ELECTRICAL MACHINES

3

A. IVANOV-SMOLENSKY

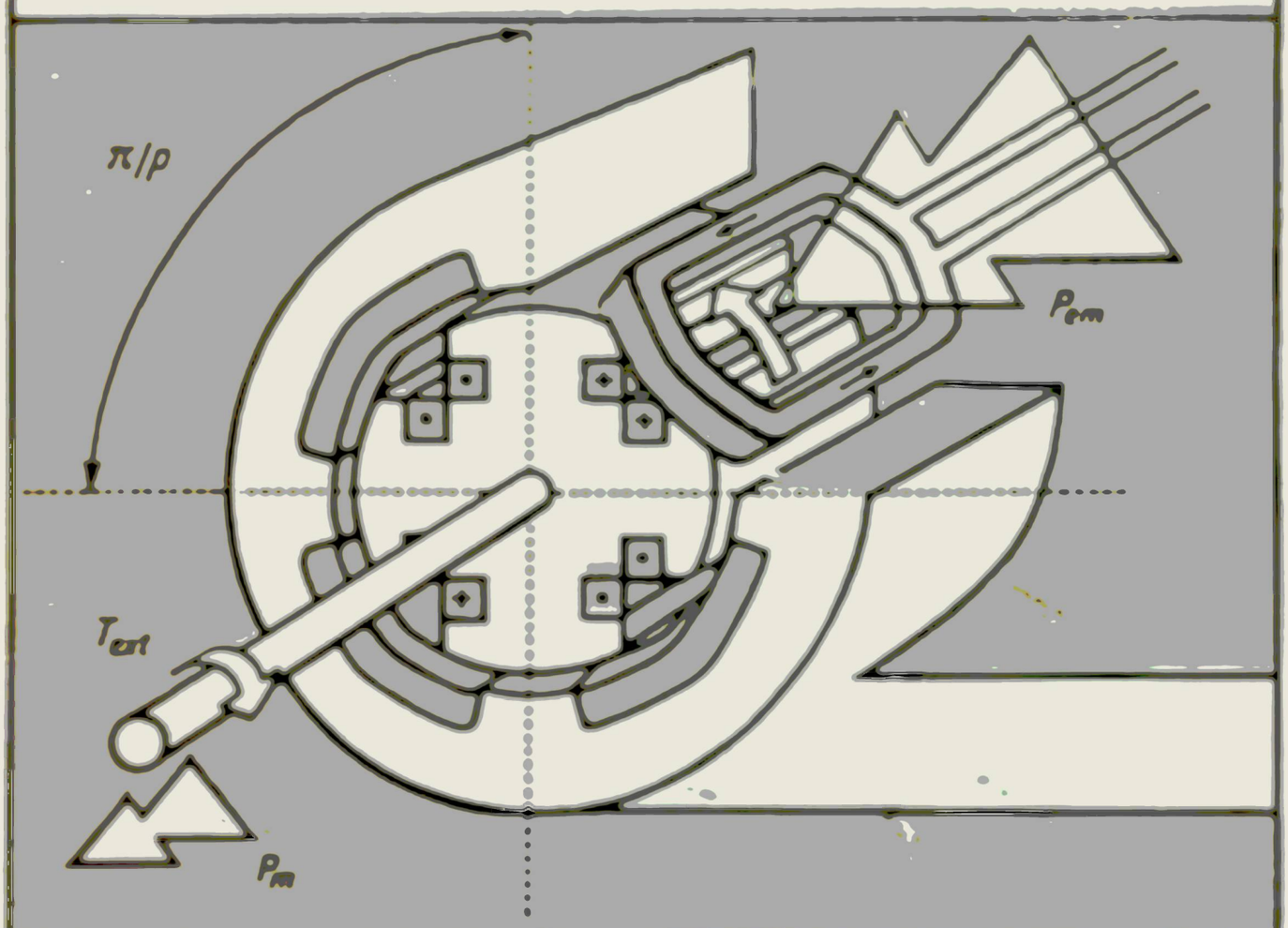

MIR Publishers Moscow

ABOUT THE BOOK

The book is in three volumes as follows.

Volume I:

Preface. Introduction. Transformers. A General Theory of Electrical Machines.

Volume II:

Classification of Electrical Machines. Mechanical, Hydraulic and Thermal Analysis and Design. Induction Machines. Synchronous Machines.

Volume III:

D.C. and Commutator Machines. Transients in Electrical Machines.

The book is intended for college and university students majoring in electrical-machine theory and design. It will also be useful to electrical power engineers.

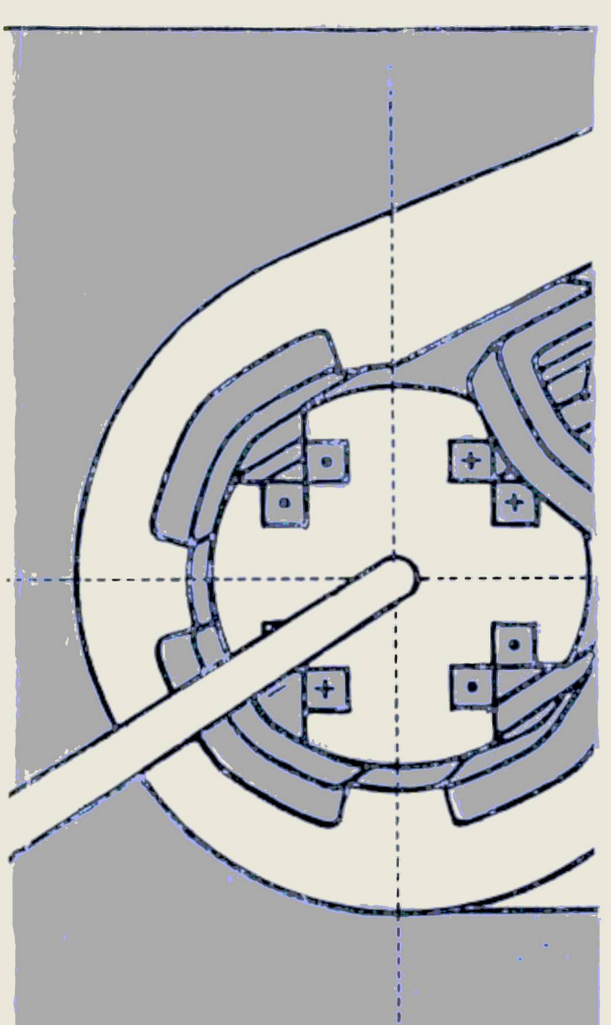

ABOUT THE AUTHOR

Professor Alexei V. IVANOV-SMOLENSKY, D. Sc. (Tech.), is a leading Soviet authority in his field. Currently, he is with the Moscow Power Institute. He has written (individually and as a coauthor) six books on electricity including the present one.

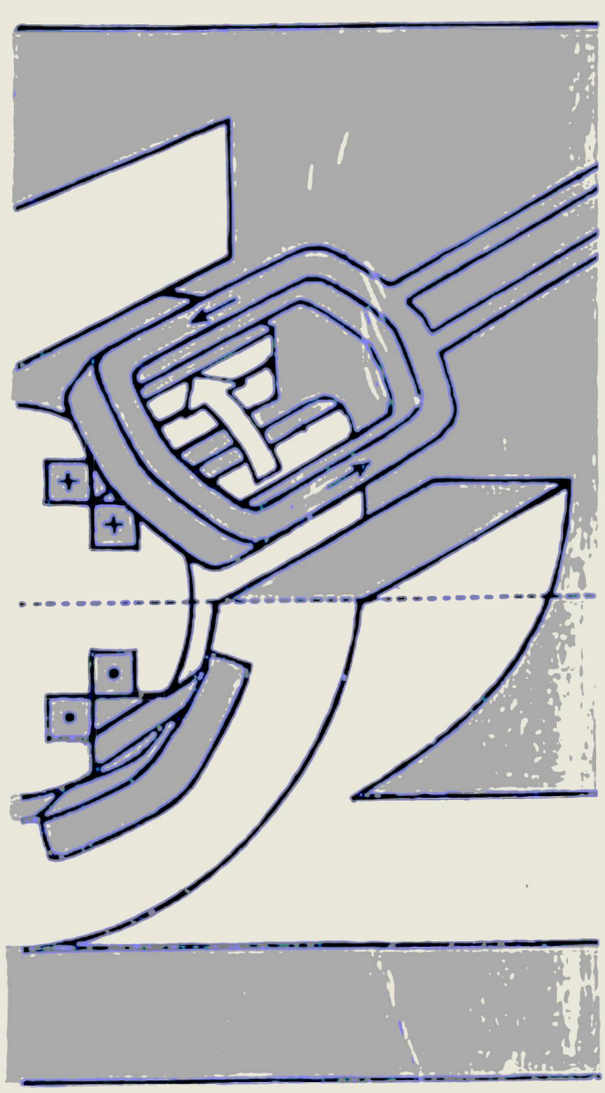

ELECTRICAL MACHINES vol. 3

A. IVANOV-SMOLENSKY

Mir Publishers Moscow

А. В. Иванов-Смоленский

ЭЛЕКТРИЧЕСКИЕ МАШИНЫ

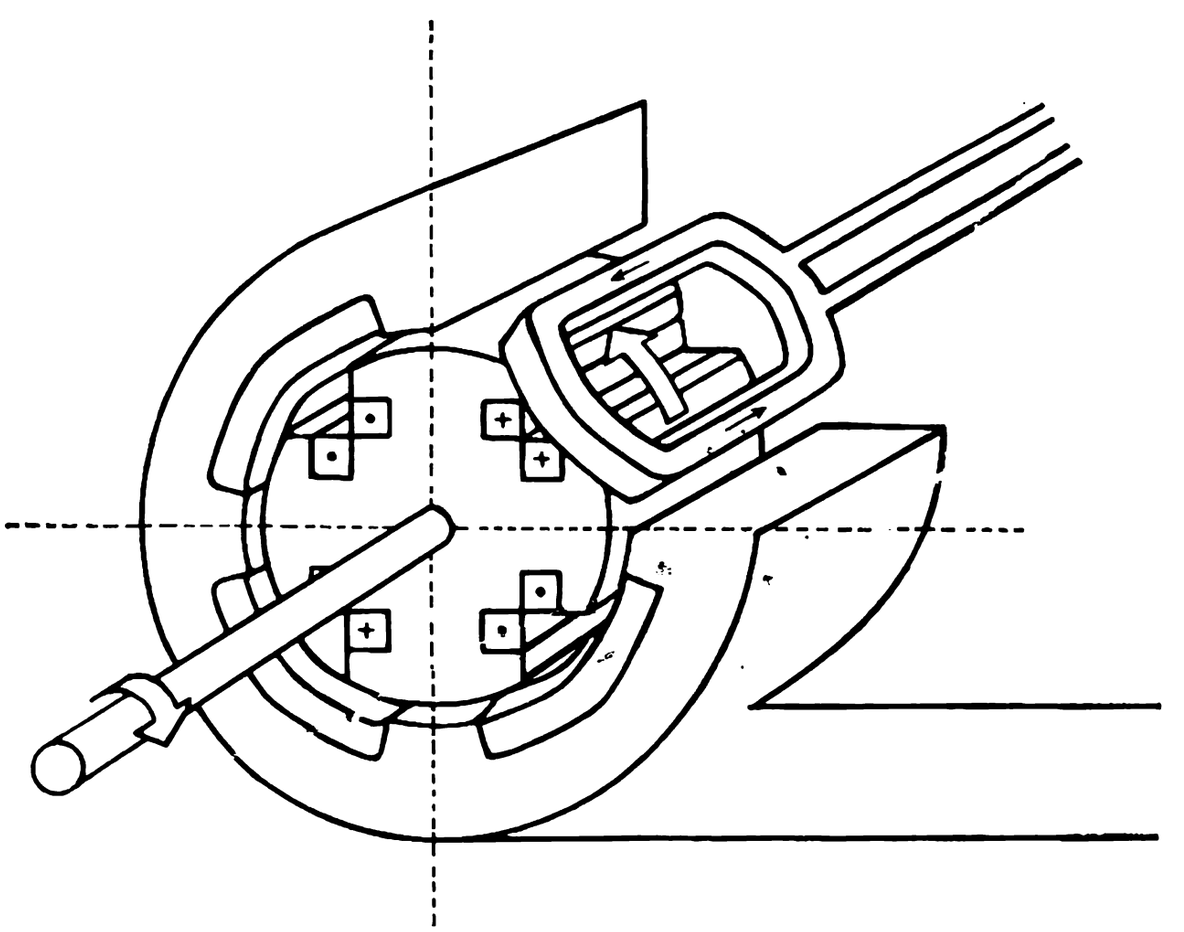

Издательство «Энергия» Москва

ELECTRICAL MACHINES

A. IVANOV-SMOLENSKY

Vol. 3

Translated from Russian
by BORIS V. KUZNETSOV

MIR Publishers Moscow

First published 1983
Revised from the 1980 Russian edition

На английском языке

© Издательство «Энергия», 1980 г.
© English translation, Mir Publishers, 1983

Contents

6 Direct-Current and Alternating-Current Commutator Machines

Chapter 64 Direct-Current Electrical Machines 9

64-1 Purpose and Applications *9*
64-2 A Brief Historical Outline *10*
64-3 Construction and Principle of Operation *13*
64-4 Armature Windings *17*
64-5 Armature EMF *30*
64-6 Electromagnetic Torque *38*
64-7 MMFs and Resistances of the Windings of a D.C. Machine *40*
64-8 Calculation of the Magnetic Circuit at No Load *43*
64-9 Calculation of the Magnetic Circuit and Voltage On Load *48*
64-10 Energy Conversion by a D.C. Machine *56*
64-11 Commutation *59*
64-12 D.C. Generators *70*
64-13 D.C. Motors *84*
64-14 A Brief Outline of Soviet-Made D.C. Machines *96*

Chapter 65 Special-Purpose D.C. Machines 100

65-1 Permanent-Magnet D.C. Machines *100*
65-2 The Krämer D.C. Generator *102*
65-3 The Split-Pole Generator *102*
65-4 The Rosenberg Variable-Speed Generator *104*
65-5 Rotary Power Amplifiers *107*
65-6 Round-Armature and Printed-Armature Motors *110*
65-7 Acyclic or Homopolar Machines *111*
65-8 Magnetohydrodynamic (MHD) D.C. Machines *113*

Chapter 66 Rotary Converters 115

66-1 Motor-Generators Sets *115*
66-2 D.C.-to-D.C. Dynamotors *116*
66-3 A.C.-to-D.C. Dynamotors *118*

Chapter 67 Solid-State Commutator D.C. Machines 121

67-1 Replacement of the Mechanical Commutator *121*

67-2 Fractional-HP Transistor D.C. Motors *124*
67-3 Thyristor-Commutated, Closed-Winding D.C. Motor *130*

Chapter 68 Alternating-Current Commutator Machines. Speed Control Systems Using Auxiliary Machines 134

68-1 Commutator Action in A.C. Machines *134*
68-2 The Commutator as a Frequency Changer *135*
68-3 Three-Phase A.C. Commutator Motors *139*
68-4 Speed and Power Factor Control Schemes for Induction Motors *148*
68-5 Single-Phase Commutator Motors *155*

7 Transient Phenomena in Electrical Machines

Introduction 165

Chapter 69 Mathematical Description of Transients in Induction Machines 166

69-1 Differential Equations Based on Phase Quantities *166*
69-2 Zero-Sequence Components of the Phase Quantities *170*
69-3 Phase Quantities in Terms of Resultant Phasors *174*
69-4 The α- and β-Axis Components of Stator Quantities and the d- and q-Axis Components of Rotor Quantities *176*
69-5 The d- and q-Axis Components of Stator Quantities and the α- and β-Axis Component of Rotor Quantities *178*
69-6 Flux Linkage Phasors in Terms of Current Phasors *179*
69-7 The Voltage Equation in Terms of the α- and β-Axis Components *181*
69-8 Voltage Equations in Terms of d- and q-Axis Components and in Terms of Components Along Axis Rotating at Arbitrary Velocity. Equivalent Circuits *183*
69-9 Electromagnetic Torque Expressed in Terms of Resultant Current and Flux Linkage Phasors and Their Components *186*
69-10 Equations of a Three-Phase Induction Machine in a Balanced Steady State *188*

Chapter 70 Transient Phenomena in Induction Machines 191

70-1 Introductory Remarks *191*

70-2 Transients with the Stator Winding Open-Circuited. Disconnection of an Induction Machine from the External Circuit *193*
70-3 Transients with the Stator Winding Short-Circuited or Connected to an External Line *195*
70-4 Switch-On of an Induction Machine *203*
70-5 Transients during a Balanced Short-Circuit in the Stator Winding of an Induction Machine *210*

Chapter 71 Mathematical Description of Transient and Asynchronous Conditions in Synchronous Machines 212

71-1 Statement of the Problem. Simplifying Assumptions *212*
71-2 Equivalent Circuits for the Damper Winding *213*
71-3 Referring the Rotor Circuits to the Stator Side *216*
71-4 Resistive and Inductive Parameters of a Salient-Pole Synchronous Machine with Referred Rotor Circuits *218*
71-5 Circuit Voltage Equations in Terms of Phase Quantities *224*
71-6 Circuit Voltage Equations in the d, q-Plane *226*
71-7 Electromagnetic and the Equation of Motion for the Rotor *232*
71-8 Equations of a Three-Phase Synchronous Machine in a Balanced Synchronous Steady State *233*

Chapter 72 Transients in Synchronous Machines Caused by Changes in and Suppression of Field Excitation 235

72-1 General Remarks *235*
72-2 Transients in a Synchronous Machine with No Damper Winding (with the Stator Winding Open-Circuited) *235*
72-3 Transients in a Synchronous Machine with a Damper Winding and with the Stator Open-Circuited *239*
72-4 Transients in a Synchronous Machine without a Damper Winding, with the Stator Short-Circuited *247*
72-5 Transients in a Synchronous Machine with a Damper Winding and the Stator Winding Short-Circuited *250*

Chapter 73 Transients Caused by a Balanced Short-Circuit on the Stator Winding of a Synchronous Machine 253

73-1 General Remarks. Initial and Terminal Conditions *253*

73-2 Equations for Transient Currents *256*
73-3 Periodic Currents *257*
73-4 Aperiodic Current Components *265*
73-5 Total Short-Circuit Currents in the *d*- and *q*-Axis Stator Circuits *268*
73-6 Currents in the Stator Phases *269*
73-7 Currents in the Rotor Windings *272*

Appendix. Conductor Materials for Electrical Machines and Transformers *277*

Bibliography **278**

Index **279**

Direct-Current and Alternating-Current Commutator Machines

6

64 Direct-Current Electrical Machines

64-1 Purpose and Applications

This part of the book will be concerned with electrical machines connected to the external circuit via what is known as the *commutator*.

The function of a commutator is to convert a.c. to d.c. in the generating mode and to invert d.c. to a.c. in the motoring mode. A commutator, in one form or another, is built into any d.c. machine because its armature winding must carry a.c.—it is only then that there will be a continuous and unidirectional energy conversion.

The most commonly used form of commutator is the *mechanical commutator*—a mechanical rectifier-inverter connected between the armature coils and the d.c. terminals. Quite aptly, such machines are called *commutator d.c. machines*. Recently, there has been a growing trend towards using electronic (or solid-state) commutators—switching arrangements based on thyristors, rectifying diodes, or transistors—to supplement or supplant the mechanical commutator function.

Unless otherwise qualified, the term "commutator d.c. machine" will refer to those fitted with a mechanical commutator. As already noted, they may be motors or generators.

D.C. motors. Direct-current motors have a broad range of speed control coupled with a high efficiency over the range, and can be built with torque-speed characteristics to suit any particular applications. This is why, although they are twice or three times more expensive to make than squirrel-cage induction motors, d.c. motors are preferable wherever their special qualities are desirable or decisive. For example, they are widely used in electric traction on

railways where their drooping torque-speed characteristic and wide range of speed control are valuable. The same goes for the d.c. motors used in cranes and other hoisting equipment. Large d.c. motors (up to 12 MW) are used as drives in blooming and slabbing mills, as main propulsion units on Diesel-electric ships. In most cars, tractors and aircraft using d.c. electric supply, all auxiliaries are driven by d.c. motors. Small d.c. motors (from a fraction of a watt to tens of watts) are employed in various automatic control applications.

Direct current for d.c. motors is supplied by d.c. generators, a.c.-to-d.c. converters or rectifiers.

D.C. generators. Direct-current generators supply d.c. for industrial purposes where low voltage is required (electrolysis, electroplating, and the like). In many cases, they serve as exciters for synchronous generators.

There are also various special-purpose d.c. generators (welding, train-lighting), d.c. rotary amplifiers (control generators), etc.

☆ 64-2 A Brief Historical Outline

In 1821, Faraday demonstrated a device in which a conductor carrying d.c. rotated around a magnet. In fact, his device was a primitive homopolar machine. In the years that followed, several more devices capable of converting electrical energy to mechanical were made. In 1824, Barlow described a device resembling a homopolar machine, in which a copper disc placed in the field of a permanent magnet would rotate when supplied with current.

In 1833, Ritchie described the first working model of a heteropolar commutator motor. In his device, the field was excited by a horse-shoe magnet between the poles of which there was an electromagnet fed with d.c. via the commutator. A unidirectional torque was produced by the interaction of the permanent magnet and the electromagnet in which the direction of current flow was reversed in a periodic fashion.

In 1834, Jacobi built an electromagnetically excited d.c. motor which could be used as a drive for various machines. It had two groups of U-shaped magnets, with four magnets per group. One group was mounted on a stationary frame, and the other on a rotating disc, so that the two

groups faced each other. The coils of all the magnets were connected in series (today, we would call it "series-excited" or "series-wound"). Direct current was supplied by a battery of primary cells. The polarity of the rotating magnets was periodically changed by a commutator. In 1838, Jacobi built a better and larger motor which could propel a small boat. In fact, it was a combination of 40 small units each of which differed from the machine of 1834 only in that the axes of the rotating and stationary magnets were arranged radially and in the same plane. A major limitation of Jacobi's motor was the pulsating torque, because both the armature and the field structure used a salient-pole core.

In 1859, Pacinotti built an electric motor which had a nonsalient-pole, distributed-winding armature and produced a practically constant torque. The armature core was a toothed steel ring mounted on the shaft by means of brass spokes. The slots received coils brought out to commutator bars. The commutator had as many bars as there were armature coils. Current was conveyed to the commutator bars by contact rolls. Placed across from the armature teeth were two electromagnets of opposite polarity, fitted with pole-pieces. The electromagnets were connected in series with the armature winding and took a small current for excitation (owing to the teeth on the armature core). For all of its advantages, Pacinotti's motor failed to become a practical machine because, like Jacobi's motor, it required an economical d.c. source which was nonexistent at that time.

Direct-current generators lagged behind d.c motors at all times. For the first time, Faraday thought of building a homopolar d.c. generator in the form of a disc rotating in a magnetic field in 1831, that is, a decade after he had built his homopolar motor. In 1832, the Pixie brothers built a heteropolar d.c. generator employing a commutator for rectification of the alternating current induced in stationary coils mounted on a U-shaped iron core. The field in the core was periodically reversed in polarity by a rotating U-shaped magnet placed opposite to the core.

For practical purposes, a permanent-magnet d.c. generator was first used by Jacobi in 1842. In contrast to the Pixii machine, the magnets were stationary and the coils were rotating. In the 1840-50s, some prominence was gained by Störer's permanent-magnet generator with three rotating

magnets. For larger output, several such machines would be combined into a single assembly. From 1856 to 1865, permanent-magnet generators of this design were produced by the Alliance Company (France). They were driven by a steam engine with a power output of 6 to 10 hp.

In 1851, Sinsteden proposed to replace the permanent magnets by electromagnets energized from another permanent-magnet generator. This idea was embodied, for example, in 1863 in Wilde's generator which was built in two modifications, as a single-phase a.c. generator (see Sec. 51-2) and as a d.c. generator. In the d.c. generator, a.c. was rectified by a simple commutator. The excitation field was produced by a U-shaped electromagnet whose pole-pieces encircled a concentrated-winding, salient-pole armature. The voltage at the brushes was a pulsating one.

In 1854, Hjort took out a patent for a self-excited machine. For "initial" excitation, he proposed to use permanent magnets, so his machine actually used a combination of excitation.

In 1856, Jedlik came out with the idea to use residual magnetization for self-excitation; in 1861, he built a self-excited d.c. generator based on his idea.

In 1866, Siemens applied self-excitation to series-wound generators—a feature which made them attractive as sources of direct current for lighting.

However, d.c. generators remained unattractive commercially until 1870 when Gramme took out a patent for a self-excited generator with a ring-shaped armature and a toroidal winding divided into a multiplicity of coils brought out to the bars of a commutator of a nearly present-day design.

Although the Gramme ring armature was basically similar to Pacinotti's invention made in 1860, it differed in two important aspects: the ring core was made of a bundle of iron wires (as a way of reducing eddy-current losses) and had no teeth (which was a step backward from Pacinotti's idea and could not but lead to an increased reluctance of the magnetic circuit). Its advantages were obvious (a practically constant terminal voltage, freedom from an additional excitation source, a relatively smaller weight, and high efficiency), and the Gramme generator quickly ousted all the other types. At that time, the principle of reversibility had been well established, and the Gramme

machine came to be used as both generator and motor.

In 1873, von Hefner-Alteneck and Siemens replaced the ring armature by a drum design in which both sides of each coil contributed to the output emf. In 1878, it was proposed to cut slots in the drum armature core, and this substantially reduced the radial gap length.

In 1879, Siemens used a series-wound generator to power the first electric railway demonstrated at the Berlin Exhibition.

In 1880, Edison proposed to build up the armature core of insulated iron laminations—a feature which led to a sizeable reduction in eddy-current losses and armature reaction. In 1884, it was proposed to add a compensating winding, and in 1885, commutating (or intermediate) poles as a way of reducing armature reaction still more and improving commutation. Thus, towards the end of the past century the d.c. machine had become almost what it is today.

64-3 Construction and Principle of Operation

As has been noted in Sec. 64-1, we shall deal with d.c. machines, that is, those connected to a d.c. system via a mechanical rectifier-inverter or, simply, a *commutator*.

To simplify the commutator design, the machine must be of inverted construction, that is, its d.c.-fed field winding must be on the stator, and the armature (output) winding on the rotor. With this arrangement, the commutator is mounted on the rotor and consists of a multiplicity of bars or segments to which the terminal leads of the armature coils are taken, and a set of stationary brushes held in contact with the commutator bars.

(a) Construction. In sketch form, the construction of a d.c. machine is shown in Fig. 64-1. Referring to Fig. 64-2, the stator consists of a yoke (or frame) *6*, the cores of main poles *1* and commutating (or intermediate) poles *3*, and the field coils encircling the poles. The number of main poles depends on the power rating and rpm. As a rule, four or six main poles are provided. Fractional-hp machines have two main poles, and very large machines up to several tens. Figure 64-2 shows the stator of a four-pole machine. The main-pole cores are built up of structural-steel sheet

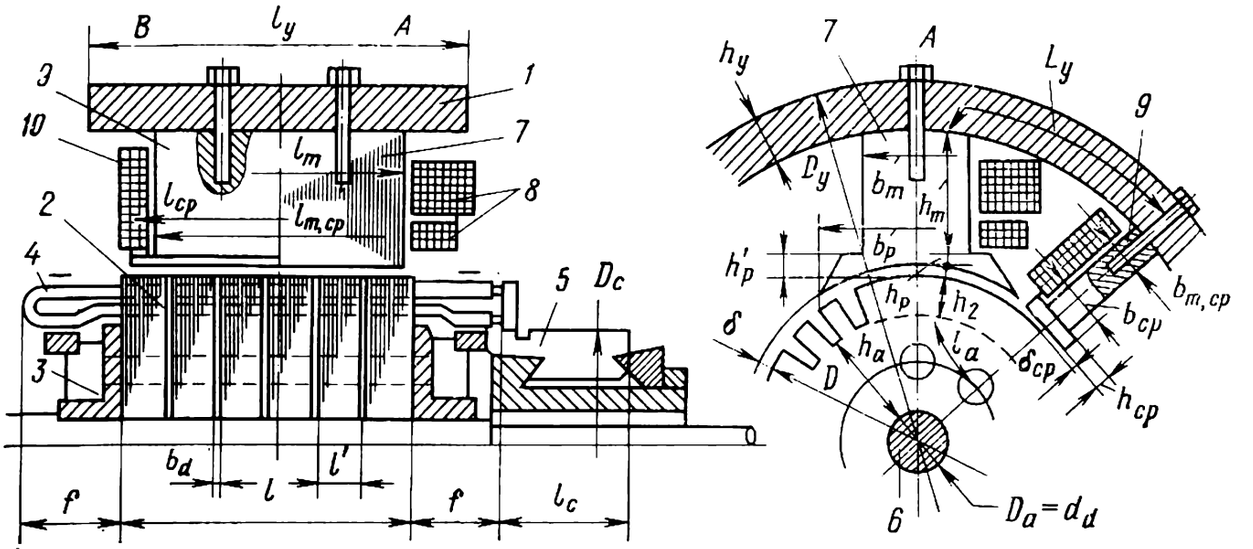

Fig. 64-1 Arrangement of a d.c. machine:
1—frame (yoke); *2*—armature core; *3*—coil-holder; *4*—armature coils; *5*—commutator; *6*—shaft; *7*—main pole core; *8*—field coils; *9*—compole core; *10*—compole coils

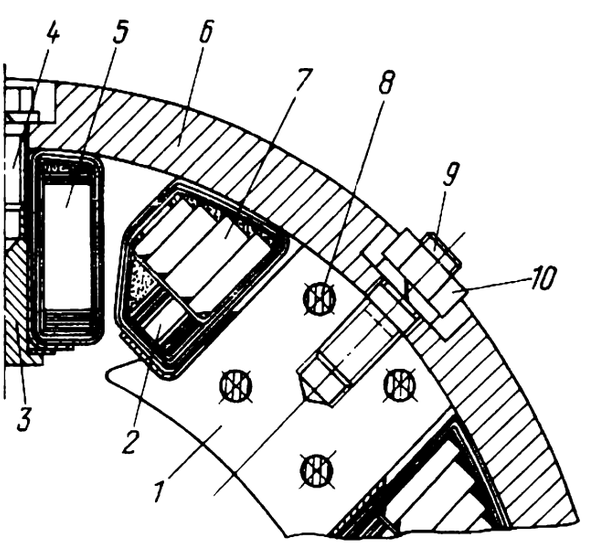

Fig. 64-2 Stator of a d.c. machine

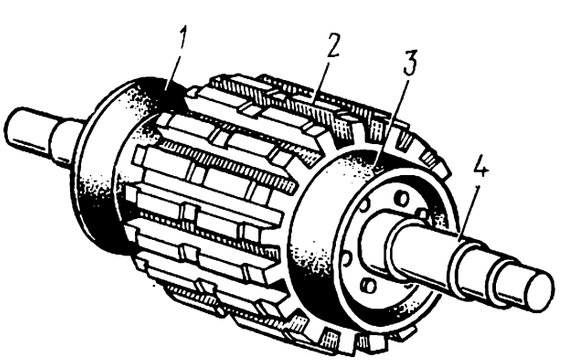

Fig. 64-3 Unwound armature

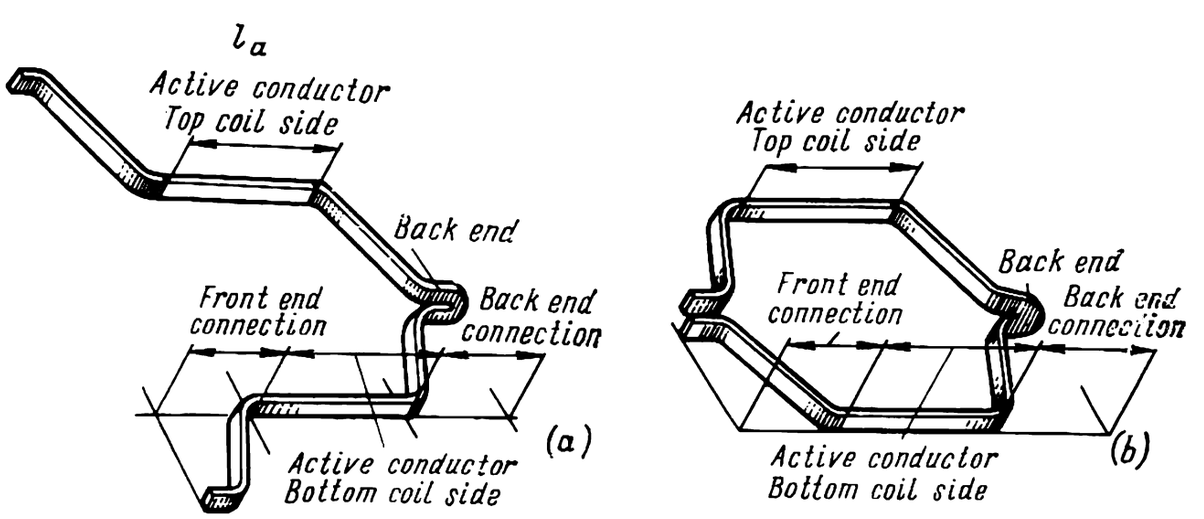

Fig. 64-4 Single-turn armature coils: *a*—wave winding; *b*—lap winding

laminations 1 or 2 mm thick, clamped together by studs *8*. Attachment of the poles to the yoke is by studs *9* screwed into the cores, and nuts *10*. The compole cores are solid pieces of iron attached to the yoke by bolts *4*.

The main poles carry the coils of one or several field windings (the series field winding *2* is traversed by the rectified armature current, the shunt field winding *7* is connected to the armature brushes and energized from an external d.c. supply). The compole coils are connected in series with the armature winding.

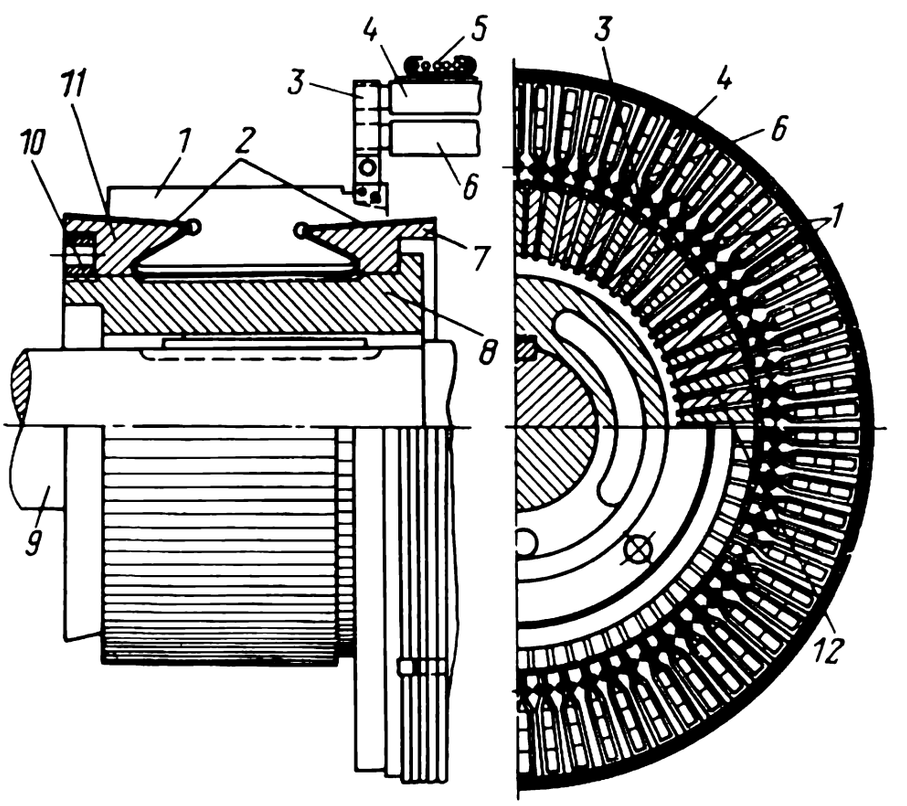

Fig. 64-5 Connection of armature coils to the commutator

As is seen from Fig. 64-3 the armature core consists of one or several blocks, *2*, of varnish-insulated electrical-sheet steel laminations 0.5 mm thick. The blocks are separated by radial ventilation ducts (not shown in the figure). The core laminations and blocks are clamped together by rings *1* and *3* which also double as coil-holders. The core armature may be mounted either directly on the shaft, *4*, or on a spider. If the outer diameter of the core exceeds 100 cm, it is assembled of segments.

The slots on the armature core receive the insulated coils of a two-layer armature winding, with the lower sides nearer to the bottom, and the upper sides nearer to the top of the slots (Fig. 64-4). As shown in Fig. 64-5, the terminal leads,

4 and *6*, of the coils are soldered to risers *3* on the commutator bars *1*. The centrifugal force of the leads is taken up by a wire binding *5*. The terminal lead *6* from the lower side of one coil is connected to the terminal lead *4* of the upper side in another coil, and all the coils are interconnected so as to form a closed winding (for the winding circuits, see Sec. 64-4).

The commutator (Fig. 64-5) is an assembly of copper bars or segments *1*. The bars are insulated from one another by mica (or micanite) spacers *12* and from the ground by tapered or cylindrical micanite washers *2*. The commutator-bar assembly is held together by a commutator shell *8* and Vee-rings *7* and *11*. In turn, the Vee-rings are held in place by a nut *10*. The commutator assembly is press-fitted on the shaft *9* and its outer surface is machined together with the bearing seats. In this way, the commutator is given a regular cylindrical shape.

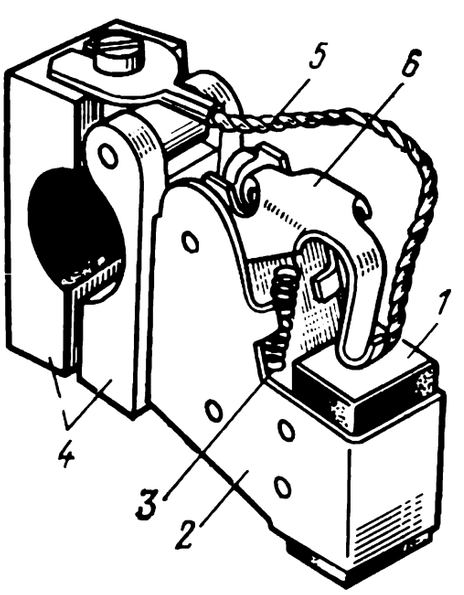

Fig. 64-6 Brush holder: *1*—brush; *2*—box; *3*—spring; *4*—brush-finger clamp; *5*—pig-tail; *6*—rocker

Electric connection between the armature winding and the external d.c. circuit is by means of brushes held in brush holders (Fig. 64-6). The brush holders are so built that the brush pressure can be adjusted at will and automatically maintained at a constant value as the brushes wear

Tangentially, a brush usually spans two or three commutator bars. Axially, the length of a brush does not exceed 3 or 4 cm. Therefore, in order to obtain a safe current density at the sliding contact, it is usual to mount several brush holders on one brush finger. The total number of brush fingers is equal to the number of poles (one half is in positive polarity, and the other, in negative polarity). The brush fingers are secured in and insulated from a rocker arm by insulating sleeves. In turn, the rocker arm is fastened to the end-shield or yoke (in the case of machines with pedestal bearings). The brush fingers of the same polarity are interconnected by brush shunts.

(b) Principle of operation. The d.c. field of a machine at no-load ($I_a = 0$) is set up solely by the mmf of the field winding which is traversed by a direct current, I_f. When the armature rotates at speed n, the emf induced in its winding has the frequency $f = p\Omega/2\pi = pn$. The commutator and brushes rectify this emf, and a direct (or, rather rectified) emf appears at the brushes.

When the machine is connected to a d.c. line or a resistive load, a current is flowing in the armature winding, its magnitude being dependent on the relative magnitude of the emf and line voltage. In the generator mode of operation (the rotation is along the arrow G in Fig 64-7), the emf exceeds the line voltage, $E > V$, the armature current is in the same direction as the emf, and the mechanical energy applied to the shaft is converted to electric energy, which is delivered to the external circuit.

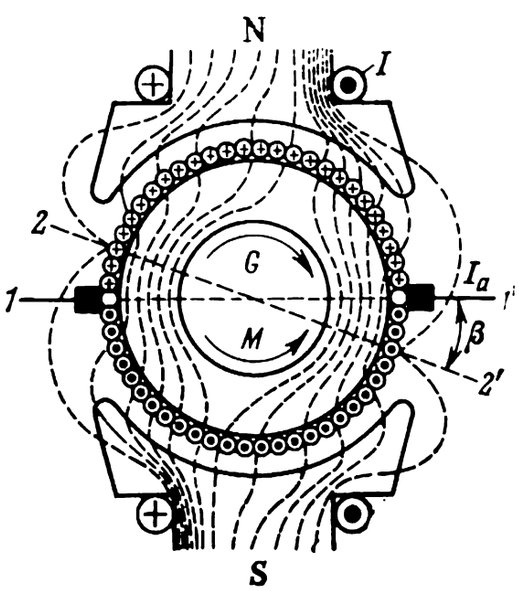

Fig. 64-7 Explaining the operating principle of a d.c. machine

In motoring (the rotation is in the direction of arrow M), the emf is smaller than the line voltage, $E < V$, the armature current is in the same direction as the line voltage and the electric energy taken in from the external circuit is converted to mechanical energy which is transferred by the shaft to the driven machine.

On load, $I_a \neq 0$, the magnetic field is set up not only by the separately excited or the shunt field winding traversed by I_f, but also by the series field and armature windings carrying I_a. This brings about a change in the flux pattern and in the gap flux distribution. As is seen from Fig. 64-7, flux line *2-2'* passing through the points on the armature surface where the flux density is zero (the physical neutral line) is displaced from its position at no-load, *1-1'*, by an angle β.

64-4 Armature Windings

Present-day d.c. machines use the *drum armature winding* in which the conductors are laid in slots on the outer surface

of the core. As a rule, this is a double-layer winding formed of insulated coils (see Fig. 64-4) interconnected at commutator bars (Fig. 64-8). A coil may consist of one turn, $w_c = 1$ (as in Figs. 64-4 and 64-8*a*) or several turns, $w_c > 1$ (as in Fig. 64-8*c*). In circuit diagrams, a multiturn coil is shown as a single-turn one.

In a slot, the coil sides are arranged in two layers (see Fig. 64-8*b*), one nearer to the bottom, and the other

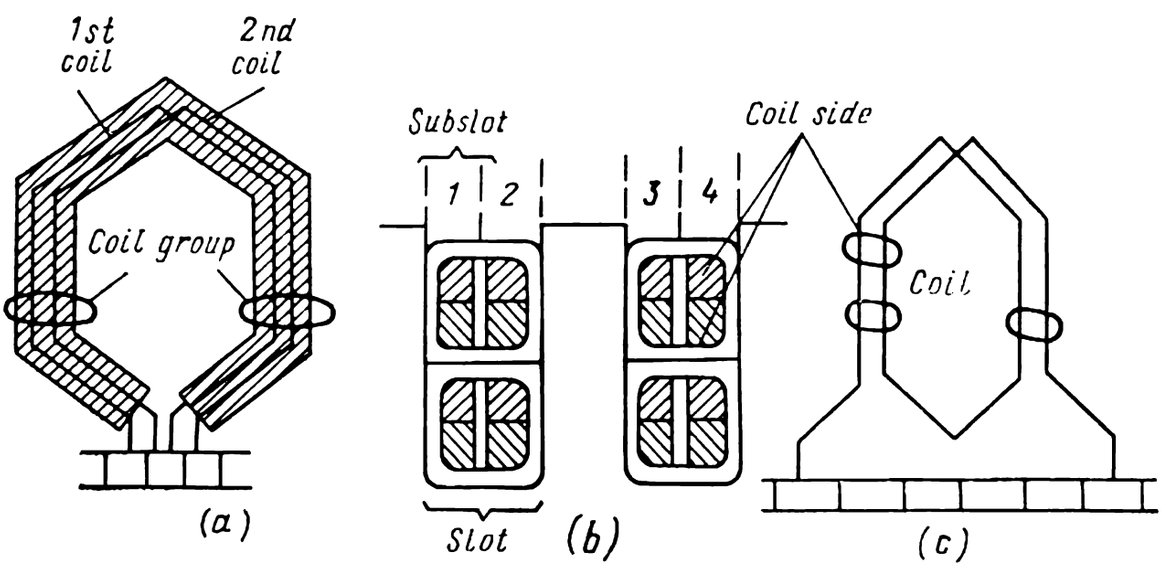

Fig. 64-8 Armature coils and coil groups: *a*—lap winding composed of single-turn coils; *b*—subslot; *c*—two-turn coil of a wave winding

nearer to the top of the slot. The several coils surrounded by common ground insulation form a *coil group* (see Fig. 64-8*a*). The number of coils in a coil group is denoted by u_c.

In a winding diagram, the coil width (also called the *front pitch*), y_f, and the spacing between adjacent coils (usually called the *back pitch*), y_b, are measured in subslots, a subslot being defined as the part of an armature slot occupied by the two coil sides lying one above the other. In Fig. 64-8*b*, the subslots are numbered *1*, *2*, *3*, and *4*. The number of subslots, Z_s, is the same as the number of coils in the winding, Z_c, and equal to the number of commutator bars, K. The remaining data characterizing an armature winding are the number of pole pairs p, the number of armature slots Z, the number of coils per coil group $u_c = Z_s/Z$, the number of effective conductors $N = 2w_cZ_s$, and the number of effective conductors per slot, $u_s = N/Z = 2w_cu_c$.

The armature winding may be *lap-wound*, *wave-wound*, or *frog-leg-wound*.

(a) Lap winding. A lap commutator winding consists of coils (or coil groups) shaped in the same manner as in an

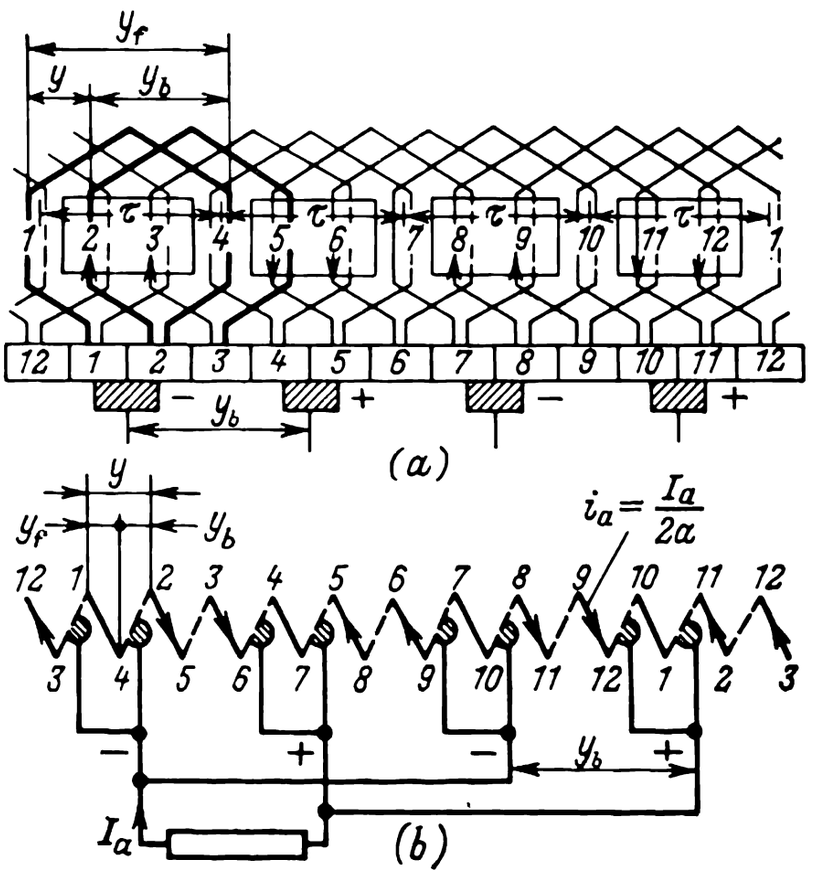

Fig. 64-9 Simple lap winding ($Z_s = 12$, $2p = 2a = 4$, $y_f = 3$, $y_b = 2$, $y = 1$, $y_b = 3$): *a*—complete diagram; *b*—simplified diagram

a.c. polyphase lap winding (see Sec. 22-2, Fig. 22-5). The coil width or front pitch, y_f, in a lap winding is chosen to be nearly equal to a pole pitch (as a rule, a bit shorter than a pole pitch). As measured in subslots, the front pitch is

$$y_f \leqslant Z_s/2p \qquad (64\text{-}1)$$

where

$$Z_s/2p = \tau$$

is the number of subslots per pole pitch.

With the above choice of the front pitch, the emf induced in a coil will have a maximum amplitude.

The simple (or simplex) lap winding shown in Fig. 64-9*a* is obtained by connecting the conductors (coils) consecutively in such a way as to form one complete ring. More specifically, starting at commutator bar No. 2, the lower (right-

hand) side of, say, coil *1* is connected to the upper (left-hand) side of the adjacent coil *2* which is diplaced from coil *1* by one subslot (or coil side).

The number of coil sides (or bars) by which the winding fails to close one time around the commutator is called the *resultant pitch*, y. For a simple lap winding, $y = 1$. Now the back pitch, y_b, can be re-defined as the distance (in subslots or coil sides) between the lower (right-hand) side of a coil and the upper (left-hand) side of the next adjacent coil (in the direction of journey around the winding). As is seen from Fig. 64-9*a* the resultant pitch of a lap winding is

$$y = y_f - y_b \qquad (64\text{-}2)$$

For the simple lap winding in Fig. 64-9, $y_f = 12/4 = 3$ and $y_b = y_f - y = 3 - 1 = 2$.

As already noted, connecting all the coils in series produces a closed winding. In it, the magnetic field reverses once every pole pitch, so the emfs in the winding add up to zero. This is because the emf in, say, coil *2* is cancelled out by the emf in the coil displaced by a pole pitch, $\tau = 3$, that is, in coil *5*, $e_2 = -e_5$, and so on. If the coils are symmetrical, the brushes must be set on the pole axes and the spacing between them, or the *brush pitch*, y_{brush}, must be equal to $K/2p$ commutator bars.

A simplified winding diagram is shown in Fig. 64-9*b* where the coils are represented by full lines and the commutator bars by dashed lines. The coils take the same numbers as the subslots where their coil sides are laid, and the commutator bars are labelled by the numerals written above them.

As is seen from Fig. 64-9, with respect to the brushes a simple lap winding has

$$2a = 2p \qquad (64\text{-}3$$

parallel paths or circuits. In Fig. 64-9, $2a = 4$.

In the case of an ideal magnetic symmetry, the emfs in all the parallel paths are the same because the paths are formed by coils displaced by a pole pitch, τ, from one another:

$$e_2 + e_3 = -(e_5 + e_6) = e_8 + e_9 = -(e_{11} + e_{12})$$

As a consequence, there are no circulating currents that would exist if the emfs were different and that would then have their paths completed through the brushes.

As the armature rotates, the coils are continually switched from one parallel path to the next adjacent. However, the sum of instantaneous emfs induced in the coils in a given parallel path remains nearly constant. If the winding has few coils, the emf of a given parallel path will contain, in addition to a constant term, also a small alternating component which owes its origin to variations in the emfs induced in the coils that are switched in that path at a given instant. With a sufficiently large number of coils the varying component practically disappears, and the emf that exists between the brushes of opposite polarity is equal to the emf of a parallel circuit. If we connect an ohmic load to the brushes, the load resistance will carry a direct current, I_a. This current will be shared equally among the parallel circuits, so that each will carry a current given by

$$i_a = I_a/2a$$

Some of the coils undergoing commutation (that is, those passing from one parallel circuit to one next adjacent) are shorted by the brushes (coils *1*, *4*, *7* and *10* in Fig. 64-9).

If the number of commutator bars is increased so that a simple lap winding will connect only to alternate bars, thereby leaving them unconnected, then a second winding, virtually in parallel electrically, can be interleaved with the first and connected to the bars that have been missed. This forms a *duplex-lap winding* for which the resultant winding pitch is 2. A further increase in the number of bars will permit additional "folds" or "plexes" in the winding (triplex, quadruplex, and so on). In this way we can obtain what is called a *multiplex lap winding* which is in effect a combination of $m = y$ simple lap windings connected to the same commutator. A multiplex lap winding has

$$2a = 2pm \qquad (64\text{-}4)$$

parallel circuits (here, m is the number of "plexes"). A schematic diagram of a duplex-lap winding is shown in Fig.64-10 (for more detail, the reader should refer to [65] and [66]).

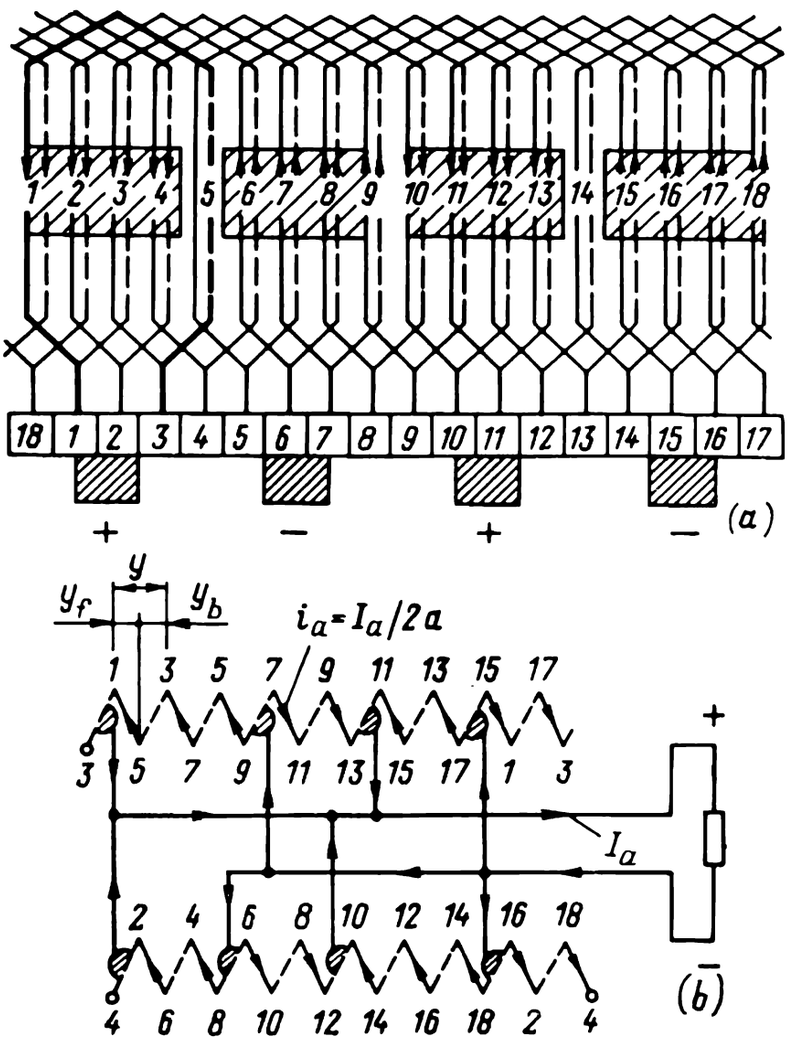

Fig. 64-10 Duplex lap winding ($Z_s = 18$, $2p = 4$, $y_f = 4$, $y_b = 2$, $y = 2$, $y_b = \tau = 4^1/_2$): a—complete diagram; b—simplified diagram

(b) Wave winding. A wave commutator winding consists of coils (or coil groups) shaped in the same manner as those of a polyphase a.c. wave winding (see Sec. 22-4, Fig. 22-7). From a lap winding, a wave winding only differs in the shape of terminal leads and end connections (see Fig. 64-4). As in other commutator windings, the front pitch, y_f, is chosen to be a bit smaller than a pole pitch

$$y_f \leqslant \tau = Z_s/2p$$

Figure 64-11a shows a *simple (or simplex) wave winding* which is formed by consecutively connecting the coils displaced from each other by two pole pitches,

$$2\tau = Z_s/p$$

The resultant winding pitch, $y \approx Z_s/p$, should be chosen such that after completing a tour around the armature the winding will not close upon itself, but will be past or before the starting conductor. In order to obtain a singly reentrant simple wave winding, it is essential that each tour around

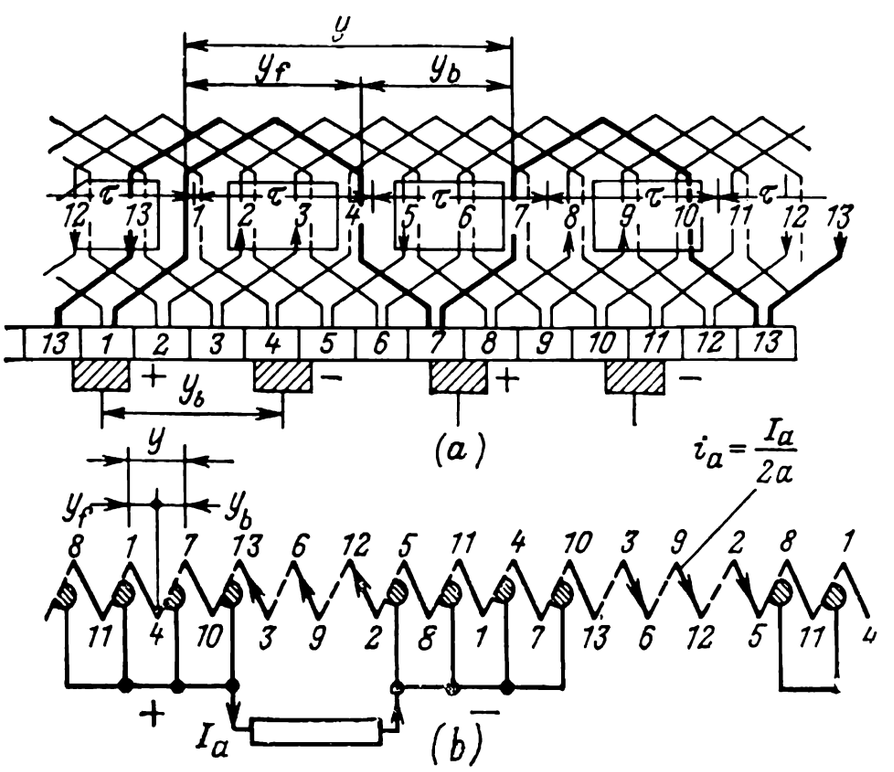

Fig. 64-11 Simple wave winding ($Z_s = 13$, $2p = 4$, $2a = 2$, $y_f = 3$; $y_b = 3$, $y = 6$, $y_b = \tau = 3^1/_4$): *a*—complete diagram; *b*—simplified diagram

the armature should include $Z_s \pm 1$ coil sides (if a tour covered Z_s sides, the winding would close upon itself). In other words, such a tour should cover p coils (one coil per pole pair). In Fig. 64-11*a*, the coils of one tour, namely coils *1* and *7*, are represented by heavy lines. As is seen, the tour covers

$$yp = 6 \times 2 = 12 \text{ sides}$$

and the next tour commences at coil *13* displaced from coil *1* by one subslot or coil side (as will be recalled, the coil No. is the No. of its upper (left-hand) side).

The throw of a tour covering p resultant pitches, y, should be such that

$$py = Z_s \pm 1$$

Therefore, the resultant pitch of a simple wave winding is given by

$$y = (Z_s \pm 1)/p \tag{64-5}$$

The back pitch of a simple wave winding, defined as the distance between the lower (right-hand) side of a coil and the upper (left-hand) side of the next adjacent coil in the direction of journey around the armature, is, as is seen from the figure, given by

$$y_b = y - y_f \tag{64-6}$$

In our example, $y = (13 - 1)/2 = 6$, $y_f = 3 \approx \tau = 13/4 = 3^1/_4$, and $y_b = 6 - 3 =$.

As in Fig. 64-9*b*, the full lines in Fig. 64-11 represent the coils taking the same numbers as the slots holding their sides, and the dashed lines represent the commutator bars which are numbered in the same sequence as the upper (left-hand) sides of the coils connected to them. The numerals labelling the upper (left-hand) coil sides are written at the top and those of the lower (right-hand) coil sides at the bottom of the diagram.

With respect to the brushes, a simple wave winding has

$$2a = 2 \tag{64-7}$$

parallel paths or circuits. Each circuit carries a current

$$i_a = I_a/2a = I_a/2$$

Some of the coils undergoing commutation are shorted by brushes of the same polarity (coils *8*, *1*, *7*, and *5*, *11*, *4* in Fig. 64-11*b*).

As with lap windings, there are *multiplex wave windings*. A multiplex wave winding is in effect a combination of m simple wave windings (here, m is the number of "folds" or "plexes" in the complete winding). Each journey of a multiplex wave winding around the armature, covering p resultant pitches y must be shorter or longer than the armature circumference by m coil sides,

$$yp = Z_s \pm m$$

Hence, the resultant pitch of an m-plex wave winding is

$$y = (Z_s \pm m)/p \tag{64-8}$$

An m-plex winding is formed by interleaving $m - 1$ simple wave windings between the first simple wave winding and connecting them to the bars that have been missed by the first.

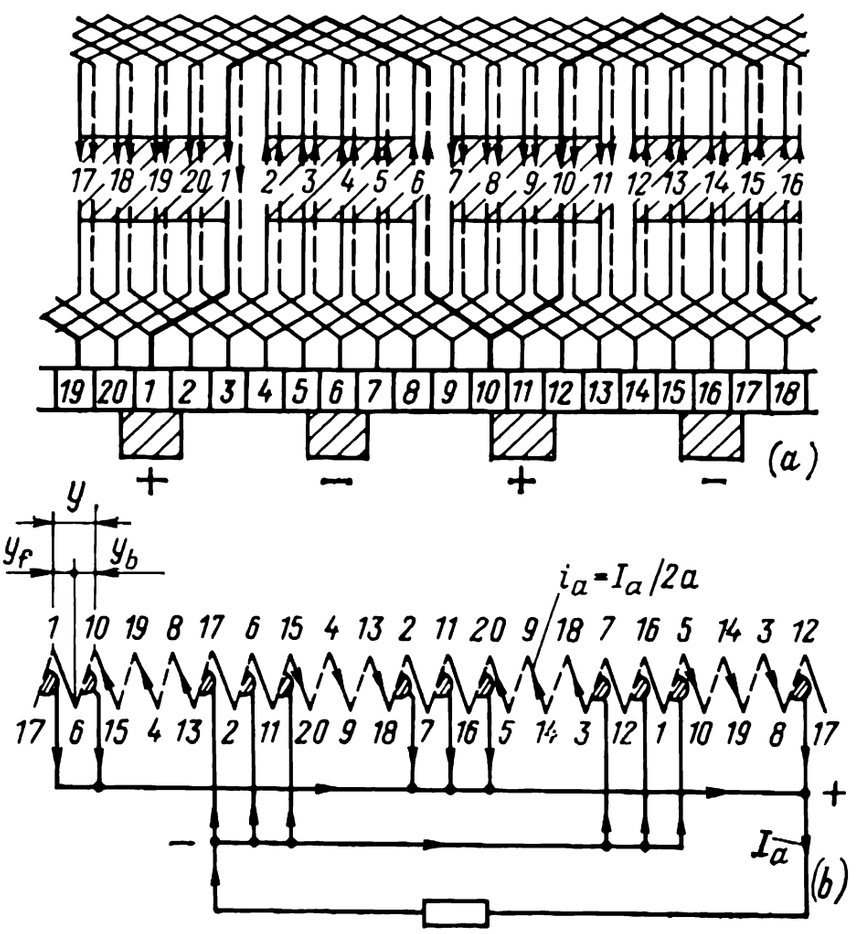

Fig. 64-12 Duplex wave winding ($Z_s = 20$, $2p = 4$, $m = 2$, $y_f = 5$, $y_b = 4$, $y = 9$, $y_b = \tau = 5$, $2a = 4$): a—complete diagram; b—simplified diagram

A schematic diagram of a duplex-wave winding ($Z_s = 20$, $m = 2$, $2p = 4$) is shown in Fig. 64-12. The resultant pitch given by Eq. (64-8) is

$$y = (20 - 2)/2 = 9$$

The front pitch is

$$y_f = 5 = 20/4$$

and the back pitch defined by Eq. (64-6) is

$$y_b = 9 - 5 = 4$$

As is seen from Fig. 64-12b, the winding has $2 \times 2 = 4$ parallel paths or circuits. In the general case, the number of parallel circuits in an m-plex wave winding is

$$2a = 2m \qquad (64\text{-}9)$$

(c) Frog-leg winding. This is a combination of a lap winding and a wave winding placed in the same slots and connected to the same commutator. Such a winding is called "frog-leg", because the coil ends resemble a frog's leg. A coil of a frog-leg winding is shown by heavy lines in Fig. 64-13. It is made up of a lap-winding coil and a wave-winding coil having the same front pitch, $y'_f = y''_f$, and the same number of turns. Because each of the component windings is two-layer, a frog-leg winding has four layers. The parameters of the lap and wave windings must be chosen such that the currents in the parallel circuits of each are the same. This requires that the two windings should have the same number of parallel circuits [see Eqs. (64-4) and (64-9)]

$$2a' = 2pm' = 2m'' = 2a'' \quad \text{or} \quad pm' = m'' \qquad (64\text{-}10)$$

where $m' = y'$ is the number of "plexes" in the lap winding, and m'' is the number of "plexes" in the wave winding.

Also, no circulating current should exist in the loops formed by the coils. This requirement will be satisfied if

$$y'_f = y''_f = Z_s/2p, \quad y'_b = y''_b, \quad y' + y'' = Z_s/p \qquad (64\text{-}11)$$

An example of a frog-leg winding ($Z_s = 24$, $2p = 6$, and $2a = 12$) is shown in Fig. 64-13. The lap winding is a simplex one:

$$m' = y' = 1$$

The wave winding is, in accord with Eq. (64-10), a triplex one:

$$m'' = pm' = 3 \times 1 = 3$$

From Eq. (64-11),

$$y'_f = y''_f = 24/6 = 4$$

and

$$y'' = (Z_s \pm m'')/p = (24 - 3)/3 = 7$$

The sum of the two pitches satisfies Eq. (64-11), that is

$$y' + y'' = 1 + 7 = 24/3 = Z_s/p$$

As is seen from Fig. 64-13, since Eq. (64-11) is satisfied, the emfs in coil *1* of the lap winding and in coil *5* of the wave winding connected in series and shorted by brushes of the same polarity add up to zero.

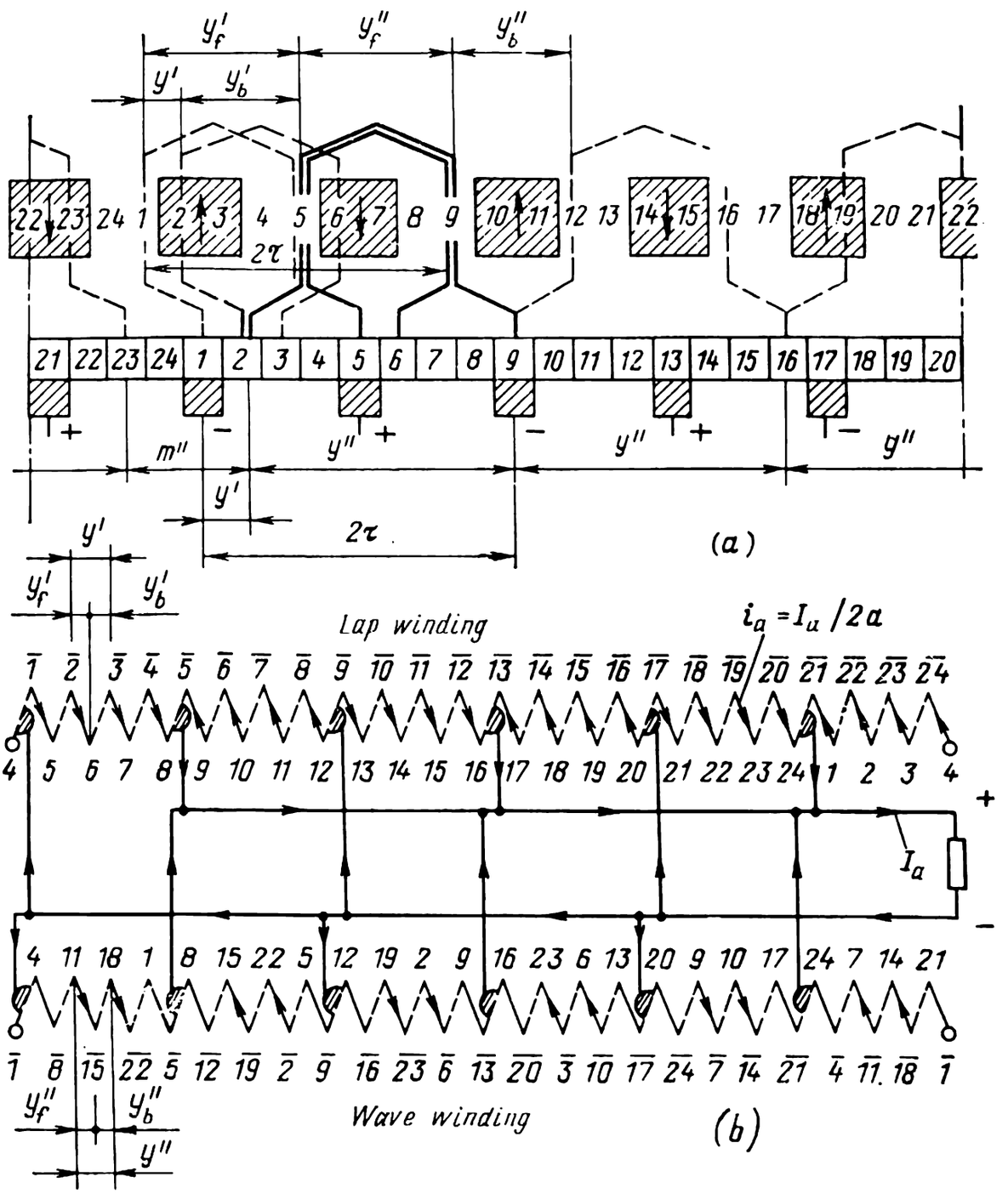

Fig. 64-13 Frog-leg winding ($Z_s = 20$, $2p = 6$, $y'_f = y''_f = 4$, $y' = m' = 1$, $y'' = 7$, $y'_b = 3$, $y''_b = 3$): *a*—complete diagram; *b*—simplified diagram

The schematic diagram of a frog-leg winding shown in Fig. 64-13*b* uses the same numbering scheme as in the previous diagrams, except that each commutator bar takes the number assigned to the left-hand (upper) side of the

lap-wound coil connected to it. The commutator bars (represented by dashed lines in the diagram) take the overscored numbers.

As is seen from Fig. 64-13, the frog-leg winding shown has $6 \times 2 = 12$ parallel circuits which take an equal share of the total current. In the general case, a frog-leg winding has

$$2a = 2a' + 2a'' = 2 \times 2a' = 4pm' \qquad (64\text{-}12)$$

parallel circuits.

(d) Equalizers for simple lap windings. In discussing the simple lap winding we assumed an ideal magnetic symmetry, so that the emfs in the parallel circuits are the same and the circuits each take an equal share of the total current. In practical machines, however, an ideal magnetic symmetry is unattainable. For example, the radial gap length may vary from pole to pole and the gap flux density will vary in a similar fashion. As a result, there will be discrepancies in the generated emfs, and these discrepancies will cause internal circulating currents which have a path through the brushes. Such currents could cause excessive heating, sparking at the brushes, and mechanical vibration.

A simple remedy is to provide a simple lap winding with what are known as *first-order equalizers.* Equalizers connect theoretically equipotential points (or tappings) on the winding, displaced by two pole pitches from each other. In this way, they form a short-circuited, double-pole-pitch "coil" superimposed, as it were, on the winding. The spacing between the tapping points expressed in coil sides or commutator bars is called the equalizer pitch

$$y_{eq} = 2\tau = Z_s/p = K/p$$

where K is the number of commutator bars.

With perfect magnetic symmetry, this "coil" would embrace equal and cancelling amounts of N-pole and S-pole flux in every armature position; there would be no net flux change and no circulating currents in the equalizers. Should there be any flux unbalance, there would be circulating currents, but they would have their path through the equalizers and not through the brushes.

It is usual to choose tapping points on commutator bars or overhangs on the side opposite from the commutator.

In the winding of Fig. 64-9, equal potentials will exist at commutator bars displaced from one another by

$$y_{eq} = Z_s/p = 12/2 = 6$$

If equalizers were connected to each commutator bar, there would be a total of Z_s/p such connectors on the armature. In our case, there would be 6 connectors. In practice, it suffices to have a half or a third as many. For example, in the winding of Fig. 64-9, we could interconnect commutator bars *1* and *7*, *3* and *9*, *5* and *11*.

In simple wave windings, the coils of each parallel path lie under all poles, so no circulating currents arise in the case of any flux unbalance. Obviously, no equalizers are needed for simple wave windings.

In multiplex lap and wave windings, the sharing of total current among the various simple windings electrically connected only by brushes will depend on the state of sliding contact and the position of the brushes relative to the commutator bars. For the same reason, the voltage between adjacent commutator bars belonging to different simple windings might exceed the limit of safety. To avoid this, equipotential points on the simple windings are electrically interconnected by *second-order equalizers.*

In making equalizer connections in a duplex winding, the Kth commutator bar of one of the simplex windings should be connected to a tapping point n on the other simplex winding where the $(K - 1)$th and $(K + 1)$th commutator bars take each an equal share of the total voltage. If in a duplex-lap winding $Z_s/p = K/p$ is an odd number, the second-order equalizers with $y_{eq} = K/p$ interconnecting the two simplex windings also double as first-order equalizers. Such equalizers can be used in the winding shown in Fig. 64-10. If $y_{eq} = Z_s/p = 18/2 = 9$, every third commutator bar must be interconnected, that is, bars *1* and *10*, *4* and *13*, *7* and *16*. If K/p is an even number, a duplex-lap winding will have both first-order and second-order equalizers. The second-order equalizers pass through the armature and connect at the opposite end the Kth commutator bar of one simple winding to the overhang of the other simple winding soldered to the $(K - 1)$th and $(K + 1)$th bars.

In m-plex wave windings, first-order equalizers are nonexistent, and the second-order equalizers are made with

$y_{eq} = Z_s/m = K/m$. If p/m is an integer, the Kth commutator bar is connected to tapping point n on the commutator. If p/m is not an integer, the tapping point is located on the overhang at the opposite end of the armature. In the duplex-wave winding of Fig. 64-12, the ratio $p/m = 2/2 = 1$, so equalizers with $y_{eq} = Z_s/m = 20/2 = 10$ may be made on the commutator. This means that every second bar should be connected, that is, bars *1* and *11*, *3* and *13*, 5 and *15*, *7* and *17*, *9* and *19*.

No equalizers are required for frog-leg windings, because (see Fig. 64-13) the lap-winding coils serve as second-order equalizers for the wave winding, whereas the wave-winding coils act as first-order equalizers for the lap winding.

64-5 Armature EMF

(a) EMF in an armature turn. The active coil sides in a machine are usually embedded in slots on the cores. As has been explained in Sec. 29-3, within the slot region occupied by conductors the flux density is practically zero, but it is a maximum in the teeth. Therefore, movement of the armature in a stationary magnetic field brings about periodic variations in the flux density at any point in that field. When a given point falls within a slot region, the flux density reduces to zero; when it lines up with a tooth, it rises to a maximum. In the circumstances, the emf induced in the coil sides can no longer be found from Faraday's equation

$$e_1 = B_{s1} l u$$

because it is true only when the travel of a conductor does not affect the stationary field itself. To demonstrate, if we substitute in the above equation the flux density obtaining within the slot region occupied by a conductor,

$$B_{s1} = B_{s2} = 0$$

we shall get

$$e_1 = 0, \; e_2 = 0$$

at any value of u, which runs counter to experience.

The value of emf induced in an armature turn can be found from Maxwell's equation for electromagnetic induction:

$$e = -d\Psi/dt$$

Let us find the emf due solely to the stationary field whose flux lines cross the air gap. The distribution of the radial component of the gap flux density, B, averaged over a slot (tooth) pitch is shown in Fig. 64-14. The flux linkage of a turn, Ψ, is the same as the flux that threads it. In the initial position labelled by the numerals *1* and *2*, where the axes of the slots taken up by the turn are x_1 and x_2,

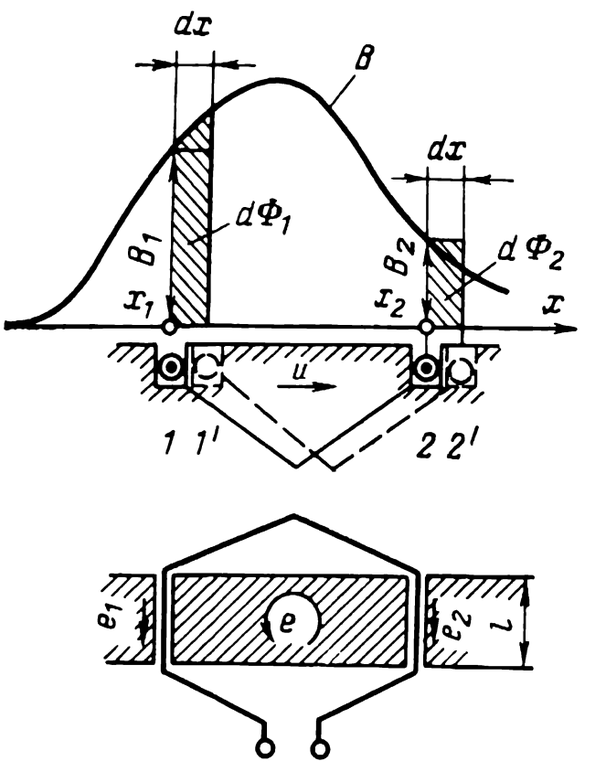

Fig. 64-14 EMF induced in an armature turn

$$\Psi = \Phi = \int_{x_1}^{x_2} Bl\,\mathrm{d}x$$

on moving through a distance $\mathrm{d}x = u\,\mathrm{d}t$ in time $\mathrm{d}t$, the turn takes up the position labelled by the numerals *1'* and *2'*, and its flux linkage is

$$\Psi' = \Psi + \mathrm{d}\Psi = \Psi + \mathrm{d}\Phi_2 - \mathrm{d}\Phi_1$$

where

$\mathrm{d}\Phi_1 = B_1 l\,\mathrm{d}x$ = change in the turn flux linkage owing to change in position of slot *1*

$\mathrm{d}\Phi_2 = B_2 l\,\mathrm{d}x$ = change in the turn flux linkage owing to change in position of slot 2

Recalling that (by Lenz's law) the current appearing under the action of an emf always opposes any change in flux linkage, the emf of a turn may be written as

$$e = -\mathrm{d}\Psi/\mathrm{d}t = \frac{(B_1 - B_2)\,lu\,\mathrm{d}t}{\mathrm{d}t} = e_1 - e_2 \qquad (64\text{-}13)$$

where

$e_1 = B_1 lu$ = emf of the left-hand turn side
$e_2 = B_2 lu$ = emf of the right-hand turn side

Thus, we have defined the emf of a turn in terms of the difference in emf between its sides. As we have seen, the

emf of a conductor in a slot can formally be described by Faraday's equation modified to include the averaged radial component of gap flux density at the axis of the slot containing the conductor.

(b) EMF of a parallel circuit of the armature winding. The instantaneous emf of a parallel circuit connected between brushes of opposite polarity is the sum of the emfs in the coils that enter the parallel circuit at a given instant or, in the final analysis, the sum of the emfs in the coil conductors, which are functions of the gap flux density B_δ at the axis of the slot containing the conductors

$$e = B_\delta l_\delta u$$

As the armature turns at a constant mechanical angular velocity, Ω, each conductor moves at a constant linear circumferential velocity

$$u = \Omega R$$

where R is the radius of the outer surface of the armature, the value of e varies with time in the same manner as the flux density around the gap periphery The time period, T, of the emf corresponds to the space period, 2τ, of flux density. The time period of the emf is the time during which the conductor moves through a distance equal to $2\tau = 2\pi R/p$, that is,

$$T = 2\tau/u = 2\pi/p\ \Omega$$

Therefore, the emf induced in the armature conductors (coils) alternates at a frequency given by

$$f = 1/T = p\Omega/2\pi = pn \qquad (64\text{-}14)$$

where

$$n = \Omega/2\pi$$

is the speed of the armature in revolutions per second.

Now we shall define the emf of a parallel circuit. As has been shown in Sec. 64-4, the conductors of the coils included in a parallel circuit at a given instant are found under several poles. In lap windings, they occur under two adjacent poles (see Figs. 64-9 and 64-10), whereas in wave windings they occur under all poles of the machine (see Figs. 64-11 and 64-12). To circumvent the difficulties involved in combining the emfs of the conductors lying under different

poles, the emf of a parallel circuit should first be expressed as the sum of the emfs due to the conductors lying under one pole (more accurately, within one pole pitch). We shall demonstrate how this is done for a parallel circuit in a simple lap winding (Fig. 64-15). With the front pitch equal to a pole pitch, the emf of the lower coil side, e_{lower}, is equal in magnitude but opposite in sign to the emf of the upper coil side, e_{upper}, i.e. $e_{\text{lower}} = -e_{\text{upper}}$. (In the figure the first and last coils of the winding are represented by heavy lines.)

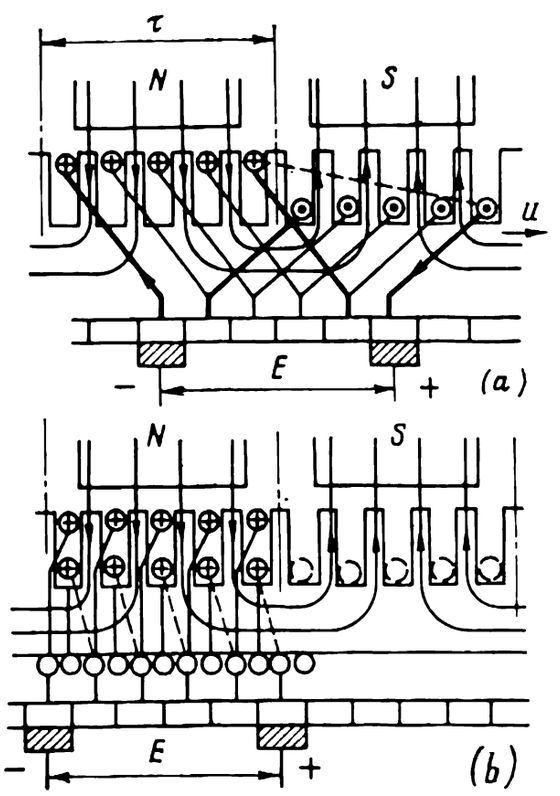

Fig. 64-15 Approximation of the emf in a parallel circuit (path) of a simple lap winding

This can readily be proved, if we recall that both at no load and on load the rotation through a pole pitch causes the field to change sign (see, for example, Fig. 64-16)

$$B_\delta (x + \tau) = -B_\delta (x)$$

Therefore, the emf of a single-turn coil, as given by Eq. (64-13), is equal to twice the emf of the upper coil side:

$$e = e_{\text{upper}} - e_{\text{lower}} = 2e_{\text{upper}}$$

Hence, the emf of a coil will remain unchanged, if the lower side conductor is replaced by an auxiliary conductor in the slot taken up by its upper side and the two conductors are combined to form a two-turn coil encircling the yoke as shown in Fig. 64-15*b*. The emf induced in such a coil will be

$$e = e_{\text{upper}} + e_{\text{upper}} = 2e_{\text{upper}}$$

Applying this procedure to all the coils in the parallel circuit, we shall obtain a group of conductors equivalent in terms of emfs, but lying only under one (in our case, a north) pole. Together with the overhangs, these conductors form a parallel circuit of what is known as the *toroidal heteropolar commutator winding* which is formed of the same

coils (or coil groups) as an a.c. toroidal winding (see Sec. 19-3). The emf appearing at the brushes that ride the commutator of a toroidal winding (Fig. 64-16) is the same

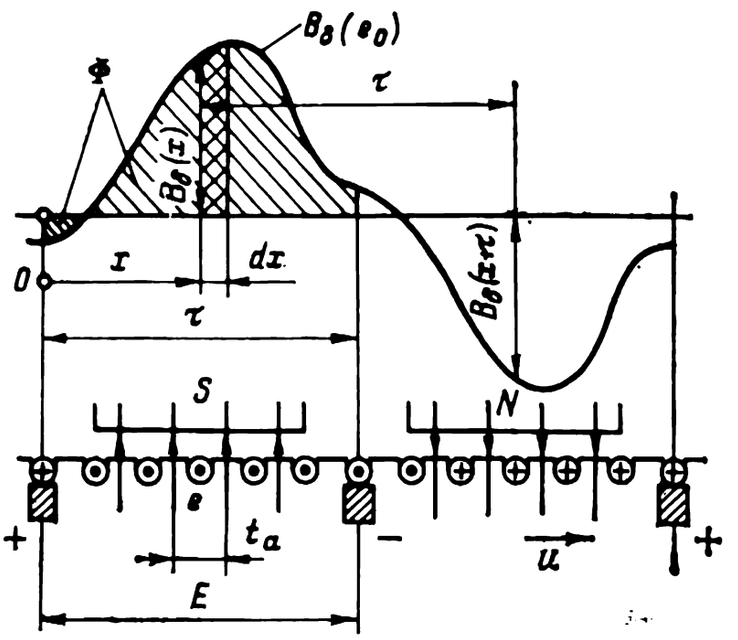

Fig. 64-16 EMF in a parallel circuit (path) of the armature winding

as that existing at the brushes of a simple lap winding (see Fig. 64-15*a*).

Similarly, it can be shown that the emf of a parallel circuit in any drum commutator winding may be derived as the sum of the emfs in the circuit conductors equidistantly distributed within a pole pitch. As is seen from Fig. 64-15, this pole pitch must be symmetrical relative to a brush of the drum winding. If the brushes are shown (for convenience) touching the conductors (as in Fig. 64-16), the conductors must be equidistantly distributed over the pole pitch bounded by two adjacent brushes.

Let us distribute the conductors of a parallel circuit equidistantly over a south pole pitch (see Fig. 64-16). If the number of active conductors in the winding is

$$N = 2Z_s u_c$$

the parallel circuit will contain

$$N_a = N/2a$$

series-connected conductors, and each conductor will occupy a fraction of a pole pitch equal to

$$t_a = \tau/N_a = 2a\tau/N$$

In Fig. 64-16, $N_a = 6$, and $t_a = \tau/6$.

Suppose that we know the distribution of the radial component of gap flux density, B_δ, within the axial gap length l_δ. Then the emf in the conductor x distant from the edge of the pole pitch will be

$$e = B_\delta l_\delta u$$

and the emf per unit length of the circumference in the conductor region will be

$$e_0 = e/t_a = p\Omega N l_\delta B_\delta / 2\pi a$$

because $\tau = \pi R/p$ and $u = \Omega R$* .

The total emf of a parallel circuit can then be found as the integral of the emfs per unit length

$$E = \int_0^\tau e_0 \, dx = \frac{p\Omega N}{2\pi a} \int_0^\tau B_\delta l_\delta \, dx$$

or

$$E = p\Omega N\Phi/2\pi a = 4fw\Phi = c_w \Omega \Phi \qquad (64\text{-}15)$$

where

$\Phi = \int_0^\tau B_\delta l_\delta \, dx$ = flux per pole, proportional to the shaded area in Fig. 64-16

$w = N/4a$ = number of turns per parallel circuit

f = frequency of the armature emf, Eq. (64-14)

$c_w = pN/2\pi a$

To sum up, the emf of a parallel circuit is proportional to the product of the mechanical angular velocity of the armature by the flux threading the pole pitch bounded by the conductors connected to the brushes.

Example 64-1. Find the emf of the simple wave winding used in a 14-kW, 220-V, 1500-rpm d.c. motor for which $Z_s = 93$, $u_c = 2$, $2p = 4$, $2a = 2$, and $\Phi = 0.01099$ Wb.

Solution. On finding

$$N = 2Z_s u_c = 2 \times 93 \times 2 = 372$$

* In deriving the above equations we neglected the fact that the coils shorted by the brushes are actually removed from the parallel circuit.

and

$$\Omega = 2\pi n = 2\pi \times 1500/60 = 157 \text{ rad s}^{-1}$$

use Eq. (64-15) to obtain

$$E = \frac{2 \times 157 \times 372 \times 0.01099}{2\pi \times 1} = 204.4 \text{ V}$$

(c) The effect of chording (short-pitching) and the number of coils per parallel circuit on the parallel-circuit emf. In deriving Eq. (64-15), we assumed the coil pitch to be equal

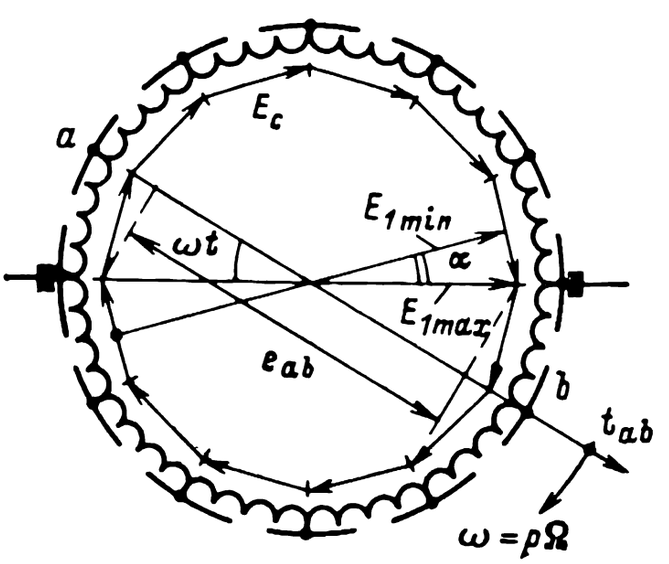

Fig. 64-17 Diagram of coil emfs

to a pole pitch and the number of conductors per parallel circuit to be infinitely large. To evaluate the effect of short-pitching (chording) and the finite number of conductors on the parallel-circuit emf, we expand the gap flux density into a Fourier series and retain the fundamental term with a peak value B_{1m} for which the corresponding flux is given by

$$\Phi_1 = (2/\pi)\, B_{1m}\, l_\delta \tau$$

The emfs in the various coils of the armature winding may be represented by phasors as for the coils or coil groups of the armature winding in a synchronous machine. Figure 64-17 illustrates how the phasors of coil emfs are combined within the closed loop formed by the winding ($2p = 2$, $Z_s = 12$, and $K = 12$). The phasors form a regular dodecagon, and the corresponding emfs add up to zero.

The peak value of a coil emf is found from Eq. (27-5).

Using the notation of the present chapter, it is

$$E_c = 2\pi f w_c k_p \Phi_{1m} \tag{64-16}$$

where

$$k_p = \sin(y_f \pi / 2\tau)$$

is the pitch factor.

The maximum emf across the brushes is equal to the vectorial sum of the emfs in a parallel circuit, and proportional to the diameter of the polygon formed by the coil emfs

$$E_{1,max} = (Z_s/2a)\, k_d E_c \tag{64-17}$$

where $Z_s/2a$ is the number of coils in a parallel circuit, and k_d is the distribution factor which, for a parallel circuit spanning a belt of π radians, is found as the ratio of the vectorial sum of the coil emfs to their arithmetic sum or (if the number of coils is sufficiently large and the polygon approximates a circle very closely) as the ratio of the diameter to half the circumference of the emf circle

$$k_d = 2R_E/\pi R_E = 2/\pi$$

Substituting in Eq. (64-17), we obtain an equation for the emf of a parallel circuit with allowance for chording

$$E_{1,max} = 4 f w k_p \Phi_{1m} \tag{64-18}$$

It differs from Eq. (64-15) in that it contains the pitch factor. However in d.c. machines k_p is unity very closely:

y_f/τ	0.9	0.95
k_p	0.988	0.996

Therefore, Eq. (64-15) yields a sufficiently accurate result.

Using the polygon of emfs (Fig. 64-17), we can approximately evaluate the likely variations in the emf of a parallel circuit as its coils move in the magnetic field. With an even number of coils or commutator bars per pole pair, the minimum value of the parallel-circuit emf is numerically equal to the distance between the opposite sides of the polygon. Its ratio to the maximum emf is

$$E_{1,min}/E_{1,max} = \cos\alpha$$

where $\alpha = \pi p/K$ is the angle shown in Fig. 64-17.

The percent deviation of the parallel-circuit voltage from its mean value is given by

$$\Delta E\% = (\Delta E/E_1) \times 100 = \frac{0.5\,(E_{1.\max} - E_{1.\min})}{0.5\,(E_{1.\max} + E_{1.\min})} \times 100$$
$$= 100 \tan^2 (\pi p/2K) \qquad (64\text{-}19)$$

This deviation rapidly decreases with increasing number of commutator segments:

K/p	4	8	10	20	40
ΔE, %	17.2	4	2.5	0.62	0.16

64-6 Electromagnetic Torque

The external torque, T_{ext}, applied to the shaft of a d.c. machine is balanced in a steady state by the electromagnetic

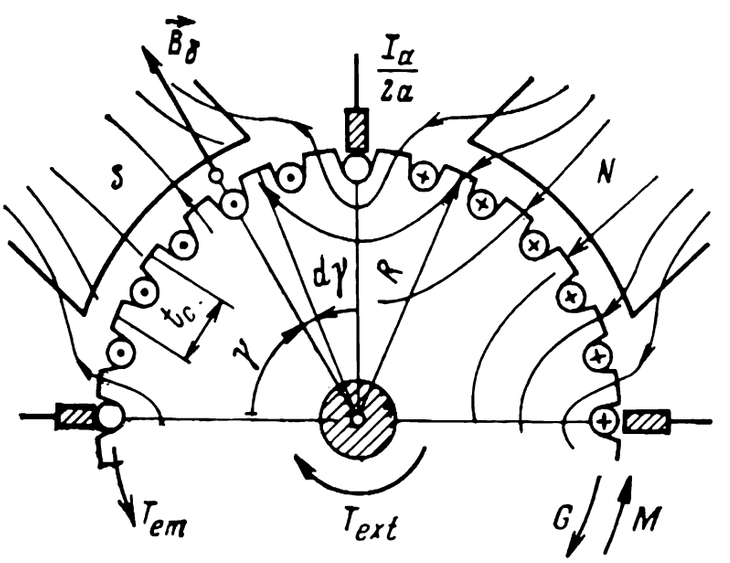

Fig. 64-18 To determining electromagnetic torque

torque, T_{em}, produced by the interaction of the armature currents with the magnetic field.

Applying the right-hand rule to find the emf and the left-hand rule to find electromagnetic forces, we can see that in the generator mode of operation, when $V < E$ and the armature currents are in the same direction as the induced emf, the electromagnetic torque is acting against the direction of rotation (as indicated by the arrow G in Fig. 64-18). In the motor mode of operation, when the currents are against the emf, the electromagnetic torque is acting in the direction of rotation (as indicated by the arrow M in the same figure).

As has been shown in Sec. 29-3, the tangential electromagnetic force produced by the interaction of the current

in a slot with the external magnetic field is proportional to the current and the mean gap flux density, and this force is applied to the core teeth. The armature conductors carry a current $I_a/2a$. A conductor displaced through an angle γ from the start of the south pole pitch (see Fig. 64-18) is associated with a tangential force

$$S_\gamma = B_\delta l_\delta I_a/2a$$

In the conductor region, the force per unit length of the circumference is

$$S_{0\gamma} = S_\gamma/t_c = NI_a B_\delta l_\delta/4\pi aR$$

where $t_c = 2\pi R/N$ is the fraction of the armature circumference per conductor. Then the electromagnetic torque acting on a circumference element of length $R\,d\gamma$ is

$$T_{em} = (S_{0\gamma} R\,d\gamma)\,R$$

The torque per pole pitch is

$$T'_{em} = \int_0^{\pi/p} S_{0\gamma} R^2\,d\gamma$$

and the torque acting on the whole armature is

$$T_{em} = 2p \int_0^{\pi/p} S_{0\gamma} R^2\,d\gamma = c_w I_a \Phi \qquad (64\text{-}20)$$

where

$$\Phi = \int_0^{\pi/p} B_\delta l_\delta R\,d\gamma$$

is the magnetic flux threading the pole pitch bounded by the brushes, and $c_w = pN/2\pi a$.

To sum up, the electromagnetic torque acting on the armature of a d.c. machine is proportional to the product of the armature current by the magnetic flux threading the pole pitch bounded by the conductors touching the brushes.

Example 64-2. Find the electromagnetic torque for the machine of Example 64-1, assuming $I_a = 72$ A.

Solution.

$$c_w = pN/2\pi a = 2 \times 372/(2\pi \times 1) = 118.4$$

Using Eq. (64-20),

$$T_{em} = 118.4 \times 72 \times 0.01099 = 93.7 \text{ Nm}$$

64-7 MMFs and Resistances of the Windings of a D.C. Machine

As with a synchronous machine, the magnetic field of a d.c. machine may be resolved into a d-axis and a q-axis component, as shown in Fig. 64-19.

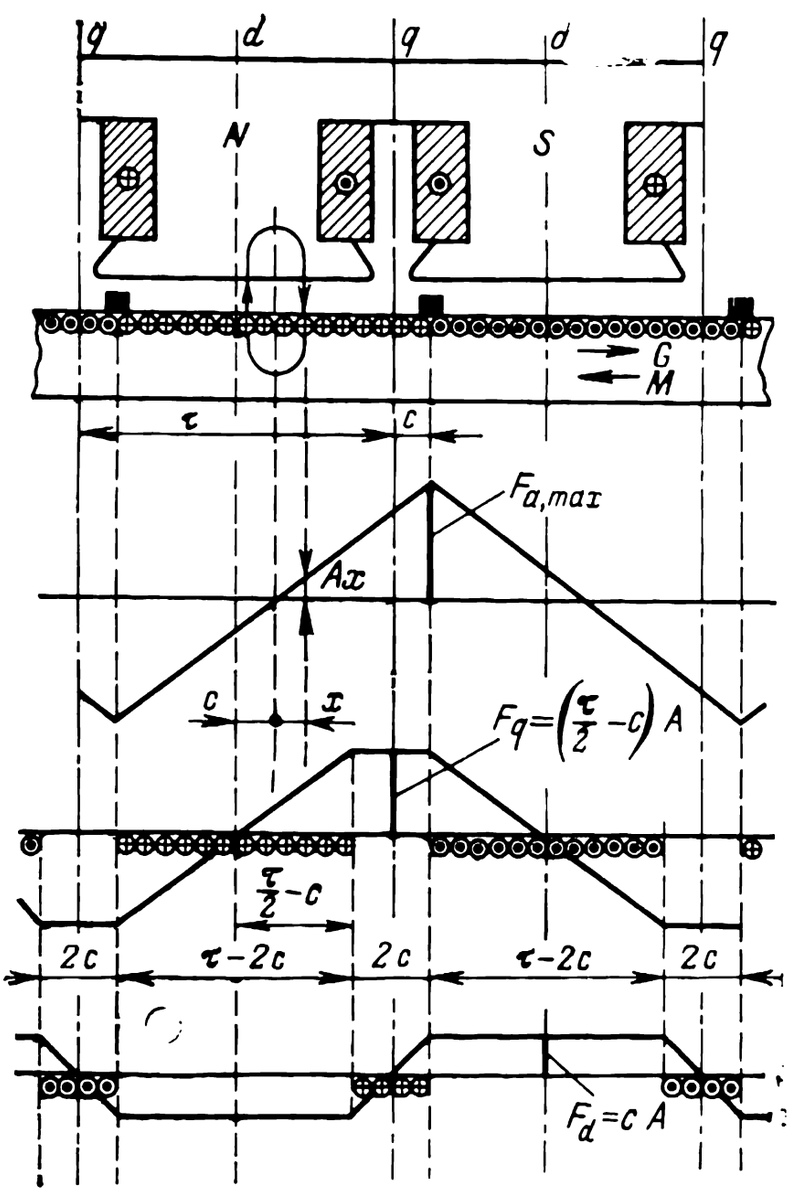

Fig. 64-19 Armature mmf and its d- and q-axis components

The magnetic field of a d.c. machine is set up by the current and mmf in the field winding, the mmf of the armature winding, and the mmfs of the compole and compensating windings (the part played by the latter two windings will be explained in Sec. 64-11).

The mmf produced by a shunt-wound (or separately excited) field winding is given by

$$F_f = w_f I_f \tag{64-21}$$

where w_f is the number of turns per pole and I_f is the field current. The mmf of a series-wound field winding is given by

$$F_s = w_s I_a \tag{64-22}$$

where w_s is the number of turns per pole in the series-wound field winding. The mmfs given by Eqs. (64-21) and (64-22) set up only the *d*-axis field (their coils encircle the main poles).

The mmf of a field winding remains unchanged over pole pitch of a given polarity and changes sign in moving to the next adjacent pole pitch. Therefore, over a pole pitch it has a rectangular waveform.

The mmf of a distributed armature winding (with a sufficiently large number of conductors per pole pitch) has a triangular waveform (see Fig. 64-19). The armature mmf is a maximum, $F_{a,max}$, in the brush region and passes through zero mid-way between the brushes. Let the armature conductors be encircled by a loop of width $2x$, symmetrically disposed about the point where the armature mmf is zero. Then the mmf x distant from that point will be equal to half the current encircled by the loop, and at $0 < x < \tau$ it will be

$$F_a = 2Ax/2 = Ax \tag{64-23}$$

where

$$A = NI_a/4a\pi R$$

is the current per unit length of the armature circumference, usually called the *electric loading* (or linear current density) of the armature, and expressed in A m^{-1}.

The armature mmf is a maximum at $x = \tau/2$

$$F_{a,max} = A\tau/2 \tag{64-24}$$

In the general case, when the brushes are c distant from the geometrical neutral axis (Fig. 64-19), the armature mmf can be resolved into a *d*-axis and a *q*-axis component. The maximum value of the *q*-axis component is

$$F_q = (\tau/2 - c)\, A \tag{64-25}$$

The maximum value of the d-axis component is

$$F_d = cA$$

When the brushes are set on the geometrical neutral axis, that is, when $c = 0$, only the q-axis mmf exists, that is,

$$F_q = F_{a,max} = A\tau/2$$

and

$$F_d = 0$$

At a temperature t, the resistance of the armature winding is given by

$$R_{a,0} = \rho_t N l_{mean}/S\,(2a)^2 \qquad (64\text{-}27)$$

where

l_{mean} = mean length of a coil half-turn
S = cross-sectional area of an effective armature conductor
ρ_t = resistivity of copper at t degrees C

The resistance of a separately excited (or shunt-wound) field winding at t degrees C is

$$R_f = \rho_t 4pw_f l_f/S_f \qquad (64\text{-}28)$$

where l_f is the length of a half-turn from Fig. 64-1, and S_f is the cross-sectional area of conductors in the field winding.

The resistances of the other pole windings are found in a similar manner.

The armature circuit resistance, including the resistance of the series-connected windings and the brush contact resistance, is given by

$$R_{ac} = R_a + R_s + R_{cpw} + R_{cw} + \Delta V_b/I_{a,R} \qquad (64\text{-}29)$$

where

ΔV_b = brush voltage drop (for conventional graphitized brushes, ΔV is about 2 V)
R_s = resistance of the series field winding
R_{cpw} = resistance of the compole windings
R_{cw} = resistance of the compensating winding

Example 64-3. Find the electric loading, the maximum mmf (with the brushes set on the neutral axis), and the resistance of the armature winding at 75°C for the machine

in Examples 64-1 and 64-2 in which $D_a = 2r = 0.195$ m, $l_\delta \approx l = 0.14$ m, $l_{mean} = 0.325$ m, and $S = 5.73$ mm^2.

Solution. Using Eq. (64-23), the electric loading and mmf of the armature are found to be

$$A = 372 \times 72/(2\pi \times 0.195) = 21\,860 \text{ A m}^{-1}$$

$$F_{a,max} = F_q = 21\,860 \times 0.153/2 = 1672 \text{ A}$$

where

$$\tau = \pi D_a/2p = \pi \times 0.195/4 = 0.153 \text{ m}$$

The resistance of the armature winding is

$$R_{ac} = 0.0214 \times 10^{-6} \times 372 \times 0.325/(5.73 \times 10^{-6} \times 2^2) = 0.113\ \Omega$$

where

$$\rho_{75} = 0.0175 \times 10^{-6}\,[1 + (75 - 20) \times 0.004] = 0.0214 \times 10^{-6} \Omega\text{m}$$

64-8 Calculation of the Magnetic Circuit at No Load

At no load (on an open circuit), when there is no current flowing in the armature winding, the magnetic field is solely set up by the mmf of the separately excited (or shunt-wound) field winding, F_f. The distribution of the gap flux density, B, obtained by calculation is shown in Fig. 64-20. The magnetic flux at no load is proportional to the shaded area

$$\Phi_f = \int_{-0.5\tau}^{+0.5\tau} B l_\delta \, dx \quad .$$

To simplify calculation of Φ_f, the actual distribution of flux density over a pole pitch is replaced with that shown by the dashed rectangle in Fig. 64-20. Its height is the same as B_δ, and its width b_δ, called the *pole arc* (the design width of the pole shoe), is chosen so as to maintain the flux unchanged (that is, so as to make the shaded area equal to the area of the rectangle)

$$\Phi_f = b_\delta l_\delta B_\delta = \alpha_\delta \tau l_\delta B_\delta \qquad (64\text{-}30)$$

where $\alpha_\delta = b_\delta/\tau$ is the *enclosure of the pole.*

From an analytical expression for the gap field, b_δ may be expressed in terms of the core dimensions (given in Fig. 64-1) as

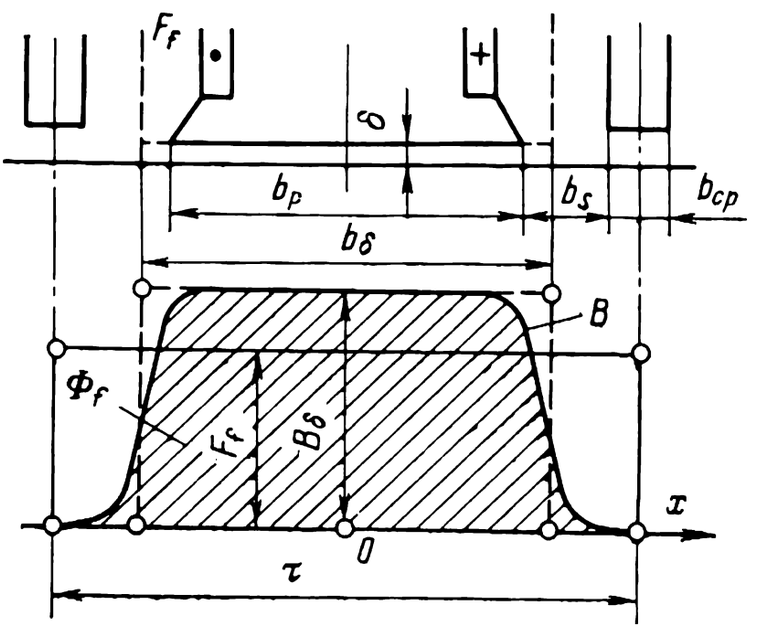

Fig. 64-20 Air-gap field at no load

$$b_\delta = \frac{1}{B_\delta} \int_{-0.5\tau}^{+0.5\tau} B \, dx = b_p + (b_0 - \gamma\delta)$$

where

$$b_0 = (\tau - b_p - b_{cp})/2;$$

$$\gamma = \frac{(b_0/\delta)^2}{5 + b_0/\delta}$$

b_p = width of the main-pole shoe
b_{cp} = width of the compole shoe
b_0 = opening between the main-pole and compole shoes

The magnetization curve at no load, $\Phi = f(F_a)$, is calculated in about the same manner as for a salient-pole synchronous machine (see Sec. 53-2), with a few exceptions. The magnetic circuit for which the characteristic dimensions are given in Fig. 64-1 is calculated for several values of the excitation flux, namely $\Phi_f = 0.5\Phi_{f,R}$, $0.8\Phi_{f,R}$, $1.1\Phi_{f,R}$, and $1.25\Phi_{f,R}$, where

$$\Phi_{f,R} = 2\pi a V_R / p\Omega N$$

is the magnetic flux at no load and rated voltage, as found from Eq. (64-15). For each value of Φ_f, one finds the flux

density in the various parts of the magnetic circuit and the corresponding mmfs.

The gap mmf, F_δ, is found as explained in Sec. 53-2. The tooth mmf, F_Z, and the armature yoke mmf, F_a, as explained in Sec. 40-2 (with the subscripts *z1* and *a1* replaced, respectively by *z* and *a*). The pole leakage flux

$$\Phi_{f\sigma} = \sigma_m \Phi_f$$

is found with σ_m approximately equal to 1.2 (here, σ_m is the pole leakage factor). The pole-core flux density, B_m, and the pole-core mmf, F_m, are found as explained in Sec. 53-2 for

$$\Phi_m = \Phi_2 = \Phi_f + \Phi_{f\sigma}$$

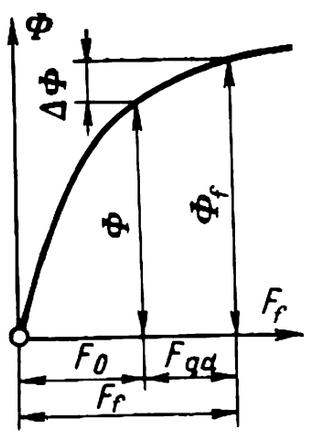

Fig. 64-21 Magnetization curve of a d.c. machine

The yoke mmf is given by

$$F_y = L_y H_y$$

where H_y is the magnetic field intensity in the yoke corresponding [13] to

$$B_y = \Phi_m / 2 l_y h_y$$

The resultant mmf at no load (per pole) is given by

$$F_f = F_\delta + F_Z + F_a + F_m + F_y \qquad (64\text{-}31)$$

The results are presented as the magnetization curve, $\Phi_f = \Phi = f(F_f)$, of the machine, the magnetization curve, $B_\delta = f(F_{\delta Z})$, of the active layer, where $F_{\delta Z} = F_\delta + F_Z + F_a$, and the no-load (or open-circuit) characteristic, $E_f = E = f(F_f)$. The above curves are plotted in Figs. 64-21 through 64-23, respectively. Because emf is proportional to flux,

$$E = c_w \Omega \Phi$$

the magnetization curves and the open-circuit characteristic are similar.

The magnetization curves and the open-circuit characteristic of a d.c. machine can readily be formalized and calculated on a computer. To facilitate the use of steady-state and transient responses in analytical calculations, the magnetization curves and open-circuit characteristic are

replaced by their approximations. One form of approximation is a parabola with a vertical axis (parallel to the axis of ordinates):

$$\begin{aligned} E &= a_E F_f^2 + b_E F_f + c_E \\ \Phi &= a_\Phi F_f^2 + b_\Phi F_f + c_\Phi \\ B_\delta &= a_B F_{\delta Z}^2 + b_B F_{\delta Z} + c_B \end{aligned} \qquad (64\text{-}32)$$

To keep the likely error to an acceptable minimum (0.5% on the axis of ordinates), the part of the magnetization curve to be approximated ought not to exceed the mmf corresponding to the middle "leg" of the curve (in Fig. 64-22,

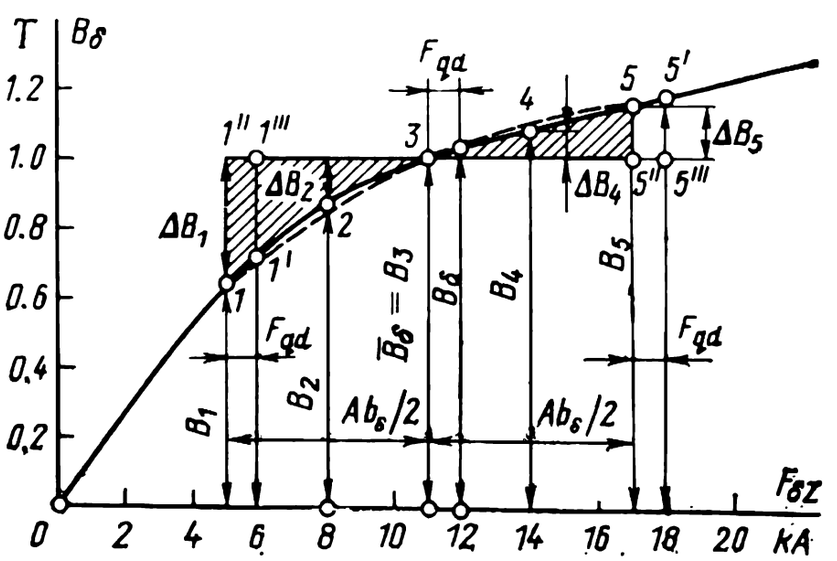

Fig. 64-22 Magnetization curve of the active layer of a d.c. machine

this mmf is about 7 kA).

In the equation

$$y = ax^2 + bx + c$$

of the parabola drawn through the known points (x_1, y_1) and (x_3, y_3) at the ends of the part being approximated, and a third point, (x_2, y_2), in the middle of that part the coefficients are given by

$$a = D_a/D, \quad b = D_b/D, \quad c = D_c/D \qquad (64\text{-}33)$$

where

$$\begin{aligned} D &= x_1^2 (x_2 - x_3) + x_2^2 (x_3 - x_1) + x_3^2 (x_1 - x_2) \\ D_a &= y_1 (x_2 - x_3) + y_2 (x_3 - x_1) + y_3 (x_1 - x_2) \\ D_b &= x_1^2 (y_2 - y_3) + x_2^2 (y_3 - y_1) + x_3^2 (y_1 - y_2) \\ D_c &= x_1^2 (x_2 y_3 - x_3 y_2) + x_2^2 (x_3 y_1 - x_1 y_3) + \\ &\quad + x_3^2 (x_1 y_2 - x_2 y_1) \end{aligned}$$

Example 64-4. Using a parabola, approximate the part of the magnetization curve in Fig. 64-22, containing points *1*, *3* and *5* whose coordinates are $x_1 = F_1 = 5$ kA, $x_2 = F_3 = 11$ kA, $x_3 = F_5 = 17$ kA, $y_1 = B_1 = 0.625$ T, $y_2 = B_3 = 1.0$ T, and $y_3 = B_5 = 1.154$ T.

Solution. Using Eq. (64-33), we find

$$D = -432$$
$$D_a = 1.326 \qquad a = -0.0030694$$
$$D_b = -48.216 \qquad b = 0.11161$$
$$D_c = -62.075 \qquad c = 0.14369$$

The parabolic approximation of the curve described by the equation

$$B = aF^2 + bF + c$$

is shown in Fig. 64-22 by a dashed line. Failure to choose the length of the part to be approximated as recommended leads to a deviation of 4% of the parabola from the given curve.

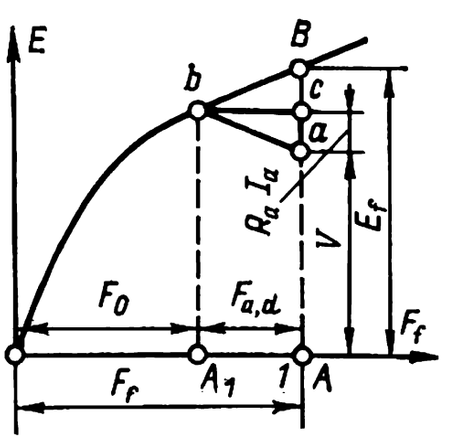

Fig. 64-23 No-load (open-circuit) characteristic

Example 64.5. Divide the part of the curve in Example 64-4 into two intervals and approximate each by a parabola of its own. The parabolas must pass through point *2* in the middle of interval *1-3* and point *4* in the middle of interval *3-5*. Their coordinate s are $F_2 = 8$ kA, $F_4 = 14$ kA, $B_2 = 0.872$ T, and $B_4 = 1.082$ T.

Solution. Using Eq. (64-33) and setting $x_1 = F_1$, $x_2 = F_2$, $x_3 = F_3$, $y_1 = B_1$, $y_2 = B_2$, and $y_3 = B_3$, write the equation of the parabola passing through points *1*, *2* and *3* in Fig. 64-22:

$$B = -0.0066111\,F^2 + 0.16827\,F - 0.051111$$

where $F_1 < F < F_3$.

On setting $x_1 = F_3$, $x_2 = F_4$, $x_3 = F_5$, $y_1 = B_3$, $y_2 = B_4$, and $y_3 = B_5$, write the equation of the parabola passing through points *3*, *4* and *5* in Fig. 64-22:

$$B = -0.0005555\,F^2 + 0.041222\,F + 0.61378$$

where $F_3 < F < F_5$. With this approximation the deviation

of the parabolas from the given curve does not exceed 0.5% (in Fig. 64-22, the parabolas merge with the curve).

64-9 Calculation of the Magnetic Circuit and Voltage on Load

On load, the magnetic field is set up by the joint action of the mmf due to the separately excited (or shunt-wound) field winding and also the mmfs of the windings carrying the armature current, the *d*-axis and *q*-axis armature mmfs F_d and F_q, and the mmf of the series field winding, F_s^*.

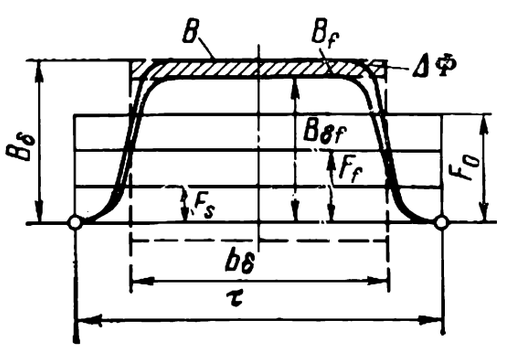

Fig. 64-24 The effect of the series-winding mmf on the gap field

(a) The effect of the series winding. The mmf produced by the series field winding has the same waveshape as the mmf produced by the separately excited (or shunt-wound) field winding. In Fig. 64-24, the mmf of the series field winding,

$$F_s = w_s I_a$$

is represented by a rectangle. The same figure also shows the mmf of the main field winding,

$$F_f = w_f I_f$$

The resultant mmf is

$$F_0 = F_f \pm F_s \qquad (64\text{-}34)$$

where the "+" sign applies when the windings are connected aiding, and the "—" sign, when they are connected in opposition.

The resultant flux density (B) curve has the same shape as the no-load flux density (B_f) curve. As at no load, the actual flux density distribution can be replaced with a constant flux density within the pole arc, b_δ (represented by the dashed rectangle in Fig. 64-24). The resultant magnetic flux Φ or the maximum gap flux density

$$B_\delta = \Phi/\alpha_\delta \tau l_\delta$$

---

* The effect of the compensating winding, the compole windings and the coils being commutated is examined in Sec. 64-11.

correspond to F_0 from the magnetization curve in Fig. 64-21. In passing from no load to on load, the flux changes by an amount represented by the shaded area in Fig. 64-24, $\Delta\Phi = \Phi - \Phi_f$.

(b) Armature reaction—the effect of the d-axis armature mmf. The d-axis armature mmf, $F_d = cA$, has a trapezoidal distribution (see Fig. 64-19). When the brushes are moved a short distance away from the geometric neutral axis, F_d affects the field in the same manner as the rectangular d-axis mmf [see (a) above]. Including the effect of the d-axis armature mmf, the resultant mmf may be written as

$$F_0 = F_f \pm F_d \qquad (64\text{-}35)$$

where the "+" sign applies when F_d has a magnetizing effect, and the "—" sign, when it has a demagnetizing effect.

As is seen from Fig. 64-19, the demagnetizing effect takes place when the brushes are shifted away from the neutral axis in the direction of rotation in the generator mode of operation and against the rotation in the motor mode of operations. The magnetizing effect occurs when the brushes are shifted in the respectively opposite directions. The resultant mmf, F_0, corresponds to the resultant flux, Φ, on the magnetization curve.

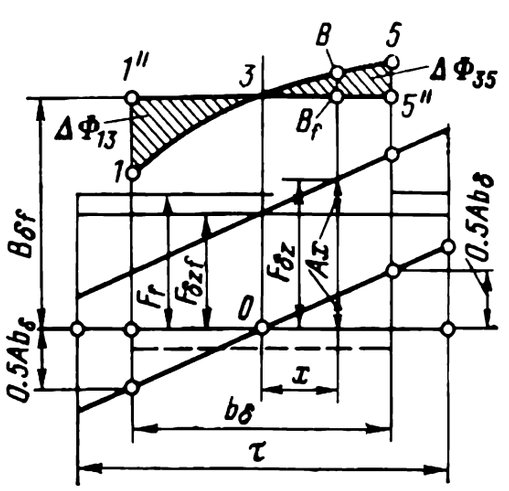

Fig. 64-25 The effect of the q-axis armature mmf on the gap field

(c) Armature reaction—the effect of the q-axis armature mmf. When the brushes are set on (or shifted a short distance c from) the neutral axis, the q-axis mmf is zero at the pole axis. Within a distance x of the pole axis, it is Ax; within a distance $b_\delta/2$, that is, half the pole arc, it is $\pm Ab_\delta/2$. The distribution of the q-axis mmf is shown in Fig. 64-25 which also shows the distribution of F_f, the excitation mmf. For simplicity, the actual pole-shoe is replaced by a pole shoe b_δ wide, within which the flux density is deemed constant. As has been explained in Sec. 64-7, if we take the gap flux density outside the pole arc equal to zero, the replacement of the

actual pole-shoe will leave the gap flux density unaffected both at no load and on load.

To begin with, let us find the design flux density distribution at no load

$$B_f = B_{\delta f} = \Phi_f / b_\delta l_\delta$$

where Φ_f corresponds to F_f on the magnetization curve of Fig. 64-21. Then the area of the rectangle bounded by the B_f curve will be proportional to $\Phi_f = B_{\delta f} b_\delta l_\delta$. Now let us turn to the field set up by the q-axis mmf at $F_f = 0$. The lines of the q-axis mmf have their paths closed within the active layer along the loops encircling the armature currents. One of these loops $2x$ wide and encircling the current $2Ax$ is shown in Fig. 64-19. As is seen, the loop includes the pole-shoe, the air gap, the teeth, and the armature yoke. Neglecting the mmf in the pole-shoe and applying Ampere's circuital law to the loop, we find the mmf in a half-loop

$$F_{\delta z} = F_\delta + F_z + F_d = Ax$$

and, from the magnetization curve for the active layer (see Fig. 64-22) the flux density $B_{\delta x}$ due to the q-axis mmf, Ax, within a distance x of the pole axis. The resultant field is along the q-axis and, because

$$B_{\delta x}(x) = -B_{\delta x}(-x)$$

the d-axis flux is zero.

To determine the resultant gap field set up by F_f and Ax, we isolate from F_f the component $F_{\delta zf}$ associated with the active layer (see Fig. 64-25) and corresponding to $B_\delta = \Phi_f / b_\delta l_\delta$ on the magnetization curve for the active layer (see Fig. 64-22). Next, we find the resultant mmf in the active layer

$$F_{\delta z} = F_{\delta zf} + Ax$$

and, referring to the curve in Fig. 64-22, the flux density B at point x in the gap. The flux density, B, at the pole axis (point *3*) thus obtained is the same as $B_{\delta f}$ at no load. In the portion *3-5* where Ax is added to $F_{\delta zf}$, it runs higher than $B_f = B_{\delta f}$. In the portion *1-3* where Ax is subtracted from $F_{\delta zf}$, it runs below $B_f = B_{\delta f}$. Because the active layer has a nonlinear magnetization curve, the decrease in the flux density within portion *1-3* (as compared with the

no-load condition) is greater than its increase within portion *1-5*. Accordingly, the decrease in the *d*-axis flux, $\Delta\Phi_{13}$, proportional to the area of the figure *1-3-1″* is greater than its increase, $\Delta\Phi_{35}$, proportional to the area of the figure *3-5-5″*. In the final analysis, the armature *q*-axis flux reduces the *d*-axis flux by

$$\Delta\Phi = \Delta\Phi_{13} - \Delta\Phi_{35} = \Phi_f - \Phi$$

Quantitatively, this reduction in flux can be obtained directly from the magnetization curve of the active layer (see Fig. 64-22). The procedure is as follows. On the magnetization curve, locate point *3* corresponding to the given flux density at no load,

$$B_3 = B_{\delta f}$$

and determine $F_{\delta Z}$ for that point. Next, locate point *1* corresponding to $F_{\delta Z} - 0.5Ab_\delta$, and point *5* corresponding to $F_{\delta Z} + 0.5Ab_\delta$. Because Ax is proportional to the distance x from the pole axis (see Fig. 64-25), the shapes bounded by the identical portions of the flux density curves and the axis of abscissae in Figs. 64-22 and 64-24 are similar, and the change in flux can be found from the shaded areas *1-3-1′* and *3-5-5′* in Fig. 64-22.

Assuming that portions *1-3* and *3-5* are approximated by appropriate parabolas, let us express the decrease in flux as

$$\Delta\Phi = \Delta\Phi_{13} - \Delta\Phi_{35} = \Delta B l_\delta b_\delta \qquad (64\text{-}36)$$

where

$$\Delta B = (\Delta B_1 + 4\Delta B_2 - 4\Delta B_4 - \Delta B_5)/12$$

is the average change in flux density caused by the *q*-axis mmf of the armature, $\Delta B_1 = B_3 - B_1$, $\Delta B_2 = B_3 - B_2$, $\Delta B_3 = 0$, $\Delta B_4 = B_4 - B_3$, $\Delta B_5 = B_5 - B_3$. Points *2* and *4* lie in the middle of portions *1-3* and *3-5*, respectively.

In order to make up for the reduction in flux, the excitation mmf on load has to be somewhat increased. Suppose that the flux on load must be equal to Φ with a flux density

$$B_{\delta,\text{mean}} = B_3 = \Phi/b_\delta l_\delta$$

If we choose F_f or $F_{\delta\, Zf}$ for this flux density from the curves in Fig. 64-21 and 64-22, the specified flux will be obtained at no load (it will be represented by the rectangle *1″-5″*

having height $B_{\delta,\,mean}$ and width $l_\delta b_\delta$ or, if drawn to the scale of Fig. 64-22, width Ab_δ. If this excitation is retained on load, the flux will be reduced by $\Delta\Phi$ owing to the difference in area between shapes *1-3-1″* and *3-5-5″*.

To make up for the reduction in flux owing to the demagnetizing effect of the q-axis mmf, the excitation mmf must be increased by F_{qd}. This increase causes points *1* and *5* to move to positions *1′* and *5′*. The value of F_{qd} must be such that the area bounded by curve *1′-5′* is equal to the area of the rectangle between curve *1″-5″* and the axis of abscissae, representing the specified flux Φ. In other words, it is required that the sum of the areas *1′-3-1‴* and *3-5′-5‴* be equal to $\Delta\Phi$, that is

$$S\,(1\text{-}1''\text{-}1'''\text{-}1') + S\,(5'' - 5 - 5' - 5''') = \Delta\Phi\,(A/l_\delta) \quad (64\text{-}37)$$

where S is the area of the shapes drawn to the scale of Fig. 64-22.

To a first approximation, if we assume the flux density biased by F_{qd} to be constant and recall Eq. (64-36), we may write

$$\Delta B_1 F_{qd} + \Delta B_5 F_{qd} = \Delta B A b_\delta$$

Hence,

$$F_{qd} = F_{d0} = \Delta B A b_\delta/(\Delta B_1 + \Delta B_5)$$

or, in per unit, with the mmf under the pole-shoe tip taken as the base quantity,

$$F_{*qd0} = F_{qd0}/0.5Ab_\delta = 2\Delta B/(\Delta B_1 + \Delta B_5) \quad (64\text{-}38)$$

If we allow for the change in flux density due to bias by F_{qd}, Eq. (64-37) takes the form

$$\Delta B_{1,\text{mean}} F_{qd} + \Delta B_{5,\text{mean}} F_{qd} = \Delta\Phi\,(A/l_\delta) = \Delta B A b_\delta \quad (64\text{-}39)$$

where

$$\begin{aligned} \Delta B_{1,\text{mean}} &= \Delta B_1 - (\mathrm{d}B/\mathrm{d}F)_1\, F_{qd}/2 \\ \Delta B_{5,\text{mean}} &= \Delta B_5 + (\mathrm{d}B/\mathrm{d}F)_5\, F_{qd}\,2 \end{aligned} \quad (64\text{-}40)$$

are the mean heights of trapezoids *1-1″-1‴-1′* and *5″-5-5′-5‴* expressed in terms of $(\mathrm{d}B/\mathrm{d}F)_1$ and $(\mathrm{d}B/\mathrm{d}F)_5$ at points *1* and *5*, respectively.

The derivatives can be expressed in terms of change in flux, if, prior to that, we approximate the flux in por-

tions *1-3* and *3-5* by parabolas, Eqs. (64-32),

$$B = a_{13}F^2 + b_{13}F + c_{13}$$

and

$$B = a_{35}F^2 + b_{35}F + c_{35}$$

Then,

$$\begin{aligned}(\mathrm{d}B/\mathrm{d}F)_1 &= 2a_{13}F_1 + b_{13} = \frac{(6\Delta B_1 - 8\Delta B_2)}{AB_\delta} \\ (\mathrm{d}B/\mathrm{d}F)_5 &= 2a_{35}F_5 + b_{35} = \frac{(6\Delta B_5 - 8\Delta B_4)}{Ab_\delta}\end{aligned} \tag{64-41}$$

Re-writing Eq. (64-39) subject to Eqs. (64-40) and (64-41), we get

$$QF_{*qd}^2 - F_{*qd} + F_{*qd0} = 0 \tag{64-42}$$

where F_{*qd0} is the per-unit d-axis mmf required to make up for the demagnetizing effect of the q-axis mmf (a first approximation based on Eq. (64-38)), and

$$Q = \frac{6\Delta B_1 - 8\Delta B_2 + 8\Delta B_4 - 6\Delta B_5}{4(\Delta B_1 + \Delta B_5)}$$

is a coefficient.

Solving Eq. (64-42) yields a second approximation for the d-axis mmf required to make up for the demagnetization effect of the q-axis mmf of the armature in per-unit

$$F_{*qd} = F_{qd}/0.5Ab_\delta = 1/2Q - \sqrt{(1/2Q)^2 - F_{qd0}/Q}$$

and in absolute terms

$$F_{qd} = 0.5F_{*qd}Ab_\delta \tag{64-43}$$

The excitation mmf required to give the desired on-load flux Φ is found from the magnetization curve as illustrated in Fig. 64-21:

$$F_f = F_0 + F_{qd} \tag{64-44}$$

where F_0 is the resultant mmf (with allowance for the effect of the q-axis mmf) corresponding to the desired flux Φ.

The magnetic flux

$$\Phi_f = B_\delta b_\delta l_\delta$$

which appears on removal of load (at $I_a = 0$) corresponds to F_f from the same magnetization curve, if the excitation

mmf is retained unchanged. The reduction in flux due to the q-axis armature mmf is

$$\Delta\Phi = \Phi_f - \Phi$$

Example 64-6. Find F_{qd} required to make up for the demagnetizing effect of the armature q-axis mmf for the machine in Fig. 64-22, if $B_{\delta,\text{mean}} = B_3 = 1$ T, $Ab_\delta = 12$ kA, $\Delta B_1 = 0.375$ T, $\Delta B_2 = 0.13$ T, $\Delta B_4 = 0.078$ T, and $\Delta B_5 = 0.153$ T.

Solution. Using Eq. (64-36), we get

$$\Delta B = (0.375 + 4 \times 0.13 - 4 \times 0.078 - 0.153)/12 = 0.03583 \text{ T}$$

As a first approximation, the compensating mmf from Eq. (64-38) is

$$F_{*qd0} = 2 \times 0.3583/(0.375 + 0.153) = 0.1357$$

$$F_{qd0} = F_{*qd0} \times 0.5 Ab_\delta = 0.1357 \times 0.5 \times 12 = 0.8142 \text{ kA}$$

As a second approximation from Eq. (64-43),

$$F_{*qd} = 1/(2 \times 0.43371) - \sqrt{\frac{1}{(2 \times 0.43371)^2} - \frac{0.1357}{0.43371}} = 0.1447$$

where

$$0.43371 = Q = \frac{6 \times 0.375 - 8 \times 0.13 + 8 \times 0.078 - 6 \times 0.153}{4\,(0.375 + 0.153)}$$

$$F_{qd} = F_{*qd} \times 0.5 Ab_\delta = 0.1447 \times 0.5 \times 12 = 0.8682 \text{ kA}$$

(d) Armature mmf on load. The resultant mmf due to the armature current may be replaced by a d-axis mmf called the *armature mmf*

$$F_{a,d} = \pm F_s \pm F_d - F_{qd} \qquad (64\text{-}45)$$

where

$$F_s = w_s I_a$$

is the mmf of the series winding,

$$F_d = cA$$

is the d-axis mmf of the armature, and F_{qd} is the mmf given by Eqs. (64-38) and (64-43) and required to compensate for the demagnetizing effect of the q-axis mmf of the armature. The "+" sign applies when a magnetizing effect takes

place, and the "—" sign, when a demagnetizing effect occurs [see the comments to Eqs. (64-34) and (64-35)].

Given I_a, I_f and Ω, the value of Φ or E can be found, using the magnetization curve (see Fig. 64-21) or the open-circuit (no load) characteristic (see Fig. 64-23), and the resultant d-axis mmf, F_0, determined with allowance for the action of all the armature mmfs,

$$F_0 = F_f + F_{a,d} \tag{64-46}$$

where $F_{a,d} > 0$, if the armature reaction produces a magnetizing effect.

Then, using the voltage equation

$$V = E - I_a R_a \tag{64-47}$$

we find the armature voltage V. The value of R_a is given by Eq. (64-29). In the generator mode of operation, $I_a > 0$. In the motor mode of operation, $I_a < 0$.

Graphically, V is determined from the open-circuit characteristic constructed for a given Ω, and from the characteristic triangle abc (see Fig. 64-23). The sides of the triangle are given by

$$bc = | F_{a,d} |, \quad ac = | I_a R_a |$$

In Fig. 64-23, the construction is done for the generator mode of operation and the demagnetizing effect of the armature reaction when

$$F_{a,d} = \pm F_s \pm F_d - F_{qd} < 0$$

If the armature reaction produces a magnetizing effect ($F_{a,d} > 0$), which can occur when the series winding is connected aiding, the apex b of the triangle must lie to the right of the apex c. In determining the armature voltage, point b must lie on the open-circuit characteristic, and the side ca must lie on the constant F_f line. The position of point a will then give the armature voltage V. For the motor mode of operation, a similar construction is used, except that the point a must lie above point c.

In determining the armature voltage by a numerical method (which is often done on a computer), the open-circuit characteristic should first be approximated by a parabola using Eq. (64-33):

$$E = a_E F^2 + b_E F + c_E - I_a R_a$$

Then, from Eq. (64-47), the armature voltage is

$$V = a_E F_0^2 + b_E F_0 + c_E - I_a R_a$$

Example 64-7. Find the voltage of a generator for which the open-circuit characteristic is approximated by a parabola

$$E = -1.54F^2 + 55F + 71.8$$

The excitation mmf is $F_f = 12$ kA, $I_a = 1000$ A, $F_{a,d} = -F_{qd} = -0.8$ kA, and $R_a = 0.015\Omega$.

Solution. Using Eq. (64-46), the resultant d-axis mmf is

$$F_0 = 12 - 0.8 = 11.2 \text{ kA}$$

and, from Eq. (64-47), the armature voltage is

$$V = -1.54 \times 11.2^2 + 55.8 \times 11.2 + 71.8 - 0.015 \times 1000 = 488.6 \text{ V}$$

64-10 Energy Conversion by a D.C. Machine

A d.c. machine converts energy in the same manner as an inverted synchronous machine, that is, one with its armature winding placed on the stator (see Sec. 56-1). In a steady-state generator operation, the mechanical (input) power

$$P_2 = T_2\Omega \qquad (64\text{-}48)$$

is transferred to the active zone of the armature by the mechanically stressed rotating elements. As has been shown in Sec. 30-1, the mechanical power flux density transferred by the rotating elements is measured in terms of the corresponding component of the Umov vector.

Some of the input power is expended as friction and windage loss $P_{f/w}$, tooth and yoke loss P_c, and stray loss P_{ad}

$$P_m = T_{em}\Omega = P_2 - P_{f/w} - P_c - P_{ad} \qquad (64\text{-}49)$$

Accordingly, the mechanical torque which balances the electromagnetic torque T_{em} acting on the armature (see Sec. 64-6) is decreased as compared with the input torque, T_{ext}:

$$T_{em} = T_2 - (P_{f/w} + P_c + P_{ad})/\Omega \qquad (64\text{-}50)$$

The above losses basically have the same origin as in a synchronous machine. In calculating $P_{f/w}$, account must be taken of friction at the brushes as well. The reason for

including P_c in Eqs. (64-49) and (64-50) is that in an inverted machine some of the input mechanical power is directly converted to magnetic losses dissipated as heat in the teeth and yoke of the armature core. In a synchronous machine with an armature on the stator, these losses are included with the electromagnetic power.

For d.c. machines, P_c is calculated for the total field, and not for the fundamental field as in the case of synchronous machines. The stray losses, P_{ad}, include the loss in the pole-shoes due to pulsation caused by the armature saliency, the increase in magnetic loss on load due to the distortion of the field waveform caused by the q-axis mmf of the armature (cross-magnetization), the loss in the armature conductors due to the radial components of the alternating magnetic fields, and the losses in the commutated coils due to eddy currents induced by the varying leakage fields.

In the active zone of the armature (that is, the region taken up by the core teeth and the armature conductors), P_m is converted to electromagnetic power which can be expressed as

$$P_{em} = T_{em}\Omega$$

Using Eq. (64-20), the electromagnetic power can be written as the product of current and emf

$$P_{em} = T_{em}\Omega = c_E I_a \Phi\Omega = EI_a \qquad (64\text{-}51)$$

The electric power picked off the armature brushes, P_a, is less than the electromagnetic power by the electric (copper) loss, P_{Cu}, in the armature circuit

$$P_a = P_{em} - P_{Cu} \qquad (64\text{-}52)$$

where $P_{Cu} = R_a I_a^2$, and R_a is defined in Sec. 64-7.

On expressing P_{em} and P_{Cu} in Eq. (64-52) in terms of E, I_a and R_a [see Eq. (64-51)], and then in terms of V, I_a and R_a. and using the voltage equation (64-47), the electric power of the armature can be written as the product of armature current and armature voltage

$$P_a = (V + R_a I_a) I_a - R_a I_a^2 = VI_a \qquad (64\text{-}53)$$

Recalling that in an electromagnetically excited generator the power expended by the separately excited or shunt-

wound field winding is

$$P_f = R_f I_f^2$$

where R_f is the resistance of the field circuit including the field control rheostat, the useful electric power in the generator mode of operation is

$$P = P_a - P_f \tag{64-54}$$

In a shunt-wound generator,

$$P_f = VI_f$$

($R_f I_f = V$), so

$$P = VI_a - VI_f = VI \tag{64-55}$$

where

$$I = I_a - I_f$$

is the current in the machine terminals.

In the final analysis, the useful electric power in the generator mode of operation is smaller than the mechanical input power, P_2, by the total losses

$$P = P_2 - \Sigma P \tag{64-56}$$

where

$$\Sigma P = P_{f/w} + P_c + P_{ad} + P_{Cu} + P_f$$

In the motor mode of operation, $V > E$, and I_a is reversed, $I_a < 0$. Accordingly, P_2, P_m, P_{em}, P, T_{em} and Ts_2 are negative, and the useful mechanical power, $|P_2|$, is smaller than the input electric power $|P|$ by the total losses

$$|P_2| = |P| - \Sigma P \tag{64-57}$$

The efficiency of a d.c. machine, as a generator is

$$\eta = P/P_2 = 1 - \Sigma P/(P + \Sigma P)$$

and as a motor,

$$\eta = |P_2|/|P| = 1 - \Sigma P/(|P_2| + \Sigma P) \tag{64-58}$$

Example 64-8. Find the voltage and efficiency in the motor and generator modes of operation for a shunt-wound d.c. machine having the following parameters: $E = 205$ V, $I_a = 72$ A, $I_f = 1.8$ A, $R_a = 0.208\ \Omega$, the total loss (less the loss in the shunt-wound field winding and the armature circuit) $P_{f/w} + P_c + P_{ad} = 730$ W.

Solution. Using Eq. (64-47), for the motor mode of operation we get:

$$V = 205 - (-72) \times 0.208 = 220 \text{ V}$$

The loss in the shunt-wound field winding is

$$P_f = VI_f = 220 \times 1.8 = 396 \text{ V}$$

The loss in the armature circuit is

$$P_{\text{Cu}} = 0.208 \times 72^2 = 1078 \text{ W}$$

In accord with Eq. (64-56),

$$\Sigma P = 730 + 1078 + 396 = 2204 \text{ W}$$

From Eq. (64-55), the input power is

$$| P | = 220 \times (72 + 1.8) = 16\,236 \text{ W}$$

From Eq. (64-58), the efficiency is

$$\eta = 1 - 2204/16\,236 = 0.8644$$

For the generator mode of operation, from Eq. (64-47) we have

$$V = 205 - 72 \times 0.208 = 190 \text{ V}$$

$$P_f = VI_f = 190 \times 1.8 = 342 \text{ W}$$

$$\Sigma P = 730 + 1078 + 342 = 2\,150 \text{ W}$$

In accord with Eq. (64-55), the power delivered to the line is

$$| P | = 190 \times (72 - 1.8) = 13\,338 \text{ W}$$

From Eq. (64-58), the efficiency is

$$\eta = 1 - 2150/(13\,338 + 2150) = 0.8613$$

☆ 64-11 Commutation

As the armature and commutator of a d.c. machine rotate the coils are continually switched out of a parallel circuit (or path) where the current is in one direction, into a parallel circuit where the current is in the opposite direction. As a result, the current in a coil being switched, or *commutated*, undergoes a reversal, whereas the coil itself is shorted by

the commutator bars and brushes for the duration of *commutation*.

The commutation process is illustrated in Fig. 64-26. The coil being commutated is shown by heavier lines. When the rotation is in the direction indicated by the arrow, the coil is switched out of the left-hand path where its current

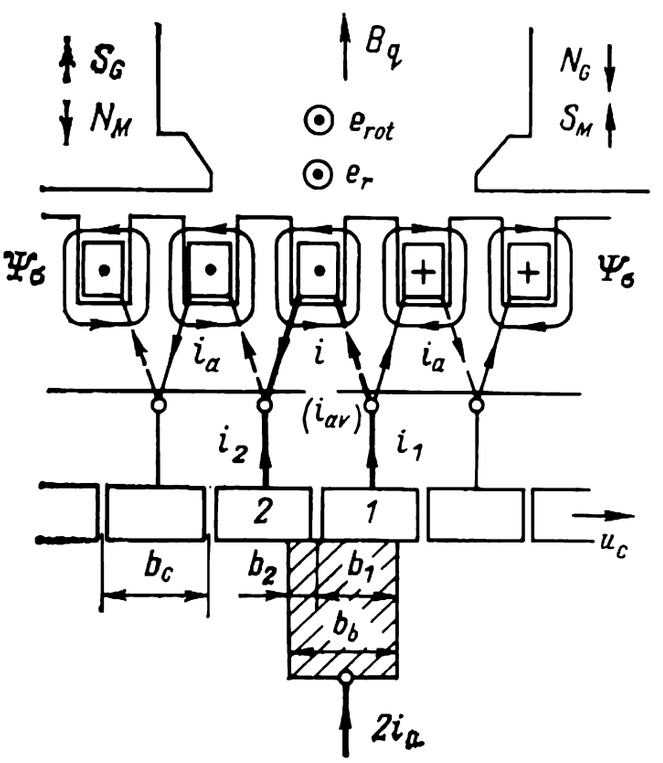

Fig. 64-26 Late commutation in a machine without compoles

is $i = i_a$ and into the right-hand path where its current is $i = -i_a$ (the positive direction of current flow is towards the reader). A reversal of the coil current occurs in a very short time. The commutation time or period, that is, the time during which a coil remains shorted by a brush depends on the brush width b_b and the peripheral speed of the commutator, u_c:

$$T_c = b_b/u_c$$

Recalling that

$$u_c = R_c\Omega = Kb_c\Omega/2\pi$$

where K is the number of commutator bars and b_c is the commutator bar width, we get

$$T_c = (2\pi/K\Omega)\,(b_b/b_c) \qquad (64\text{-}59)$$

When $b_b > b_c$, several coils will be in the process of commutation at a time.

Example 64-9. Find the commutation time for a machine with $n = 1500$ rpm, $K = 93$, and $b_b/b_c = 2$.

Solution. The mechanical angular velocity is

$$\Omega = 2\pi n/60 = 2\pi \times 1500/60 = 157 \text{ rad s}^{-1}$$

Hence,

$$T_c = 2\pi \times 2/(93 \times 157) = 0.0008 \text{ s}$$

In a loaded machine, several coils are being commutated at any given instant of time. Their commutation is completed in T_c, and the coils following them enter the process of commutation. To a stationary observer, this process appears recurring periodically at a frequency

$$f_c = 1/T_c$$

which may be as high as several kilohertz.

Commutation gives rise to electromagnetic oscillations which, if no measures to the contrary are taken, might disrupt or interfere with radio communication. Most frequently, radio interference due to commutation is minimized or suppressed altogether by shielding (or screening) the associated d.c. line and by switching in capacitors which act in combination with the windings in the armature circuit as LC-filters.

(1) Current reversal during commutation. To simplify analysis, let the brush width be equal to the commutator bar width. Also assume that the thickness of the insulation between commutator bars is small in comparison with their width, and brush contact resistance (that is, one between the brush and commutator) is independent of current density.

Consider the loop containing the coil being commutated and carrying a current i, the conductors connecting the coil to commutator bars *1* and *2* and carrying the currents i_1 and i_2, and the brush touching the bars.

Suppose that a time t has elapsed since the onset of commutation and that the brush covers commutator bar *2* over a width

$$b_2 = u_c t$$

and commutator bar *1* over a width

$$b_1 = b_b - b_2 = u_c T_c - u_c t = u_c (T_c - t)$$

On writing the Kirchhoff current equation for the two nodes where the coil terminal leads join the left- and right-hand paths and the conductors leading to the commutator bars, we shall see that the currents in the elements of the loop will be connected by equations of the form

$$i_1 = i_a + i, \quad i_2 = i_a - i \tag{64-60}$$

In addition, write the Kirchhoff loop (or mesh) voltage equation

$$R_c i + i_1 (R_1 + R_{cond}) - i_2 (R_2 + R_{cond}) = \Sigma e \tag{64-61}$$

where R_c is the coil resistance, R_{cond} is the resistance of the conductor connecting the coil to the commutator bar, R_1 and R_2 are the brush contact resistances at bars *1* and *2*, and Σe is the sum of the emfs induced in the coil being commutated.

At a constant resistivity, the brush contact resistances R_1 and R_2 are inversely proportional to the contact surface areas, S_1 and S_2.

$$R_1 = R_b S_b / S_1 = R_b T_c / (T_c - t) \tag{64-62}$$
$$R_2 = R_b S_b / S_2 = R_b T_c / t$$

where $R_b = \rho_b / S_b$ is the total resistance between the brush and commutator

$$R_1 = \rho_b / S_1$$
$$R_2 = \rho_b / S_2$$
$$S_1 = l_b b_1 = l_b u_c (T_c - t)$$
$$S_2 = l_b b_2 = l_b u_c t$$

In solving Eq. (64-60) for i, it is legitimate to neglect R_c and R_{cond} in comparison with R_1 and R_2. Also, let Σe in Eq. (64-61) be a constant quantity equal to the emf averaged over the commutation period. Then, in view of Eq. (64-42), we get

$$i = i_a (1 - 2t/T_c) + (\Sigma e / R_b) [t/T_c - (t/T_c)^2] \tag{64-63}$$

Equation (64-63) offers insight into the effect of various factors on the current i in the coil being commutated.

(a) *Linear (straight-line) commutation.* This form of commutation occurs at $\Sigma e = 0$, when the current in the coil being commutated varies linearly from $i = i_a$ at $t = 0$ to

$i = -i_a$ at $t = T_c$ (Fig. 64-27*a*). In this case, the current density under the brush remains constant and the same for the leading commutator segment (*1*) and the trailing commutator segment (*2*)

$$J_1 = i_1/S_1 = 2i_a/S_b = i_2/S_2 = J_2$$

where

$$i_1 = 2i_a\,(1 - t/T_c)$$

is the current in the leading commutator segment and

$$i_2 = 2i_a t/T_c$$

is the current in the trailing commutator segment in accord with Eq. (64-60). This is because i_1 and i_2 vary in proportion to S_1 and S_2.

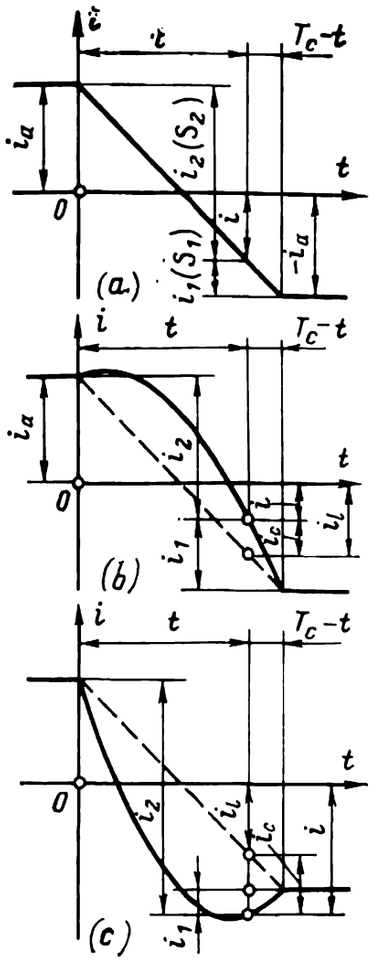

Fig. 64-27 Various forms of commutation: *a*—linear; *b*—late; *c*—early

(b) *Late commutation* (*undercommutation*). This form of commutation occurs at $\Sigma e > 0$, that is, when the average emf in the coil being commutated gives rise to a complementary commutation current, i_c, acting in the same direction as i_a which existed in the coil prior to the onset of commutation. The current i_c is added to the linear commutation current i_1, as found at $\Sigma e = 0$, and slows down the reversal of the coil current

$$i = i_1 + i_c$$

(Fig. 64-27*b*). Because the current under the trailing edge of the brush

$$i_1 = i_a + i = i_a + i_1 + i_c$$

decreases at a slower rate than the contact surface S_1 (Fig. 64-27*a*), the current density under the trailing edge

$$J_1 = i_1/S_1 = (i_a + i_1)/S_1 + i_c/S_1 = 2i_a/S_b + i_c/S_1$$

exceeds the current density $2i_a/S_b$ which would exist in the case of linear commutation.

(c) *Early commutation* (*overcommutation*). This form of commutation takes place at $\Sigma e < 0$, that is, when the

complementary current i_c produced by the average emf aids the current $(-i_a)$ which exists in the coil after the commutation. Now i_c is subtracted from the linear commutation current found at $\Sigma e = 0$, and speeds up the reversal of the coil current

$$i = i_1 - i_c$$

(Fig. 64-27*c*). Because the current under the trailing edge of the brush

$$i_1 = i_a + i = i_a + i_1 - i_c$$

is now decreasing at a faster rate than the contact surface S_1 (Fig. 64-27*a*), the current density under the trailing edge

$$J_1 = i_1/S_1 = (i_a + i_1)/S_1 - i_c/S_1 = 2i_a/S_b - i_c/S_1$$

is less than the current density $2i_a/S_b$ which would exist in the case of linear commutation. If

$$\Sigma e = -2i_a R_b$$

the current at the end of current reversal, proportional to $(di_1/dt)_{t=T_c}$ reduces to zero. When

$$|\Sigma e| > 2i_a R_b$$

the current density under the trailing edge even goes negative (as illustrated by the current curve in Fig. 64-27*c*).

The current in the coil undergoing commutation has some effect on the main field of the machine. This effect depends on the magnitude of the coil current as given by Eq. (64-63), and its direction averaged over a commutation period

$$i_{av} = \frac{1}{T_c}\int_0^{T_c} i\,dt = \frac{1}{T_c}\int_0^{T_c} i_c\,dt = 2i_{c,\max}/3$$

where

$$i_{c,\max} = i_{c(t=0.5T_c)} = \Sigma e/4R_b$$

is the maximum complementary current in the coil undergoing commutation.

The average current, i_{av}, in the coil undergoing commutation gives rise to a *d*-axis mmf

$$F_{d,c} = i_{av} w_c = w_c \Sigma e/6R_b$$

With linear commutation, the mmf of the coil being commutated is zero. With late commutation, $\Sigma e > 0$, and $i_{av} > 0$ is flowing in the coil as shown in Fig. 64-26. In the generator mode of operation, $F_{d,c}$ weakens the main field, whereas in the motor mode of operation it strengthens the main field. With early commutation, $\Sigma e < 0$, and $i_{av} < 0$ in the coil undergoing commutation is flowing as shown in Fig. 64-28. In the generator mode of operation $F_{d,c}$ strengthens the main field; in the motor mode of operation it weakens the main field.

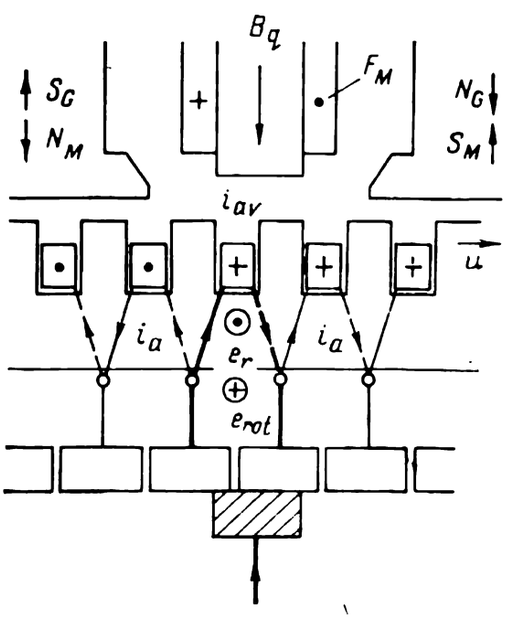

Fig. 64-28 Early commutation in a compole machine

(2) Brush sparking causes and remedies. Sparking under the brushes in a d.c. machine may be caused by mechanical and electromagnetic factors. Heavy sparking may cause an accelerated wear to the brushes and commutator. Therefore, it is important to take appropriate measures to the contrary.

As regards mechanical causes of sparking, it is important to give a correct shape to the commutator, to use brushes having an adequate mechanical strength, to permit free movement of the brushes in the brush holders, to maintain a correct brush pressure and a correct stiffness of the springs that hold the brushes against the commutator bars.

The commutator must be the shape of a cylinder and retain its shape under centrifugal forces and the stresses caused by temperature variations. The out-of-roundness and eccentricity of the commutator ought not to exceed a few hundredths of a millimetre.

A proper brush pressure is essential as a way of preventing brush vibration and bounce. An insufficient pressure would aggravate both, whereas an excessive pressure would lead to an accelerated wear of the brushes and commutator.

Of no less importance is the atmosphere in which the brush-commutator contact exists. Under normal atmospheric pressure (at not over 1000 m above sea level and $\pm 40°C$), a strong film of copper and carbon oxides is formed on the

commutator surface. This oxide film absorbs the atmospheric water and oxygen to form a kind of lubricant. If the atmospheric humidity is too low (which often happens at over 6000 m above sea level), the lubricating action of the oxide film is drastically reduced, and the mechanical losses at the sliding contact and the temperature of the commutator rise several-fold. This leads to the destruction of the oxide film, a reduction in the brush contact resistance and, in the long run, to poor commutation.

As regards electromagnetic factors responsible for sparking under the brushes, special mention must be made of commutation. As we have seen, preference should be given to early commutation. With it, the current density under the trailing edge of the brush can be made equal to zero very nearly, and this will prevent sparking. If, however, no special measures are taken, Σe will be positive, and late (or delayed) commutation will take place, least favourable in terms of sparking. To demonstrate, as is seen from Fig. 64-26 showing a machine without commutating (or intermediate) poles in the generator mode of operation, only positive emfs are induced in the coils undergoing commutation (that is, the emfs in the same direction as the coil current that existed prior to commutation).

These emfs include, firstly, the emf of self-induction

$$e_L = -\mathrm{d}\Psi_\sigma/\mathrm{d}t$$

associated with a change in the leakage flux linkage of the coil. Because commutation brings about a reversal in the flux linkage (the positive flux linkage gives way to a negative flux linkage, as is shown in Fig. 64-26),

$$\mathrm{d}\Psi_\sigma < 0$$

and

$$e_L > 0$$

The value of this emf averaged over the commutation period is called the *reactance emf* (or *voltage*) of the coil

$$e_r = \frac{1}{T_c}\int_0^{T_c} e_L\,\mathrm{d}t = -L_\sigma\,(\mathrm{d}i/\mathrm{d}t)_{av} = L_\sigma\,(2i_a/T_c) > 0 \qquad (64\text{-}64)$$

where

$$L_\sigma = \Psi_\sigma/i_a$$

is the leakage self-inductance of the coil.* As is seen from Fig. 64-26, the reactance emf of the coil is directed towards the reader (out of the paper).

Secondly, a *rotational emf* is induced in the coil undergoing commutation

$$e_{\text{rot}} = 2B_q l_\delta w_c u \qquad (64\text{-}65)$$

where B_q = average flux density in the conductor region of the coil undergoing commutation
w_c = coil turns
u = peripheral speed of the armature.

When the brushes are in neutral, B_q is produced by $F_{q,\max} = A\tau/2$, the q-axis mmf of the armature:

$$B_q = (\mu_0 F_{q,\max}/\delta)\sqrt{c_q/(c_q+1)}$$

where

$$c_q = [2\delta/(\tau - b_p)]^2$$

where b_p is the pole-shoe width (pole arc).

Using the right-hand rule, it is an easy matter to prove that $e_{\text{rot}} > 0$. Thus, in a machine without commutating poles, the commutation will always be late. This also goes for the motor mode of operation, except that the polarity of the main pole shown in Fig. 64-26 will be reversed.

Early commutation can be obtained by reversing the sign of e_{rot}. In turn, this can be done by reversing the sense of the q-axis field in the region of the coil being commutated. Practically, this can best be done by providing intermediate (or commutating) poles (interpoles or compoles for short), as shown in Fig. 64-28. For the first time, they were proposed by Menges in 1884, and today they are fitted on all d.c. machines over 1 or 2 kW in rating.

Because e_{rot}, Eq. (64-55), must compensate for the reactance emf, Eq. (64-64), proportional to i_a, the compole winding is connected in series with the armature winding and is fed with i_a. The mmf due to the compole winding, F_{cp}, must be such that it will compensate for $F_{q,\max}$ and have an excess to set up a q-axis field in the opposite sense:

$$F_{cp} = F_{q,\max} + \beta_{cp} B_q \delta_{cp} k_{\delta,cp}/\mu_0$$

* If $b_b > b_c$ and several coils undergo commutation at a time the coil emf must be found with allowance for mutual inductance between the coils.

where

δ_{cp} = air gap under the compoles

β_{cp} = 1.2 = factor taking care of the mmf drop in the iron parts of the magnetic circuit of the compoles

$k_{\delta,\,cp}$ = air gap factor for the compoles.*

To set up such an mmf, the compole must have

$$w_{cp} = F_{cp}/i_a \text{ turns}$$

To obtain early commutation, $|e_{rot}|$ is taken to exceed e_r by about 15%, that is,

$$\Sigma e = e_r - e_{rot} = e_r - 1.15e_r = -0.15e_r < 0$$

Then, subject to Eqs. (64-64) and (64-65), we find that in order to obtain the desired value of $|e_{rot}|$, the gap flux density under a compole must be

$$B_q = 1.15L_\sigma i_a/T_c l_\delta w_c u$$

As the load is varied, early commutation will be maintained automatically if e_{rot} and e_r are varied in proportion to the armature current. To meet this requirement, the magnetic circuit of the compoles must be unsaturated both in the region of the compole cores and in the parts common with the main magnetic circuit.

A violent change in load upsets compensation because of the eddy currents that are induced in massive parts and prevent the compole flux from following changes in the armature current. This is the reason why in machines for suddenly alternating load the compole cores and, sometimes, the yoke are built up of electrical sheet steel laminations. It is also important to remember that the compoles compensate for the reactance emf only in average over a commutation period, and may fail to do so at some instants. So, if the reactance emf is too large, the compoles may fail to prevent sparking. Because of this, in designing a d.c. machine, its dimensions are chosen such that the reactance emf defined by Eq. (74-64) will not exceed 3.5 V.

(3) Flashover. Compensating winding. In very large machines that undergo violent changes of load, the sudden and

---

* In a machine with a compensating winding, the compole mmf may be reduced by the mmf, $Ab_1/2$, produced by the compensating winding.

large changes of armature current may induce large emfs that flash over the commutator segments and cause an arc to circle round the whole of the commutator. This is an extreme case of armature reaction and may cause severe damage to the commutator and brush holders or even knock the machine out of action.

As investigations have shown, a flashover can occur if the maximum voltage between the commutator segments, $v_{c,max}$, exceeds 30 or 35 V. The voltage between the commutator segments is the same as the voltage across the coil which is connected to the segments. The coil voltage differs but little from the coil emf and is proportional to the flux density in the region of coil sides. Because of this, the distribution of voltage between commutator segments is similar to that of gap flux density over a pole pitch, $v_c \sim B$. The average voltage between commutator segments,

$$v_{c,av} = 2pV/K$$

is proportional to the average gap flux density, $B_{\delta,av}$. The maximum voltage between segments is proportional to the maximum gap flux density, $B_{\delta,max}$. The relation between them is the same as that between the two flux densities, namely

$$v_{c,max} = v_{c,av} c_{max} = (2pV/K)\, c_{max}$$

where

$$c_{max} = B_{\delta,max}/B_{\delta,av}$$

At no load, $c_{max} \approx 1/0.7 = 1.42$. On load, the q-axis armature reaction comes into play (see Sec. 64-9, Fig. 64-22), the maximum flux density is 1.2 or 1.3 times the average flux density, and

$$c_{max} = (1.2 \text{ to } 1.3)/0.7 = 1.7 \text{ or } 1.8$$

A substantial decrease in $v_{c,max}$ on load can be obtained by balancing out the q-axis mmf of the armature. This is done with a *compensating winding*. The conductors of the compensating winding are put in the main pole faces and connected in series with the armature winding in such a way that their respective mmfs oppose each other

(Fig. 64-29). When the electric loading of the compensating winding, A_{cp}, is equal to that of the armature winding, A, the q-axis mmf of the armature, Ax, will be balanced out by the mmf of the compensating winding, $A_{cp}x$, at any distance from the pole axis ($x < 0.5b_p$).

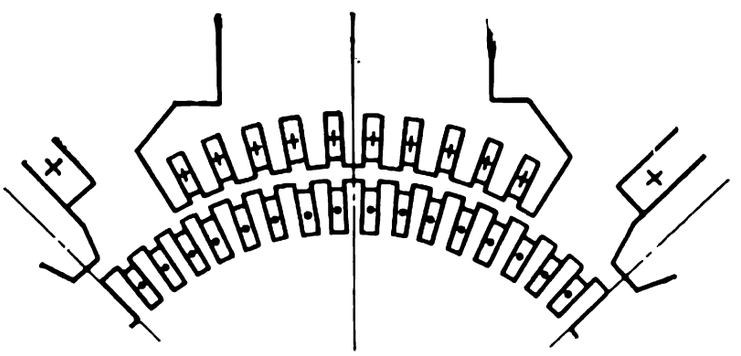

Fig. 64-29 Cross-sectional view of a machine with a compensating winding

Compensation is maintained automatically at any value of load, and the field under the pole-shoes remains the same as at no load. This reduces the maximum voltage between commutator segments and eliminates the demagnetizing action of the q-axis armature reaction ($F_{qd} = 0$).

Because compensating windings complicate machine design, they are only used on large units.

64-12 D.C. Generators

The behaviour of a d.c. generator depends on the manner in which its field winding is connected to the d.c. excitation source. Two general possibilities exist: the field winding may be connected to a d.c. source which is electrically independent of the machine, resulting in a *separately excited generator*, shown in Fig. 64-30*a*; or it may be recognized that the armature itself constitutes a d.c. source capable of supplying electric power not only to the load on the machine but also to its own field winding, resulting in a *self-excited generator* (Fig. 64-30*b* through *d*).

The field winding of self-excited generators can be supplied in three different ways. The machine in Fig. 64-30*b* is a *shunt-wound* (or simply, *shunt*) *d.c. generator*, because its field winding is connected in parallel with its armature winding. The machine in Fig. 64-30*c* is a *series-wound* (or

simply *series*) *d.c. generator*, because its field winding is connected in series with its armature. Finally, the machine in Fig. 64-30*c* is a *compound-wound* (or simply *compound*)

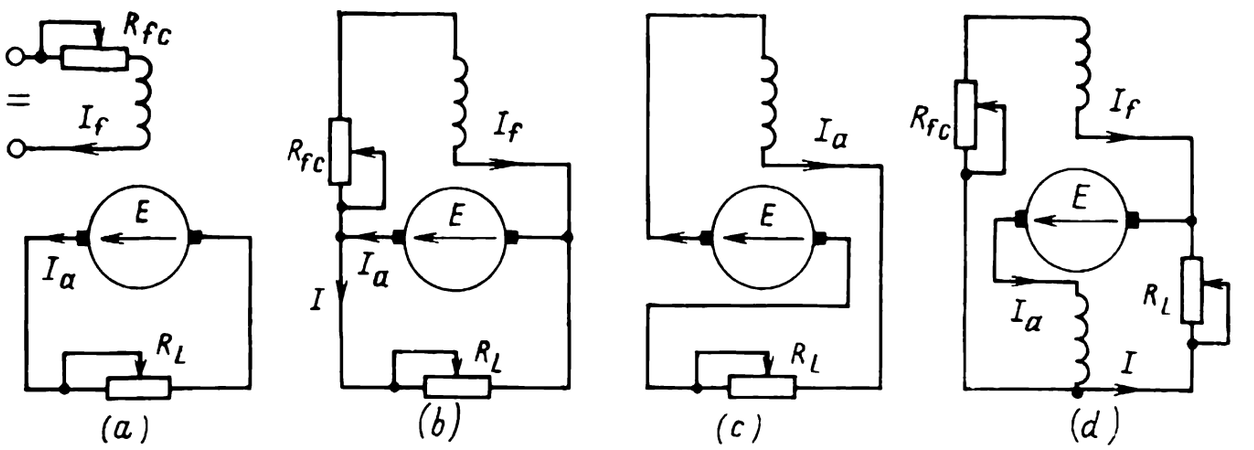

Fig. 64-30 Form of excitation for d.c. generators: R_L = load resistance; R_{fc} = field-control rheostat

d.c. generator because it has both a shunt and a series field winding. Shunt d.c. generators are often used as exciters for large synchronous machines. As a way of *extending the range of voltage control*, they are fitted with *three* windings, namely, separately excited, shunt, and series.

In the diagrams of Fig. 64-30, the compole and compensating windings are omitted.

The performance of a d.c. generator at no load, $I = 0$, can be described by its no-load (or open-circuit) characteristic (see Sec. 64-8). On load, the performance of a d.c. generator can be described, using its external, armature, output, and short-circuit characteristics which relate its terminal voltage V, load current I, and field current I_f.

The construction of the above characteristics is dealt with in Sec. 64-9. For normal d.c. machines with compoles, with the brushes in neutral, and with the mmf of the coils undergoing commutation neglected (see Sec. 64-11), the armature mmf and the field current equivalent to that mmf may be taken approximately proportional to the armature current and found from

$$F_{a,d} = \pm F_s - F_{qd} = F_{a,dR}\,(I_a / I_{aR})$$

and

$$F_{a,d}\, w_f = (F_{a,dR}\, w_f)\,(I_a / I_{a,R}) \qquad (64\text{-}66)$$

where

$$F_{a,dR} = \pm F_{s,R} - F_{qdR}$$

is the armature mmf at $I = I_R$ and $\Phi = \Phi_R$.

When the actual flux deviates from Φ_R by a large amount, Eq. (64-66) leads to an appreciable error. Where high accuracy is essential, F_{qd} must be found as advised in Sec. 64-9 for each value of flux and current (by the method of successive approximation, if necessary).

The characteristics of d.c. generators can conveniently be calculated on small computers. For higher accuracy, the no-load (open-circuit) characteristic should preferably be divided into two or three portions, and each portion should be approximated by a parabola of its own.

(i) A separately excited or separately-series-excited d.c. generator

In this type of generator, the field current and terminal voltage can be varied with a rheostat, R_{fc}, (see Fig. 64-30*a*) over a wide range. Therefore, such machines are used in cases where the terminal voltage must be gradually varied from zero to V_R.

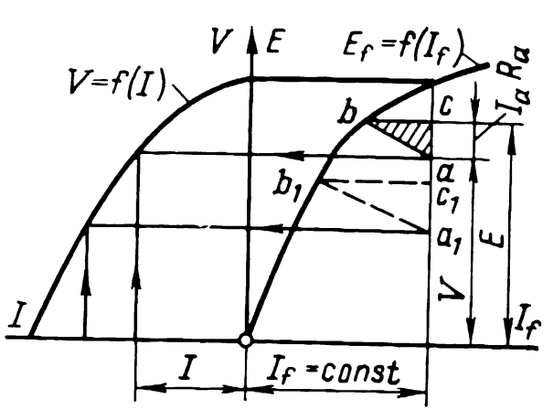

Fig. 64-31 External characteristic of a separately excited generator

(a) External characteristic, $V = f(I)$. This characteristic is plotted for constant $R_{f0} = R_f + R_{fc}$ or constant I_f as shown in Fig. 64-31, using the open-circuit (no-load) curve and the characteristic "load" triangle (see Sec. 64-9). The open-circuit characteristic is a curve relating the output (terminal) voltage to the field current on open-circuit, that is, with no load. The side *bc* of the characteristic triangle is calculated by Eq. (64-66) to give the field current

$$bc = F_{a,d}/w_f$$

equivalent to the armature mmf.

To construct the external characteristic, a range of values is assumed for the armature current, and for each value the triangle is positioned so that its apex *b* lies on the open-

circuit characteristic, and the apex c on the constant I_f line. Then the distance from point a to the axis of abscissae will give the value of V.

The characteristic in Fig. 64-31 has been plotted for the case where the armature reaction produces a demagnetizing effect. In this case, $F_{a,d} < 0$, and point b lies to the left of point c.

For a generator in which the separately excited and the series excited field windings are connected aiding, so that the series mmf, F_s, exceeds $|F_{qd}|$ and $F_{a,d} = F_s - F_{qd} > 0$, a similar construction applies, but point b will lie to the right of point c.

For the external characteristic to be expressed analytically, the first step is to approximate the open-circuit characteristic over the interval of interest with a parabola

$$E = a_E I_{f0}^2 + b_E I_{f0} + c_E \qquad (64\text{-}67)$$

The next step is to express the resultant field current as a function of I_a:

$$I_{f0} = I_f + F_{a,d}/w_f = I_f + c_a I_a$$

where

$$c_a = F_{a,dR}/w_f I_{aR}$$

Then, using Eq. (64-47), the equation of the external characteristic may be written as

$$V = a_V I_a^2 + b_V I_a + c_V \qquad (64\text{-}68)$$

where

$$a_V = a_E c_a^2$$
$$b_V = c_a (2 I_f a_E + b_E) - R_a$$
$$c_V = E_f = a_E I_f^2 + b_E I_f + c_E$$

Because a_V, like a_E, is negative always, the external characteristic of the d.c. generator in question is a parabola with the vertex turned upwards. At $I_a = 0$,

$$V = c_V = E_f$$

The manner in which the output (terminal) voltage varies with a rise in load (or in current I_a) depends on the sign of the coefficient b_V. At $b_V = 0$,

$$(dV/dI_a)_{I_a=0} = (2a_V I_a + b_V)_{I_a=0} = b_V = 0$$

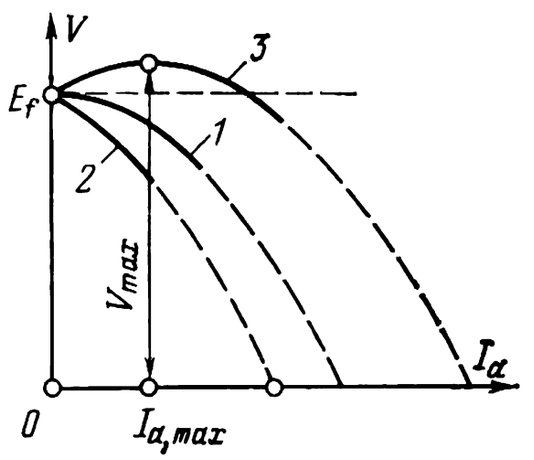

Fig. 64-32 External characteristics of separately/series-excited d.c. generator

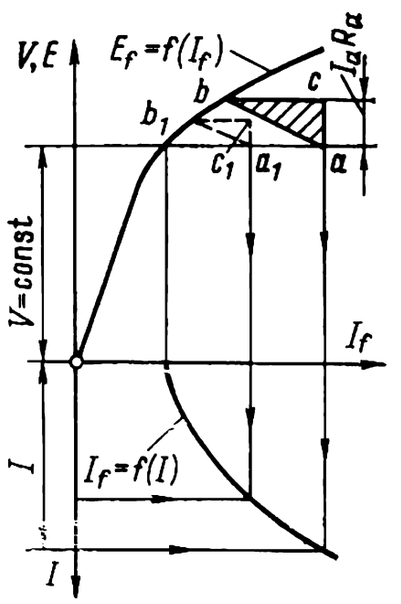

Fig. 64-33 Armature characteristic of a separately excited generator

and the voltage follows curve *1* in Fig. 64-32. The $b_V = 0$ case occurs in separately/series-excited generators where

$$c_a = R_a/(2I_f a_E + b_E)$$

When $b_V < 0$, the voltage falls off with a rise in load at a much higher rate than when $b_V = 0$ (curve *2*). This happens in separately/series aiding or separately excited generators, where

$$c_a < R_a/(2I_f a_E + b_E)$$

Finally, when $b_V > 0$, the voltage first rises with increasing load, reaches its maximum value, V_{max}, at $I_{a,max} = -b_V/2a_V$, then falls off along curve *3*. This happens in separately/series aiding excited generators, when

$$c_a > R_a/(2I_f a_E + b_E)$$

In the above expressions, the quantity $(2I_f a_E + b_E)$ is the slope of the open-circuit characteristic, dE/dI_f, for a given I_f.

On putting $V = 0$ in Eq. (64-67), we find the armature current at which the external characteristic cuts the axis of abscissae

$$I_{a(V=0)} = (-b_V + \sqrt{b_V^2 - 4a_V c_V})/2a_V \qquad (64\text{-}69)$$

(b) Armature characteristic, $I_f = f(I_a)$. This characteristic is plotted for a constant output (terminal) voltage as shown in Fig. 64-33. As before, several fixed values of I_a are chosen and for each value the characteristic triangle is positioned so that points a and a_1 lie on the constant V

line, and points b and b_1 lie on the open-circuit characteristic. Then the distance from point a to the axis of ordinates will give the required field current. The characteristic in Fig. 64-33 applies when $F_{a,d} < 0$. When $F_{a,d} > 0$, point b will lie to the right of point c.

For the armature characteristic plotted for a constant V to be expressed analytically, the same approximation, Eq. (64-67), may be used. To begin with, a value of I_a is chosen, and the emf (generated voltage)

$$E = V + R_a I_a$$

is found. Then, using Eq. (64-67), the resultant field current, I_{f0}, corresponding to the above emf is determined

$$I_{f0} = \frac{-b_E + \sqrt{b_E^2 - 4a_E(c_E - E)}}{2a_E}$$

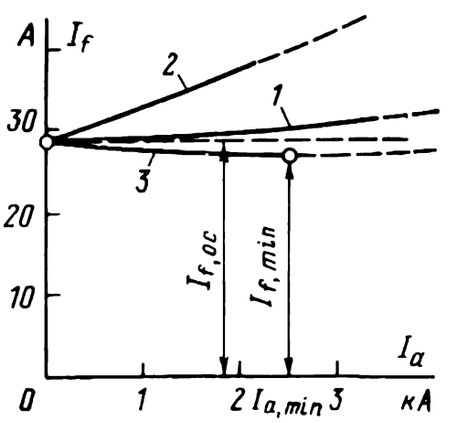

Fig. 64-34 Armature characteristics of a separately/series-excited generator

and also the field current, $I_f = I_{f0} - c_a I_a$, at which V is constant,

$$I_f = [-b_E + \sqrt{b_E^2 - 4a_E(c_E - V - R_a I_a)}]/2a_E - c_a I_a \quad (64\text{-}70)$$

This is an analytical expression for the armature characteristic, $I_f = f(I_a)$. The shape of the characteristic depends on the effect of the armature reaction and the voltage drop in the armature circuit. At $I_a = 0$, all curves pass through a point

$$I_{f,oc} = -b_E + \sqrt{b_E^2 - 4a_E(c_E - V)}$$

on the axis of ordinates. From that point, the curves emanate at an angle

$$(dI_f/dI_a)_{I_a=0} = c_{a,0} - c_a$$

where

$$c_{a,0} = \frac{R_a}{\sqrt{b_E^2 - 4a_E(c_E - V)}} > 0$$

When $c_a = c_{a,0}$, the angle is zero, and an increase in I_a brings about an insignificant rise in the field current (curve *1* in Fig. 64-34). When $c_a < c_{a,0}$, which occurs with separate excitation or in the case of a weak series winding connected

aiding with the separately excited winding, the angle is positive, and an increase in I_a produces a larger increase in the field current (curve *2* in the same figure). When $c_a > c_{a,0}$, which happens in the case of a strong series winding connected aiding with the separately excited winding, the angle is negative, and an increase in I_a first leads to a reduction in the field current which drops to a minimum, $I_{f,\min}$, at

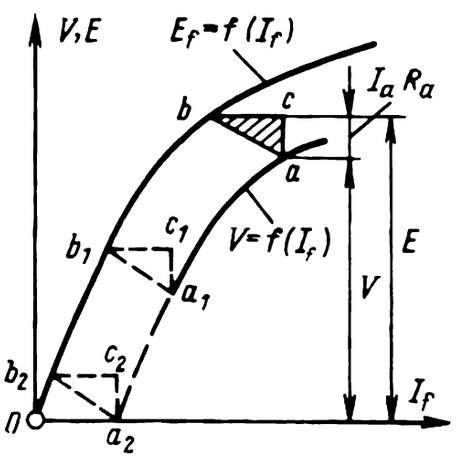

Fig. 64-35 Output characteristic

$$I_{a,\min} = \frac{R_a^2 - c_a^2 [b_E^2 - 4a_E (c_E - V)]}{4a_E R_a c_a^2}$$

then rises along curve *3*.

Example 64-10. Given: A separately excited generator whose open-circuit characteristic is approximated by a parabola

$$E = a_E I_f^2 + b_E I_f + c_E$$

where $a_E = -0.2464\ \text{VA}^{-2}$, $b_E = 22\ \Omega$, $c_E = 71.8\ \text{V}$, and for which $I_{a,R} = 1000$ A, $w_f = 400$, $R_a = 0.015\ \Omega$, and $F_{qd,R} = 800$ A.

To find: An armature characteristic for $V = 500$ V and also armature characteristics if the machine is fitted with a series winding such that $c_{a,0}$ and $c_a = 0.003$.

When separately excited,

$$c_a = F_{a,dR}/w_f I_{a,R} = -800/(400 \times 1000) = -0.002$$

where

$$F_{a,dR} = -F_{qd} = -800\ \text{At}$$

The characteristic for $c_a = -0.002$, as calculated by Eq. (64-70), is curve *2* in Fig. 64-34.

$$c_{a,0} = \frac{0.015}{\sqrt{22^2 - 4(-0.2464)(71.8 - 500)}} = 0.001905$$

The characteristic for $c_{a,0}$ is curve *1*: for $c_a = 0.003$, curve *3*.

(c) Output characteristic, $V = f(I_f)$. This characteristic (Fig. 64-35) is plotted for constant armature current. Given the rated voltage, this current corresponds to a certain

characteristic "load" triangle, *abc*. To a first approximation, it is assumed that the size of the triangle remains unchanged as the field current is varied. Then, moving the triangle so that point *b* falls on the open-circuit characteristic, we can find the desired relation. The distance from point *a* to the axis of abscissae gives the value of V, and the distance from point *a* to the axis of ordinates gives the value of I_f.

The output characteristic can readily be expressed analytically with the aid of Eq. (64-67):

$$V = a_I I_f^2 + b_I I_f + c_I$$

where

$$a_I = a_E$$
$$b_I = b_E + 2a_E c_a I_a$$
$$c_I = c_E - R_a I_a + b_E c_a I_a + a_E c_a^2 I_a^2$$

(d) Armature current on short-circuit. To a first approximation, the armature current on short-circuit can be found from Eq. (64-69). When the excitation corresponds to the rated voltage on load, the short-circuit current may be tens times the rated value. This current is particularly heavy in generators having their separately excited and shunt field windings connected aiding.

(ii) Shunt and Compound D.C. Generators

Shunt and compound d.c. generators (see Fig. 64-30*b* and *d*) need no external d.c. source to feed the field winding. Instead, they operate by self-excitation—a feature which explains why they have found a broad field of application.

The rated current in the shunt field winding, $I_{f,R}$ ranges from 0.01 to 0.05 of the rated armature current, $I_{a,R}$.

For purposes of analysis, the load current is assumed to be

$$I = I_a - I_f \approx I_a$$

(a) Conditions for self-excitation (generator-build up). Consider first the conditions for self-excitation (generator buildup) at no load, when the armature circuit is open, $R_L = \infty$. Suppose that the generator is spinning at a mechanical angular velocity Ω. Its open-circuit characteristic

for this speed is shown in Fig. 64-36 which also shows lines *1* through *4* which represent the voltage drop across the shunt field winding

$$V_f = R_{f0} I_f$$

for several values of field resistance

$$R_{f0} = R_f + R_{fc}$$

Because the field winding (see Fig. 64-30*b*) is connected across the terminals of the armature winding,

$$E = V_f = R_{f0} I_f$$

and the steady-state voltage is represented by the intersection of the $V_f = R_{f0} I_f$ line and the open-circuit characteristic. As R_{f0} is decreased, $R_{f01} < R_{f02}$, the terminal voltage, $V = E = V_f$, increases.

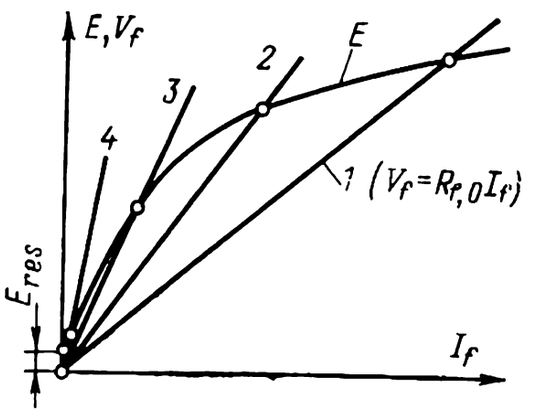

Fig. 64-36 Conditions for self-excitation of a shunt-wound generator

The largest critical resistance at which generator buildup still can occur is given by

$$R_{f03} = (\mathrm{d}E/\mathrm{d}I_f)_{I_f=0}$$

At

$$R_{f0} \leqslant (\mathrm{d}E/\mathrm{d}I_f)_{I_f=0} \qquad (64\text{-}71)$$

generator buildup will occur, whereas at

$$R_{f0} > (\mathrm{d}E/\mathrm{d}I_f)_{I_f=0}$$

it will not, and the terminal voltage will remain nearly equal to the residual voltage.

For generator buildup to take place at $R_{f0} < R_{f03}$, it is essential that the generator should have a residual magnetization corresponding to E_{res}. Also, the field winding must be connected so that the current produced in it by E_{res} will boost the residual magnetic field. If the above requirements are satisfied, E_{res} will produce in the field winding a current whose buildup to a steady-state value can be described by a nonlinear differential equation of the form

$$E - R_{f0} I_f = L_f \, \mathrm{d}I_f/\mathrm{d}t \qquad (64\text{-}72)$$

where $E = f(I_f)$ is the current value of armature emf at I_f,

$$L_f = L_{f\sigma} + \mathrm{d}\Psi/\mathrm{d}I_f = 2pw_f k_{f\sigma}\mathrm{d}\Phi/\mathrm{d}I_f$$
$$= (2pw_f k_{f\sigma}/c_w\Omega)\,(\mathrm{d}E/\mathrm{d}I_f)$$

is the dynamic self-inductance of the field winding, and $k_{f\sigma}$ is the mean leakage factor.

Generator buildup will take place at

$$E = f(I_f) > R_{f0}I_f$$

Then

$$dI_f/\mathrm{d}t > 0$$

and the current buildup will continue until $\mathrm{d}I_f/\mathrm{d}t$ becomes equal to zero (which happens at the intersection of the $V_f = I_f R_{f0}$ line and the open-circuit characteristic).

To define conditions for self-excitation of a d.c. generator loaded into a constant R_L (see Fig. 64-30*d*), let us write voltage equations for its loops:

$$V = E - R_a I_a, \quad V = R_{f0}I_f, \quad V = R_L I_a$$

and approximate the open-circuit characteristic with a parabola which passes through the point ($I_f = 0$, $E = E_{res} = c_E$):

$$E = a_E I_{f0}^2 + b_E I_{f0} + c_E$$

Recalling that

$$I_{f0} = I_f + c_a I_a$$

and writing I_{f0} as a function of voltage

$$I_{f0} = k_V V$$

where

$$k_V = 1/R_{f0} + c_a/R_L$$

we obtain the following quadratic voltage equation

$$a_{sh}V^2 + b_{sh}V + c_E = 0$$

where

$$a_{sh} = a_E k_V^2$$
$$b_{sh} = b_E k_V - R_a/R_L - 1$$

Thus, at the end of buildup, the terminal voltage is given by

$$V = \frac{-b_{sh} \pm \sqrt{b_{sh}^2 - 4a_{sh}c_E}}{2a_{sh}}$$

On putting $c_E = E_{res} = 0$ for simplicity, the roots of the above equation are found to be:

$$V = 0 \text{ and } V = -b_{sh}/a_{sh}$$

For buildup to be successful, that is, for a positive terminal voltage, $V > 0$, to be generated at $a_{sh} < 0$, it is essential that

$$b_{sh} = b_E k_V - R_a/R_L - 1 \geqslant 0$$

or

$$b_E R_L/(R_a + R_L - b_E c_a) \geqslant R_{f0} \qquad (64\text{-}73)$$

The above condition implies that the $V = f(I_f)$ characteristic plotted for constant R_L and $I_f = 0$ must go steeper than that of the field voltage. (It is an easy matter to check that the left-hand side of the above inequality is equal to $(dV/dI_f)_{I_f=0}$ at constant R_L.)

In a special case when $R_L = \infty$ and $I_a = 0$, the condition defined by (64-73) reduces to Eq. (64-71) derived for no load,

$$b_E = (dE/dI_f)_{I_f=0} \geqslant R_{f0}$$

For a series generator, when $R_{f0} = \infty$ and $I_f = 0$, Eq. (64-73) takes the form

$$b_E c_a - R_a \geqslant R_L$$

where

$$b_E c_a - R_a = (dV/dI_a)_{I_a=0}$$

is the slope of the $V = f(I_a)$ curve, and R_L is the slope of the load voltage,

$$V_L = R_L I_a$$

(b) External characteristics of a compound d.c. generator. The construction of the external characteristic, $V = f(I_a)$, of a differential-compound generator ($c_a < 0$) for constant

R_{f0} is shown in Fig. 64-37. The open-circuit characteristic is plotted for a given constant Ω. The field voltage is represented by the $R_f = R_{f0}I_f$ line. Assuming several values of armature current and varying the dimensions of the characteristic ("load") triangle abc ($a_1b_1c_1$) in proportion, we position the triangle so that point a lies on the V_f line, and point b on the open-circuit characteristic. Then the distance from point a to the axis of abscissae will give the value of V. The construction in Fig. 64-37 holds for $F_{a,d} < 0$ and $c_a < 0$. A similar construction for a cumulative-compound generator (one with its shunt and series field windings connected aiding, that is, with $c_a > 0$) is shown in Fig. 64-38.

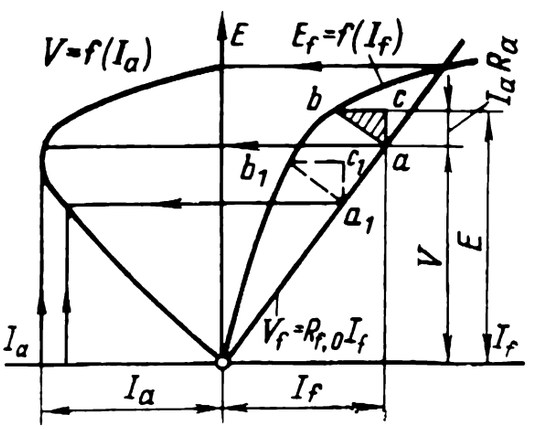

Fig. 64-37 External characteristic of a differential-compound generator ($c_a < 0$)

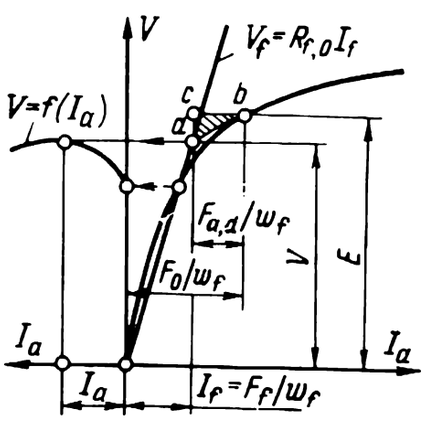

Fig. 64-38 External characteristic of a cumulative-compound generator ($c_a > 0$)

Using a parabolic approximation, it is an easy matter to derive an equation describing the external characteristic. To begin with, we write the voltage equation

$$V = a_E (I_f + c_a I_a)^2 + b_E (I_f + c_a I_a) + c_E - R_a I_a$$

express the field current in terms of terminal voltage

$$I_f = V/R_{f0} = VY_f$$

and solve the above equation for terminal voltage

$$V = (R_{f0}^2/2a_E) [-(b_E Y_f - 1) - 2a_E c_a Y_f I_a \pm \sqrt{(b_E Y_f - 1)^2 + 4a_E Y_f (Y_f R_a - c_a) I_a}] \quad (64\text{-}74)$$

On open circuit, that is, at $I_a = 0$, the terminal voltage is found to be solely dependent on the shape of the open-circuit characteristic (a_E, b_E) and the field resistance R_{f0}:

$$V_0 = -R_{f0} (b_E - R_f)/a_E \quad (64\text{-}75)$$

The shape of the external characteristic depends on the armature circuit resistance R_a and the coefficient c_a. When $c_a < R_a/b_E$ the characteristic takes the form shown in Fig. 64-37. When $c_a > R_a b_E$, it takes the form shown in Fig. 64-38. Here, R_a/c_a is the tangent of the angle b in the triangle abc, and

$$b_E = (\mathrm{d}E/\mathrm{d}I_f)_{I_f=0}$$

is the slope of the open-circuit characteristic at $I_f = 0$.

A fundamental difference between the two characteristics (one in Fig. 64-37 and the other in Fig. 64-38) consists in that in the former the emf (generated voltage) on load is smaller than the terminal voltage at no load, whereas in the latter the reverse is true. Accordingly, when $c_a < R_a/b_E$ the point b of the characteristic triangle lies on the open-circuit characteristic between $E = V_0$ and $E = E_{res} \approx 0$ (see Fig. 64-37), and for each value of armature current the triangle may take up any one of two positions each corresponding to a particular value of terminal voltage. This explains the unusual shape of the external characteristic in Fig. 64-37. As the load resistance decreases from $R_L = \infty$ (at no load or open-circuit), the decrease in current is accompanied by a decrease in voltage. At a certain value of load resistance, $R_{L,max}$, the current attains a maximum value,

$$I_a = I_{a,max}$$

As the load resistance keeps decreasing, $R_L < R_{L,max}$, both the current and voltage fall off, tending to zero at $R_L = 0$ (on short-circuit).

When $c_a > R_a/b_E$, point b lies on the open-circuit characteristic above point $E = V_0$ (see Fig. 64-38), and for each value of armature current the triangle abc may only take up one position corresponding to only one value of terminal voltage. Now the characteristic is not unlike that of a separately series-excited generator: on a short-circuit, when $R_L = 0$ and $V = 0$, the current attains a maximum value rather than drops to zero as it does in Fig. 64-37. It can be shown that when

$$R_a/b_E < c_a < R_a/(2R_{f0} - b_E)$$

the generator has a drooping external characteristic, whereas when

$$c_a > R_a/(2R_{f0} - b_E)$$

the generator has a rising external characteristic, as in Fig. 64-38: as the current rises, the voltage first goes up until it reaches a maximum value, then goes down.

(c) Armature and output characteristics of a compound d.c. generator. If we assume $I = I_a$, these characteristics will not differ from those of the same generator when its shunt field winding is energized from a separate d.c. source.

(iii) Parallel Operation of D.C. Generators

Direct-current generators may be brought in for parallel operation, if their terminal voltages and terminal polarities are the same,

$$V_1 = V_2$$

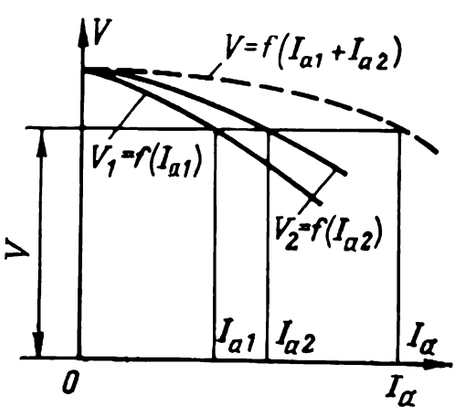

Fig. 64-39 Current sharing between paralleled generators

Before the incoming generator may be put on line, it is important to check that the voltage difference is zero

$$V_1 - V_2 = \Delta V = 0$$

The current distribution between the generators operating in parallel depends on the shape of their external characteristics (Fig. 64-39). Assuming several values of terminal voltage,

$$V = V_1 = V_2$$

we can find I_{a1} and I_{a2}, the total load current

$$I_a = I_{a1} + I_{a2}$$

and the relation

$$I_{a1}/I_{a2} = f(I_a)$$

or

$$I_{a1}/I_{a2} = f(V)$$

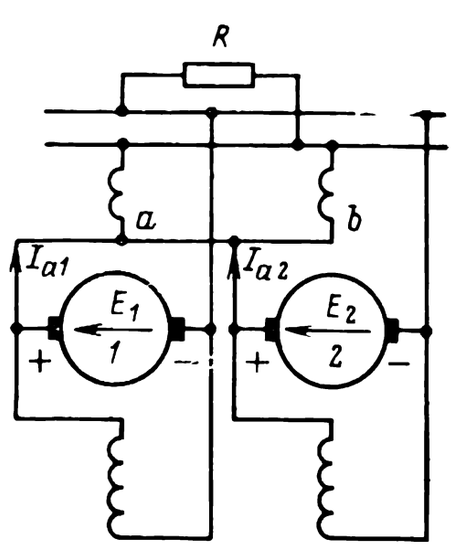

Fig. 64-40 Compound-wound generators in parallel

As a rule, identical generators are used for parallel operation. Then they will take the same share of total load, that is,

$$I_{a1}/I_{a2} = 1$$

if their external characteristics are identical.

When cumulative-compound generators (those with $c_a > 0$) are connected for parallel operation, their performance may prove unstable (if there is no connection between points

a and *b* in Fig. 64-40). This instability manifests itself in that with a chance increase in I_{a1} (and a decrease in I_{a2}), the mmf of the series winding will cause E_1 to rise (and E_2 to fall). This will lead to a further increase in I_{a1} and a further decrease in I_{a2}. This form of instability can be avoided by placing an electric connection between points *a* and *b* (see Fig. 64-40) which ensure an equal distribution of current between the series windings of identical generators.

64-13 D.C. Motors

Direct-current motors may have the same excitation forms as electromagnetically excited d.c. generators. Most fre-

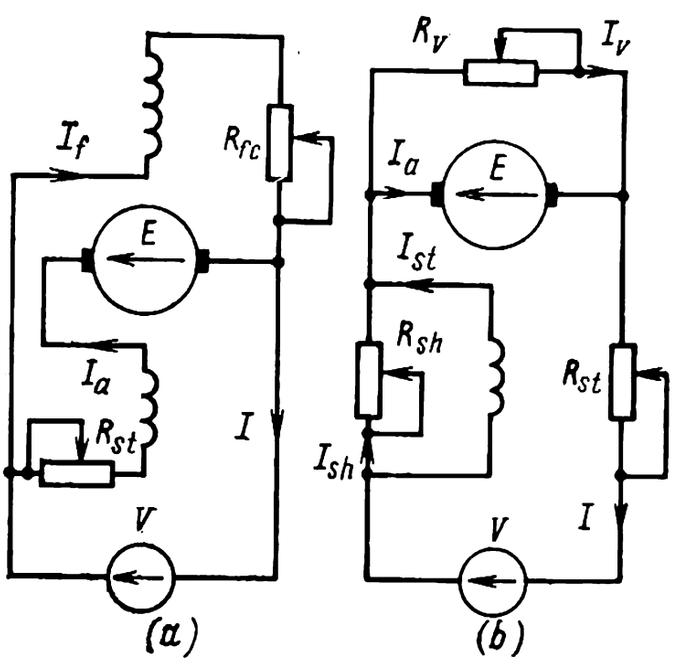

Fig. 64-41 Electromagnetically excited d.c. motors: R_{fc} = field-control rheostat in the shunt winding; R_{sh} = rheostat shunting the series winding; R_s = starting rheostat; R_V = rheostat shunting the armature

quently, however, they are built as compound motors (Fig. 64-41*a*) and series motors (Fig. 64-41*b*). They differ from the corresponding generator designs only in that they have additional rheostats for starting and speed control.

(i) Starting

When a d.c. motor is started "direct-on-line" from standstill, a current begins to flow in its armature circuit

$$I_a = V/R_a$$

where V is the supply voltage and R_a is the armature circuit resistance.

Should $V = V_R$, the field current will exceed the rated armature current tens of times. Therefore, direct-on-line start may only be used for motors with ratings not over several hundred watts. In all other motors, the armature current at starting is limited by a starting rheostat R_s placed in series with the armature (see Fig. 64-41). The initial value of this rheostat, $R_s = R_{s0}$, at $\Omega = 0$ is chosen such that the initial starting current

$$I_{a0} = \frac{V}{R_a + R_{s0}}$$

is 1 to 1.5 times the rated armature current.

At the end of all transients, the currents flowing in the machine's windings, namely I_{a0} and $I_f = V/R_{f0}$, set up a magnetic flux Φ_0. When the initial electromagnetic torque

$$T_{emo} = c_0 I_{a0} \Phi_0$$

exceeds the initial external (load) torque, T_{ext}, the armature sets in motion and picks up speed with an angular acceleration given by

$$d\Omega/dt = (T_{em,0} - T_{ext,0})/J$$

where J is the moment of inertia of the rotating parts of the machine.

In the motor mode of operation, the emf opposes both I_a and V. Therefore, for the armature current in a running motor

$$I_a = (V - E)/(R_a + R_s)$$

to be sufficiently large (1 to 1.5 times $I_{a,R}$), R_s must be gradually reduced as Ω and E increase. This should be done so that at any instant during a start the difference between the electromagnetic torque, $T_{em} = c_w I_a \Phi$, and the external torque, T_{ext}, controlling the acceleration, $d\Omega/dt = (T_{em} - T_{ext})/J$ is sufficiently large.

To obtain a sufficiently large T_{em} and to cut down the starting time, it is usual to pass maximum safe currents in the shunt and series field windings (in Fig. 64-41, $R_{fc} = 0$ and $R_{sh} = \infty$). By the instant when the starting is completed the starting rheostat is fully brought out of circuit ($R_s = 0$), and the rheostats in the series and shunt field circuits (R_{fc} and R_{sh}) are adjusted so that the desired torque is obtained, $T_{em} = T_{ext}$, at the desired rpm.

(ii) Steady-State Characteristics of a D.C. Motor

The performance of a d.c. motor in a steady state is primarily described by its speed-torque characteristic, $\Omega = f(T_{em})$ plotted for constant V, R_{fc}, R_{sh} and R_V (see Fig. 64-41).

The equation of the speed-torque characteristic is derived by considering together the emf equation (64-15), the voltage equation (64-47) and the electromagnetic torque equation (64-20) which in the motor mode of operation, are re-written for positive current.

$$\Omega = (V - R_a I_a)/c_w\Phi = V/c_w\Phi - R_a T_{em}/c_w^2\Phi^2 = f(T_{em}) \quad (64\text{-}76)$$

where $\Phi = f(I_a)$.

Also, an idea about the performance of a d.c. motor can be gleaned from its speed-vs-armature current characteristic, $\Omega = f(I_a)$, written in the form of Eq. (64-76) and its torque-vs-armature current characteristic, $T_{em} = f(I_a)$, identical with Eq. (64-20).

To determine the relation $\Phi = f(I_a)$ which enters all of the above characteristics, we should go back to Sec. 64-9 and recall the notes made at the start of Sec. 64-12. The flux should preferably be determined from the open-circuit characteristic at rated mechanical angular velocity Ω_R, that is,

$$E_0 = f(I_f)$$

rather than from the magnetization curve, because

$$\Phi = f(I_f) = E_0/(c_w\Omega_R)_0$$

Then the flux may be defined, using the parabolic approximation found from Eq. (64-33) for a part of the open-circuit characteristic

$$E_0 = a_E(I_f + c_a I_a)^2 + b_E(I_f + c_a I_a) + c_E = f(I_f, I_a) \quad (64\text{-}77)$$

and the equations of the speed-torque and speed-current characteristics may be written as

$$\Omega = \frac{(V - R_a I_a)}{E_0}\Omega_R = (\Omega_R/E_0)(V - R_a T_{em}\Omega_R/E_0) \quad (64\text{-}78)$$

where $T_{em} = I_a E_0/\Omega_R$

The best way to find the characteristics of d.c. motors is with the aid of a computer, especially when a family of curves is to be obtained. In cases where the characteristics are to be found over a wide range of voltage values, the accuracy can be enhanced by dividing the open-circuit characteristic into two or three parts and by approximating each part with a parabola of its own.

In finding the steady-state mechanical angular velocity of a d.c. motor, it is important to consider the speed-torque characteristics of both the driving motor and the driven machine or tool. The steady-state speed will be at the intersection of the two curves. As has been shown for induction motors, the operation will be steady, if

$$\mathrm{d}T_{\mathrm{ext}}/\mathrm{d}\Omega > \mathrm{d}T_{\mathrm{em}}/\mathrm{d}\Omega$$

With a constant external torque and $\mathrm{d}T_{\mathrm{ext}}/\mathrm{d}\Omega = 0$, the motor will give a stable performance if it has a drooping speed-torque characteristic, that is, when an increase in T_{em} brings about a decrease in speed, and

$$\mathrm{d}T_{\mathrm{em}}/\mathrm{d}\Omega < 0 = \mathrm{d}T_{\mathrm{ext}}/\mathrm{d}\Omega$$

(iii) Compound-Wound D.C. Motor

(a) Characteristics. Using Eqs. (64-77) and (64-78), it is an easy matter to write the torque-vs-armature current and speed-vs-armature current characteristics of a compound d.c. motor in analytical form

$$T_{\mathrm{em}} = I_{\mathrm{a}}E_0/\Omega_{\mathrm{R}} = (I_{\mathrm{a}}/\Omega_{\mathrm{R}})\,(a_0 I_{\mathrm{a}}^2 + b_0 I_{\mathrm{a}} + c_0) \qquad (64\text{-}79)$$

$$\Omega = (V - R_{\mathrm{a}}I_{\mathrm{a}})\,\Omega_{\mathrm{R}}/(a_0 I_{\mathrm{a}}^2 + b_0 I_{\mathrm{a}} + c_0) \qquad (64\text{-}80)$$

where

$$a_0 = a_E c_{\mathrm{a}}^2$$

$$b_0 = 2a_E c_{\mathrm{a}} I_f + b_E c_{\mathrm{a}}$$

$$c_0 = a_E I_f^2 + b_E I_f + c_E = E_{f0}$$

In the above equations, the coefficient c_0 has the meaning of E_{f0} due to I_f at $I_{\mathrm{a}} = 0$ and $\Omega = \Omega_{\mathrm{R}}$.

It is difficult to derive the speed-torque characteristic of a compound motor in canonical form, that is, as the relation $\Omega = f(T_{\mathrm{em}})$, because this would necessitate solving the cubic equation (64-79) for I_{a}. However, in parametric form,

the speed-torque characteristic is in effect described by Eqs. (64-79) and (64-80) where I_a is the independent variable.

For insight into the effect of the various variables, it is convenient to write Eqs. (64-79) and (64-80) in per unit, the base quantities being V_R, $I_{a,R}$, Ω_R, and

$$T_{em,b} = I_{a,R} V_R / \Omega_R$$

denoting $I_{f,b}$ the field current corresponding to the rated voltage at no load ($I_a = 0$) and rated mechanical angular velocity, Ω_R.

After re-arranging Eqs. (64-79) and (64-80), the per-unit torque and the per-unit velocity can be written as functions of per-unit current

$$T_{*em} = T_{em}/T_{em,b} = I_{*a}\,(a_{*0} I_{*a}^2 + b_{*0} I_{*a} + c_{*0}) \qquad (64\text{-}81)$$

$$\Omega_* = \Omega/\Omega_R = (V_* - R_{*a} I_{*a})/(a_* I_{*a}^2 + b_* I_{*a} + c_{*0}) \qquad (64\text{-}82)$$

where

$$I_{*a} = I_a/I_{a,R} \qquad a_{*0} = a_{*E} c_{*a}^2$$

$$V_* = V/V_R \qquad b_{*0} = c_{*a}\,(2a_{*E} I_{*f} + b_{*E})$$

$$R_{*a} = R_a I_{a,R}/V_R \qquad c_{*0} = E_{*f0} = E_{f0}/V_R = a_{*E} I_{*f}^2 + b_{*E} I_{*f} + c_{*E}$$

$$a_{*E} = a_E I_{f,b}^2/V_R \qquad c_{*E} = c_E/V_R$$

$$b_{*E} = b_E I_{f,b}/V_R \qquad c_{*a} = c_a I_{a,R}/I_{f,b}$$

The coefficient c_{*a} is the mmf due to the initial armature current

$$F_{ad,R} = w_f c_a I_{a,R}$$

expressed as a fraction of the base field mmf

$$F_{f,b} = w_f I_{f,b}$$

that is,

$$c_{*a} = F_{ad,R}/w_f I_{f,b}$$

where

$$F_{ad,R} = \pm F_{s,R} - F_{qd,R}$$

(see Sec. 64-9 and Eq. (64-54)).

Figure 64-42 shows a family of per-unit speed-torque characteristics, $\Omega_* = f(T_{*\mathrm{em}})$ plotted on the basis of the data given in Example 64-11. For all the curves, V_*, I_{*f}, $R_{*\mathrm{a}}$, a_{*E}, b_{*E} and c_{*E}, are taken the same, and the difference between them is solely due to variations in $c_{*\mathrm{a}}$ characterizing the effect of $F_{\mathrm{a}d}$, the direct-axis mmf of the armature.

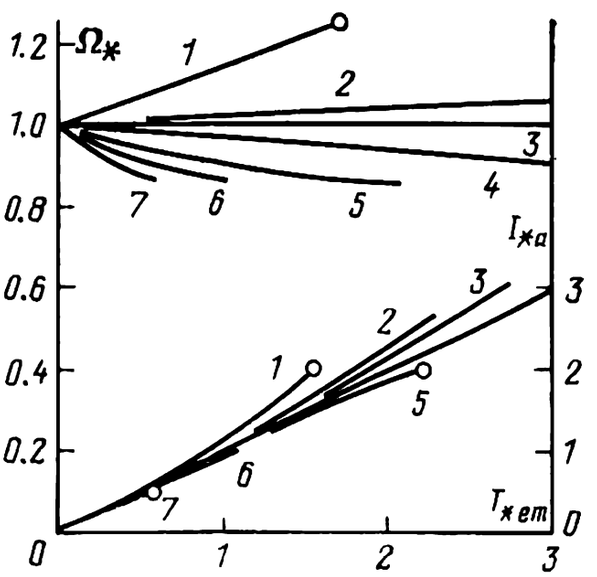

Fig. 64-42 Speed-torque characteristics of compound-wound motor (curves *1*, *2*, *3*, *4*, *5*, *6*, and *7* correspond to $c_{\mathrm{a}} = -0.2$ or -0.1; $c_{\mathrm{a}\Omega} = -0.063, 0, 0.2, 0.6$, and 1.0)

In a cumulative-compound motor ($c_{*\mathrm{a}} > 0$), an increase in $I_{*\mathrm{a}}$ brings about an increase in the flux

$$\Phi \approx E_{*0} = a_{*0}I_{*\mathrm{a}}^2 + b_{*0}I_{*\mathrm{a}} + c_{*0}$$

and drooping speed-torque curves are obtained,

$$(\mathrm{d}\Omega_*/\mathrm{d}T_{*\mathrm{em}})_{I_{*\mathrm{a}}=1} < 0$$

Conversely, for a differential-compound motor ($c_{*\mathrm{a}} < 0$), rising characteristics (curves *1* and *2*) are obtained. A transition from drooping to rising characteristics occurs at $c_{*\mathrm{a}\Omega}$

$$= \frac{V_*(2a_{*E}+b_{*E}) - \sqrt{V_*^2(2a_{*E}+b_{*E})^2 + 4R_{*\mathrm{a}}E_{*f0}a_{*E}(1-2V_*)}}{2a_{*E}(1-2V_*)}$$

$$\approx -\frac{R_{*\mathrm{a}}E_{*f0}}{V_*(2a_{*E}I_{*f} + b_{*E})} < 0 \qquad (64\text{-}84)$$

which corresponds to curve *3* with a slope equal to

$$(\mathrm{d}\Omega_*/\mathrm{d}T_{*\mathrm{em}})_{I_{*\mathrm{a}}=1} = 0$$

(In deriving Eq. (64-83), the derivative $\mathrm{d}\Omega_*/\mathrm{d}T_{*\mathrm{em}} = (\mathrm{d}\Omega_*/\mathrm{d}I_{*\mathrm{a}})/(\mathrm{d}T_{*\mathrm{em}}/\mathrm{d}I_{*\mathrm{a}})$ is found by differentiating Eqs. (64-81) and (64-82).)

Thus, cumulative-compound motors ($c_{\mathrm{a}} > c_{\mathrm{a}\Omega}$) have drooping speed-torque characteristics which are conducive to a stable running (see item (b) below).

As the number of turns in the series winding of a cumulative-compound motor is increased ($c_{*\mathrm{a}}$ increases), the speed-

torque characteristic becomes increasingly more drooping. However, compound motors are most often employed in drives which are required to give a constant rpm and a variable torque. Therefore, in general-purpose compound motors every effort is made to obtain a maximally flat response*.

To this end, the number of turns in the series field winding is chosen such that its mmf balances out the demagnetizing effect of the armature mmf. Then, $c_{*a} \approx 0$, and the mechanical angular velocity falls but little as the load is increased from its no-load to full (rated value):

$$\Omega_{I_{*a}=-1}/\Omega_{I_{*a}=0} = 1 - R_{*a} \approx 0.9 \text{ to } 0.97$$

Shunt and differential-compound motors ($c_a \leqslant c_{a\Omega}$) have rising speed-torque characteristics which do not ensure a stable performance.

Example 64-11. For a compound motor with $V_R = 500$ V, $I_{a,R} = 1000$ A, $I_{f,b} = 28.7$ A, $F_{qd,R} = 1000$ A, $w_f = 349$, $R_a = 0.015\Omega$, $a_E = -0.2464\,\text{V/A}^2$, $b_E = 22\,\text{V/A}$, and $c_E = 71.8$ V, construct per-unit speed-torque characteristics for $V = 506.5$ V, $I_f = 29.5$ A, and various numbers of turns in the series field winding: $w_s = 1$ (differential compounding), and 0, 1, 3, 7, and 11 (cumulative compounding).

Solution. Using Eq. (64-83),

$$a_{*E} = -0.2464 \times 28.7^2/500 = -0.405$$

$$b_{*E} = 22 \times 28.7/500 = 1.26$$

$$c_{*E} = 71.8/500 = 0.1436$$

and also

$$V_* = 506.5/500 = 1.013$$

$$I_{*f} = 29.5/28.7 = 1.03$$

$$R_{*a} = 0.015 \times 1000/500 = 0.03$$

$$c_{*0} = E_{*f0} = -0.405 \times 1.03^2 + 1.26 \times 1.03 + 0.1436 = 1.013$$

---

* The flatness of a speed-torque characteristic is expressed in terms of *speed regulation*, that is, the change in speed when the load is increased from no-load to full value divided by no-load speed, at constant I_f and V.

$$(\Omega_{I_{a*=0}} - \Omega_{I_{*a=1}})/\Omega_{I_{*a=0}}$$

The values of c_{*a}, a_{*0} and b_{*0}, which are functions of the number of turns in the series field winding, are tabulated below.

w_s	1 (diff. comp)	0	(1/k)*	1 (cumulative compounding)	3	7	11
c_{*a}	−0.2	−0.1	−0.0626	0	0.2	0.6	1.0
a_{*0}	−0.016	−0.00405	−0.00159	0	−0.016	−0.146	−0.405
b_{*0}	−0.0854	−0.0427	−0.0267	0	0.0854	0.256	8.427
Curve in Fig .64-42	*1*	*2*	*3*	*4*	*5*	*6*	*7*

* Non-real for any integer k.

The no-load mechanical angular velocity (in per-unit) is $\Omega_{*(I_a=0)} = 1.013/1.013 = 1.0$

The per-unit armature current-vs-torque characteristics, $I_{*a} = f(T_{*em})$ constructed by Eq. (64-81) and the per-unit speed-torque characteristics, $\Omega_* = f(T_{*em})$ constructed by Eqs. (64-81) and (64-82) are given in Fig. 64-42. It also shows the characteristics found for $c_{*a\Omega} = -0.0626$, as calculated by Eq. (64-84).

(b) Speed control. This is done by varying I_f or V. The simplest way to control speed is to vary the field current with a field rheostat, R_{fc} (see Fig. 64-41*a*):

$$I_f = V/(R_f + R_{fc})$$

As I_f is decreased, the magnetic flux, $\Phi = f(I_f)$, and E_0 proportional to Φ and given by Eq. (64-77), are also decreased. At constant armature voltage, this leads to an increase in Ω (see Eqs. (64-76), (64-78), and (64-80)). As a function of I_f, the per-unit no-load angular velocity is found from Eq. (64-82)

$$\Omega_{*(I_a=0)} = \Omega/\Omega_R = V_*/E_{*f0} = V_* \ (a_{*E}I_{*f}^2 + b_{*E}I_{*f} + c_{*E})$$

where $I_{*f} = I_f/I_{f,b}$

If V, T_{em} and I_f are known, the angular velocity on load will be given by the intersection of the constant T_{em} line with the speed-torque characteristic plotted by Eqs. (64-81)

and (64-82) for constant armature voltage and field current.

Motors are designed so that they will give a stable performance at any angular velocity over the specified speed control range. On the other hand, a decrease in I_f leads to an increase in $F_{qd,R}$,* which is accompanied by a decrease in c_{*a} (see Eq. (64-83)) and an increase in the slope of the speed-torque characteristic

$$(d\Omega_*/dT_{*em})_{I_{*a}=0} = \frac{-R_{*a}E_{*f} - V_*(b_{*E} + 2a_{*E}I_{*f})c_{*a}}{E_{*f}^3} \quad (64\text{-}85)$$

Therefore, a decrease in field current might make the characteristic flatter, so that at $I_f = I_{f,R}$ (curve *2* in Fig. 64-43), a drooping speed-torque characteristic could at, say, $\Omega_* \approx 1.5$, become a rising one (curve *4*), which is not conducive to stable performance. To avoid this, the number of turns in the series field winding must be increased so that at any required angular velocity F_{qd} could be balanced and c_{*a} could be positive. For example, if in a motor which has speed-torque characteristics represented by curves *2* and *4* (c_{*a} being 0 and —0.05, respectively) at $w_s = 1$ and $V = V_R$, we make $w_s = 2$, its characteristics will be curves *1* and *3* (c_{*a} becoming 0.05 and 0, respectively), and the motor will give a stable performance in the speedrange 1 : 1.5.

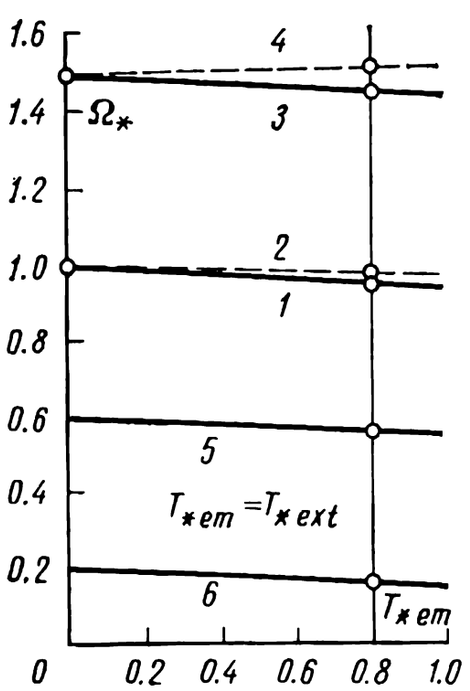

Fig. 64-43 Speed-torque characteristics of a compound-wound motor for several constant values of V_* and I_{*f}

With the above method, speed is controlled upwards from the rated value. The limits of control are set by the commutation conditions.

Speed control downwards from the rated value is effected by reducing the armature voltage, V. As follows from

* It should be stressed that for each value of I_f differing markedly from the base value, $F_{qd.R}$ must be found separately as explained in Sec. 64-9.

Eq. (64-82), the angular velocity at no load is proportional to armature voltage, $\Omega_* = V_*/E_{f0*}$ (with I_{*f} held constant). At load, the angular velocity is determined by the intersection of the constant T_{em} line with the speed-torque characteristics plotted on the basis of Eqs. (64-81) and (64-82) for constant V_* and I_{*f}. Curves *1*, *5*, and *6* in Fig. 64-43 represent the speed-torque characteristics of a motor for $V_* = 1$, 0.6, 0.2, and for $I_{*f} = I_{*f;R}$. As follows from Eq. (64-85), a decrease in V_* leads to an increase in the slope of the characteristics (the slope becomes less negative), but the characteristics remain drooping and their flatness even decreases. In this way, speed can be varied from rated to zero.

How economical speed control by voltage reduction can be depends on the manner in which it is effected. If this is done with a rheostat placed in the armature circuit, the efficiency decreases in proportion to the armature voltage and angular velocity

$$\eta_V = V/V_s = \Omega/\Omega_s$$

where V is the armature voltage, V_s is the supply voltage, Ω is the angular speed at V, and Ω_s is the angular speed at V_s. If the supply voltage comes from a regulated (stabilized) d.c. supply (such as a rotary or static converter), the loss is the sum of the loss in the motor and converter. Therefore, although the efficiency decreases as the speed goes down, it remains higher at any angular velocity than when speed control is effected with a rheostat in the armature circuit.

(iv) Series-Wound D.C. Motors

In a series-wound d.c. motor, the field is established solely by the armature current (see Fig. 64-41$_b$). As the load and armature current increase, the flux builds up, and the angular velocity which is inversely proportional to the flux goes down by an appreciable amount [see Eq. (64-76)]. Such motors are mainly employed as drives for traction, hoisting and conveyance. Their speed-torque characteristic is such that the motor will automatically slow down as its torque increases (say, in moving uphill) and pick up speed as its torque decreases (say, in moving downhill).

(a) Characteristics. In per-unit, the speed-torque and current-torque characteristics of a series-wound motor can be described by Eqs. (64-81) and (64-82) derived for compound motors. In calculating the coefficients in the above equations,

(1) deem the shunt-winding current equal to zero;

(2) use as the base quantities the current in the series field winding, $I_{s,b}$, and the series-winding mmf, $w_s I_{s,b}$, such as will induce $E = V_R$ at no load and at $\Omega = \Omega_R$.

Because some of the armature current divides into R_{sh} (see Fig. 64-41*b*), the resultant *d*-axis mmf is

$$F_0 = F_s - F_{qd}$$
$$= w_s I_a R_{sh}/(R_s + R_{sh}) - F_{qd}$$

In per-unit,

$$F_{*0} = F_0/w_s I_{s,b} = c_{*a} I_{*a} \qquad (64\text{-}86)$$

where

$$c_{*a} = F_{0,R}/w_s I_{s,b}$$
$$= \frac{R_{sh} I_{a,R}}{(R_{sh} + R_s) I_{s,b}} - \frac{F_{qd,R}}{w_s I_{s,b}}$$

is the resultant rated armature mmf as a fraction of the series-winding mmf.

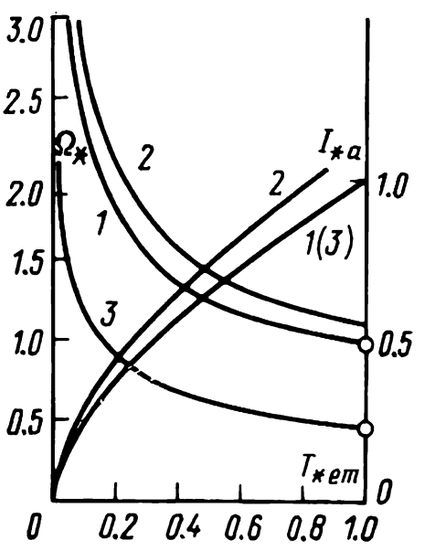

Fig. 64-44 Speed-torque and armature current-torque characteristics of a series-wound motor: *1* — $V_* = 1$; $c_{sh} = R_{sh}/(R_{sh} + R_s) = 1$; *2* — $V_* = 1$, $c_{sh} = 0.725$; *3* — $V_* = 0.5$, $c_{sh} = 1$

If we approximate the open-circuit characteristic, $E = f(I_s)$ at rated angular velocity by a parabola

$$E = a_E I_s^2 + b_E I_s + c_E$$

and assume that the shunt-winding current is zero, the following equations can be written with the aid of Eq. (64-83) for the coefficients in Eqs. (64-81) and (64-82):

$$a_{*0} = a_E I_{s,b}^2 c_{*a}^2/V_R$$
$$b_{*0} = b_E I_{s,b} c_{*a}/V_R \qquad (64\text{-}87)$$
$$c_{*0} = c_E/V_R$$

Figure 64-44 shows a family of speed-torque characteristics plotted on the basis of Eqs. (64-81) and (64-82) for the motor in Example 64-12. In all the characteristics, R_{*a}, a_{*0},

b_{*0} and c_{*0} are taken the same, and the difference between them is solely due to variations in V_* and c_{*a} (changes in R_{sh}).

In all cases, the characteristics have high slope. At $T_{em} = 0$, the angular velocity might (theoretically) increase to infinity. Therefore, to avoid damage due to centrifugal forces, series-wound motors cannot be operated at no load.

The same figure shows per-unit armature current-vs-torque characteristics for various values of c_{*a} and V_*.

Example 64-12. For a series-wound motor with V_R 500 V, $I_{a,R} = 1000$ A, $w_s = 11$, $F_{s,b} = 910$ A, $F_{qd,R} = 980$ At, $R_a = 0.015$ Ω, $a_E = -0.000244$ VA^{-2}, $b_E = 0.692$ V/A, $c_E = 71.8$ V, construct per-unit speed-torque characteristics for $V = 500$ V, $c_{sh} = R_{sh}/(R_{sh} + R_s) = 1$; $V = 250$ V, $c_{sh} = 1$; $V = 500$ V and $c_{sh} = 0.725$.

Solution. Using Eqs. (64-80) and (64-87) and assuming $c_{sh} = 1$, we find:

$$c_{*a} = 1000/910 - 980/(910 \times 11) = 1.0$$

$$a_{*0} = -0.000244 \times 910^2 \times 1^2/500 = -0.405$$

$$b_{*0} = 0.692 \times 910 \times 1/500 = 1.26$$

$$c_{*0} = 71.8/500 = 0.143$$

For $c_{sh} = 0.725$, we obtain:

$$a_{*0} = -0.000244 \times 910^2 \times 0.7^2/500 = -0.198$$

$$c_{*a} = 1000 \times 0.725/910 - 980/(910 \times 11) = 0.7$$

$$b_{*0} = 0.692 \times 910 \times 0.7/500 = 0.882$$

$$c_{*0} = 0.143$$

The $\Omega_* = f(T_{*em})$ and $I_{*a} = f(T_{*em})$ curves based on Eqs. (64-81) and (64-82) and plotted for the above values of coefficients are shown in Fig. 64-44.

(b) Speed control. For this type of motor, speed control is effected by varying the current in the series field winding, I_s, or the armature voltage, V. To reduce the series field current, some of the armature current is divided into a shunt, R_{sh} (see Fig. 64-41*b*):

$$I_s = I_a R_{sh}/(R_{sh} + R_s)$$

Because this leads to a reduction in c_{*a}, a_{*0} and b_{*0} [see Eqs. (64-86) and (64-87)], the flux Φ also decreases and so does

$$E_{*0} = a_{*0}I_{*a}^2 + b_{*0}I_{*a} + c_{*0}$$

which is proportional to flux, and the mechanical angular velocity Ω_* goes up. The speed-torque characteristics plotted for $R_{sh}/(R_{sh} + R_s) = 0.75$ and $V = V_R$ (curve *2*) runs above the one plotted for $R_{sh}/(R_{sh} + R_s) = 1$ and $V = V_R$ (curve *1*). The range of speed control by shunting the series field winding is limited by commutation conditions.

The angular velocity of the motor can be brought down by reducing the armature voltage, V. The speed-torque curve plotted for $R_{sh}/(R_{sh} + R_s) = 1$ and $V_* = 0.5$ (curve *3*) runs below that for $R_{sh}/(R_{sh} + R_s) = 1$ and $V_* = 1$ (curve *1*). Speed control by armature voltage reduction can give any angular velocity from rated to zero. As regards the economy of this method of speed control, everything said with respect to compound motors holds.

☆ 64-14 A Brief Outline of Soviet Made D.C. Machines

Soviet makers turn out all the types of d.c. machines discussed in the previous sections. Except for very large units in the topmost rating bracket (mainly motors and generators used in drives for rolling mills), they are produced in quantity.

As is customary, the bulk of machine output falls in a standard range covering all the desired ratings and speeds. In addition, special-purpose machines are available commercially, such as motors for traction, hoisting, conveyance, marine service, car accessories, aircraft, automatic control, and the like.

A general-purpose industrial d.c. motor is shown in Fig. 64-45.

In general-purpose d.c. machines, speed control is effected by weakening the main-pole field, so that the ratio top-speed/base-speed can be as great as 2/1. They have a shunt field winding and a small stabilizing winding. They are built into a protected enclosure and have a flat speed-torque characteristic.

Special-purpose d.c. motors are of enclosed construction. They come with a gamut of speed-torque characteristics and

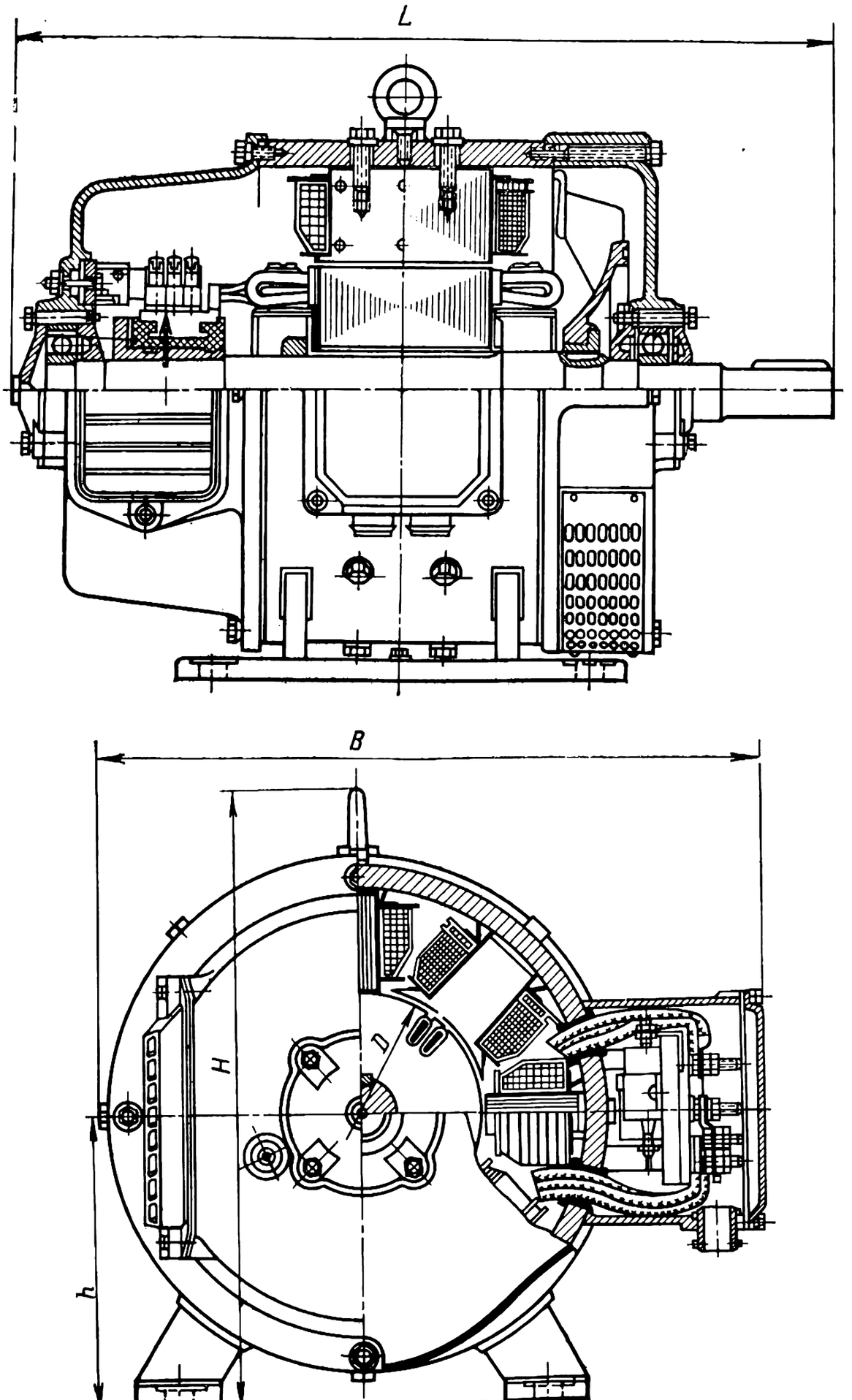

Fig. 64-45 14-kW, 220-V, 1500-rpm d.c. motor

a wide range of speed control which can be effected not only by weakening the main-pole field, but also by varying the armature voltage.

General-purpose d.c. generators are shunt- or compound-wound and have a flat external characteristic. They serve to feed d.c. motors and control circuits, and as exciters for large d.c. generators.

Special purpose d.c. generators are employed as battery chargers, supply sources for special-purpose d.c. motors, etc.

The standard range of d.c. machines is divided into three groups as follows:

—machines with ratings from 0.3 to 200 kW (sizes 1 through 11)

—machines with ratings from 200 to 1400 kW (sizes 12 through 17)

—machines with ratings above 1400 kW (sizes 18 through 26).

Sizes 1 through 11 include both general- and special-purpose motors and generators. Their performance and other data are summarized in Table 64-1.

If not otherwise specified, the machines come in splash-proof enclosures (see Fig. 64-45); motors also come in enclosed construction (see Sec. 33-2).

The rated voltage for motors is 110 V, 220 V, or 440 V; for general-purpose generators, 115 V, 230 V, and 460 V.

Machines in sizes 12 through 17 have ratings from 55 kW at 300 rpm to 1400 kW at 1000 rpm. Motors in these sizes are intended for use as drives of rolling mills, large metal-cutting machine-tools, and similar applications.

All d.c. motors of sizes 12 through 17 have a compensating winding. Generators may be compensated or uncompensated. They are built protected or enclosed (generators may also be of open construction). The rated voltage for motors in sizes 12 through 17 is 220 V, 330 V, 440 V, or 660 V. The rated speed is 300 rpm, 400 rpm, or 500 rpm. For generators in the above sizes, the rated voltage is 230 V, 330 V, 460 V, or 660 V, and their speed is 1000 rpm.

Machines in sizes 18 through 22 are rated from 460 kW at 24 rpm to 5400 kW at up to 750 rpm. This size bracket also includes special-purpose motors used in drives of metal-making plant. The machines are of enclosed construction, forced-ventilated from a separate blower.

Table 64-1 Basic Data of Standard-Range Motors (1500 rpm) and Generators (1450 rpm)

Size designation	Motors		Generators		Dimensions, mm (Fig. 64-45)					J, kg/m²	Weight, kg
	P_R, kW	Efficiency, %	P_R, kW	Efficiency, %	*B*	*L*	*H*	*h*	*D*		
12	.45	70	—	—	348	397	210	112	83	.0037	23.5
22	1	76.5	—	—	447	458	310	140	106	.013	44.0
32	2.2	83.5	—	—	493	541	336	150	120	.29	67.5
42	4.5	80.5	—	—	537	569	355	160	138	.45	80
52	8.0	84.5	—	—	620	639	400	180	162	.1	124
62	14	86.5	—	—	694	662	484	225	195	.16	187
72	25	85.5	—	—	882	847	540	250	210	.4	330
82	42	88.0	35	87.5	975	892	600	280	245	.775	435
92	75	89.0	70	89.0	990	1187	694	315	294	1.75	705
102	125	90.0	110	90.5	1095	1304	783	355	327	3.0	985
112	200	91.0	190	92.5	1200	1447	884	400	368	5.75	1370

Notes: P_R = power rating (for generators, electric power delivered to the system) for motors, mechanical power available at the shaft). J = moment of inertia of the rotating parts; B = width, L = length, H = height of a machine; h = shaft height; D = outside diameter. The size designation gives (1) the standard size code (the first numeral) and (2) the standard length code (the second numeral).

65 Special-Purpose D. C. Machines

65-1 Permanent-Magnet D.C. Machines

Permanent-magnet d.c. (PMDC) machines are those which use permanent magnets for excitation. Obviously, their magnetic system differs from that of electromagnetically excited machines. The likely designs of PMDC machines (less the field windings) are shown in Fig. 65-1. The designs in Fig. 65-1*a*, *b* and *c* using radial permanent magnets are advantageous in multipolar machines with $2p \geqslant 4$. Because the permanent magnets are short along the lines of flux, these designs are prone to suffer from the demagnetizing effect of the armature mmf. One way to minimize this effect is to make the permanent magnets from materials having a high coercive force (ferrite-barium magnets) and to fit them with pole-shoes from magnetically soft materials (as in Fig. 65-1*a*). The design in Fig. 65-1*c* is especially attractive for cases where $2p = 2$, and the tangentially disposed permanent magnets have an appreciable length in the direction of magnetization. In such cases, use may be made of materials having a relatively small coercive force, but a large specific energy (Alni, Alnico, Magnico). The same goes for the design in Fig. 65-1*d* where the magnetic system is a suitably magnetized ring from a magnetically hard material. An advantage of this design is structural simplicity; a disadvantage is an impaired commutation because of the small air gap along the q-axis and an increased armature field.

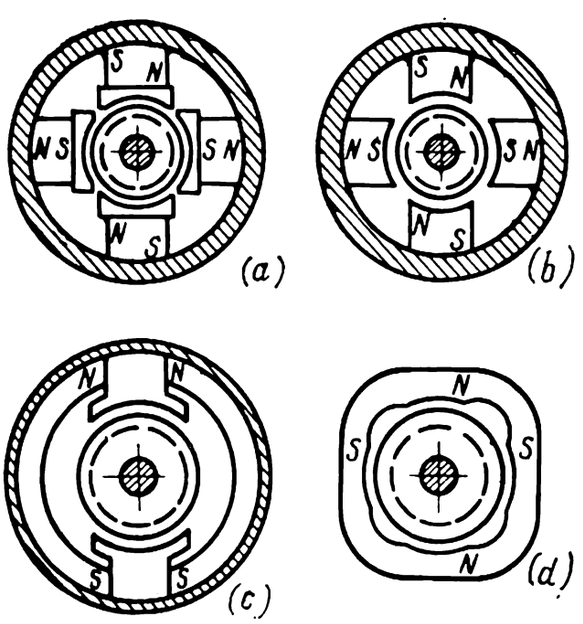

Fig. 65-1 Magnetic circuits of permanent-magnet d.c. (PMDC) machines: *a*—radial magnets with pole-shoes; *b*—same, without pole-shoes; *c*—tangential magnets; *d*—ring magnets

The materials that go to make permanent magnets are the same as are used for permanent-magnet synchronous machines (see Sec. 63-6).

No commutating (or intermediate) poles are used in

PMDC machines, as they must be excited electromagnetically for fundamental reasons.

PMDC motors with ratings from a few watts to hundreds of watts are widely used in low-power drives for cars, aircraft, and automatic control systems. Most frequently, they operate in short-time or intermittent duty. They are started and reversed without any rheostats in the armature circuits. Their speed is controlled by varying the armature voltage, although pulse speed control is also used. Pulse speed control is effected with a relay controlled by a tachogenerator which periodically shorts out a series resistor in the armature circuit. Larger PMDC motors use combined excitation. In such a case, a PMDC motor is fitted with a field winding whose mmf is sufficient to control the magnetic field within the desired limits.

PMDC generators have found a more limited field of application than their synchronous counterparts. Notably, they are employed as tachogenerators to stabilize automatic control systems.

Generators operating under a varying load use combined excitation systems as they give better voltage stabilization. The mmf of the field winding is chosen to be sufficient for balancing out the voltage drop across the armature circuit and the armature reaction.

In motor-generator sets, the voltage of the PMDC generator is stabilized by automatic control of the motor's rpm.

In designing a PMDC machine, it is important to take account of the armature reaction. Although it is weaker than in permanent-magnet synchronous machines, its effect remains substantial [59].

Because PMDC machines have no field windings and are free from field-winding losses, they compare favourably with electromagnetically excited machines in terms of efficiency, cooling, size, weight and cost (for low-power machines), and excitation (the flux of permanent magnets is independent of speed, armature voltage, and temperature). On the demerit side, the rpm of PMDC motors and the output voltage of PMDC generators cannot be controlled by varying the field; at ratings in excess of several tens of watts they are inferior to electromagnetically excited machines in terms of size, weight and cost; the permanent magnets have to be made from scarce materials; and, finally, the permanent magnets are rather difficult to make and magnetize.

☆ 65-2 The Krämer D.C. Generator

In this form of d.c. generator due to Krämer, there are a shunt, a series, and a separately-fed field winding. The series winding is connected in opposition with respect to the other two (see Fig. 64-30).

Because the series winding produces a demagnetizing effect the external characteristic of the Krämer generator is steeply drooping: the armature current, I, is nearly equal to the short-circuit current over a wide range of variations in V (Fig. 65-2). This type of external characteristic is valuable in, say, arc-welding generators, because the current in the arc depends but little on the arc length (that is, the distance from the electrode to the workpiece), and will rise very little even in the case of a short-circuit (when the electrode is touched to the workpiece). A steeply drooping characteristic is likewise valuable for generators feeding the motors that may come to a stop in operation (for example, the motor of an excavator). This avoids damage to the driven machine when its tool is jammed, because even on a short-circuit (when the motor comes to a complete standstill), the armature current and, as a consequence, the torque of the motor are limited. The same objective is achieved when such generators are used to feed the traction motors on Diesel-electric locomotives.

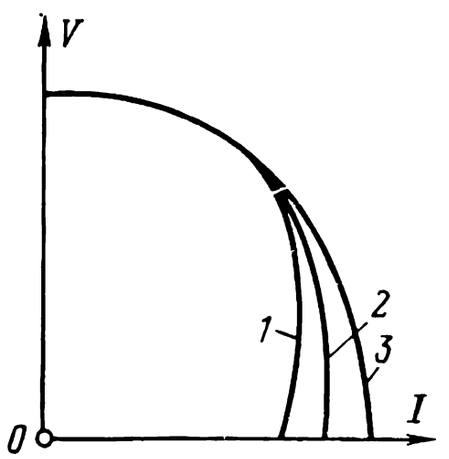

Fig. 65-2 External characteristics of the Krämer generator

To some extent, the external characteristic of the Krämer generator can be varied (curves *1* through *3* in Fig. 65-2) by adjusting the resistances in the shunt and separately fed windings and by shunting the series winding.

☆ 65-3 The Split-Pole Generator

Split-pole generators are used as sources of electricity for arc welding. As their name implies, their poles (Fig. 65-3) are split into two parts (the N pole is made up of cores

N_1 and N_2, and the S pole is made up of cores S_1 and S_2). The N_1 and S_1 cores are made wider than the N_2 and S_2 cores.

A split-pole generator has two field windings. Winding *1* encircles the wider N_1 and S_1 poles, and winding *2* encircles

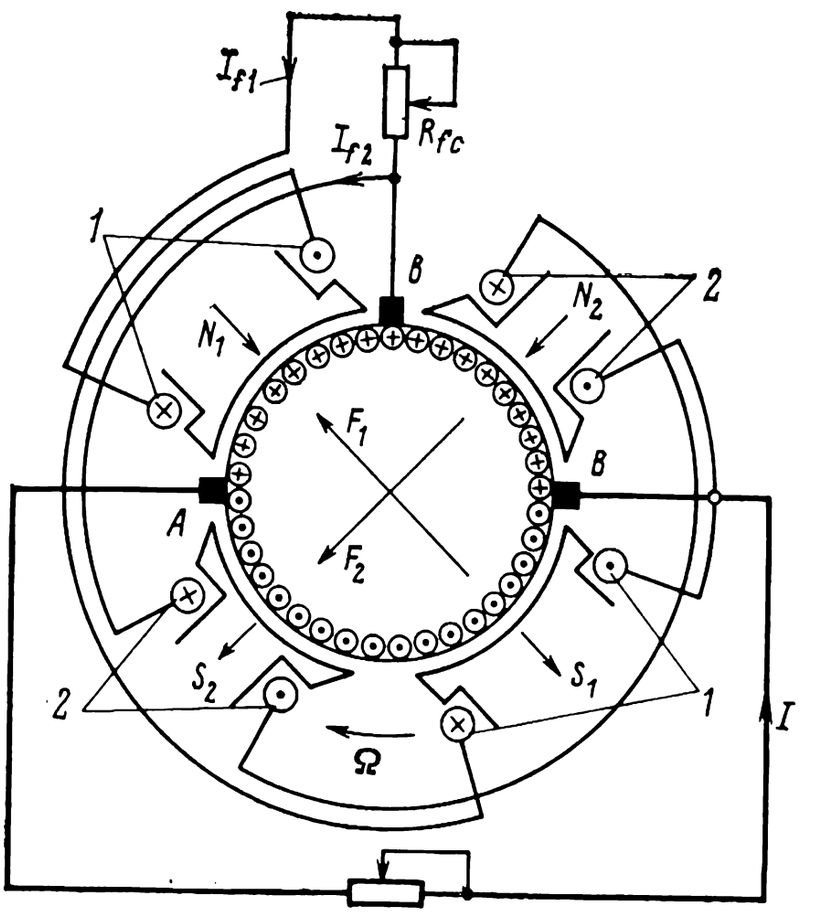

Fig. 65-3 Split-pole welding generator

the narrower N_2 and S_2 poles. Both field windings are connected in parallel to a main brush B and an auxiliary brush b positioned on the commutator midway between the main brushes A and B. The circuit of field winding *1* contains a field rheostat, R_{fc}. The direction of rotation for the armature is chosen such that F_2 (one of the components of armature mmf) boosts the field of poles N_2 and S_2, whereas F_1 (the other component of armature mmf) bucks the field of poles N_1 and S_1. Then the total magnetic flux of like poles

$$\Phi = \Phi_1 + \Phi_2$$

will decrease with increasing I_1, because the amount by which the flux Φ_1 of the unsaturated poles N_1 and S_1 is greater than the small amount by which the flux Φ_2 of

the poles N_2 and S_2 is augmented (as it is limited by saturation). However, this results in a very small change in the voltage between the brushes B and b, proportional to the nearly constant flux Φ_2. In consequence the field currents I_{f1} and I_{f2} remain practically unchanged, and this prevents an excessive de-excitation of the generator. With this form of excitation, the generated voltage drastically decreases as current rises, so the current is not excessive even on a short-circuit. Precisely this drooping external characteristic makes the split-pole generator ideally suited for arc welding.

The slope of the characteristic can be controlled by varying the setting of R_{fc} (an increase in R_{fc} leads to an increase in no-load voltage and a decrease in short-circuit current). For better commutation, the generator can be fitted with commutating (or intermediate) poles positioned midway between the unlike main poles.

In the Soviet Union, split-pole generators are available with a rated voltage of 35 V and a rated current of up to 500 A.

☆ 65-4 The Rosenberg Variable-Speed Generator

This form of generator, originally proposed by Rosenberg of Germany, has two sets of brushes shifted from each other

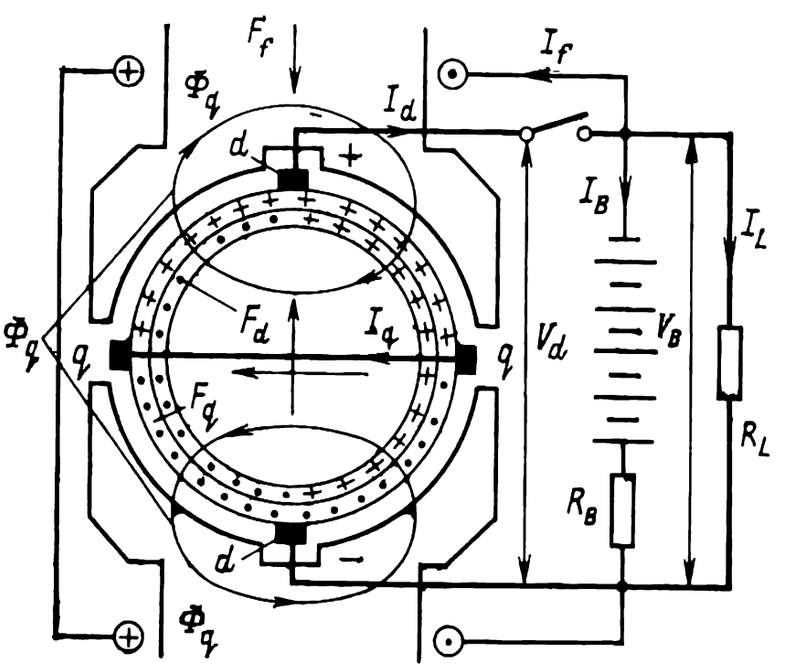

Fig. 65-4 Rosenberg variable-speed generator

by a half-pole pitch. One set consists of two d-axis brushes, d-d, connected to load; the other set consists of two q-axis brushes, q-q, shorted together (Fig. 65-4). The width and

height of the pole-shoes are increased so as to boost the q-axis flux, Φ_q. In their middle, the pole-shoes have slots which serve to weaken the d-axis field locally in the commutation zone of current I_d.

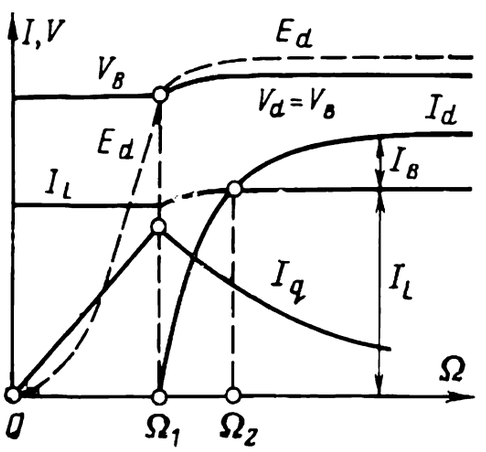

Fig. 65-5 Characteristics of the Rosenberg generator operating in parallel with a storage battery

At present, Rosenberg variable-speed generators are mainly used for train lighting. The shunt field winding is connected to a storage battery. When the train is stationary or moving slowly, the generator voltage is smaller than the battery voltage, so a relay disconnects the generator from the battery, and the load R_L draws I_L from the battery. The constant field current, I_f, sets up a d-axis flux

$$\Phi_d = \Lambda_d F_f$$

whereas in the circuit of the shorted q-q brushes an emf

$$E_q = c_w \Omega \Phi_d$$

is induced, which gives rise to a q-axis current, mmf and flux proportional to F_f and the angular velocity

$$I_q = E_q/R_a, \quad F_q = k_1 I_q, \quad \Phi_q = \Lambda_q F_q = \Lambda_q k_1 \Lambda_d c_w \Omega F_f/R_a$$

The emf induced across the open-circuited d-d brushes is

$$E_d = c_w \Omega \Phi_q = k_3 \Omega^2 F_f/R_a$$

where

$$k_3 = c_w^2 \Lambda_d \Lambda_q k_1$$

As the machine picks up speed, both I_q and $V_d = E_d$ go up, as shown in Fig. 65-5. At Ω_1, when $V_d = V_b$, the generator is switched in parallel with the battery. As the speed keeps on rising, E_d exceeds the battery voltage, V_b, and a current

$$I_d = (E_d - V_b)/R_a$$

begins to flow in the circuit of the d-d brushes. Variations in this current can conveniently be followed if we assume $R_b = 0$ and a constant $V_b = E_b$. Also, account must be taken of the demagnetizing effect of I_d. The d-axis current gives rise to

$$F_d = k_2 I_d$$

(Fig. 65-5) which always opposes F_f, whatever the direction of rotation. This leads to a reduction in the d-axis flux:

$$\Phi_d = \Lambda_d (F_f - F_d)$$

and slows down the rise in the d- and q-axis emfs with increasing velocity

$$E_q = c_w \Lambda_d \Omega (F_f - k_2 I_d)$$
$$E_d = k_3 \Omega^2 (F_f - k_2 I_d)/R_a$$

Substituting E_q into the equation for I_d, we can readily obtain a relation connecting the current to the angular velocity

$$I_d = (E_{d,f} - V_b)(R_a + k_2 k_3 \Omega^2/R_a)^{-1}$$

where

$$E_{d,f} = k_3 \Omega^2 F_f/R_a$$

is the d-axis emf due to I_f, and see that I_d tends to a limit

$$\underset{(\Omega \to \infty)}{I_{d\infty}} = F_b/k_2$$

It can easily be verified that the mmf produced by the d-axis current

$$F_{d\infty} = I_{d\infty} k_2 = F_f$$

completely balances out the field mmf.

For proper charging of the battery, $I_{d\infty}$ should somewhat exceed the charging current, I_b, and the load current, I_L. At

$$\Omega_1 = \sqrt{V_b R_a/F_f k_3}$$

where $E_{d.f} = V_b$ the direct-axis current is zero. At Ω_2, $I_d = I_L$. In the interval $\Omega_1 < \Omega < \Omega_2$, when $I_d < I_L$, the load is jointly sustained by the generator and the battery, the current drawn from the battery being

$$I_b = I_L - I_d$$

At $\Omega > \Omega_2$, the generator takes over all of the load and is charging the battery with

$$I_b = I_d - I_L$$

The characteristics in Fig. 65-5 have been plotted with allowance for the internal resistance of the battery, R_b.

Its effect consists in an increase in the voltage across the *d-d* brushes, the battery voltage

$$V_d = V_b = E_b + I_b R_b$$

and the load current

$$I_L = V_b / R_L$$

as the speed is increased. Because of this, the velocity Ω_2 found for $R_b = 0$ must be somewhat increased.

The polarity of the *d-d* brushes is independent of the direction of armature rotation. This property of the Rosenberg generator is especially valuable in the case of railway cars as they may move in either direction. Recently, however, the Rosenberg generator has been giving way to the more reliable solid-state-commutator d.c. generators.

65-5 Rotary Power Amplifiers

Direct-current generators (along with vacuum-tube, solid-state, and magnetic amplifiers) can be used in automatic control system to amplify power received from various measuring elements (transducers). Because of this, they are often called *control generators.*

(1) The separately excited generator as a power amplifier. Power amplification by a factor of 50 to 100 can be obtained with a separately excited generator driven by a prime mover at constant speed. The input (field winding) of such an amplifier receives input (or control) power, $P_{in} = I_{in} V_{in}$, and its output (armature winding) delivers output power, $P_{out} = I_{out} V_{out}$, which is k_{amp} times the input power. The coefficient k_{amp}, known as the *gain factor*, is defined as

$$k_{amp} = P_{out} / P_{in}$$

and may be as high as 50 to 100. Power amplification is effected at the expense of the power supplied by a prime mover,

$$(P_{out} - P_{in}) / \eta_{amp}$$

where η_{amp} is the efficiency of the amplifier.

If the magnetic circuit of a rotary power amplifier is unsaturated and the residual voltage is low, the gain factor will be constant and, in a steady state, P_{out} will be proportional to P_{in}.

Variations in P_{out} usually lag behind those in V_{in}, and this time lag is associated with the time constants of the rotary-amplifier windings. It is usually stated in terms of an equivalent time constant, T_{amp}, which characterizes the speed of response of the rotary amplifier as a whole. To minimize the retarding effect of eddy currents induced during transients, the core of rotary amplifiers is built up of insulated electrical-steel sheet laminations 0.35 to 0.5 mm thick.

(2) The double-armature rotary power amplifier. A substantially larger power amplification can be obtained with a double-armature rotary amplifier. This is a cascade connection of two d.c. generators in which the control signal (or input power, P_{in}) is applied to the field winding of the first generator, and its armature energizes the field winding of the second generator. The output power, P_{out}, is transferred from the armature of the second generator to the driven machine.

One form of the double-armature rotary amplifier is produced by Siemens-Schuckert of West Germany under the proprietary name of *Rapidyne*. To minimize the overall weight and size, the two armatures are mounted on a common shaft, and the two magnetic systems are built into a common frame. The gain factor of the Rapidyne is

$$k_{amp} = k_{amp1} \times k_{amp2} = \text{approx. } 10\,000$$

(3) The cross-field rotary power amplifier. A similar performance in terms of power amplifications is shown by cross-field rotary amplifiers. One of its form, known as the *Amplidyne*, has been developed by the General Electric Company, USA.

The Amplidyne is a cross-field, nonsalient-pole generator driven by a motor at a constant speed (see Sec. 65-4).

Referring to the circuit diagram of the Amplidyne in Fig. 65-6, it is seen that the control flux, Φ_c, is established by the current I_c traversing the control winding, *CW*. This flux induces in the circuit of the shorted q-q brushes an emf

$$E_q = c_w \Omega \Phi_c$$

which gives rise to a q-axis current, I_q. Flowing in the armature winding and the bias q-axis winding, *BW*, this current sets up an mmf, $F_q + F_{q,b}$, and a q-axis flux

$$\Phi_q = \Lambda_q (F_q + F_{q,b}) k_1 I_c$$

In turn, Φ_q induces an emf

$$E_d = c_w \Omega \Phi_q$$

in the output circuit containing the *d-d* brushes. When this circuit is closed through a load, a current

$$I_{out} = I_d = E_d/(R_L + R_a)$$

begins to flow in it, and a voltage appears across the output terminals

$$V_d = E_d - R_a I_d = V_{out}$$

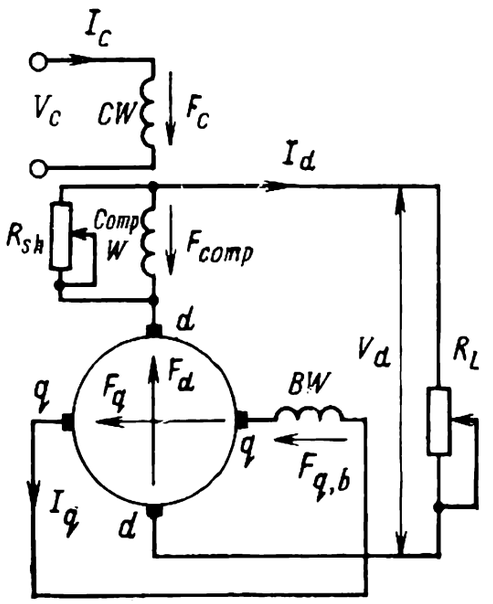

Fig. 65-6 Cross-field rotary amplifier

The gain factor of the Amplidyne is

$$k_{amp} = V_{out} I_{out}/V_c I_c$$

where

$$V_c = I_c R_c$$

The *d*-axis mmf produced by I_d is balanced out by F_{comp} due to a compensating winding, Comp *W* (see Sec. 64-11). Owing to compensation, the *d*-axis field in the Amplidyne is set up solely by I_c, and I_d has no demagnetizing effect on the field, as it does in the Rosenberg generator (see Sec. 65-4). Adjustment of the compensating winding so that $F_{comp} = F_d$ is effected with R_{sh}. For exact compensation to be possible, the compensating winding must be capable of some overcompensation, that is, $F_{comp} > F_d$ at $R_{sh} = \infty$.

The bias winding, *BW*, reduces the value of I_q required to set up the desired Φ_q, thereby improving the commutation conditions for the *q-q* brushes (see Sec. 64-11). Commutating (or intermediate) poles are installed only for the coils commutated by the *d-d* brushes. The compole winding (omitted in the figure) is connected in series with the compensating winding

Sometimes, the Amplidyne can be provided with a demagnetizing winding which encircles the stator yoke and is fed with direct current. Its purpose is to reduce the residual voltage and the effect of hysteresis on the performance of the machine. The demagnetizing winding produces an alternating flux which has its path through the stator yoke.

65-6 Round-Armature and Printed-Armature Motors

In contrast to conventional d.c. machines, a *round-armature motor* has no slots and its armature winding is bonded to the smooth surface of a ferromagnetic cylinder (Fig. 65-7*a*). This design became possible with the advent of materials capable of bonding conductors to a smooth core (glass-fibre tape, epoxy and other resins). Owing to the absence of slots, the gap flux density may be nearly doubled. For the same reason, the self-inductance of the armature winding and that of the coil undergoing commutation is reduced to a small fraction, so that the reactance emf (see Sec. 64-11) is kept within the limits acceptable from considerations of commutation, whereas the electric loading of the armature may be increased substantially.

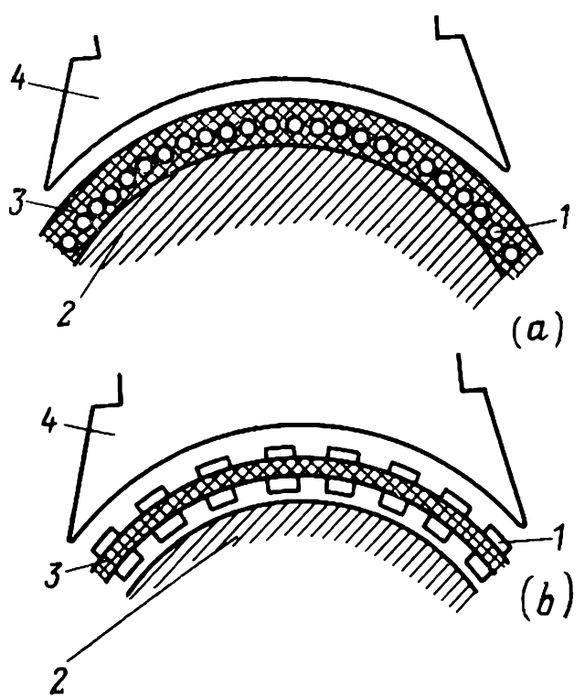

Fig. 65-7 Motors with (*a*) a round armature and (*b*) a printed armature: *1*—armature conductors; *2*—round armature; *3*—insulation; *4*—pole

Because of this, the armature diameter can be markedly reduced, leading not only to a low self-inductance and electromagnetic time constant of the armature, but also to a reduced moment of inertia and a reduced electromechanical time constant. These properties of a round-armature motor are valuable when it is employed as a fast-response servo motor in automatic control systems.

On the other hand, the armature winding placed on the periphery of a smooth core increases the nonmagnetic gap several-fold. In order to produce twice as large a flux density in such an air gap, the field mmf must be substantially larger than in conventional motors. The field winding takes up so much space that a round-armature motor has a larger weight than a conventional toothed-armature motor.

Control (servo) motors of this type come in ratings up to several kilowatts.

Printed-armature motors also have a high speed of response (Fig. 65-7*b*). In the axial type, the armature core *2* is stationary; the rotor is a hollow insulating cylinder *3*, with conductors bonded to its inner and outer surfaces to form an armature *1*. In fact, the armature conductors are formed by a process adopted in the printed-circuit technology. Instead of a cylindrical armature as in Fig. 65-7*b*, there may be a disc-type armature which is a thin, ironless disc with printed-circuit windings etched on the two sides, rotating in a double-sided air gap between fixed outer and inner iron circuits. This is known as the radial type.

In the axial type, the commutator is of conventional design. In the radial type, the function of a commutator is performed by a zone of active armature conductors.

Owing to better cooling, the current density in the armature conductors may be as high as 30 or 40 A mm^{-2}. In terms of electromagnetic properties, the printed-armature motor is comparable with the round-armature motor. Motor ratings range from units to hundreds of watts.

Printed-circuit motors are mainly used in automatic control systems.

Because in the round-armature and the printed-armature types the armature conductors lie in the air gap where the peak value of flux density may be as high as 2 T, the eddy currents induced in them are hundreds of times heavier than when the conductors are embedded in slots (in the latter case, the peak value of flux density does not exceed 0.02 to 0.05 T). To minimize the associated power losses, special measures need to be taken (such as reduction in the tangential dimensions of conductors or strands).

65-7 Acyclic or Homopolar Machines

Acyclic or homopolar machines differ from all other d.c. machines in that a continuous, or direct, emf is induced in their armature directly. Therefore, they need not have any commutator or its equivalent inevitable in all conventional heteropolar d.c. machines.

A likely design of an acyclic or homopolar d.c. generator is shown diagrammatically in Fig. 65-8. The armature (rotor) *1* is a substantial iron body rotating in the excitation flux Φ_f. This field flux established by the stationary

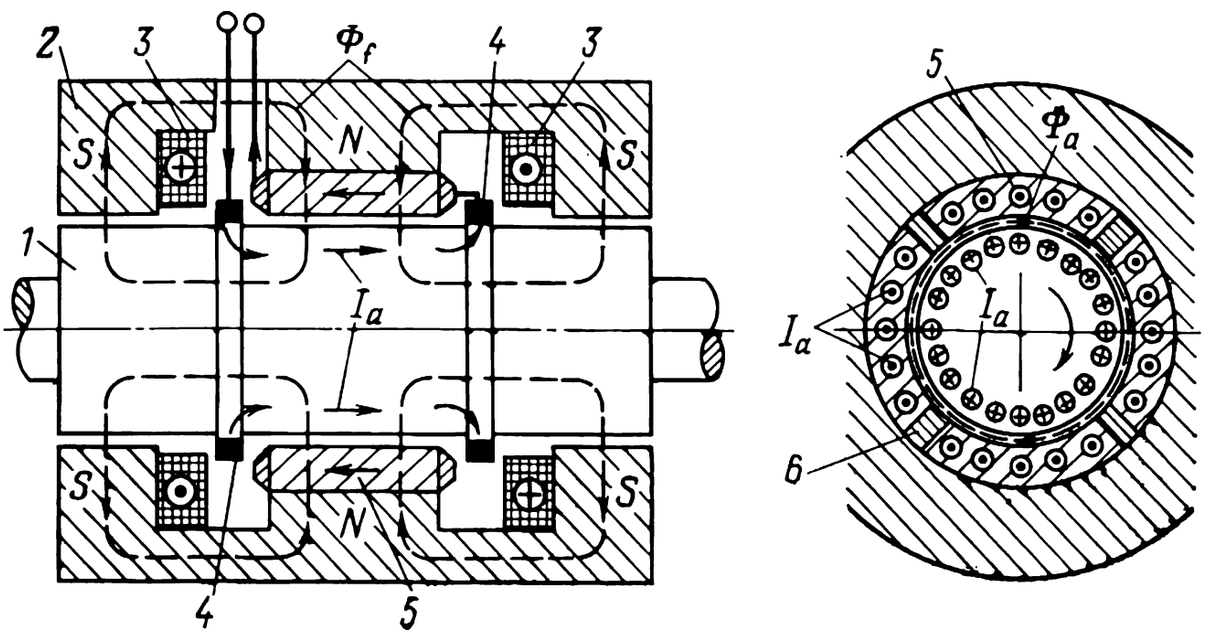

Fig. 65-8 Homopolar (acyclic) generator

coils *3* of a ring field winding completes its path by crossing the air gap twice, threading the core *2* and the rotor. The resultant field is symmetric, and a circular pole of a particular polarity (an N pole in our case) is formed in the active zone (between brushes *4*). Therefore, the same constant emf is induced in all the axial rotor elements lying between the stationary brushes, namely

$$E = Bl_\delta u$$

where B is the gap flux density, l_δ is the axial gap length (the design or effective core length), and u is the peripheral speed of the rotor.

If we connect a load resistance R_L to the brushes, E will give rise to I_a which will be equally shared between the parallel connected axial elements of the conducting rotor (it is assumed that the brushes are equidistantly disposed around the slip rings). As in conventional d.c. machines, the armature mmf has a demagnetizing effect on the excitation field. In fact, if no measures are taken to the contrary, its effect in a homopolar machine is far more pronounced. This is because the circular lines of flux have their paths within the low reluctance rotor or stator. Accord-

ingly, the armature mmf might set up a tangential flux, Φ_s, heavily saturating the rotor and stator and substantially weakening the field flux, Φ_f. The armature reaction is ordinarily minimized by a compensating winding (at *5* in Fig. 65-8) and nonmagnetic radial inserts *6*. Similar nonmagnetic inserts may be made in the rotor. Other designs of the homopolar machine are also known.

Homopolar generators are used to supply heavy currents (up to 1.5×10^5 A in continuous duty and 1.8×10^6 A in pulse duty) at low voltage (1 to 100 V in continuous duty and up to 800 V in pulse duty). Homopolar machines in the top rating bracket are built with liquid-metal (sodium or potassium) current collecting arrangements.

In the current and voltage ranges stated above, homopolar generators outperform commutator d.c. machines, as they are free from main and additional magnetic and other power losses.

The field of application for homopolar generators includes electrolysis, feeding the electromagnets of particle accelerators, and electromagnetic conduction pumps (see Sec. 65-8).

65-8 Magnetohydrodynamic (MHD) D.C. Machines

For its operation, an MHD machine depends on the motion of a fluid interacting with a magnetic field. The fluid must be a good conductor of electricity, so it can be a liquid metal or, more usually, an ionized gas or plasma.

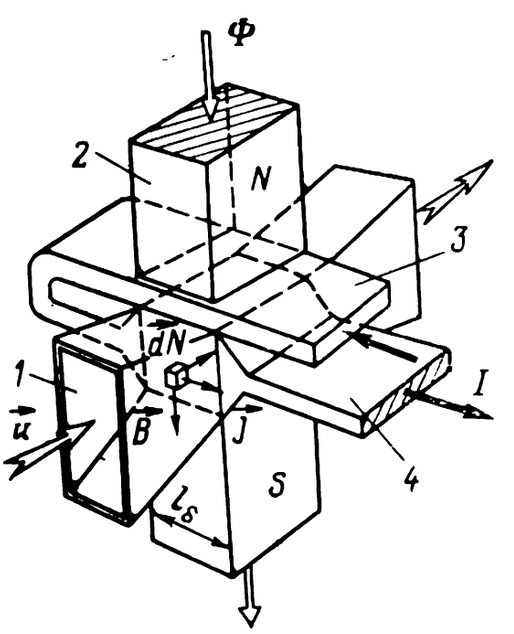

Fig. 65-9 D.C. electromagnetic pump

An example of a simple MHD motor is an electromagnetic d.c. pump for liquid metals (Fig. 65-9). In this pump, the duct, *1*, containing a conducting fluid (ordinarily, mercury, molten lithium, sodium or potassium) is placed between the N and S poles of an electromagnet, *2*. Electrodes, *4*, connected to an external supply of voltage V and held in contact with the liquid convey a direct current I to the liquid. Since current is supplied to the liquid by conduction, this type of pump is called a *conduction pump*.

The electromagnetic force acting on an elementary volume dV of the fluid is given by

$$\mathbf{dN} = \mathbf{JB}\, dV$$

The resultant pressure causes the fluid to flow at a velocity u such that a balance of voltages is struck:

$$V - E = R_a I$$

where

$$E = Bl_\delta u$$

This velocity is a function of the hydraulic resistance presented by the duct in which the fluid is flowing (see Chap. 36).

To minimize the demagnetizing effect of the quadrature-axis field established by the current I, a compensating conductor, *3*, is placed between the poles and the duct. This conductor carries the same current, but in the opposite direction.

A major advantage of electromagnetic d.c. pumps is freedom from moving parts, valves, seals or glands, so the fluid circuit can be made perfectly tight. This is the reason why electromagnetic pumps have found wide application at nuclear plants for circulating liquid metal used as coolant.

For their operation, d.c. conduction pumps need a heavy current at a low voltage. This purpose can best be served by homopolar generators.

In all probability, MHD d.c. motors in the form of plasma engines will find application in space vehicles to produce small thrust at large distances from planets. The working fluid in such plasma engines, as their name implies, will be the plasma, or an ionized gas raised to 2000-4000°C or even more.

Like all other electromechanical converters, MHD machines are reversible, so they can serve as MHD generators as well. For example, the energy converting device in Fig. 65-9 can supply direct current. To this end, a conducting fluid (liquid or gas) must be passed through its duct or channel *1* at velocity u. If the magnetic field around the duct has a flux density B, the emf that will exist across the electrodes will be given by

$$E = Bl_\delta u$$

When the "armature" circuit is closed through a load resistance, R_L, a current

$$I = E/(R_L + R_a)$$

will begin to flow in the external circuit.

At present, plasma MHD-generators are being used to produce large blocks of power per pulse.

Currently, large-scale development work is underway in the Soviet Union, the United States and some other countries on large MHD-generators which would appreciably improve the efficiency of thermal power stations. The working fluid for such generators will be the plasma produced by burning conventional fossil fuel or by heating a gas in nuclear reactors.

66 Rotary Converters

66-1 Motor-Generator Sets

A motor-generator set, as its name implies, consists of two machines mechanically coupled to, but electrically isolated from, each other. Sometimes, the two machines may be built into a common frame, and their rotors mounted on a common shaft.

Most commonly, motor-generator sets are employed to convert a.c. to d.c. The motor is an induction or a synchronous machine.

If it is desired to obtain a constant voltage, the d.c. generator can be made with shunt or compound excitation. Where the objective is continuous voltage control over a broad range, separate excitation for the generator is preferable.

A motor-generator set is reversible—when fed from a d.c. line, it can supply a.c. with a continuously variable frequency owing to speed control of the d.c. machine operating as a motor.

As sources of direct current with a continuously variable voltage, motor-generators are widely used in many fields and compete favourably with solid-state (static) converters. They are also used in Ward-Leonard drives to feed armature-controlled motors. A combination of a motor-generator set and a heteropolar or homopolar d.c. generator can supply very heavy currents such as are needed for electrolysis.

On the merit side, motor-generators offer a wide range of voltage control, reliability in operation, and the possibility of using stock-produced units. On the demerit side, they suffer from a relatively low efficiency (the total efficiency is equal to the product of the efficiency of the motor and generator), a higher cost, and a larger size.

☆ 66-2 D.C.-to-D.C. Dynamotors

The *dynamotor* is similar to the motor-generator set except that its two armature windings *1* and *2*, are on the same

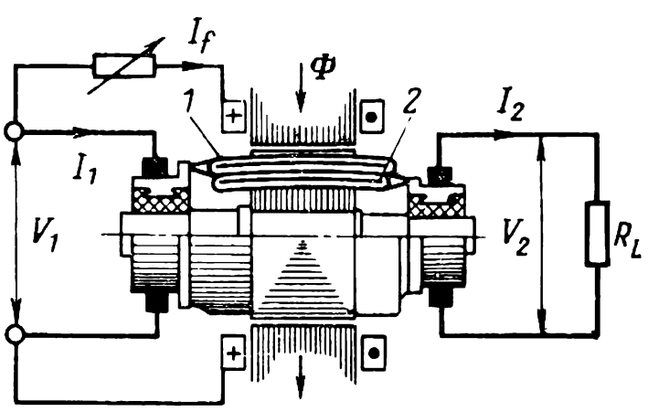

Fig. 66-1 D.C.-to-D.C. dynamotor

core and move in the same magnetic field (Fig. 66-1). When a dynamotor is used for d.c.-to-d.c. conversion, each armature winding is connected to a commutator of its own.

The brushes on the primary side are connected to a d.c. supply at V_1, and from that side the dynamotor operates as a motor drawing a current I_1 from the supply. As a result, the armature revolves at an angular mechanical velocity

$$\Omega = (V_1 - R_{a1}I_1)/c_{w1}\Phi$$

where

$$c_{w1} = pN_1/2\pi a_1$$

On the secondary side, the dynamotor operates as a generator delivering a current I_2 to the load resistance, R_L, connected to the secondary brushes.

The direct-axis flux Φ is set up by a field winding usually connected to V_1. The current in the field winding can be adjusted with a rheostat.

Because E_1 and E_2 are induced by the same flux:

$$E_1 = c_{w1}\Omega\Phi$$

and

$$E_2 = c_{w2}\Omega\Phi$$

where

$$c_{w2} = pN_2/2\pi a_2$$

their ratio, called the *emf* (or *voltage*) *conversion factor*, depends solely on the winding data, see Eq. (64-15):

$$E_2/E_1 = c_{w2}/c_{w1} = N_2a_1/N_1a_2$$

The difference between the electromagnetic torques produced by the primary and secondary currents is very small and equal to the torque remaining on making up for the magnetic and mechanical losses. If we neglect the losses, we may write

$$T_{em1} = c_{w1}I_1\Phi = c_{w2}I_2\Phi = T_{em2}$$

and also,

$$I_2/I_1 \approx c_{w1}/c_{w2}$$

In the circumstances, the electric loading on the primary and secondary windings, see Eq. (64-23), is the same

$$A_1 = N_1I_1/4a_1\pi R = N_2I_2/4a_2\pi R = A_2$$

Owing to this, the q-axis mmfs due to the opposing currents I_1 and I_2 cancel out nearly completely

$$F_{q1} - F_{q2} = A_1\tau/2 - A_2\tau/2 = 0$$

and the magnetic flux on load is about the same as it is at no load. Recalling that

$$I_2 = E_2/(R_{a2} + R_L)$$

and using the relation between currents and the expression for angular velocity, we can readily see how the angular velocity of the armature varies with load

$$\Omega = \frac{V_1c_{w1}(R_{a2} + R_L)}{[c_{w1}^2(R_{a2} + R_L) + c_{w2}^2R_{a1}]\Phi}$$

On an open circuit, when $R_L = \infty$,

$$\Omega = \Omega_0 = V_1/c_{w1}\Phi$$

as it is in a d.c. motor. As the load and the currents I_1 and I_2 are increased, the voltage ratio somewhat decreases

$$V_2/V_1 = \frac{E_2(1 - I_1R_1/V_1)}{E_1(1 + I_2R_2/V_2)}$$

From the above equations it follows that E_2 or V_2 cannot be varied by varying the field current (or flux Φ), for an

increase in, say, Φ would reduce the rpm, and E_2 would remain unchanged.

At one time, dynamotors were widely used in mobile radio equipments to step up the voltage supplied by storage batteries from 12-24 V to 750-1500 V. At present, they have almost completely been ousted by solid-state converters.

☆ 66-3 A.C.-to-D.C. Dynamotors

In contrast to the d.c.-to-d.c. dynamotor examined in the previous section, an a.c.-to-d.c. unit (Fig. 66-2) has its armature winding on the a.c. side brought out to slip (or

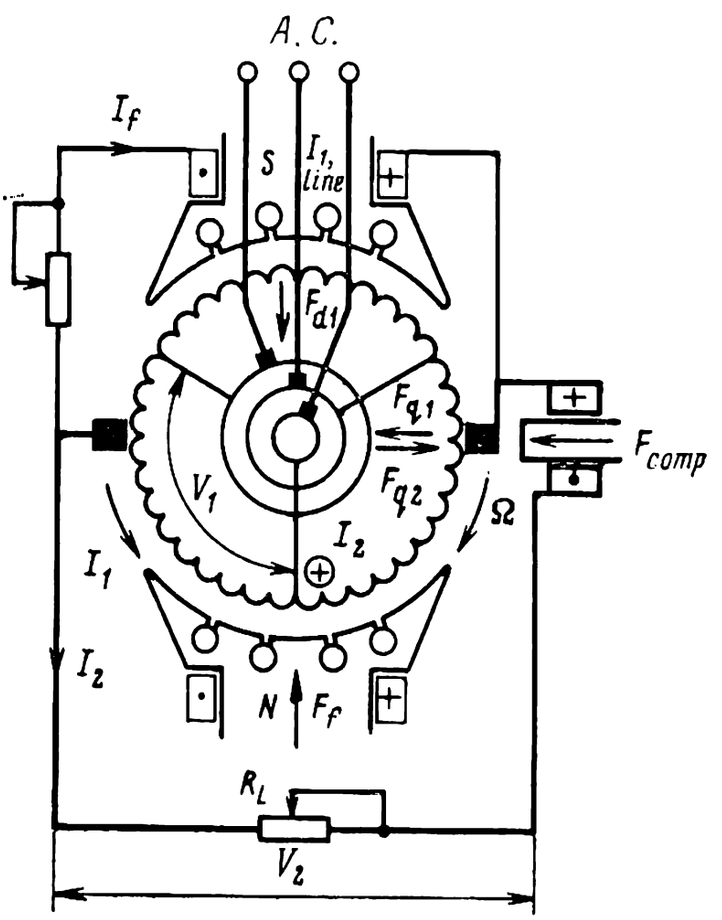

Fig. 66-2 A.C.-to-D.C. dynamotor

collector) rings, of which there are as many (m) as phases in the dynamotor (provided $m \geqslant 3$). Connection of the slip-rings to an a.c. line is via a transformer which provides both voltage and phase transformation. On the d.c. side, the armature winding is brought out to a commutator.

The armature usually carries a lap winding with $2a = 2p$ parallel circuits (or paths) in terms of d.c. Each slip-ring is connected to a equipotential points on the armature

winding, so that with respect to the a.c. supply (the transformer secondary), the armature winding is a polygon with m phases and a parallel circuits. The slip-rings also double as equalizers of the first kind for the direct current flowing in the winding.

In a steady state, the a.c.-to-d.c. dynamotor is excited by a current, I_f, and a voltage V_1, which is the phase voltage for a polygon winding, is applied to its slip-rings. As viewed from the a.c. side, the dynamotor operates as an inverted synchronous motor drawing a phase current I_1 and a line current

$$I_{1,\,\text{line}} = 2I_1 \sin(\pi/m)$$

The armature rotates at a synchronous angular velocity

$$\Omega = 2\pi f/p$$

proportional to the supply-line frequency f. On the d.c. side, the dynamotor operates as a generator delivering a current I_2 rectified by the commutator and brushes, to the load resistance R_L.

Neglecting the weak q-axis field and assuming a sinusoidal distribution for the d-axis field in the gap, we can derive a relation connecting the slip-ring and brush voltages from the emf polygon (see Fig. 64-17) which, given a sufficiently large number of coils, approaches a circle very nearly. Because the brush emf, E_2, is numerically equal to the diameter of the circle, and peak slip-ring emf, $\sqrt{2}E_1$, is numerically equal to the chord subtending the central angle $2\pi/m$, the voltage ratio may be written as

$$V_2/V_1 \approx E_2/E_1 = \sqrt{2}\sin(\pi/m)$$

In practice, the d-axis field distribution is other than sinusoidal, and the above ratio may vary by as much as 5%.

The current ratio,

$$I_2/I_{1,\,\text{line}} = m\eta\cos\varphi/2\sqrt{2}$$

can be deduced from the power balance

$$m_1 V_1 I_1 \eta \cos\varphi = V_2 I_2$$

As is seen, the current ratio strongly depends on the phase angle φ between V_1 and I_1. In turn, as is the case with a conventional synchronous machine (see Sec. 58-9), the phase angle is a function of the field current. When I_f is

such that $\cos \varphi = 1$, the line current is a minimum:

$$I_{1,\ \text{line},\ \min} = 2\sqrt{2}\, I_2/m\eta$$

Overexcitation or underexcitation leads to a decrease in $\cos \varphi$, and the line current goes up

$$I_{1,\ \text{line}} = I_{1,\ \text{line},\ \min}/\cos \varphi > I_{1,\ \text{line},\ \min}$$

An a.c.-to-d.c. dynamotor shows a better efficiency than a corresponding motor-generator set, especially in operation at unity power factor, when the opposing currents in the coils cancel out almost completely. In the circumstances, the copper loss of a three-phase dynamotor is 56% of the figure observed in a d.c. generator (for a six-phase dynamotor, the respective figure is 27%). Also, the friction, windage, hysteresis and excitation losses are nearly halved.

As a rule, an a.c.-to-d.c. dynamotor is started as a synchronous motor (induction starting). To this end, the pole-shoes carry a damper (starting) winding (see Fig. 66-2). If a d.c. supply is available, the dynamotor can be started as a d.c. motor, after which it can be put in parallel operation with the a.c. line by exact synchronizing (see Sec. 59-1).

To improve commutation, a.c.-to-d.c. dynamotors are fitted with compoles (one compole with F_{comp} is shown in Fig. 66-2). Because a larger proportion of F_{2q} is balanced out by the opposing F_{1q} due to $I_{1q} = I_1 \cos \beta \approx I_1 \cos \varphi$, the compole mmf may be taken substantially smaller than for a conventional d.c. machine.

At one time, a.c.-to-d.c. dynamotors were widely employed to supply direct voltage for street cars, trolley buses, and electric-traction railways. At first, they gave way to mercury-arc rectifiers, then to solid-state (thyristor) converters. Today, they are only used in special applications. An a.c.-to-d.c. dynamotor may also be used in the inverted mode to supply a.c. at a controlled frequency (such as for group drives).

On small river and sea craft, an a.c.-to-d.c. dynamotor driven by a prime mover serves as an a.c./d.c. generator. To obtain standard voltages, its armature carries separate windings for a.c. and d.c.

67 Solid-State Commutator D. C. Machines

67-1 Replacement of the Mechanical Commutator

The reliability of the brushgear and commutator in a d.c. machine depends on a number of factors, above all the electric and magnetic loading on the machine, commutation conditions, workmanship, environmental factors, and the wear and tear of the commutator and brushes.

To be sufficiently reliable, the active parts of the brushgear and commutator must be made sufficiently large, of scarce materials, to close tolerances, and so on. In the final analysis, this leads to an increase in the weight and size of the machine, the moment of inertia of its rotor, and in the overall cost. In corrosive media and at high altitudes (see Sec. 64-11), the sliding contact provided by brushes cannot operate safely, if at all.

This explains why so much effort has been put into the replacement of the mechanical commutator by a better arrangement. Early machines in which the switching function was performed by mercury-arc rectifiers, thyratrons or ignitrons appeared in the late 1920s. They were used as d.c. generator-exciters for turbogenerators.

The first motor with rectifier-assisted commutation was proposed by Kern in 1933. In the Soviet Union, major advances in this field date back to 1934-37 and were mainly associated with generators using mercury-arc rectifiers for commutation. A new vista was opened up with the advent of transistors in 1948.

In this chapter, we shall be concerned with several designs of d.c. machines in which the switching function is performed by solid-state (electronic) devices. The simplest of them are solid-state commutator d.c. machines intended for use solely as generators (under fairly lenient requirements for the quality of rectification). The generator is usually a three-phase synchronous machine whose armature winding is connected to load via a rectifier bridge circuit, as shown in Fig. 67-1. The rectifying elements may be semiconductor diodes or (in larger units) silicon controlled rectifiers, SCR, or thyristors. The output voltage can be controlled by varying the field current of the generator or

the firing angle of the thyristors. The rectified voltage contains a noticeable alternating component. In cases where the presence of an alternating component is undesirable, the winding must be of closed multi-coil construction (as in the motor described in Sec. 67-3).

In an electromagnetically excited, solid-state commutator machine, the armature winding is stationary, and the slid-

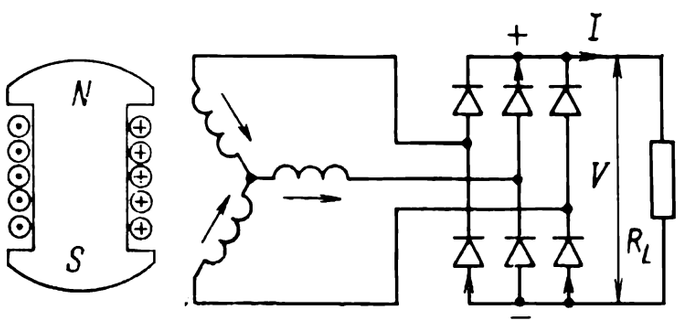

Fig. 67-1 D.C. generator with a solid-state commutator

ing contact is retained only in the field circuit. Sliding contact can be eliminated completely, if (a) excitation is supplied by permanent magnets (see Sec. 63-5 ; (b) the rotor core has claw-shaped poles and stationary ring field coils (see Sec. 63-3); or (c) the field winding is energized via rotating rectifiers from the armature of an a.c. exciter mounted on the same shaft (see Sec. 52-2).

A solid-state (electronic) commutator d.c. motor is a synchronous motor fed from a d.c. line via a solid-state inverter. In the case of an independently controlled inverter, when its output frequency is independent of the operating conditions, the motor has all the properties of a conventional synchronous motor (see Sec. 62-4). An electronic-commutator d.c. motor will have the characteristics typical of d.c. commutator motors (see Sec. 64-13) only if its excitation is controlled by a shaft-position sensor, SPS. The performance of such a motor depends on (a) the manner in which the controlled rectifiers are commutated; (b) the manner in which the rectifiers and coils are connected; (c) the number of coils; and (d) whether or not the direction of current flow in the coils can be reversed.

Small solid-state commutator motors (up to several hundred watts) are built with transistor commutators (see Sec. 67-2). In larger motors, use is made of thyristors controlled by various capacitor circuits. A major limitation of this form

of commutation is the need for a bank of capacitors comparable in size and weight with the motor itself. As regards controlled electric drive, the best promise is held out by motors with a closed, multicoil winding and thyristors controlled by rotational emf (see Sec. 67-3).

Solid-state commutator motors can use closed, radial, series, and shunt windings [69, 70]. The best choice (especially with a sufficiently large number of coils) is the *closed*,

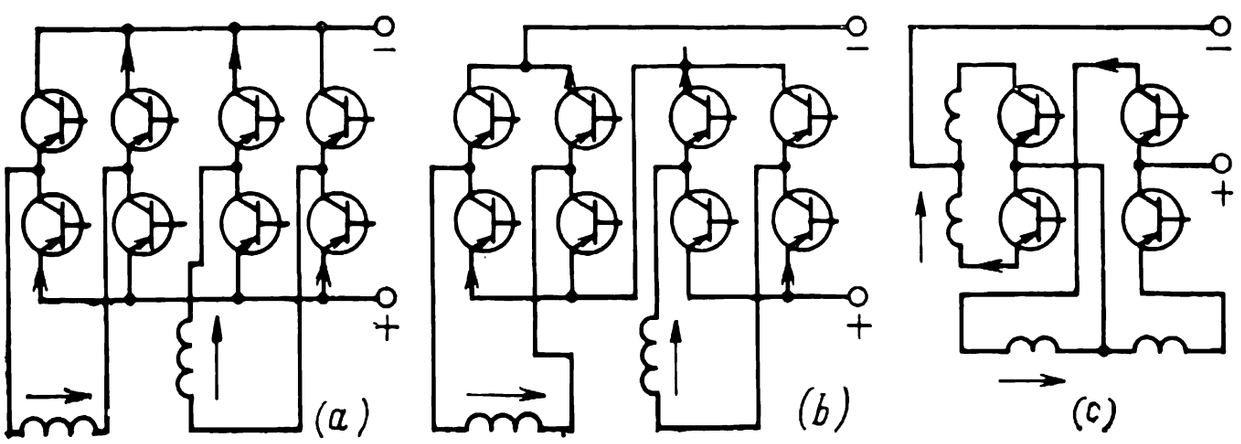

Fig. 67-2 Series and shunt windings of brushless (transistor-controlled) motors: *a*—reversibly fed two-coil shunt winding; *b*—reversibly fed two-coil series winding; *c*—nonreversibly fed four-coil winding

reversibly fed winding (Fig. 67-7) which gives the motor the performance of a d.c. commutator motor. With a small number of coils (less than five), the harmonic currents circulating in the closed loop of this winding may introduce additional losses. Given the same number of coils, the same performance will be ensured by the radial, reversibly fed winding (Fig. 67-1). With three coils, the radial winding compares favourably with the closed winding in terms of additional losses. Conversely, with a large number of coils, the closed winding is preferable, because the rectifiers operate then under easier conditions.

Nonreversibly fed, radial windings with three coils (see Fig. 67-3) and four coils come with an electronic commutator consisting of three (or four) power-transistor switches. They are used in small motors (not over 100 W) which may have a reduced efficiency (0.5 or 0.6 with three coils, 0.6 or 0.7 with four coils). Their principal advantage lies in the simplicity and small size of the electronic commutator.

With more than two coils, *reversibly fed shunt* and *series windings* (Fig. 67-2*a* and *b*) are equivalent in performance to

closed or radial windings, but need twice as many power-transistor switches. With two coils, they need as many power-transistor switches and have the same characteristics as four-coil closed or radial windings.

A *nonreversibly fed, four-coil series winding* (Fig. 67-2*c*) is electromagnetically equivalent to the two-coil series winding of Fig. 67-2*b*, but needs half as many power-transistor switches and twice as large space for the coils (each coil operates in one direction only).

Nonreversibly fed one- and two-coil shunt windings will not start the motor unless the rotor takes up a particular position. So they call for provision of a device that would position the rotor as necessary.

67-2 Fractional-HP Transistor D.C. Motors

One of the simplest designs in this class of motors is shown diagrammatically in Fig. 67-3. The motor uses a radial armature winding consisting of three coils (*AW1*, *AW2*,

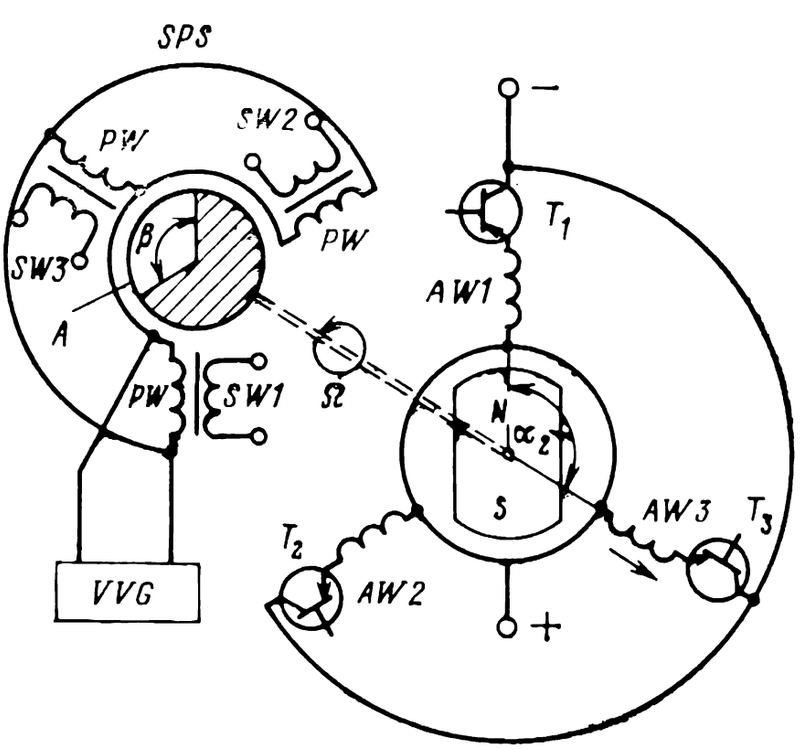

Fig. 67-3 Transistor-controlled d.c. motor with a nonreversibly fed three-coil armature winding

and *AW3*) displaced from one another through 120° in space. The field is set up by a rotating permanent magnet, *N-S*. Because the coils are nonreversibly fed, the transistor commutator consists of as few as three identical power-tran-

sistor switches, T_1, T_2 and T_3. The input signal for the switches is the voltage taken off the secondary windings (*SW1*, *SW2*, and *SW3*) of the transformers in the shaft-position sensor, *SPS*. The primary windings, *PW*, of these transformers are energized with a rectangular waveform voltage from a variable voltage generator, *VVG*. The generator operates at a frequency, f_g, which is ten to twenty times the frequency of the currents in the coils,

$$f_{max} = p\Omega_{max}/2\pi$$

at the maximum angular velocity of the motor. As a rule, f_g ranges between 3000 and 7000 Hz. For example, at $\Omega_{max} = 1000$ rad s^{-1}, and $p = 1$, $f_g \geqslant 1650$ to 3300 Hz. The variable-voltage generator is a transistor square-wave voltage converter.

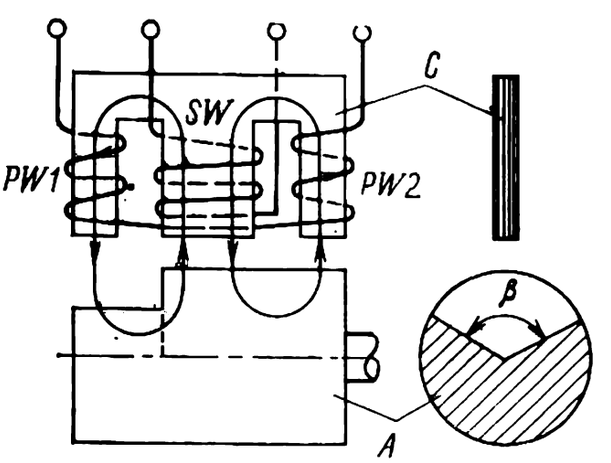

Fig. 67-4 Transformer-type shaft position sensor

The shaft position sensor may be of any one of several designs, but nearly the best choice is a differential transformer with a rotating magnetic armature, shown diagrammatically in Fig. 67-3. The sensor has as many transformers as there are controlled transistor switches. Each transformer (Fig. 67-4) uses an E-shaped core *C* the outer limbs of which carry the primary windings, *PW1* and *PW2*, connected in series opposition. The fluxes set up by the primary windings close through the middle limb carrying the secondary, or output, winding, *SW*. The armature, *A*, is cylindrical in shape at the right-hand outer and middle limbs, and has symmetrically disposed sector cutouts at the left-hand outer limb. The number of cutouts is equal to that of pole pairs, p, on the field structure, and each subtends an angle β/p. In the two-pole machine of Fig. 67-3, each sector cutout subtends an angle β.

When the shaft takes up a position in which the rotor presents a smooth, cylindrical surface to all the limbs and the air gap is everywhere the same, the opposing fluxes in the middle limb balance each other, and the emf of the sec-

ondary (output) winding is zero. The balance is, however, upset when the sector cutout lines up with the left-hand limb, and a maximum emf is induced in the output winding.

The rectified voltages taken from the secondary windings, *SW1*, *SW2* and *SW3*, serve as signals which control the respective power-transistor switches, T_1, T_2 and T_3. In the no-signal condition, they are turned off. Upon arrival of a signal from an output winding, the respective transistor turns on, connects the corresponding coil to the supply, and remains in the ON state until the control pulse ceases.

The sequence and time for a particular coil to be connected to the supply are determined by the angular position of the transformer in the shaft position sensor and the angular size β of the sector cutout, called the signal sector. Because the armature of the shaft position sensor is mechanically coupled to the field structure, the transistor commutator connects the kth coil to the supply for as long as the emf induced in that coil, e_k, opposes the supply voltage.

The emf of a coil is proportional to its mean flux density, B_k, and the angular velocity Ω of the field structure, or mathematically,

$$e_k = c_c B_k \Omega$$

where

$$c_c = 2w_c l_\delta R$$

is a constant coefficient proportional to the axial gap length (or the effective armature length), the armature radius R, and the number of turns per coil, w_c.

If we limit ourselves to the fundamental term of the gap flux density, we may write B_k as a function of the angular position of a given coil as follows:

$$B_k = B_m \sin \alpha_k$$

where B_m is the peak value of the mean flux density, $a_k = \omega t = p\Omega t$ is the electrical angle between the coil axis and the field axis (in Fig. 67-3, $\alpha_k = \alpha_3$). The difference between the supply voltage V and the emf induced in the kth coil, e_k, gives rise to a current i_k which can be found from the differential equation of voltage balance

$$V - e_k = Ri_k + L\, di_k/dt$$

where L is the inductance of the coil with allowance for the effect of the other coils, and R is the ohmic resistance of the coil.

Neglecting the coil inductance, we obtain a very simple expression for the instantaneous coil current

$$i_k = (V - e_k)/R$$

which holds for $V > e_k$, when a control signal is applied to the switch T_k and its transistor is on.

The interaction of i_k with the magnetic field produces an instantaneous electromagnetic torque

$$T_{\text{em},\,k} = c_c i_k B_k$$

The current i_k and the torque $T_{\text{em},k}$ at constant velocity are plotted on a per-unit basis in Fig. 67-5. They are non-zero over a fraction of a cycle equal to β, when a control signal is applied to transistor T_k and the angle α lies in the interval $\beta_1 < \alpha < \beta_2$, where $\beta_1 = \pi/2 - \beta/2$ and $\beta_2 = \beta/2 + \pi/2$. In the figure, this interval is shown cross-hatched.

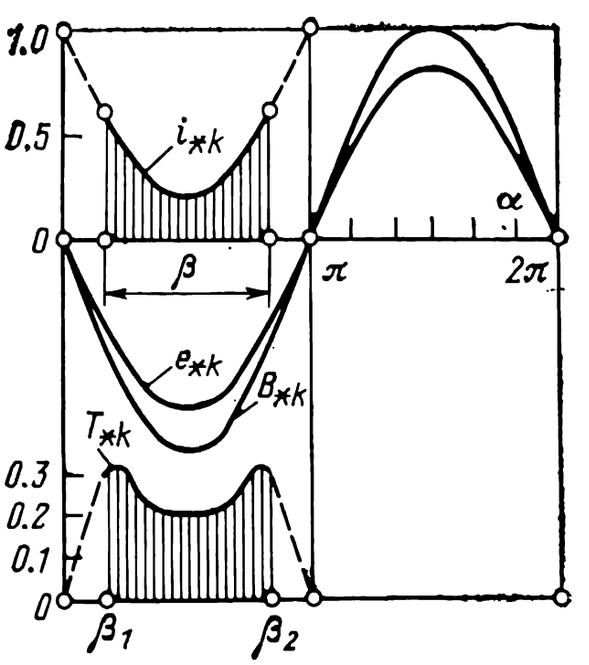

Fig. 67-5 Coil current and torque of a transistor-controlled motor at $\Omega_* = 0.8$

It is convenient to carry out all the necessary calculations in dimensionless form. To this end, we shall adopt the following set of consistent base quantities:

$$e_b = V,\ i_b = V/R,\ B_b = B_m,\ \Omega_b = V/c_c B_m$$

$T_{\text{em},k,b} = c_c B_m i_b$ (the base torque per coil)

$T_{\text{em},b} = S T_{\text{em},k,b}$ (the base torque of the motor)

where S (= 3) is the number of coils, and

$$P_b = T_{\text{em},b}\Omega_b \text{ (the base power of the motor)}$$

Then, on dropping the subscript "k" on α, $\alpha_k = \alpha$, we get the following per-unit expressions for the quantities

involved:

$$\Omega_* = \Omega/\Omega_b$$
$$B_{*k} = B_k/B_m = \sin\alpha$$
$$e_{*k} = e_k/V = e_k/c_c B_m \Omega_b = \Omega_* \sin\alpha$$
$$i_{*k} = i_k/i_b = 1 - \Omega_* \sin\alpha$$
$$T_{*em,k} = T_{em,k}/T_{em,k,b} = i_{*k} B_{*k}$$

A current is flowing in a coil at $\beta_1 < \alpha < \beta_2$, so the average torque per coil is

$$T_{em,k,av} = \frac{1}{2\pi} \int_{\beta_1}^{\beta_2} T_{em,k} d\alpha$$

and the average torque of the motor is

$$T_{em} = S T_{em,k,av}$$

Writing the average torque of the motor in per-unit, we get

$$T_{*em} = T_{em}/T_{em,b} = \frac{1}{2\pi} \int_{\beta_1}^{\beta_2} B_{*k} i_{*k} \, d\alpha$$

$$= \frac{1}{\pi} \sin(\beta, 2) - (\Omega_*/4\pi)(\beta + \sin\beta)$$

To obtain an idea about the efficiency of the motor, let us find the average copper loss per armature coil

$$P_{*Cu} = P_{Cu}/P_b = (S/P_b)\left[\frac{1}{2\pi} \int_{\beta_1}^{\beta_2} i_k^2 \, d\alpha\right] = \frac{1}{2\pi} \int_{\beta_1}^{\beta_2} i_{*k}^2 \, d\alpha$$

whence,

$$P_{*Cu} = \beta/2\pi - (2\Omega_*/\pi) \sin(\beta/2) + (\Omega_*^2/4\pi)(\beta + \sin\beta)$$

The mechanical power developed by the motor is

$$P_{*m} = T_{*em} \Omega_*$$

and the input power coming from the supply (neglecting all losses, except P_{*Cu}) is

$$P_{*m} + P_{*Cu} = \beta/2\pi - (\Omega_*/\pi) \sin(\beta/2)$$

Finally, the ideal efficiency of the motor is

$$\eta = \frac{P_{*m}}{P_{*m} + P_{*Cu}} = \frac{4\Omega_* \sin\beta/2 - \Omega_*^2(\beta + \sin\beta)}{2\beta - 4\Omega_* \sin\beta/2}$$

All of the above relations hold for a nonreversibly-fed motor only when $V - e_k \geqslant 0$, so that i_k is positive and can flow across an "ON" transistor. This condition is satisfied at $0 < \Omega_* < 1$. In fractional-hp motors this is the case practically always. At $\Omega_* > 1$, when during a fraction of a cycle $V - e_k < 0$ and $i_k = 0$, the above equations are valid up to a certain point because in their derivation we assumed that transistors could conduct in either direction. With this in view, and on setting $T_{*em} = 0$, the angular velocity on a perfect open circuit will be:

$$\Omega_{*0} = \frac{4 \sin (\beta/2)}{\beta + \sin \beta}$$

At $\beta = \pi$, $\Omega_{*0} = 4/\pi = 1.27$. At $\beta = 2\pi/3$, $\Omega_{*0} = 1.17$.

The characteristics of the motor for $\beta = \pi$ are shown in Fig. 67-6. In the range $1 < \Omega_* < \Omega_{*0}$, the characteristics are represented by the dashed curves. The motor has a maximum efficiency of 0.395 at $\Omega_* = 0.9$. The efficiency is low because over a sizeable fraction of a half-cycle (see Fig. 67-5) the emf fails to balance out the voltage, a heavy current is induced in the coil, and the i^2R loss is substantial. The useful mechanical power over that fraction of a half-cycle is small because the coil finds itself in a region of low flux density. If we reduce the signal sector to, say, $\beta = 2\pi/3$ (see Fig. 67-5), we will eliminate from the half-cycle the fractions associated with excessive currents and improve the efficiency substantially. The efficiency curve for $\beta = 2\pi/3$ runs markedly higher than that for $\beta = \pi$. The maximum efficiency is 0.7.

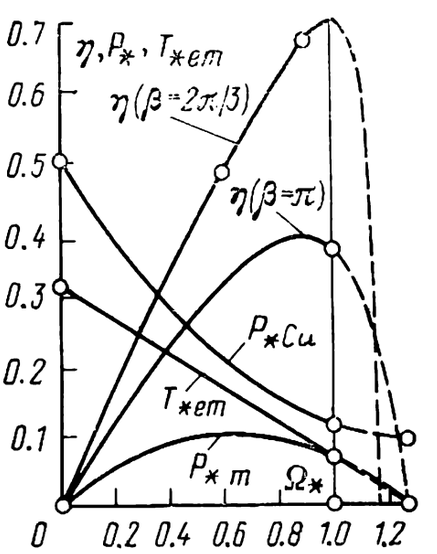

Fig. 67-6 Plots of efficiency, mechanical power and torque as functions of speed of a transistor-controlled motor

Along with valuable properties (freedom from sliding contact, simple control circuitry, and so on), a transistor-commutator motor with a small number of coils and transistor switches suffers from several limitations. Among them are the relatively low efficiency and variations in angular velocity.

To a first approximation, we deemed the angular velocity

constant, despite appreciable variations in the torque (see Fig. 67-5). Pulsations in the angular velocity can be found as follows. Combine the torques of the coils (with allowance for their displacement through a third of a cycle), find the average electromagnetic torque balanced by the external torque, and use the equation of rotor motion

$$\Sigma T_{\text{em},\,k} - T_{\text{em}} = J\,\mathrm{d}\Omega/\mathrm{d}t$$

to find the deviation of Ω from Ω_{av}:

$$\Omega - \Omega_{\text{av}} = \int_0^t \frac{\Sigma T_{\text{em},\,k} - T_{\text{em}}}{J}\,\mathrm{d}t$$

A major limitation of transistor-commutator motors lies in the very method of commutation by fully controlled transistors. The point is that the transistors turn off when the current in a coil is a maximum (see Fig. 67-5). So, if no measures are taken to the contrary, the energy stored by the magnetic field of the coil being commutated is not returned to the supply line, but is dissipated in the control circuit components.

67-3 Thyristor-Commutated, Closed-Winding D.C. Motor

The arrangement of the motor is shown in Fig. 67-7. The closed armature winding, A, is embedded in slots on the stator core and is wound exactly as it would for a d.c. commutator machine. As a rule, it is a cylindrical lap- or wave-winding. For simplicity, Fig. 67-7 shows a toroidal lap winding. It is formed by connecting identical coils into a polygon (in Fig. 67-7, the winding has 20 coils). The winding is fed from a d.c. line via a thyristor commutator, TC.

The thyristor commutator has two groups of thyristors, an anode group (marked with a "+" sign) in which all the anodes are connected electrically, and a cathode group (marked with a "—" sign) in which all the cathodes are tied together electrically. A pair of thyristors is connected to the junction of two adjacent coils, one thyristor being from the "+" group, and the other from the "—" group. In our discussion, each thyristor will take the number of the junction where it is connected to the winding and will be labelled with a "+" sign if it is from the anode group or with a "—"

sign if it is from the cathode group (for example 1^+, 1^-, 2^+, 2^-, etc.).

The rotor is similar to that of a synchronous machine and may be salient or nonsalient. The heteropolar field winding *FW* on the rotor is energized from a d.c. supply

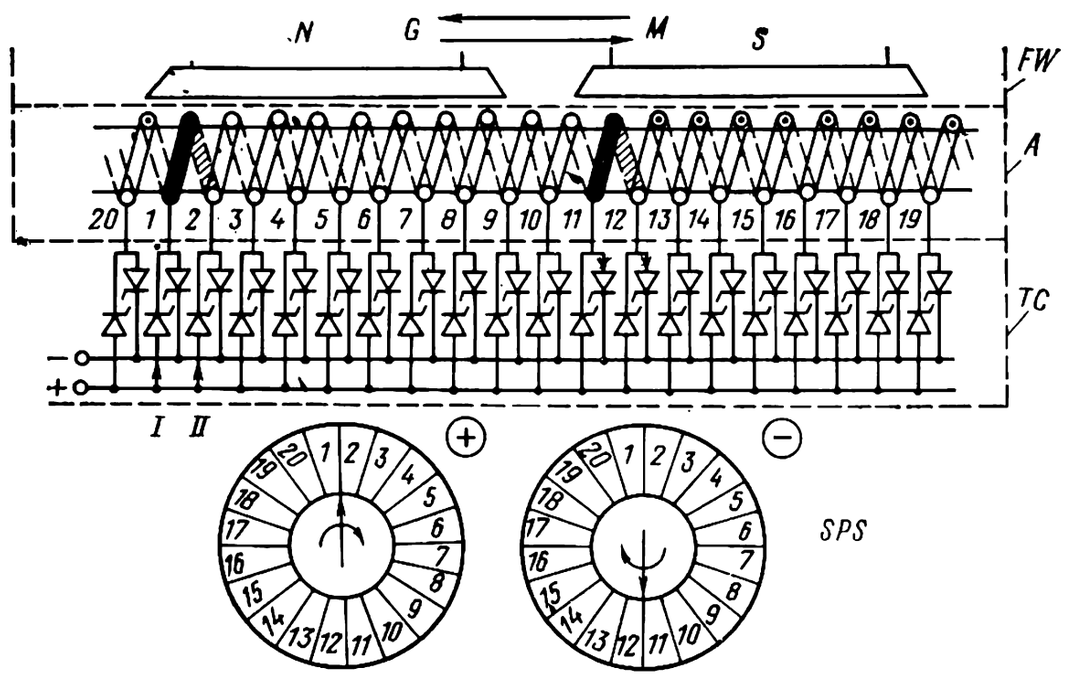

Fig. 67-7 Thyristor-controlled d.c. motor with a closed multicoil armature winding

(Fig. 67-7 shows a two-pole motor). The motor shaft is mechanically coupled to a shaft position sensor, *SPS*, which is basically the same in construction as in transistor-commutated motors (see Sec. 67-2) and only differs in that it has a larger number of output windings whose output signals control the firing of thyristors. Figure 67-7 also shows the firing diagram for the "+" and "—" thyristors. A signal for the respective thyristor to fire arrives when the rotating arrows fall within the control sector of that thyristor.

The thyristor machine converts energy in the same manner as a d.c. commutator machine, and obeys the same basic equations (for emf, electromagnetic torque, and armature mmf). From a d.c. commutator machine, it differs in the manner in which the coils are commutated. The shaft position sensor is adjusted so that with respect to the conducting thyristors in the "+" and "—" groups the winding is divided into two parallel arms (see Fig. 67-7) one of which lies under the *S* pole, and the other under the *N* pole. (In the general

case, the number of parallel paths is the same as in a d.c. commutator machine.)

In the rotor mode of operation, the active sides of the coils being commutated and connected to the conducting thyristors must lie under the trailing tips of the poles (the direction of rotation of the poles in the motor mode of operation is marked by the letter *M*). In Fig. 67-7, the circuits taking part in commutation at the instant corresponding to the position of the arrows in the firing diagram are represented by heavy lines. The circles and dots indicate the direction of current flow in the coil sides. The desired firing instant is secured through a proper adjustment of the shaft position sensor. The instants at which the thyristors are extinguished are not related to the sensor signals. In a coil shorted by two adjacent conducting thyristors, current reversal proceeds as follows. As the poles travel past the short-circuited loop being commutated (say, loop *1-2-II-I*), a rotational emf is induced in that loop. When the coil undergoing commutation comes under the trailing pole tips, the rotational, or switching, emf will, in the motor mode of operation, be directed against the current that existed in the coil prior to the onset of commutation. In other words, the switching emf opposes the current in the previously fired thyristor 1^+ and aids the current in the newly fired thyristor 2^+. As a result, the current in thyristor 2, is boosted to the full value of armature current, and that in thyristor 1^+ vanishes. By that instant, the firing signal is no longer fed to the control circuit of thyristor 1^+, and the latter turns off. Then thyristor 3^+ fires to form a new closed loop, and the sequence of events is repeated all over again.

In the generator mode of operation, the switching action proceeds similarly, but the coil to be switched must lie at the leading pole tip.

The commutation by rotational emf described above is not unlike the commutation that takes place in a d.c. commutator machine with compoles (see Sec. 64-11). However, commutation by rotational emf as it takes place in a thyristor-controlled motor offers unquestionable advantages: the switching field need not be accurately adjusted, nor should a proportional relation be maintained between the switching flux density and the armature current; the increased flux density in the region of the active sides in the coil undergoing commutation improves the commutation. Of no less importance

is the fact that a thyristor-controlled d.c. motor needs no compoles, so its design and construction are simplified. Still another advantage is that the switching circuit is simple to design and build, because it contains only power thyristors and no auxiliary components (the control circuit of a transistor switching arrangement is far more complex, see Sec. 67-2).

The only drawback of commutation by rotational emf is that it cannot be effected at zero rotational speed. There is a minimum circumferential speed, called the critical speed, u_{cr}, just sufficient for the commutation to take place under a steady state. As is shown in [70], however, this critical speed depends in a substantial manner on the rated torque and the size of a machine, so that in large motors ($D^2l > 0.1$ m^3) it is as low as a few rpm. In fact, fairly large motors can be started without resort to any ancillaries to control commutation at low speed. This can happen, if in starting from rest, the coil undergoing commutation is switched for the first time before it crosses the neutral axis and enters the magnetic field of opposite sign. In turn, this requires that the acceleration of the rotor be such that as the speed is raised from 0 to u_{cr} the coil will travel a distance substantially shorter than a pole pitch. This requirement is met in fairly large motors ($D^2l > 0.1$ m^3), but is hard to meet in small motors.

The maximum rpm for thyristor-controlled motors using commutation by rotational emf depends on the reverse recovery time of the thyristors. Assuming this time equal to 0.5×10^{-3} s, we will find that from considerations of commutation the maximum safe speed for a two-pole motor is 20 000 rpm which is beyond the limits fixed by other considerations. Thus, large motors may be built for markedly heavier electric and magnetic loading and smaller moments of inertia than d.c. commutator motors. They can be directly cooled and, in the long run, they may well supplant d.c. commutator motors in controlled drives of high power rating.

68 Alternating-Current Commutator Machines. Speed Control Systems Using Auxiliary Machines

68-1 Commutator Action in A.C. Machines

An a.c. commutator machine is a suitably designed and built induction machine whose rotor carries a closed armature winding connected to a commutator and made exactly as the armature winding of a d.c. machine (see Sec. 64-4). In some cases, the armature winding is also brought out to slip-rings.

An a.c. commutator machine is an induction, or asynchronous, machine because its rotor (armature) rotates at a speed other than synchronous.

In an a.c. commutator machine, the commutator and brush arrangement serves to convert current at one frequency, existing in the armature winding, to a current at another frequency in the circuit connected to the brushes. Using the mechanical commutator, an additional slip-frequency emf is injected into the secondary winding. This slip-frequency emf has the same frequency as the emf induced in the secondary winding as it cuts the flux. As is shown in Sec. 45-6, the injection of this emf enables the speed of the motor to be controlled continuously and over a wide range. Also, slip power is utilized over the entire control range, so that fairly high efficiency and power factors can be obtained.

In the Soviet Union, a.c. commutator motors are only used in low-power, single-phase drives, because they suffer from a number of shortcomings, namely:

(1) their power and speed control range are limited by commutation conditions;

(2) they are more elaborate in design and construction than induction and d.c. motors, so they are more difficult to operate and maintain;

(3) the cost of three-phase a.c. commutator motors is 1.5 or 2 times the cost of d.c. motors and 3 to 5 times the cost of squirrel-cage induction motors.

For some reasons, the share of a.c. commutator motors in industrial drives (except single-phase fractional-hp a. c. commutator motors) has continuously been decreasing. For

one thing, the wide use of static capacitors, synchronous motors, and synchronous compensators has made unnecessary the employment of a.c. commutator motors for the purpose of power factor improvement. Since the advent of uncontrolled and controlled solid-state rectifiers, there has been a steady expansion in the field of application for d.c. motors which permit speed control over a broader range and are more reliable in service than a.c. commutator motors. Undoubtedly, solid-state converters and inverters will expand still more the applicability of speed control by frequency adjustment to induction and synchronous motors. In fact, solid-state (static) switching arrangements are nearly completely ousting the conventional commutator. This trend will continue in the future, so our discussion will be limited to the most commonly used types of a.c. commutator motors.

68-2 The Commutator as a Frequency Changer

The voltage at frequency f_1 in the armature winding of an a.c. commutator machine can be obtained in any one of two ways: (1) conductively and (2) inductively.

In the former case (Fig. 68-1*a*), the armature winding is energized from an a.c. line via slip-rings connected to points SR_1, SR_2 and SR_3; the frequency and voltage in the armature phases (f_1 and V_{1m}) are determined by the supply.

In the latter case, there are no slip-rings, and the phase voltage is induced by a magnetic field rotating relative to the armature winding at an electric angular velocity ω_1. The phase voltage and frequency are determined by the field parameters:

$$f_1 = \omega_1/2\pi \quad \text{and} \quad V_{1m} = \omega_1 \Psi_{1m}$$

where Ψ_{1m} is the peak flux linkage with an armature phase.

Because the manner in which the armature-winding frequency, f_1, is converted to the brush frequency, f_b, is independent of how the voltage is obtained, we shall discuss this conversion by reference to a commutator frequency changer.

Diagrammatically, a three-phase commutator frequency changer is shown in Fig. 68-1*a*. It consists of a rotor carrying a closed armature winding which is connected to a commutator and three slip-rings, and a stator. There is no winding

on the stator, and the stator iron is present merely to provide a low-reluctance path for the working flux. To minimize the magnetizing current, the air gap between the rotor and stator is made as small as practicable. As was suggested by Scheribus, the stator may be omitted altogether, and the rotor can be made with deep closed slots. Then the rotor will consist, as it were, of two yokes, inner and outer, coupled by teeth between which the conductors are embedded. Because of the lines of flux completely close on themselves within iron and meet no air gap on their path, the magnetizing current in such a design is very small.

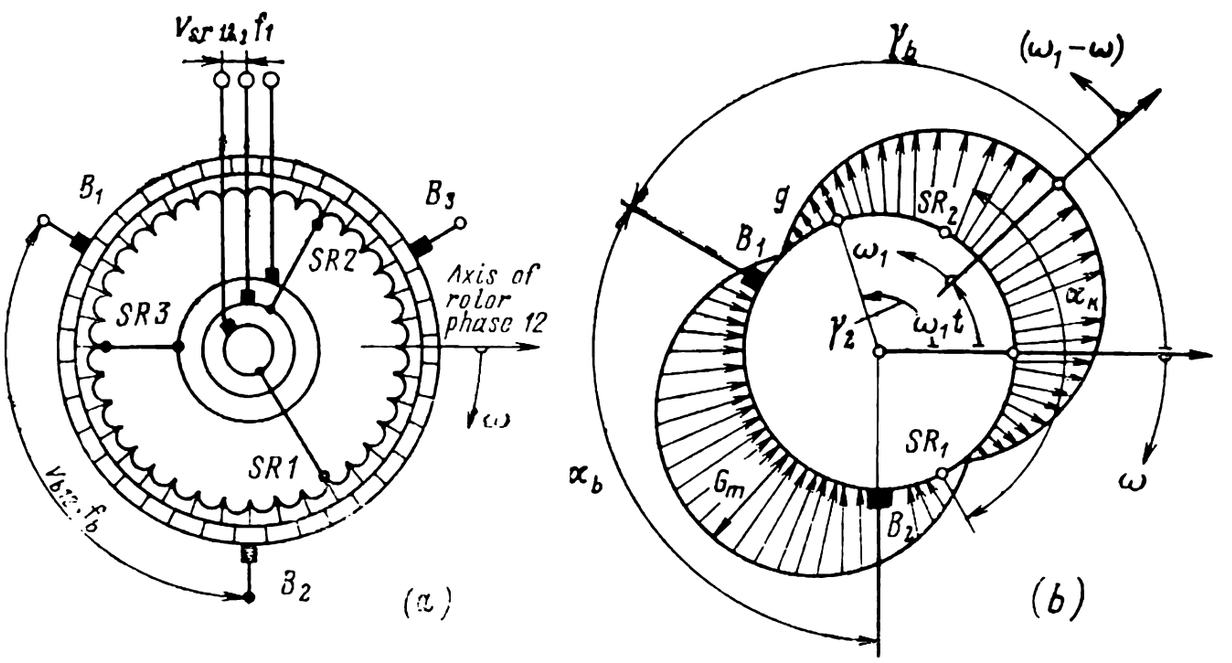

Fig. 68-1 Frequency conversion by a mechanical commutator

The three slip-rings, SR_1, SR_2 and SR_3, connect the three-phase rotor winding to a line supply voltage at f_1. The voltage existing at the slip-rings of phase *12* is

$$v_{sr,12} = V_{1m} \cos \omega_1 t$$

where $\omega_1 = 2\pi f_1$. It gives rise to currents and a magnetic field rotating at an electrical angular velocity ω_1. Because we limit ourselves only to the fundamental component of the rotating field, the emfs induced in the various coils of the closed winding and the voltages balancing them are distributed around the periphery harmonically. This also applies to the distribution of instantaneous voltage per unit electrical angle (or the specific voltage),

$$g = \partial v / \partial \gamma_2 \text{ (at constant } t)$$

around the periphery of a two-pole model

$$g = G_m \cos(\gamma_2 - \omega_1 t) \tag{68-1}$$

where G_m is the peak specific voltage.

Figure 68-1*b* shows the distribution of g at time t when the axis of the g wave makes an angle $\omega_1 t$ with the axis of rotor phase *12* (it is assumed that at $t = 0$ the two axes run together and the voltage of phase *12* is a maximum).

To derive the relationship connecting the slip-ring voltage $v_{sr,12}$ and the brush voltage $v_{b,12}$, let us write them in terms of g. The slip-ring voltage (see Fig. 68-1*b*) is found by adding together, at constant t, the voltages

$$dv = g d\gamma_2$$

in the elements bounded by points SR_1 and SR_2, that is, in the angle range from $\gamma_2 = -\alpha_{sr}/2$ to $\gamma_2 = +\alpha_{sr}/2$, where α_{sr} is the electrical angle spanned by a phase:

$$v_{sr,12(t=\text{const})} = \int_{-\alpha_{sr}/2}^{\alpha_{sr}/2} g\, d\gamma_2 = V_{1m} \cos \omega_1 t \tag{68-2}$$

where

$$V_{1m} = 2G_m \sin(\alpha_{sr}/2)$$

The brush voltage (see Fig. 68-1*b*) is found by combining, at constant t, the voltages

$$dv = g\, d\gamma_2$$

in the winding elements bounded by brushes B_1 and B_2, that is, in the angle interval from $\gamma_2 = \gamma_b$ to $\gamma_2 = \gamma_b + \alpha_b$, where α_b is the electrical angle between the brushes, $\gamma_b = \gamma_{b0} + \omega t$ is the electrical angle between brush B_1 and the axis of the rotor spinning at an electrical angular velocity ω against the g wave, and γ_{b0} is the mechanical angle between brush B_1 and the rotor axis at $t = 0$. The brush voltage is then given by

$$v_{b,12(t=\text{const})} = \int_{\gamma_b}^{\gamma_b+\alpha_b} g d\gamma_2$$

$$= V_{b,m} \cos[\alpha_b/2 + \gamma_{b0} - (\omega_1 - \omega) t] \tag{68-3}$$

where

$$V_{b,m} = 2G_m \sin(\alpha_b/2)$$

If, at $t = 0$, the rotor axis lies midway between the two brushes in question and $\gamma_{b0} = -\alpha_b/2$, then

$$v_{b,12} = V_{b,m} \cos(\omega_1 - \omega) t$$

Using Eq. (68-2), it is an easy matter to express the peak specific voltage in terms of the peak slip-ring voltage

$$G_m = V_{1m}/2 \sin(\alpha_{sr}/2) \qquad (68\text{-}4)$$

where $\alpha_{sr} = 2\pi/m_{sr}$, and m_{sr} is the number of phases on the slip-ring side.

From a comparison of Eqs. (68-2) and (68-3), we may write

$$V_{b,m}/V_{1m} = \sin(\alpha_b/2)/\sin(\alpha_{sr}/2) \qquad (68\text{-}5)$$

where $\alpha_b = 2\pi/m_b$, and m_b is the number of phases on the brush side.

In the most commonly encountered special case where $m_b = m_{sr}$ and $\alpha_{sr} = \alpha_b$, the peak values of slip-ring and brush voltages are the same

$$V_{b,m} = V_{1m}$$

As follows from Eq. (68-3), the electrical angular frequency of the brush voltage, ω_b, is the same as the electrical angular velocity of the g-wave or of the rotating field relative to the brushes

$$\omega_b = \omega_1 - \omega = \omega_1 s \qquad (68\text{-}6)$$

where

$$s = (\omega_1 - \omega)/\omega_1$$

is the slip of the g-wave relative to the brushes.

Proceeding to a similar ratio of voltage frequencies,

$$f_b = sf_1$$

we note that the frequency in the circuit connected to the brushes is expressed in the same manner as the frequency in the secondary winding of an induction motor, f_2. This is why a commutator frequency changer can be used as a source of the additional (slip-frequency) emf, E_Δ, that is injected into the secondary winding of an induction machine in order to control its power factor, $\cos\varphi$, and its rotor angular velocity, ω.

From the above analysis it is clear that a similar slip-frequency emf, E_Δ, can be obtained from the brushes held

in contact with the commutator of the armature winding in which the rotating field induces an emf at ω_1. The required magnetic field rotating at ω_1 can be set up either by the winding itself owing to the magnetizing current fed in from the brush side, or by any other polyphase winding (in such a case, there will be no connection between the armature winding and the line via slip-rings).

☆ 68-3 Three-Phase A.C. Commutator Motors

(1) The rotor-fed, three-phase shunt-wound commutator motor. This type of motor was proposed in 1910 independently by Schrage and Richter (although it is more commonly called the *Schrage motor*).

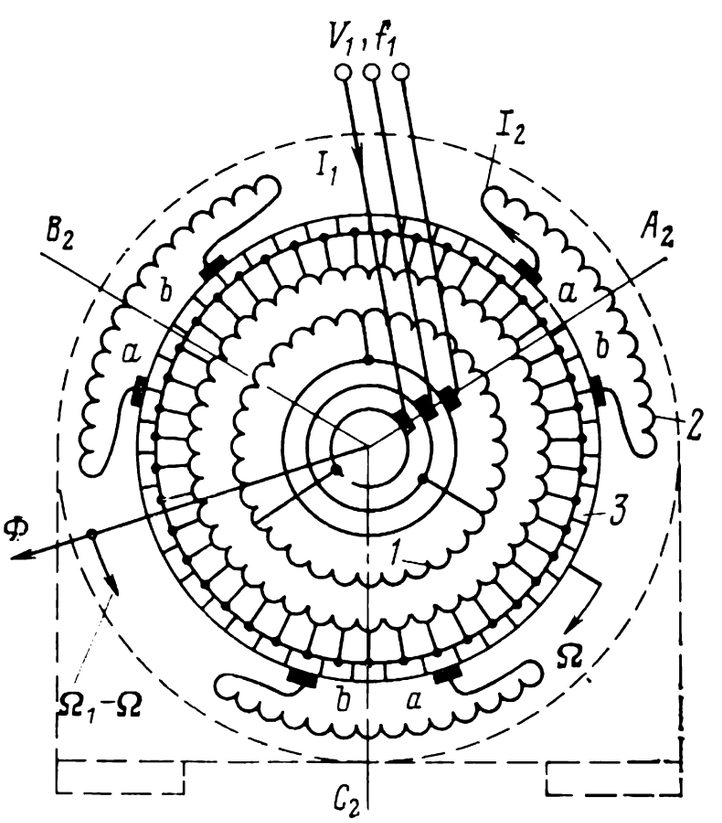

Fig. 68-2 Schrage motor

Referring to Fig. 68-2, the primary winding *1* is embedded in slots on the rotor and is an ordinary, star- or delta-connected three-phase winding with its terminal leads brought out to slip-rings. The primary winding is energized via a sliding brush contact from a line at V_1 and f_1. The same slots hold a closed armature winding, *3*, connected to a commutator. The secondary winding *2* is embedded in slots on the stator and is a symmetrical (balanced) three-phase winding.

Its phase terminal leads are connected to two sets of brushes (a and b) held in contact with the commutator of the armature winding.

The brushes in set a are connected to the starts of phases A_2, B_2 and C_2 of the secondary winding; the brushes in set b are connected to the phase finishes. In each set, a or b, the brushes are mounted on a separate rocker-arm with a shift of $2\pi/3$ (electrical). The rocker-arms can be shifted by a mechanical arrangement so as to vary the angular spacing α_{ab} between the brush sets a and b.

The speed of the motor is controlled by injecting an additional emf, E_Δ, at a slip-frequency of $f_2 = sf_1$ (see Sec. 45-6) into the secondary winding. This slip-frequency emf is induced by the flux Φ in the coils of the armature winding *3* bounded by brushes a and b. Because Φ is rotating at

$$\Omega_1 = \omega_1/p$$

where $\omega_1 = 2\pi f_1$, the slip-frequency emf in the coils of winding *3* alternates at the same frequency f_1. After conversion by the mechanical commutator (see Sec. 68-2), E_Δ at $f_b = sf_1 = f_2$ is injected into the secondary phase connected to brushes a and b. Here, $s = (\Omega_1 - \Omega)/\Omega_1$ is the slip of the field relative to the brushes or the secondary winding, and Ω is the mechanical angular velocity of the rotor.

The rms value of E_Δ is proportional to the number of turns w_3 in winding *3* bounded by brushes a and b, and to the corresponding winding factor k_{w3}:

$$E_\Delta \sim w_3 k_{w3}$$

where

$$w_3 = w\alpha_{ab}/2\pi, \quad k_{w3} = \sin(\alpha_{ab}/2)/(\alpha_{ab}/2)$$

and w is the total number of turns in the armature winding. The rms value of E_2 induced at $s = 1$ by the same field is proportional to the number of turns in a secondary phase, w_2, and the corresponding winding factor k_{w2}:

$$E_2 \sim w_2 k_{w2}$$

Therefore, the ratio of E_Δ to E_2 is solely dependent on the angular separation between the brushes

$$k_\Delta = E_\Delta/E_2 = \frac{w}{\pi w_2 k_{w2}} \sin(\alpha_{ab}/2) \qquad (68\text{-}7)$$

The angle between $\dot{E}_\Delta$ and $\dot{E}_2$ induced in a secondary phase at $s = 1$ depends on the position of brushes a and b relative to the axes of phases A_2, B_2 and C_2 of the secondary winding. The position of the brushes in which the injected emf

$$\dot{E}_\Delta = (k'_\Delta + jk''_\Delta)\,\dot{E}_2 = k_\Delta \exp(j\gamma)\,\dot{E}_2$$

increases the slip is shown in Fig. 68-3*a*. As is seen, brush a is shifted from phase axis A_2 by an angle α_a in the direction of rotation ($\alpha_a > 0$), and brush b by an angle α_b against the direction of rotation ($\alpha_b < 0$). If we place the brushes symmetrically about phase axis A_2 (as shown by the dashed lines), phase axis A_3 will line up with phase axis A_2, and

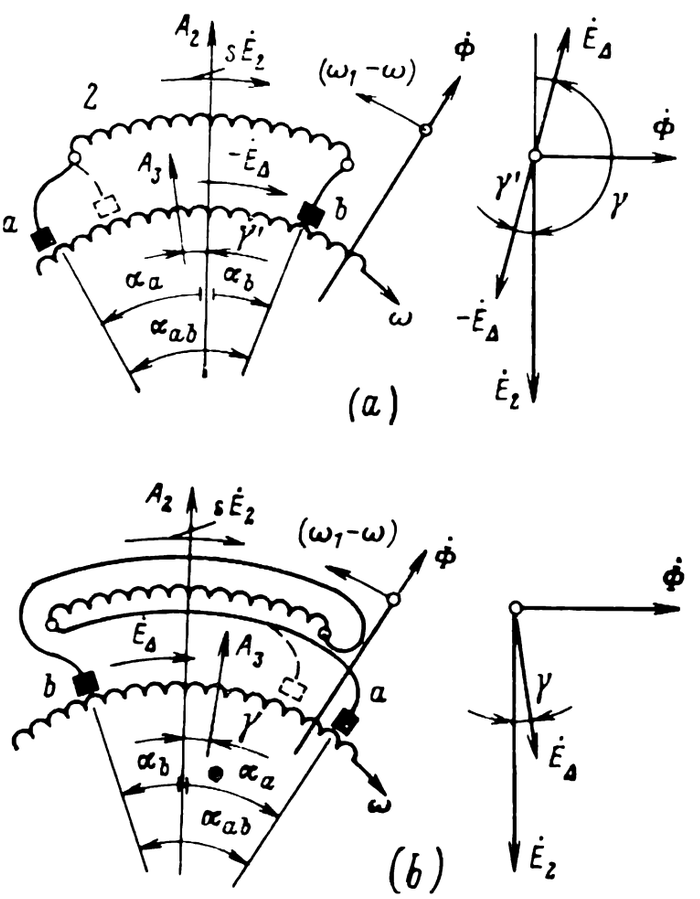

Fig. 68-3 Effect of brush shift on the injected emf

E_Δ will be in anti-phase with E_2 ($\gamma = \pi$, $k'_\Delta < 0$), thereby leading to an increase in the slip. For power factor improvement (see Sec. 45-6), $\dot{E}_\Delta$ must contain a component

$$\dot{E}'_\Delta \quad jk''_\Delta \dot{E}_2$$

leading $\dot{E}_2$ in phase, which requires that $|\alpha_a| > |\alpha_b|$.

Then the angle between the A_2 and A_3 axes will be

$$\gamma' = (\alpha_a + \alpha_b)/2$$

and $\dot{E}_\Delta$ will lead $\dot{E}_2$ by an angle $\gamma = \pi - \gamma'$ so that

$$k'_\Delta = k_\Delta \cos \gamma < 0 \quad \text{and} \quad k''_\Delta = k_\Delta \sin \gamma > 0$$

The position of the brushes in which the injected emf, $\dot{E}_\Delta$, tends to decrease the slip is shown in Fig. 68-3*b*. As is seen, brush *a* is shifted against the direction of rotation ($\alpha_a < 0$) and brush *b*, in the direction of rotation ($\alpha_b > 0$). If we position the brushes symmetrically about the A_2 axis, the A_3 axis will line up with the A_2 axis, and $\dot{E}_\Delta$ will be in phase with $\dot{E}_2$ ($\gamma = 0$ and $k'_\Delta > 0$), thereby leading to a decrease in the slip (see Sec. 45-6). For power factor improvement, it is required that $|\alpha_a| > |\alpha_b|$. Then the angle between the A_2 and A_3 axes will be

$$\gamma = (|\alpha_0| - |\alpha_b|)/2$$

and $\dot{E}_\Delta$ will lead $\dot{E}_2$ by an angle γ, so that

$$k'_\Delta = k_\Delta \cos \gamma > 0$$

and

$$k''_\Delta = k_\Delta \sin \gamma > 0$$

The electromagnetic processes taking place in an a.c. commutator motors can be described, using Equations (40-17), (41-4), (41-13) and (41-24) derived for induction machines. Additionally account must be taken of $\dot{E}_\Delta$ injected into the secondary winding and of the mmf $\dot{F}_3$ due to $\dot{I}_2$ flowing in the armature winding. This mmf can readily be expressed in terms of the secondary mmf $\dot{F}_2$:

$$\dot{F}_3 = \dot{F}_2 (k'_\Delta + jk''_\Delta) = \dot{F}_2 k_\Delta \exp(j\gamma)$$

Accordingly, the resistance and reactance of the secondary winding, R_2 and X_2, must each be taken as the sum of R_{20} and X_{20} and of the resistance and reactance of the part of winding *3* bounded between brushes *a* and *b*:

$$R_2 = R_{20} + R_3, \quad X_2 = X_{20} + X_3$$

where

$$R_3 = R_{20} (w_3/w_2) (q_2/q_3)$$

$$X_3 = X_2 (w_3/w_2)^2 (\Lambda_{\sigma 3} Z_2 / \Lambda_{\sigma 2} Z_3)$$

q_2 and q_3 are the cross-sectional areas of conductors in windings *2* and *3*; $\Lambda_{\sigma 2}$ and $\Lambda_{\sigma 3}$ are the leakage conductances per slot for windings *2* and *3*; Z_2 and Z_3 the number of slots on the stator and rotor, respectively; and w_3 is the number of turns in winding *3*.

Leaving the equations for $\dot{V}_1$ and $\dot{E}_1 = \dot{E}'_2$ unchanged, we obtain the following set of equations:

$$\dot{V}_1 = -\dot{E}_1 + (R_1 + jX_1)\,\dot{I}_1 \tag{68-8}$$

$$-\dot{E}_1 = -\dot{E}'_2 = (R_0 + jX_0)\,\dot{I}_0 \tag{68-9}$$

$$\dot{F}_1 = \dot{F}_0 - \dot{F}_2 - \dot{F}_3$$

or

$$\dot{I}_1 = \dot{I}_0 - \dot{I}'_2\,(1 + k'_\Delta + jk''_\Delta) \tag{68-10}$$

or

$$\left.\begin{aligned} s\dot{E}'_2 + \dot{E}'_\Delta &= (R'_2 + jX'_2)\,\dot{I}'_2 \\ \dot{E}'_2 &= (R'_\Delta + jX'_\Delta)\,\dot{I}'_2 \end{aligned}\right\} \tag{68-11}$$

where

$$R'_\Delta = \frac{R'_2(s+k'_\Delta) + sk''_\Delta X'_2}{(s+k'_\Delta)^2 + (k''_\Delta)^2} \quad \text{and} \quad X'_\Delta = \frac{sX'_2(s+k'_\Delta) - k''_\Delta R'_2}{(s+k'_\Delta)^2 + (k''_\Delta)^2} \tag{68-12}$$

are the equivalent resistance and reactance in the secondary circuit of the Schrage motor.

Using the above set of equations and assuming fixed values for V_1, s, α_a and α_b, we can find the desired currents, emfs, power factor and, using Eq. (41-32), electromagnetic torque of the motor:

$$\dot{I}_1 = \dot{V}_1 \left(Z_1 + \frac{Z_0 Z_{\Delta 3}}{Z_0 + Z_{\Delta 3}}\right)^{-1}$$

$$\dot{E}'_2 = \dot{E}_1 = -\dot{V}_1 + Z_1 \dot{I}_1$$

$$\dot{I}'_2 = \dot{E}'_2 / Z'_\Delta$$

$$T_{\text{em}} = (m_1/\Omega_1)\,E'_2 I'_2 \cos\beta_2$$

$$= (m_1/2\Omega_1)\,(\dot{I}'_2 \dot{E}'^{*}_2 + \dot{I}'^{*}_2 \dot{E}'_2)$$

$$\cos\varphi_1 = (\dot{I}_1 \dot{V}^*_1 + \dot{I}^*_1 \dot{V}_1)/2I_1 V_1$$

where

$$Z_1 = R_1 + jX_1$$
$$Z'_\Delta = R'_\Delta + jX'_\Delta$$
$$Z_{\Delta 3} = Z'_\Delta/(1 + k'_\Delta + jk''_\Delta)$$

Taking several values of slip, we can plot a family of torque-slip curves for several brush positions.

Figure 68-4 shows a family of torque-slip curves for a motor whose speed can be controlled in the proportion 2.5 : 1. For all curves, $k''_\Delta = 0$. The following values of k''_Δ are taken: +0.5 for curve *1*, +0.25 for curve *2*, 0 for

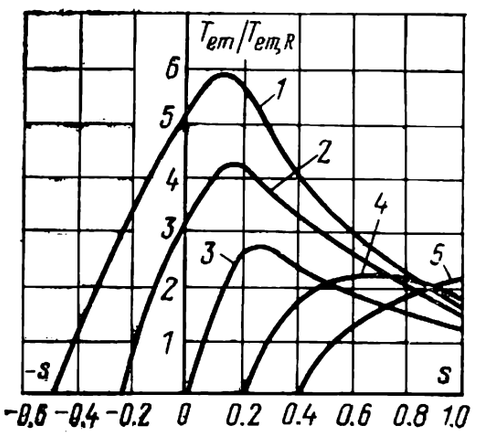

Fig. 68-4 Torque-slip characteristic of the Schrage motor

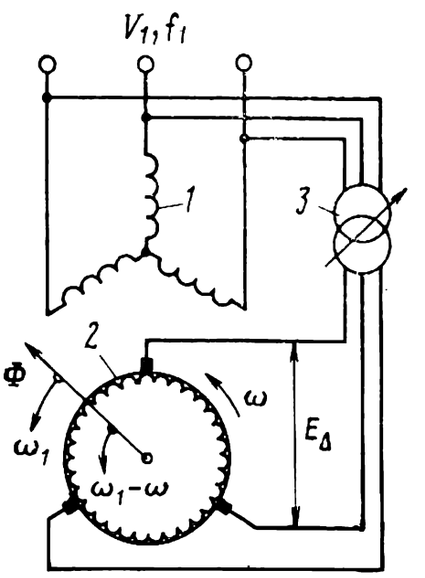

Fig. 68-5 Stator-fed, shunt-wound three-phase a.c. commutator motor

curve *3*, —0.2 for curve *4*, and —0.4 for curve *5*. As is seen, the characteristics are flat for any position of the brushes.

Schrage motors are built in power ratings from 1.5 to 150 kW (sometimes, up to 250 kW). The normal range of speed control is from 2 : 1 to 4:1. At synchronous speed, the power factor is the same as that of a conventional induction motor. At speeds above synchronous, the power factor is improved and can be as high as unity. At speed below synchronous, a sufficiently high power factor can only be obtained if the brushes are shifted asymmetrically (which can only be done in nonreversible motors). The efficiency is a bit lower than it is in a conventional motor at and above synchronous speed (owing to brush friction, brush contact resist-

ance, and increased hysteresis loss). At speeds below synchronous, the efficiency is reduced appreciably.

The Schrage motor is started "direct-on-line". In motors with a normal range of speed control, the starting torque is 1.2 to 2 times the rated value, and so is the starting current.

As compared with other three-phase a.c. commutator motors, the rotor-fed motor is far more widely used, especially in nonreversible drives with a broad and continuous speed control (printing presses, paper-making machines, the textile and cement-making industries).

(2) The three-phase, stator-fed, a.c. commutator, shunt-wound motor. The circuit of this motor is shown in Fig. 68-5. Its stator is similar to that of a conventional induction motor. Its three-phase winding is energized from a source of V_1 at f_1 and is the primary winding, *1*, of the motor. The secondary is the closed armature winding, *2*, embedded in slots on the rotor and brought out to a commutator. The injected emf, E_Δ, required for speed control is induced in the secondary winding of an induction regulator *3* whose primary is connected in parallel with the stator winding.

The frequency of E_Δ in the brush circuit is proportional to the angular velocity of the voltage wave, ω_1, relative to the brushes,

$$f_b = f_1 = \omega_1/2\pi$$

The frequency of E_Δ in the rotor winding after conversion by the mechanical commutator is proportional to the angular velocity of the voltage wave relative to the rotor:

$$f_2 = (\omega_1 - \omega)/2\pi = sf_1$$

and is the same as the frequency of the emf $s\dot{E}_2$ induced in the rotor phases by the rotating field. (In contrast to the rotor-fed type discussed in Sec. 68-2, the rotor in a stator-fed type rotates in the same direction as the voltage wave). The purpose of the induction regulator (usually of the twin type) is to control the magnitude of E_Δ without affecting its phase. Instead of an induction regulator, a variable-ratio transformer may well serve this purpose. Where the phase of E_Δ relative to E_2 must also be changed, resort may be made to brush shifting.

The electric power drawn by the stator winding from the supply line, less the losses, is transferred by the rotating magnetic field to the rotor. Some of this power, proportional

to $(1 - s)$, is converted to the mechanical power developed by the motor. The remainder, proportional to the slip, less the power lost in the rotor, is returned via the induction regulator to the supply line. At speeds above synchronous, when $s < 0$ and $1 - s > 1$, the mechanical power available at the shaft exceeds the electromagnetic power transferred to the rotor by the magnetic field. The difference proportional to $| s |$ is transferred to the rotor from the supply line via the induction regulator (or its equivalent). Therefore, the induction regulator and the mechanical commutator must be designed for the power transferred at the maximum slip, $|s_{max}|$, that is,

$$m_1 E_{\Delta, max} I_{2R} \sim | s_{max} | P_{1R}$$

Given a certain position of the induction regulator, the injected emf will be independent of load and related to E_2 so that

$$\dot{E}_\Delta = (k'_\Delta + jk''_\Delta)\, \dot{E}_2$$

where both k'_Δ and k''_Δ are constant. Therefore, the stator-fed motor has characteristics similar to those of the Schrage motor. At $E_\Delta = 0$ and with the brushes short-circuited, the stator-fed motor will be operating as a conventional induction motor.

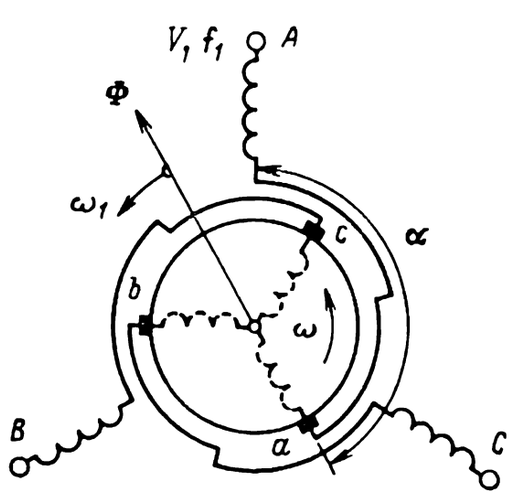

Fig. 68-6 Three-phase series commutator motor

Because there are no slip-rings in the primary circuit, stator-fed motors can be built for high voltages. As a rule, their power ratings do not exceed 150 to 200 kW, although some units are known to have ratings up to 1500 kW.

(3) The three-phase, a.c. commutator, series-wound motor. The circuit of this motor is shown in Fig. 68-6. It differs from a shunt-wound motor in that its rotor winding is connected via a mechanical commutator in series with the stator winding. Sometimes, as a way of reducing the voltage a step-down transformer is interposed between the stator and rotor winding. It is designed for the power that is injected into the rotor circuit for speed control. The supply voltage

V at frequency f_1 is shared between the series-connected phases of the stator and rotor. The stator phase voltage is V_1, and the equivalent rotor phase voltage is E_Δ. After conversion of E_Δ by the mechanical commutator to the slip frequency, $f_2 = sf_1$, this emf is injected into the rotor coils for speed control. In contrast to shunt-wound motors, however, E_Δ at constant V markedly changes with changes in load, because V is shared between the series-connected phases of the stator and rotor. As a result, the slip substantially increases with rising load, and the torque-slip characteristics of the motor resemble those of a series-wound d.c. motor. The shape of the characteristics depends on the electrical angle α betw.en the axes of the series-connected rotor and stator phases, and this is in turn dependent on the position of the brushes on the commutator. If α is zero or 180°, the axes of the fields set up by the stator and rotor are aligned, and the electromagnetic torque acting on the rotor is zero. Applying the left-hand rule to the rotor conductors, it can readily be found that the electromagnetic forces acting on the rotor depend on the direction in which the brushes are shifted from the axes of the stator phases. If the brushes are shifted in the direction of rotation, the electromagnetic forces tend to turn the rotor against the rotation of the field. If the brushes are shifted against the rotation of the field, the electromagnetic forces act in the direction of field rotation. In the latter case, the rotor is running with the field, so the frequency of cyclic magnetization of the rotor and the transformer emf in the coils undergoing commutation are reduced. This is why the brushes are usually shifted by an angle α of 130° to 160° against the rotation of the field.

Speed control is effected by brush shifting, which is done with the aid of a brush shifter.

Series-wound a.c. commutator motors are used on a limited scale, mostly in drives where the torque strongly depends on speed (fans, centrifugal pumps and the like). Speed can be controlled in the proportion 4 : 1.

(4) Commutation of three-phase, a.c. commutator motors. As the rotor of a three-phase, a.c. commutator motor rotates, the coils of its armature winding pass from one phase to another. During such a transition, the coils are short-circuited by the brushes, and their current changes by the difference in instantaneous value between the adjacent phases.

In the Schrage motor which has two sets of brushes a coil undergoing commutation passes from the zone occupied by a phase into a de-energized zone (or the other way around), and its current changes by the instantaneous current in the phase involved. Thus, in the general case, the current during commutation changes by the instantaneous current flowing through the brush in question. This change of current induces in the coil undergoing commutation the same reactance emf, e_r, as in d.c. machines (see Sec. 64-11). This reactance emf is equal to the sum of the emfs of self- and mutual induction in the commutated coil and differs from the reactance emf in d.c. machines only in that it is proportional to the current through the brush at the instant of commutation. Therefore, the reactance emf decreases as the number of phases is increased. However, apart from the reactance emf, a transformer emf, e_t, is also induced in the commutated coils of a three-phase, a.c. commutator motor. In a.c. commutator machines, this transformer emf owes its origin to changes in the flux linkage of the main rotating field with the coil undergoing commutation. The transformer emf is proportional to the speed at which the field travels past the coil and is independent of the brush current. In rotor-fed motors, e_t is independent of the rotor speed. In stator-fed motors, the transformer emf decreases as the angular velocity of the rotor approaches the angular velocity of the field. It is this transformer emf and the fact that it cannot be balanced out (because there are no compoles in three-phase a.c. commutator motors) that set the limit for the magnetic and electric loading and the maximum power.

☆ 68-4 Speed and Power Factor Control Schemes for Induction Motors

The speed and power factor of an induction motor can be controlled by cascading it with a commutator or a rectifier-commutated machine. There are schemes capable of power factor control only.

The function of the commutator or rectifier-controlled machine in such a scheme is to supply the slip-frequency emf, E_Δ, that is injected into the rotor circuit of the induction machine. The effect of this injected emf is discussed in detail in Sec. 45-6. For speed control, E_Δ must contain

a component, E'_Δ, which is in phase or in anti-phase with sE_2. For power factor control, it must contain another component, E''_Δ, which leads E_2 by an angle $\pi/2$.

The slip power needed for speed (or power-factor) control,

$$P_\Delta = m_2 E_\Delta I_2 \cos \beta_\Delta$$

is returned by the rotor of the controlled induction motor to the regulating commutator machine or the rectifier-inverter, whichever is used. This recovery can be effected

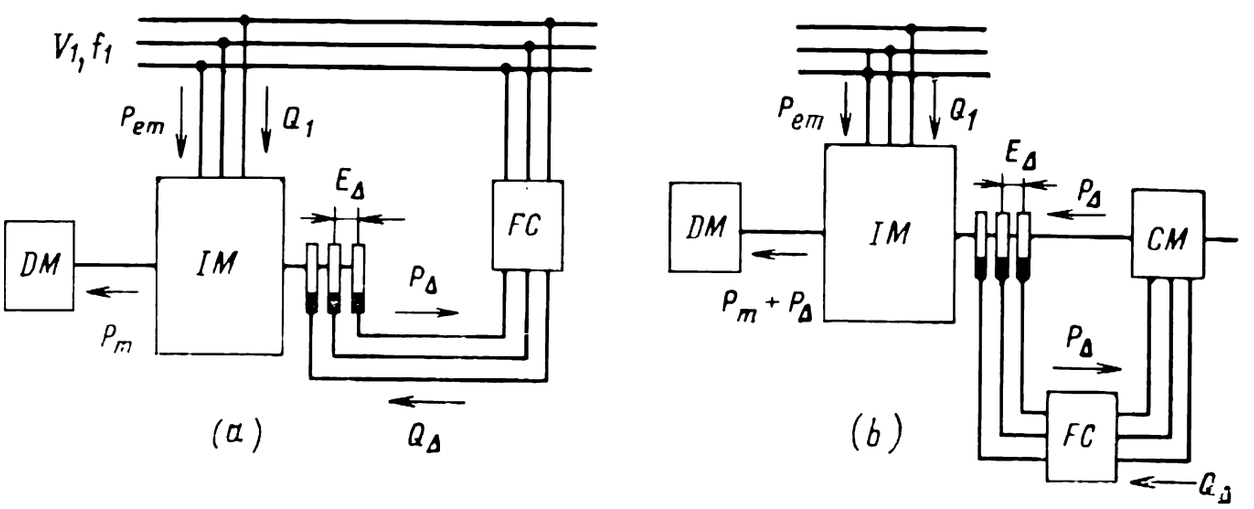

Fig. 68-7 Speed control schemes for an induction motor

in one of several ways. Accordingly, speed control schemes may be *all-electric* or *electromechanical*.

In an *all-electric speed control scheme* (Fig. 68-7*a*), the slip power is returned to or absorbed from the line by the rotor of the induction motor via a rotary or rectifier frequency changer, *FC*. In either case, the mechanical power developed by the induction motor

$$P_m = P_{em} - P_{Cu2} \pm P_\Delta = P_{em}\left(1 - \frac{P_{Cu2} \mp P_\Delta}{P_{em}}\right) = P_{em}(1 - s)$$

is smaller than the electromagnetic power by an amount equal to

$$P_{Cu2} \mp P_\Delta = sP_{em}$$

which is partly dissipated as heat in the copper of the rotor, P_{Cu2}, and is partly returned to the supply line,

$$P_\Delta = sP_{em} - P_{Cu2}$$

At speeds above synchronous, when $s < 0$, the mechanical power of the induction motor exceeds its electromagne-

tic power, and the balance, P_{Δ}, is coming from the line to the rotor of the induction motor via the frequency changer.

In addition to speed control, an all-electric scheme can be adapted to control the power factor. In such a case, some of the reactive power required to set up a magnetic field in the motor is injected via a frequency changer, *FC*, as Q_{Δ} into the rotor circuit of the induction motor. Because in a rotor-fed motor the reactive power is less than it is in a stator-fed motor (see Sec. 45-6), the total reactive power upon the injection of Q_{Δ} is always brought down (if $|s| < 1$). A special case of an all-electric scheme which also serves to control the power factor is one in which only a reactive power, Q_{Δ}, is injected into the rotor, whereas P_{Δ} is zero.

In an *electromechanical scheme* (Fig. 68-7*b*), the slip power P_{Δ} of the induction motor is transferred electrically (via a frequency changer or directly) to the commutator machine, *CM*, whose rotor is mechanically coupled to the rotor of the induction motor. At speeds below synchronous ($s > 0$), some of the electromagnetic power, P_{em}, is transferred electrically as

$$P_{\Delta} = sP_{em} - P_{Cu2}$$

to the commutator machine *CM* which operates as a motor and converts it to mechanical power. At speeds above synchronous ($s < 0$), the commutator machine operates as a generator and draws from the main motor a mechanical power which is converted to electrical power

$$|P_{\Delta}| = |s|P_{em} + P_{Cu2}$$

transferred to the rotor of the induction motor.

In the final analysis, irrespective of the mode of operation, the mechanical power transferred in an electromechanical scheme to the driven machine, *DM*, is the sum of

$$P_m = P_{em} - P_{Cu2} - P_{\Delta} = P_{em}(1 - s)$$

developed by the main induction motor, *ID*, and

$$P_{\Delta} = sP_{em} - P_{Cu2}$$

drawn from the commutator machine, *CM*. Therefore, the total mechanical power in an electromechanical scheme, less the losses, is equal to

$$P_m + P_{\Delta} = P_{em} - P_{Cu2}$$

where $P_\Delta > 0$ when $s > 0$, and the losses in the commutator machine are neglected.

The overall torque, T_o, applied to the shaft of the driven machine, DM, is the sum of the torque T_{em} developed by the main motor and the torque $T_\Delta = Ts/(1 - s)$ supplied by the commutator machine, that is

$$T_o = T_{em} + T_\Delta$$

At $s > 0$, when the commutator machine is operating as a motor $T_\Delta > 0$. At $s < 0$, when the commutator machine is operating as a generator, $T_\Delta < 0$.

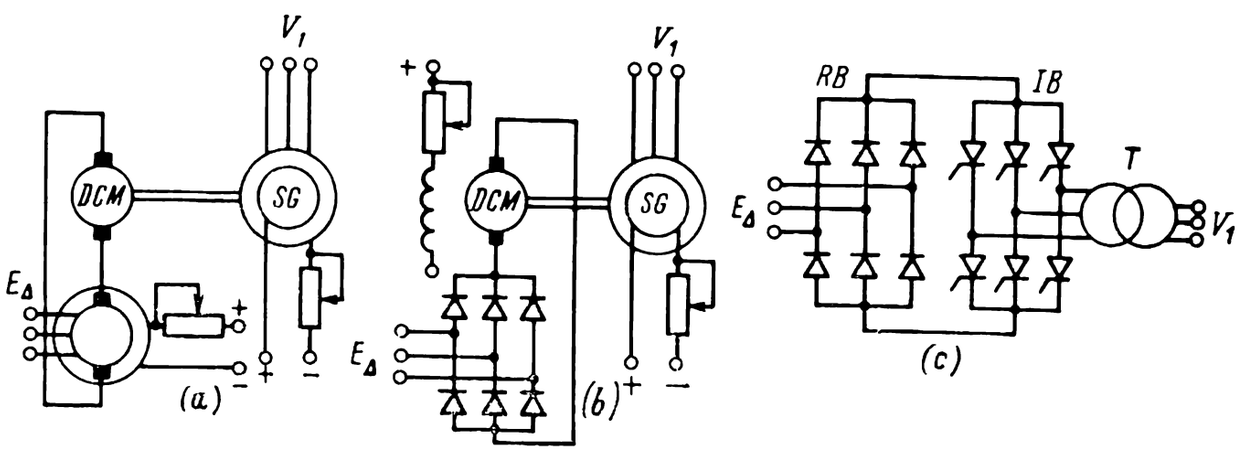

Fig. 68-8 Likely arrangements of a frequency changer for d.c. link speed control schemes

Figure 68-8 illustrates several arrangements of the frequency changer, FC (see Fig. 68-7*a*), for *all-electric schemes with an intermediate d.c. link*. In such a scheme, the current at slip frequency f_2 flowing in the rotor circuit is first converted to direct current, then to an alternating current at frequency f_1 and delivered to the external circuit. The arrangement in Fig. 68-8*a* is known as the *Scheribus scheme* or *drive*. In this scheme, the current and injected emf, E_Δ, at frequency f_2 are rectified by an a.c.-d.c. dynamotor, D, whose slip-rings are connected to the rotor winding of the induction motor. The second stage of conversion is effected by a constant-speed set consisting of a d.c. machine, DCM, energized from the rotor of the dynamotor, and a synchronous generator, SG, connected to the line operating at f_1.

Because at low slip ($s < 0.1$), a dynamotor tends to lose stability, the Scheribus scheme can only control speed downwards from synchronous (from about 0.9 to 0.5 of the rated

value, Ω_1). The slip power, P_Δ, is drawn by the dynamotor which operates as a motor on the slip-ring side and is transferred to the d.c. machine *DCM* which drives the synchronous generator *SG*. The latter returns P_Δ (less the conversion losses) to the external circuit at f_1. The speed of the induction motor is controlled by varying the field current of the d.c. machine.

Speed control over a wider range (up to 10:1) downwards from synchronous can be obtained, if the dynamotor is replaced by a set composed of a synchronous motor and a d.c. generator. In this *induction-synchronous scheme* the slip power is solely limited by the rating of the motor-generator set (usually built into a common frame). Therefore, induction-synchronous drives can be built with a main motor rated up to 30 MW and with a speed control range up to 8:1.

Of late, advances in power semiconductor devices have led to the replacement of rotary converters by the more reliable and economical *static converterss.* In such a scheme (see Fig. 68-8*b*), the dynamotor is replaced by a rectifier bridge, *RB*, composed of uncontrolled crystal (or gas-filled) rectifier diodes. Direct current is inverted to an alternating current at frequency f_1 in the same way as in the Scheribus scheme.

In a still more advanced scheme, the constant-speed set (consisting of a d.c. motor and a synchronous generator) is replaced by an inverter bridge, *IB*, using controlled crystal (or gas-filled) rectifiers (thyristors or thyratrons). An all-electric d.c.-link scheme in which both stages of current conversion are effected by rectifiers may well be named an *induction-rectifier scheme* (or drive). The circuit of such a scheme comprising a rectifier bridge, *RB*, an inverter bridge, *IB*, and a matching mains transformer, *T*, is shown in Fig. 68.8*c*.

Speed-control d.c.-link schemes have a successful rival in the form of a *direct-coupled scheme* (Fig. 68-9) in which the rotor current of an induction motor at frequency f_2 is directly converted to a current at the line frequency f_1. Some of the arrangements for the frequency changer (see Fig. 68-7*a*) used in such schemes are illustrated in Fig. 68.9*a* and *b*. In the arrangement of Fig. 68-9*a*, the conversion is effected by a three-phase a.c. commutator shunt-wound motor, *CM*, (see Sec. 68-3) which, energized with a current

at f_2 from the rotor of the induction motor, draws slip power P_Δ, and drives (at constant speed) a synchronous generator, *SG*, connected to the line operating at f_1. Speed control is effected by varying the value of the injected emf, E_Δ, induced in the rotor winding of the a.c. commutator motor. In turn, this is done by varying its field current with a regulating device, *RD*. Speed in the above drive can only

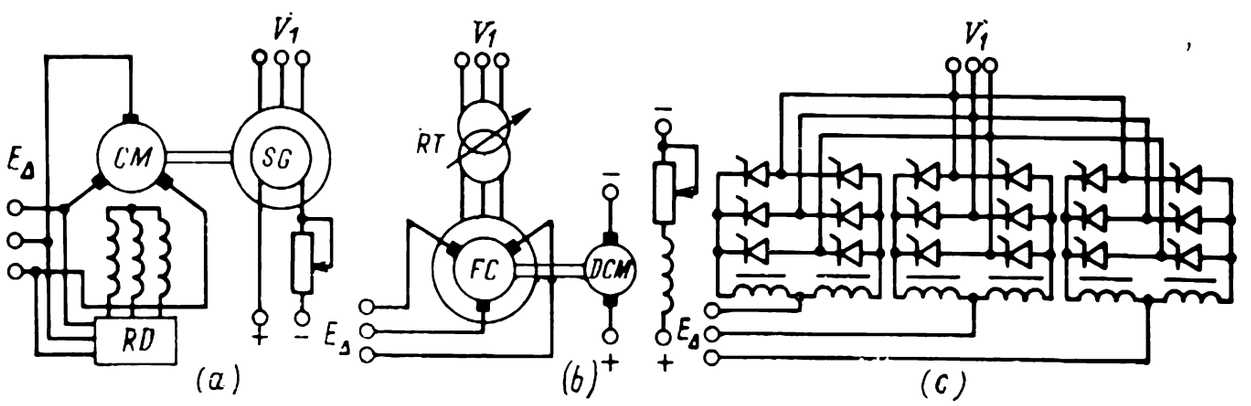

Fig. 68-9 Likely arrangements of a frequency changer for direct-connected speed control schemes

be controlled downwards from synchronous, because at $s = 0$ the commutator machine would lose excitation. The speed must be not less than 0.7 of the synchronous one, because at lower speed the brush frequency of the commutator machine would exceed 15 Hz, thereby upsetting normal commutation.

In the arrangement of Fig. 68-9*b*, using a commutator frequency changer (see Sec. 68-2), speed can be controlled both downwards and upwards of synchronous, because the slip-frequency injected emf is independent of the regulating transformer, *RT*, and of the main-motor slip. The slip power, P_Δ, is transferred from the rotor of the induction motor via the frequency changer and regulating transformer to the line.

The d.c. motor, *DCM*, driving the frequency changer is designed solely to make up for the losses occurring in the frequency changer. Using the d.c. motor, the speed of the frequency changer can be adjusted so that the frequency of its brush emf is the same as the slip frequency of the induction motor. Because of the commutation conditions existing in the commutator frequency changer, the speed of the entire scheme can be controlled within 0.75 to 1.25 of the synchronous.

As an alternative, the frequency changer in a direct-connected speed control scheme can be fully made of rectifiers. The circuit of such an arrangement is shown in Fig. 68-9*c*. The *bidirectional converter* in this scheme consists of three single-phase units built around controlled rectifiers (thyristors). The input to the bidirectional converter is a voltage V_1 at f_1, and its output is an emf E_Δ at f_2.

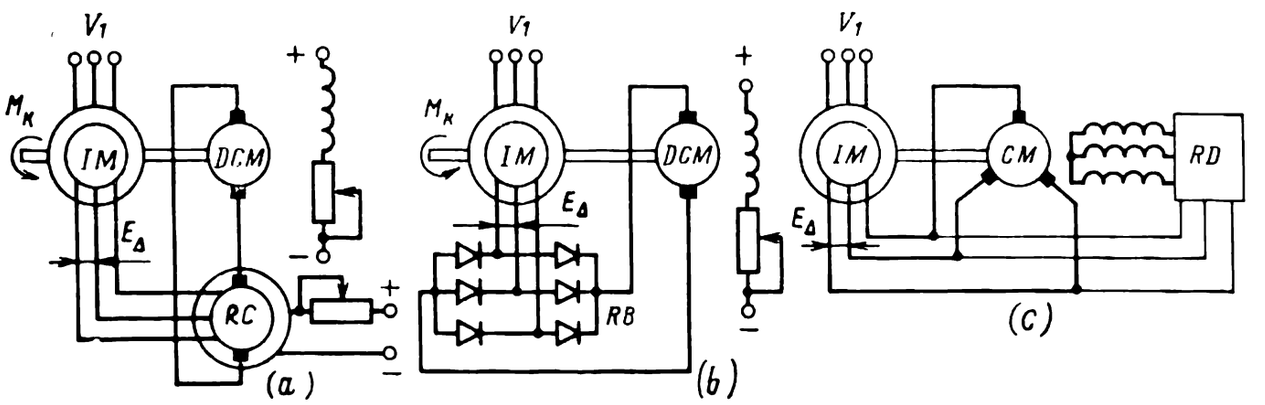

Fig. 68-10 Various electromechanical speed control schemes

The bidirectional converter acts in response to control signals coming from a control unit. The output frequency can be varied by changing the number of input voltage half-cycles that can be accommodated in a half-cycle of output voltage. The value of E_Δ can be controlled by varying the firing angles of the thyristors.

A bidirectional converter speed control scheme permits speed control both downwards and upwards from synchronous. However, special measures need to be taken to ensure stability of operation at speeds above synchronous.

Some of the likely arrangements for eletromechanical speed control schemes are shown in Fig. 68-10. They may have an intermediate d.c. link (as in Fig. 68-10*a* and *b*), or they may be built without a d.c. link (as in Fig. 68-10*c*).

In an *electromechanical speed-control scheme with an intermediate d.c. link*, the slip power P_Δ is returned to the induction motor by a d.c. motor, *DCM*, energized from the rotor winding of the induction motor via a frequency changer or, rather, a rectifier. It rectifies the incoming current and E_Δ at frequency f_2 to a direct current and a direct emf.

The arrangement shown in Fig. 68-10*a* is better known as the *Krämer scheme* (system or drive). In this system, the slip energy of the main induction motor is transformed into direct current by a rotary converter, *RC*, or dynamotor

rather than by a rectifier. Because of this, the Krämer scheme suffers from the same drawbacks as the Scheribus scheme (see above), namely: it can control speed only downwards from synchronous; at $s < 0.1$ the rotary converter is liable to lose stability; and power rating is limited. Because of this, high-power schemes employ a motor-generator set consisting of a synchronous motor and a d.c. generator instead of a rotary converter.

In the arrangement shown in Fig. 68-10*b*, the current at f_2 is rectified by a rectifier bridge *RB* consisting of uncontrolled semiconductor rectifiers (crystal diodes).

A likely arrangement for a *direct-connected speed-control scheme* is shown in Fig. 68-10*c*. There is no frequency changer at all, and the motor utilizing the slip-power P_Δ is an a.c. commutator motor, *CM* (in the example discussed it is a three-phase, a.c. commutator shunt-wound motor, see Sec. 68-3). In a three-phase a.c. commutator motor, the frequency of E_Δ across the motor brushes is the same as that of its field current, f_2. Therefore, it can be used to inject the slip-frequency emf, E_Δ, into the rotor of the induction motor. This emf and, as a consequence, the slip of the main motor can be varied with a regulating device, *RD*. For the same reasons as in a scheme using a commutator motor, speed can only be controlled downwards from synchronous. Speeds above synchronous can be obtained if the field winding of the commutator motor is energized from an independent source of voltage at slip-frequency. Because of the limitations imposed by commutation, the power rating in such a scheme may not exceed 150-200 kW and that of the drive as a whole (with speed control down to 0.7 of synchronous), 450 to 600 kW.

At present, commutator-machine sets have almost completely been ousted by rectifier-machine and static converter schemes which may be built for any power ratings and any speed control ranges and offer a number of other advantages.

☆ 68-5 Single-Phase Commutator Motors

In arrangement, a single-phase commutator motor is not unlike a d.c. motor. Its rotor carries a closed armature winding connected to a commutator. The stator core may be salient or nonsalient. To minimize iron (core) losses, it

is built up of electrical-sheet steel laminations. The slots on the stator receive a heteropolar, concentrated or distributed single-phase winding.

In a *series single-phase commutator motor*, the stator and rotor windings are series-connected conductively (see Fig. 68-12). In a *single-phase repulsion motor* (see Fig. 68-15), the stator and rotor windings are coupled inductively (by transformer action).

(i) Electromagnetic Processes in Single-Phase Commutator Motors

(a) EMFs in the rotor winding. The alternating mutual flux Φ produced by alternating currents in the windings of a single-phase commutator motor may be resolved into two components, a d-axis flux Φ_d and a q-axis flux Φ_q (Fig. 68-11). As the rotor moves in the d-axis field, a rotational (or motional) emf, e_{rot}, is induced across its brushes, proportional to the instantaneous d-axis flux. If Φ_d varies in time sinusoidally at frequency f_Φ, then e_{rot} will likewise vary sinusoidally and in phase (in the generator mode of operation) or in anti-phase (in the motor mode of operation) with Φ_d. Its instantaneous value can be found from the equation derived for d.c. machines (see Sec. 64-5). Extending this equation to the peak rotational mmf, $E_{\text{rot}\,m}$, and recalling that $E_{\text{rot}\,m} = \sqrt{2}E_{\text{rot}}$, the rms rotational emf is found to be

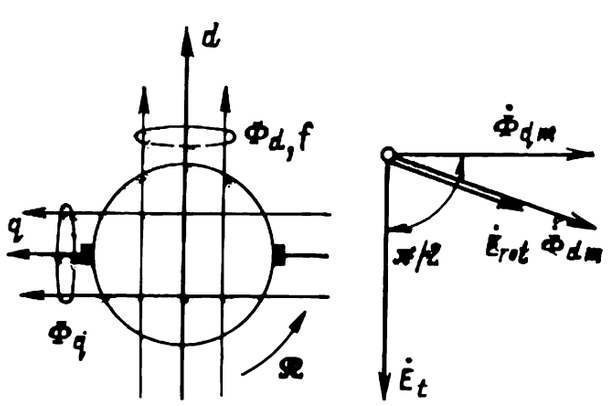

Fig. 68-11 EMF in the rotor winding of a single-phase commutator motor

$$E_{\text{rot}} = c_w \Omega \Phi_{dm} / \sqrt{2} = 2\sqrt{2}\, f u \Phi_{dm} \qquad (68\text{-}13)$$

where Φ_{dm} is the peak d-axis flux, $f = p\Omega/2\pi$ is the frequency of the rotor, and Ω is the angular velocity of the rotor.

Also, a transformer emf, e_t, is induced in the parallel path of the rotor winding connected between the brushes. The transformer emf is induced by variations in the q-axis

flux at frequency f_Φ and is of the same origin as the emf in the secondary winding of a transformer. Its rms value is given by

$$E_t = \frac{2\pi}{\sqrt{2}} f_\Phi k_w w \Phi_{qm} = 2\sqrt{2} f_\Phi w \Phi_{qm} \qquad (68\text{-}14)$$

where Φ_{qm} is the peak q-axis flux, and $k_w = k_p k_d \approx 2/\pi$ is the winding factor (see Sec. 64-5).

The transformer emf is independent of the rotor speed and lags behind Φ_{qm} by $\pi/2$.

(b) Electromagnetic torque. The instantaneous electromagnetic torque acting on the rotor of a single-phase motor may be found from the equation derived for a d.c. machine (see Sec. 64-6):

$$T_{em} = c_w i \Phi_d$$

where

$$i = I_m \cos \omega_\Phi t$$

is the instantaneous rotor current, and

$$\Phi_d = \Phi_{dm} \cos (\omega_\Phi t - \beta)$$

is the instantaneous d-axis flux.

On writing the instantaneous electromagnetic torque as a function of time,

$$T_{em} = \frac{c_w I_m \Phi_{dm}}{2} [\cot (2\omega_\Phi t - \beta) + \cos \beta]$$

we note that it contains a constant (direct) component proportional to $\cos \beta$ and a variable (alternating) component proportional to $\cos (2\omega_\Phi t - \beta)$ which alternates at a double frequency

$$2f_\Phi = 2\omega_\Phi / 2\pi$$

The average electromagnetic torque is found by integrating the instantaneous electromagnetic torque over the period $T = 1/f_\Phi = 2\pi/\omega_\Phi$,

$$T_{av} = \frac{1}{T} \int_0^T T_{em}\, dt = \frac{c_w I_m \Phi_{dm}}{2} \cos \beta \qquad (68\text{-}15)$$

This torque is involved in the energy conversion by a single-phase motor. The electromagnetic power converted by the motor into mechanical power can readily be written as

$$P_{em} = P_m = T_{av}\, \Omega = E_{rot}\, I \cos \beta \qquad (68\text{-}16)$$

where

$$E_{\text{rot}} = c_{\text{w}} \Omega \Phi_{dm} / \sqrt{2}$$

is the rms rotational emf and

$$I = I_m / \sqrt{2}$$

is the rms armature current.

As is seen from Eq. (68-16), the electromagnetic power of, and energy conversion by, a single-phase motor are solely related to its rotational emf.

(c) Commutation. As in three-phase a.c. commutator motors, three emfs differing in origin are induced in the rotor coils undergoing commutation in a single-phase motor. They are a reactance emf, a rotational (or motional) emf, and a transformer emf. The *reactance* emf, E_{react} associated with variations of current in the commutated coil is proportional to the instantaneous rotor current and rotational speed; it is a quantity varying in phase with the rotor current. The *rotational* (or motional) emf, $E_{\text{rot, c}}$ is induced in the coil being commutated as it moves in the q-axis field; it is likewise proportional to the rotational speed and current of the rotor and is a quantity varying in phase with the rotor current. The *transformer* emf, $E_{\text{t, c}}$, is induced in the coil undergoing commutation owing to variations in the d-axis flux at supply frequency f_Φ; its rms value is proportional to Φ_d and the supply frequency, and it lags in phase behind the flux by $\pi/2$. The transformer emf substantially impairs the commutation in single-phase commutator motors in comparison with d.c. motors.

(ii) Single-Phase Compensated Series Motor

Diagrammatically, a single-phase compensated series motor is shown in Fig. 68-12. It differs but little in arrangement from a series-wound d.c. motor. In addition to a field winding, FW, connected in series with the rotor winding, the stator carries two more windings, likewise series-connected with the rotor. They are a compole winding, CPW, and a compensating winding, CW.

The motor current, I, can be found from the voltage equation

$$\dot{V} = -\dot{E}_{\text{rot}} + R\dot{I} + jX\dot{I}$$

where R is the resistance of the series-connected rotor, field, compensating and compole windings, and X is their reactance. Owing to the compensating action of the compole and compensating windings, their reactance is small in comparison with that of the rotor winding.

The diagram answering the above voltage equation appears in Fig. 68-13. Because in an unsaturated machine the

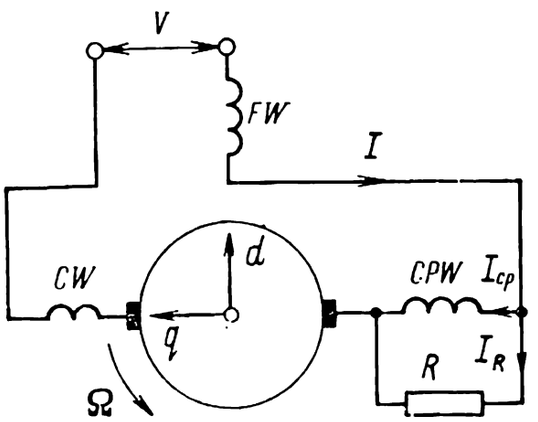

Fig. 68-12 Single-phase series motor

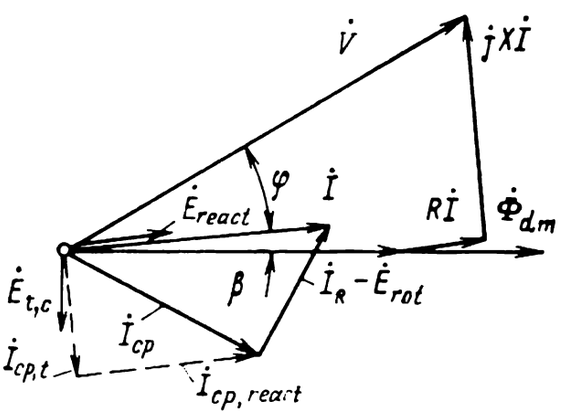

Fig. 68-13 Phasor diagram of a series commutator motor

d-axis flux is produced by the current I in the field winding and is proportional to that current, the rotational emf, Eq. (68-13), should preferably be expressed in terms of I as

$$\dot{E}_{\text{rot}} = -\Omega_* r_\Omega \dot{I}$$

where r_Ω is a proportionality factor found from the magnetization curve and is a function of I (if a linearized curve is used, r_Ω is constant); $\Omega_* = \Omega/\Omega_\Phi$ is the per-unit angular velocity, and $\Omega_\Phi = 2\pi f_\Phi/p$ is the base angular velocity which has the meaning of synchronous velocity at supply frequency.

Considering the equations for $\dot{V}$ and $\dot{E}_{\text{rot}}$ together, we get

$$I = |\dot{I}| = \left| \frac{\dot{V}}{R + r_\Omega \Omega_* + jX} \right| = \frac{V}{\sqrt{(R + r_\Omega \Omega_*)^2 + X^2}}$$

It is convenient to express the electromagnetic torque of a single-phase compensated series motor in terms of its electromagnetic power from Eq. (68-16).

$$T_{\text{av}} = P_{\text{em}}/\Omega = E_{\text{rot}} I \cos(\beta)/\Omega$$

$$= V^2 r_\Omega/\Omega_\Phi \left[(R + r_\Omega \Omega_*)^2 + X^2\right]$$

The construction of a family of speed-torque characteristics for a single-phase compensated series motor on the basis of the above equation is illustrated in Fig. 68-14. They are drooping characteristics, as is the case with a d.c. series-wound motor.

The speed of a single-phase compensated series motor can be controlled over a wide range by varying voltage with a regulating transformer. Motor reversal is accomplished by interchanging the connections of the field winding so that its current is reversed.

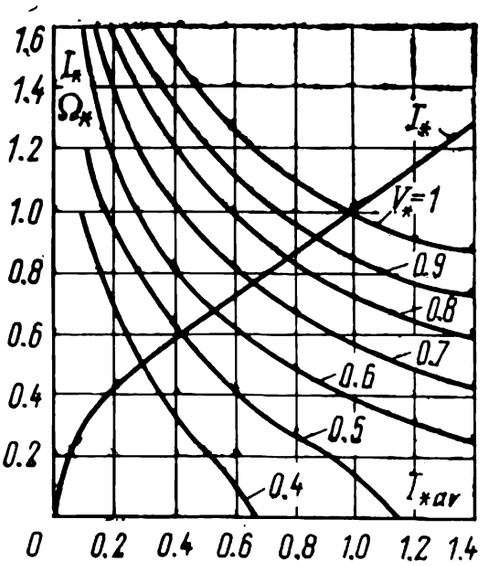

Fig. 68-14 Speed-torque characteristics of a single-phase series commutator motor

Large single-phase series motors have only found use in electric traction. For better commutation, they are fed with a reduced supply frequency ($16^2/_3$ or 25 Hz). To keep the brush voltage within the limits set by the commutation requirements (300 V at 25 Hz and 500 V at $16^2/_3$ Hz), they are connected to the supply line (usually operating at 10-25 kV) via step-down tranformers.

Traction single-phase motors have a high efficency (about 90%), a high power factor (0.96 to 0.97 at $16^2/_3$ Hz) and good starting performance. With the input voltage reduced to 40% or 50% of the rated value, the initial (static) starting torque and current are close to their rated values. Traction motors come in ratings up to 2.5 MW.

Recently, however, traction single-phase motors on electric railways have been giving way to d.c. motors supplied from a.c. overhead contact lines via solid-state rectifiers.

Small single-phase series motors (up to about 0.5 kW) designed for operation from a 50-Hz or 60-Hz supply are widely used in high-speed (up to 30 000 rpm) and regulated drives (in vacuum cleaners, floor polishers, sewing machines, electric drills, and the like).

Small single-phase series motors up to about a few tens of watts are commonly designed to operate either on direct or alternating current and are known as *universal motors*. The field winding of a universal motor has an additiona1

tap which, in operation on a.c., permits some of the turns to be switched out, thereby reducing the winding reactance so that the speed is the same as in operation on d.c.

(iii) Single-Phase Repulsion Motors

Whereas in a single-phase series motor the stator and rotor windings are connected conductively, in a repulsion motor they are coupled inductively (by transformer action). One form of the repulsion motor with two series-connected stator winding was proposed by Atkinson. In his motor, one stator winding produced a *d*-axis flux, and the other, a *q*-axis flux. The brushes were short-circuited and a current was produced in the rotor winding by a transformer emf, E_t, Eq. (68-14), induced by changes in the *q*-axis flux at frequency f_Φ.

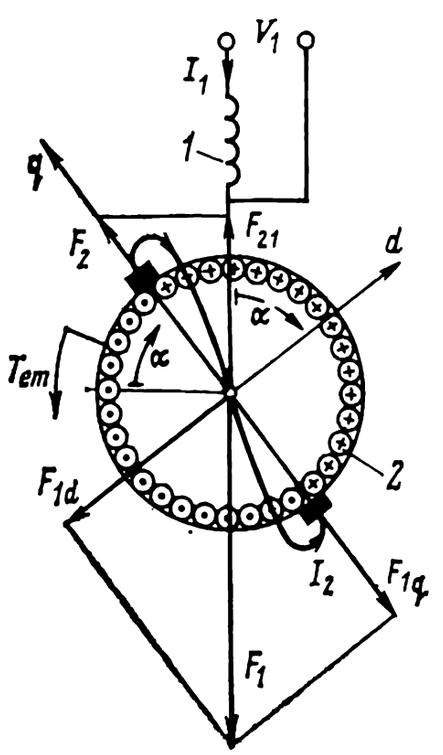

Fig. 68-15 Repulsion (Thompson) motor

In another form of the repulsion motor due to Arnold, the two stator windings, one aligned on the *d*-axis and the other on the *q*-axis of the rotor, were replaced by one winding (at *1* in Fig. 68-15). The armature winding *2* was short-circuited via a conductive path between the brushes. A suitable device could shift the brushes to any position relative to the stator axis. In this form, known as the *Thompson motor*, repulsion motors found a fairly broad field of application at one time.

The repulsion motor can be direct-on-line started, and its speed can be controlled by shifting the brushes (without any external adjusting or starting devices).

The performance of a repulsion motor substantially depends on the angular position of the brushes, or the *brush angle* which is the angle α between the *d*-axis and the stator axis (Fig. 68-15). For better insight into the matter, let us resolve the pulsating stator mmf F_1 into two components,

$$F_{1q} = F_1 \sin \alpha$$

directed along the q-axis, and

$$F_{1d} = F_1 \cos \alpha$$

directed along the d-axis which is at right angles to the brush axis. The q-axis mmf induces in the stationary rotor winding a transformer emf, E_{2t}, as in the secondary of a transformer, and this emf gives rise to a current I_2 which sets up an mmf, F_2, opposing F_{1q}. The interaction of I_2 with Φ_d produced by F_{1d} gives rise, in accord with Eq. (68-15), to an electromagnetic torque

$$T_{em} = c_w I_2 \Phi_d \cos(\beta)/\sqrt{2}$$

always acting in the direction opposite to the brush shift from the stator axis (that is, from $\alpha = 0$). So long as the brushes are on the stator axis ($\alpha = 0$), the secondary current is zero ($I_2 = 0$), and the d-axis flux is a maximum, $\Phi_d = \Phi_{d,\,max}$. When the brushes are shifted from the stator axis through 90°, the d-axis flux is zero, but the secondary current is a maximum $I_2 = I_{2,\,max}$. Accordingly, at $\alpha = 0$ and $\alpha = 90°$, the initial starting torque is zero. The starting torque is a maximum at α ranging between 75° and 80°. After the electromagnetic torque sets the rotor in motion, a rotational (motional) emf, $E_{2,\,rot}$, is induced in the rotor winding in addition to the transformer emf, $E_{2,\,t}$. Therefore, with the repulsion motor running, the steady state can be described by the following voltage equations:

$$\dot{V}_1 - \dot{I}_1 Z_1 = -\dot{E}_{1,\,t} \qquad (68\text{-}17)$$

$$\dot{E}'_{2,\,t} + \dot{E}'_{2,\,rot} = \dot{I}'_2 Z'_2 \qquad (68\text{-}18)$$

where $\dot{E}'_{2,\,t}$ is the transformer emf referred to the primary side. Because of pulsations, $\dot{E}'_{2,\,t}$ has the same frequency f_Φ as the resultant q-axis flux, Φ_q, produced by the resultant q-axis mmf

$$\dot{F}_{1q} + \dot{F}_2 = \dot{F}_1 \sin \alpha + \dot{F}_2 \sim \dot{I}_1 \sin \alpha + \dot{I}'_2$$

Therefore,

$$\dot{E}'_{2,\,t} = -j2\sqrt{2} f_\Phi w \dot{\Phi}_q = -j(I_1 \sin \alpha + \dot{I}'_2) X_0 \qquad (68\text{-}19)$$

where X_0 is the mutual reactance between the stator and rotor windings, referred to the stator winding.

The transformer emf, $\dot{E}_{1,\,t}$ in the stator winding is induced by pulsations in the resultant mmf directed along the stator axis,

$$\dot{F}_1 + \dot{F}_{21} = \dot{F}_1 + \dot{F}_2 \sin\alpha \sim \dot{I}_1 + \dot{I}'_2 \sin\alpha$$

Therefore,

$$\dot{E}_{1,\,t} = -j\,(I_1 \sin\alpha + \dot{I}'_2)\,X_0 \qquad (68\text{-}20)$$

The rotational (or motional) rotor emf referred to the stator, $\dot{E}'_{2,\,rot}$ is induced as the conductors of the rotor rotating at Ω cut the lines of d-axis flux, Φ_d, set up by

$$\dot{F}_{1d} = \dot{F}_1 \cos\alpha \sim \dot{I}_1 \cos\alpha$$

Using Eq. (68-13), we get

$$\dot{E}'_{2,\,rot} = 2\sqrt{2}\,fw\,\dot{\Phi}_d = X_0\Omega_*\dot{I}_1 \cos\alpha \qquad (68\text{-}21)$$

where

$$\Omega_* = \Omega/\Omega_\Phi$$

is the per-unit angular velocity, and

$$\Omega_\Phi = 2\pi f_\Phi/p$$

is the synchronous angular velocity at f_Φ.

Considering Eqs. (68-17) through (68-21) together, we obtain

$$\begin{aligned}\dot{I}_1 &= \dot{V}_1\,[Z_1 + C_0\,(Z'_2 + \Omega_* X_0 \sin\alpha\cos\alpha + jX_0\cos^2\alpha)]\\ \dot{I}'_2 &= -\dot{I}_1 C_0\,(\sin\alpha + j\Omega_*\cos\alpha)\end{aligned} \qquad (68\text{-}22)$$

where

$$C_0 = X_0/(X_0 + Z'_2)$$

is a complex coefficient.

The electromagnetic torque can be found from Eqs. (68-15) and (68-16):

$$T_{av} = (E'_{2,\,rot} I'_2 \cos\beta)/\Omega = \mathrm{Re}\,[\dot{E}_{2,\,rot}\dot{I}^*_2/\Omega]$$

Repulsion motors have speed-torque characteristics similar to those of a single-phase series motor. Under rated conditions, the brush angle α is usually 65° to 75°. The speed of a repulsion motor can be controlled between the speed limits 0.3 and 1.1 (in per unit) by brush-shifting.

Among the other forms of the repulsion motor, the best starting and speed-control performance is shown by the *Deri motor*. In contrast to the Thompson motor, it has two sets of short-circuited brushes (that is, the number of brushes is twice as great as that of poles). Owing to easier commutation conditions, the Deri motor can be built in larger sizes (up to 200 kW at 50 Hz) and their speed can be controlled between 0 and 1.1 (in per unit).

Transient Phenomena in Electrical Machines

7

Introduction

The term 'transients' refers to phenomena appearing during the transition from one steady state (operating condition) to another. In electrical machines they occur because of changes in line voltages, winding or load impedances, or the external (applied or load) torque. Such changes may be introduced intentionally (by routine switching operations) or occur as a result of abnormal situations (such as short or open circuits in the external circuit or the machines themselves).

What may be called 'normal' transients appear when, say, an induction motor is being connected to an a.c. supply line and brought up to speed, when synchronous motors are being induction-started, or synchronous generators are being put on line (synchronized) for parallel operation.

Examples of 'abnormal' transients are those caused by sudden balanced and/or unbalanced faults to ground or between phases in synchronous and induction machines.

Transient currents may be several times their rated value. The same is true of electromagnetic torque and electromagnetic forces. It may so happen that the voltages in some parts of the machine may exceed the limit of safety.

It is customary to class the transients associated with electrical machinery into electromagnetic and electromechanical. During electromagnetic transients, the speed of the machine may be deemed constant. During electromechanical transients, the speed and kinetic energy of the machine are subject to appreciable variations.

An electrical machine must be designed to withstand the expected transients without damage. To this end, theory must be able to predict how routine (operational) transients may proceed (for example, it should define the conditions for the machines being synchronized to pull into synchro-

nism). Advance analysis of 'fault' (abnormal) transients is essential for protective facilities to be tuned up as appropriate.

The theory of transient phenomena in electrical machines is a complex and ramified subject. This text is limited to the most important aspects of transient theory as applied to induction and synchronous machines of conventional designs. Where necessary, references are made to Part 2, "A General Theory of A. C. Machines".

69 Mathematical Description of Transients in Induction Machines

69-1 Differential Equations Based on Phase Quantities

The complete system of equations describing transients should include the differential equations of winding voltages and the equations of motion for the rotating parts of the machine.

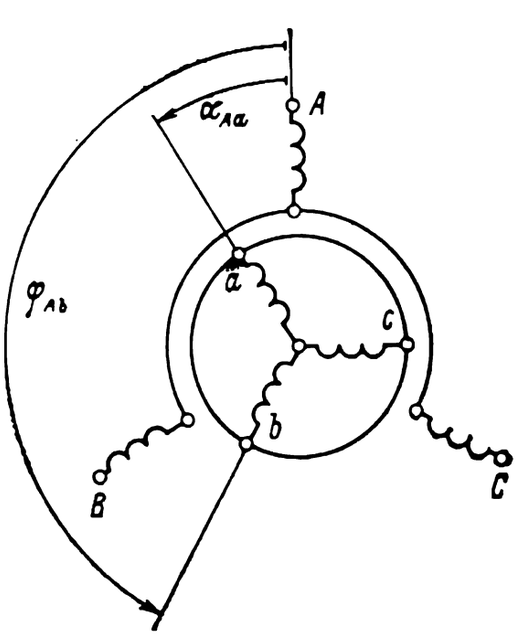

Fig. 69-1 An induction machine with a three-phase stator and a three-phase rotor winding (a two-pole model)

At commercial frequency (50 Hz), the windings of a machine can be treated as lumped-constant electric circuits, because the length of an electromagnetic wave is many times the linear dimensions of the windings. We shall discuss an induction machine with $2p$-pole, three-phase balanced stator and rotor windings. A two-pole model of such a machine is shown in Fig. 69-1. The stator winding is connected to an a.c. external circuit. The rotor winding is closed through impedances. We assume to know in advance all the quantities associated with the initial steady state prior to the transient, namely the instantaneous phase

voltages and currents ($v_{1A\Sigma}$, $v_{1B\Sigma}$, $1_{1C\Sigma}$, $v_{2a\Sigma}$, $v_{2b\Sigma}$, $v_{2c\Sigma}$, $i_{1A\Sigma}$, $i_{1B\Sigma}$, $i_{1C\Sigma}$, $i_{2a\Sigma}$, $i_{2b\Sigma}$, and $i_{2c\Sigma}$) and the initial mechanical angular velocity of the rotor, Ω. Initially, the electromagnetic torque T_{em} is balanced by the external torque T_{ext} applied to the rotor. The angular acceleration is zero ($d\Omega/dt = 0$), and the rotor is spinning at a constant angular velocity.

A transient may be initiated by a balanced or an unbalanced change in the time phase or peak value of the a.c. voltages fed to the stator winding (for example, by a change in the peak values of symmetric positive-, negative-, or zero-phase sequence voltage components, $\sqrt{2}V_{11}$, $\sqrt{2}V_{21}$ or $\sqrt{2}V_{01}$, respectively). A transient may be initiated by a sudden change in T_{ext}, leading to a disbalance of torque, a resultant acceleration and, finally, a new value of speed.

To determine the currents during a transient, given initial conditions, we should solve a set of differential equations for the instantaneous voltages of the stator phases

$$\begin{aligned} v_{1A\Sigma} &= R_1 i_{1A\Sigma} + d\Psi_{1A\Sigma}/dt \\ v_{1B\Sigma} &= R_1 i_{1B\Sigma} + d\Psi_{1B\Sigma}/dt \\ v_{1C\Sigma} &= R_1 i_{1C\Sigma} + d\Psi_{1C\Sigma}/dt \end{aligned} \tag{69-1}$$

and the instantaneous voltages of the rotor phases

$$\begin{aligned} v_{2a\Sigma} &= R_2 i_{2a\Sigma} + d\Psi_{2a\Sigma}/dt \\ v_{2b\Sigma} &= R_2 i_{2b\Sigma} + d\Psi_{2b\Sigma}/dt \\ v_{2c\Sigma} &= R_2 i_{2c\Sigma} + d\Psi_{2c\Sigma}/dt \end{aligned} \tag{69-2}$$

Equations (69-2) are written in terms of the rotor quantities referred to the stator side (the referring prime is usually omitted). The rotor quantities are referred to the stator side so as to simplify the discussion and calculations. In referring, use is made of the equations derived in Sec. 42-2.

If the magnetic circuit of the machine is unsaturated, the flux linkages with the stator and rotor phases can be written in terms of the phase currents and the corresponding inductances. Thus, for the A phase of the stator,

$$\begin{aligned} \Psi_{1A\Sigma} = {} & L_{AA\Sigma} i_{1A\Sigma} + L_{AB\Sigma} i_{1B\Sigma} + L_{AC\Sigma} i_{1C\Sigma} \\ & + L_{Aa} i_{2a\Sigma} + L_{Ab} i_{2b\Sigma} + L_{AC} i_{2c\Sigma} \end{aligned} \tag{69-3}$$

and for the a phase of the rotor,

$$\Psi_{2a\Sigma} = L_{aa\Sigma} i_{2a\Sigma} + L_{ab\Sigma} i_{2b\Sigma} + L_{a\Sigma c} i_{2c\Sigma} + L_{aA} i_{1A\Sigma} + L_{aB} i_{1B\Sigma} + L_{aC} i_{1C\Sigma} \quad (69\text{-}4)$$

The flux linkages with the other phases can be written in a similar way.

The equations of flux linkages contain (see Chap. 28) the phase inductances

$$\begin{aligned} L_{AA\Sigma} &= L_{AA\sigma} + L_{AA} \\ L_{BB\Sigma} &= L_{BB\sigma} + L_{BB} \\ &\cdots\cdots\cdots \\ L_{aa\Sigma} &= L_{aa\sigma} + L_{aa} \\ L_{bb\Sigma} &= L_{bb\sigma} + L_{bb} \\ &\cdots\cdots\cdots \end{aligned} \quad (69\text{-}5)$$

the mutual inductances between the stator phases

$$\begin{aligned} L_{AB\Sigma} &= L_{AB\sigma} + L_{AB} \\ L_{AC\Sigma} &= L_{AC\sigma} + L_{AC} \end{aligned}$$

the mutual inductances between the rotor phases

$$\begin{aligned} L_{ab\Sigma} &= L_{ab\sigma} + L_{ab} \\ L_{ac\Sigma} &= L_{ac\sigma} + L_{ac} \end{aligned}$$

and the mutual inductances between the rotor and stator phase (L_{Aa}, L_{Ab}, L_{Ac}, L_{Ba}, L_{Bb}, L_{Bc}, etc.).

If we include the gap field harmonics only in calculating the self- and mutual leakage inductances ($L_{AA\sigma}$, $L_{AC\sigma}$ . . ., $L_{aa\sigma}$, $L_{ac\sigma}$, . . .), then all the other self- and mutual inductances (L_{AA}, L_{AB}, . . ., L_{aa}, L_{ab}, L_{Aa}, L_{Ab}, . . .) will be associated solely with the fundamental terms of the gap field and can be found using the equations for the main (useful) self- and mutual inductances (see Chap. 28).

Noting that all the rotor quantities must be referred to the stator side, it is usual to replace the rotor winding variables in all the equations by the respective stator variables (w_1 instead of w_2, k_{w1} instead ok k_{w2}, and m_1 instead of m_2)*. After referring to the stator side, the main self-indu-

* Here and in the subsequent chapters, the number of pole pairs will be denoted by p_τ to avoid confusion with the differential operator, $p = \mathrm{d}/\mathrm{d}t$.

ctances of all phases turn out to be the same and independent of the angular position taken up by the rotor

$$L_{AA} = L_{BB} = L_{CC} = L_{aa} = L_{bb} = L_{cc} = L_m$$

where

$$L_m = (4\mu_0/p_\tau \pi^2)\,(w_1 k_{w1})^2\,(\tau l_\delta/\delta k_\delta) \qquad (69\text{-}6)$$

is the maximum referred mutual inductance between the stator and rotor phases.

The main mutual inductances between stator phases

$$L_{AB} = L_{AC} = L_{BC} = -L_m/2 \qquad (69\text{-}7)$$

and the mutual inductances between the rotor phases

$$L_{ab} = L_{ac} = L_{bc} = -L_m/2 \qquad (69\text{-}8)$$

are seen to be likewise the same and independent of the angular position of the rotor.

In contrast, the mutual inductances between the rotor and stator phases depend on the angular position of the rotor, that is, the angle γ between the axes of phases A and a:

$$L_{Aa} = L_{Bb} = L_{Cc} = L_m \cos \alpha_{Aa}$$
$$L_{Ab} = L_{Bc} = L_{Ca} = L_m \cos \alpha_{Ab}$$
$$L_{Ac} = L_{Ba} = L_{Cb} = L_m \cos \alpha_{Ac}$$

and generally,

$$L_{kn} = L_m \cos \alpha_{kn} \qquad (69\text{-}9)$$

where α_{kn} are the electrical angles between the axes of the stator phases ($k = A, B, C$) and the axes of the rotor phases ($n = a, b, c$), defined as

$$\alpha_{Aa} = \alpha_{Bb} = \alpha_{Cc} = \alpha = p_\tau \gamma$$
$$\alpha_{Ab} = \alpha_{Bc} = \alpha_{Ca} = \alpha + 2\pi/3$$
$$\alpha_{Ac} = \alpha_{Ba} = \alpha_{Cb} = \alpha + 4\pi/3$$

As the rotor revolves at a constant speed, the angle between the axes of phases A and a increases in a linear fashion

$$\gamma = \gamma_0 + \Omega_0 t$$

or, generally,

$$\gamma = \gamma_0 + \int_0^t \Omega \, dt \qquad (69\text{-}10)$$

In cases where variations in the angular velocity of the rotor must be considered, the above equations should be extended to include the equation of rotor motion

$$T_{em} + T_{ext} = J \, d\Omega/dt \qquad (69\text{-}11)$$

where J is the moment of inertia of the machine*, and also an equation for the angular velocity of the rotor

$$\Omega = \Omega_0 + \int_0^t (d\Omega/dt) \, dt \qquad (69\text{-}12)$$

On the assumptions made, the electromagnetic torque in Eq. (69-11) is expressed in terms of the derivatives of the winding inductances with respect to the angle γ and the phase current, and may in the general case be found from Eq. (18-6) which contains only the derivatives of the mutual inductances between a rotor phase and a stator phase

$$T_{em} = \sum_{k=A, B, C,} i_{1k\Sigma} \sum_{n=a, b, c} i_{2n\Sigma} \, dL_{kn}/d\gamma \qquad (69\text{-}13)$$

The differential equations including Eqs. (18-6) and (69-13) give a complete description of the transients in a three-phase induction machine. Unfortunately, their direct solution presents serious difficulties for two reasons:

(1) they contain too many unknowns (six stator and rotor phase variables);

(2) they involve periodically varying mutual inductances L_{Aa}, L_{Ab}, etc., because of which some coefficients of the current derivatives in Eqs. (69-1) and (69-2) are periodic functions of time.

To simplify the solution, the original set of equations is transformed in such a way that the natural variables (currents, flux linkages, phase voltages) are expressed in terms of other, more convenient variables.

69-2 Zero-Sequence Components of the Phase Quantities

If the phase quantities contain zero-sequence components, the latter must be separated. For example, if the instantaneous phase currents do not add up to zero

$$i_{1A\Sigma} + i_{1B\Sigma} + i_{1C\Sigma} \neq 0$$

* The moment of inertia of the rotor is found with allowance for the effect of the parts driven by the machine.

and contain a zero-sequence current

$$i_{01} = (i_{1A\Sigma} + i_{1B\Sigma} + i_{1C\Sigma})/3 \qquad (69\text{-}14)$$

they must be written as the sum of two components, namely the zero-sequence current in each phase, and the currents that do not contain zero-sequence components

$$i_{1A} = i_{1A\Sigma} - i_{01}, \quad i_{1B} = i_{1B\Sigma} - i_{01}, \quad i_{1C} = i_{1C\Sigma} - i_{01}$$

and add up to zero

$$i_{1A} + i_{1B} + i_{1C} = (i_{1A\Sigma} + i_{1B\Sigma} + i_{1C\Sigma}) - 3i_{01} = 0 \qquad (69\text{-}15)$$

Similarly, the phase voltages ($v_{1A\Sigma}$, $v_{1B\Sigma}$, . . .) and flux linkages ($\Psi_{1A\Sigma}$, $\Psi_{1B\Sigma}$, . . .) should be written as the sums of zero-sequence components (v_{01} and Ψ_{01}) and the components ($v_{1A} = v_{1A\Sigma} - v_{01}$, . . ., $\Psi_{1A} = \Psi_{1A\Sigma} - \Psi_{10}$) which, when added together to include all the phases, sum up to zero

$$\begin{aligned} v_{1A} + v_{1B} + v_{1C} &= 0 \\ \Psi_{1A} + \Psi_{1B} + \Psi_{1C} &= 0 \end{aligned} \qquad (69\text{-}16)$$

Similarly, the phase rotor quantities are resolved into the zero-sequence components and the components that do not contain zero-sequence components:

$$\left.\begin{aligned} i_{2a\Sigma} &= i_{2a} + i_{02}, \quad i_{2b\Sigma} = i_{2b} + i_{02}, \quad \ldots \\ v_{2a\Sigma} &= v_{2a} + v_{02}, \quad v_{2b\Sigma} = v_{2b} + v_{02}, \quad \ldots \\ \Psi_{2a\Sigma} &= \Psi_{2a} + \Psi_{02}, \quad \Psi_{2b\Sigma} = \Psi_{2b} + \Psi_{02}, \quad \ldots \end{aligned}\right\} \qquad (69\text{-}17)$$

where

$$\begin{aligned} i_{2a} + i_{2b} + i_{2c} &= 0 \\ v_{2a} + v_{2b} + v_{2c} &= 0 \\ \Psi_{2a} + \Psi_{2b} + \Psi_{2c} &= 0 \end{aligned}$$

When the terms of Eqs. (69-1) and (69-2) are written as sums of the above components, the set of equations divides into two sets of equations, one involving the phase quantities that do not contain zero-sequence terms

$$v_{1A} = R_1 i_{1A} + \mathrm{d}\Psi_{1A}/\mathrm{d}t, \quad v_{1B} = R_1 i_{1B} + \mathrm{d}\Psi_{1B}/\mathrm{d}t \ldots \qquad (69\text{-}18)$$

$$v_{2a} = R_2 i_{2a} + \mathrm{d}\Psi_{2a}/\mathrm{d}t, \quad v_{2b} = R_2 i_{2b} + \mathrm{d}\Psi_{2b}/\mathrm{d}t \ldots$$

and the other involving zero-sequence terms

$$v_{01} = R_1 i_{01} + \mathrm{d}\Psi_{01}/\mathrm{d}t, \quad v_{02} = R_2 i_{02} + \mathrm{d}\Psi_{02}/\mathrm{d}t \ldots \qquad (69\text{-}19)$$

If we express the currents in the flux-linkage equations (69-3) and (69-4) as sums of two components and recall Eqs. (69-15), (69-17), (69-6), (69-7) and (69-8), equations for flux-linkage components can be written:

$$\left.\begin{aligned} \Psi_{1A\Sigma} &= \Psi_{1A} + \Psi_{01}, \quad \Psi_{1B\Sigma} = \Psi_{1B} + \Psi_{01} \ \ldots \\ \Psi_{2a\Sigma} &= \Psi_{2a} + \Psi_{02}, \quad \Psi_{2b\Sigma} = \Psi_{2b} + \Psi_{02} \ \ldots \end{aligned}\right\} \qquad (69\text{-}20)$$

where

$$\begin{aligned} \Psi_{1A} &= L_1 i_{1A} + L_{Aa} i_{2a} + L_{Ab} i_{2b} + L_{Ac} i_{2c} \\ \Psi_{1B} &= L_1 i_{1B} + L_{Ba} i_{2a} + L_{Bb} i_{2b} + L_{Bc} i_{2c} \\ \Psi_{2a} &= L_2 i_{2a} + L_{aA} i_{1A} + L_{aB} i_{1B} + L_{aC} i_{1C} \\ \Psi_{2b} &= L_2 i_{2b} + L_{bA} i_{1A} + L_{bB} i_{1B} + L_{bC} i_{1C} \\ &\ldots\ldots\ldots\ldots\ldots\ldots\ldots \end{aligned}$$

are the flux linkages that do not contain zero-sequence components, and

$$\Psi_{01} = L_{01} i_{01}, \quad \Psi_{02} = L_{02} i_{02}, \ \ldots$$

are the zero-sequence flux linkages.

Also, the flux-linkage equations contain

$$L_1 = L_{11} + L_{1\sigma}$$

which is the stator-phase inductance for the set of currents i_{1A}, i_{1B} and i_{1C} that does not contain zero-sequence currents (with allowance for the effect of the other phases);

$$L_{11} = L_{AA} - L_{AB} = 3L_m/2$$

which is the stator-phase inductance component associated with the fundamental term of the mutual field;

$$L_{1\sigma} = L_{AA\sigma} - L_{AB\sigma}$$

which is the stator-phase inductance component associated with the leakage fields;

$$L_2 = L_{22} + L_{2\sigma}$$

which is the rotor-phase inductance for the set of currents i_{2a}, i_{2b}, and i_{2c}, that do not contain zero-sequence currents (with allowance for the effect of the other phases);

$$L_{22} = L_{aa} - L_{ab} = 3L_m/2$$

which is the rotor-phase inductance component associated with the fundamental term of the mutual field;

$$L_{2\sigma} = L_{aa\sigma} - L_{ab\sigma}$$

which is the rotor-phase inductance component associated with the leakage fields; and

$$L_{01} = L_{AA\sigma} + L_{AB\sigma} + L_{AC\sigma} \text{ and}$$

$$L_{02} = L_{aa\sigma} + L_{ab\sigma} + L_{ac\sigma}$$

which are the stator and rotor phase inductances for the zero-sequence currents (with allowance for the effect of the other phases).

In deriving equations for Ψ_{01}, Ψ_{02} and L_{01}, L_{02} account is taken of the fact that

$$L_{AA} + L_{AB} + L_{AC} = 0,\ L_{aa} + L_{ab} + L_{ac} = 0, \text{ and}$$

$$L_{Aa} + L_{Ab} + L_{Ac} = 0$$

The above equalities can be verified, using Eqs. (69-6) through (69-9), recalling that

$$\cos \alpha_{Aa} + \cos \alpha_{Ab} + \cos \alpha_{Ac}$$

$$= \text{Re}\,[\exp(j\alpha_{Aa}) + \exp(j\alpha_{Ab}) + \exp(j\alpha_{Ac})]$$

$$= \text{Re}\,[\exp(j\alpha)(1 + a + a^2)] = 0$$

where

$$a = \exp(j2\pi/3)$$

This implies that the system of zero-sequence currents produces only leakage fields and does not set up any mutual fields. That is why $L_{01} \ll L_1$ and $L_{02} \ll L_2$.

For the same reason the electromagnetic torque receives no contribution from zero-sequence currents, so it can be expressed solely in terms of the components that do not contain zero-sequence currents. This can be verified on writing the currents in Eq. (69-13) as sums of two components. Thus,

$$T_{em} = \sum_{k=A,B,C} i_{1k} \sum_{n=a,b,c} i_{2n} \mathrm{d}L_{kn}/\mathrm{d}\gamma$$

Recalling that

$$L_{kn} = L_m \cos \alpha_{kn}$$

where

$$\alpha_{kn} = \alpha + \Delta\alpha_{kn}, \quad \alpha = p_\tau\gamma, \text{ and } \Delta\alpha_{kn} \neq f(\gamma)$$

we may write the electromagnetic torque in terms of currents and the angles between phases, α_{kn} [see Eq. (69-9)] as

$$T_{em} = -p_\tau L_m \sum_{k=A,B,C} i_{1k} \sum_{n=a,b,c} i_{2n} \sin \alpha_{kn} \quad (69\text{-}21)$$

69-3 Phase Quantities in Terms of Resultant Phasors

Steady-state theory uses phasors whose projections on the phase axes represent positive-sequence phase quantities (see Sec. 25-3). By analogy, in transient analysis the phase quantities that do not contain zero-sequence components may be expressed in terms of what we call resultant phasors. Let us show how the resultant phasor of the stator current can be found.

We introduce a complex (α, β)-plane stationary relative to the stator of a two-pole model (Fig. 69-2). Its real (α-) axis is placed co-linear with the axis of stator phase A. Then the unit phasors $a = \exp(j2\pi/3)$ and a^2 will line up, respectively, with the axes of phases B and C, whereas the unit phasor $\exp(j\alpha_{Aa})$, where $\alpha_{Aa} = p_\tau\gamma$, will give the direction of the axis of rotor phase a. The resultant phasor of the stator current can then be written in terms of instantaneous phase currents as

$$\tilde{I}_1 = (2/3)(i_{1A} + i_{1B}a + i_{1C}a^2) \quad (69\text{-}22)$$

and its plot appears in Fig. 69-2.

As is seen, the projections of the resultant phasors on the phase axes represent the respective phase currents to scale. This can be verified analytically. The projection of $\tilde{I}_1 = I_1 \exp(j\varphi_1)$ on an arbitrary direction $s = \exp(j\varphi_0)$ is

$$I_1 \cos(\varphi_1 - \varphi_0) = \text{Re}[\tilde{I}_1 s^*] = (\tilde{I}_1 s^* + \tilde{I}_1^* s)/2 \quad (69\text{-}23)$$

where an asterisk stands for complex conjugate, viz.

$$s^* = \exp(-j\varphi_0)$$

Therefore, the projection of $\tilde{I}_1$ on, say, the axis o phase B or on the direction $a = \exp(j2\pi\ 3)$ as found from Eq. (69-23), does represent to scale (provided $i_{1A} + i_{1B} + i_{1C} = 0$)

the instantaneous current of that phase

$$\begin{aligned}\mathrm{Re}\,[\tilde{I}_1 a^*] &= \mathrm{Re}\,[2\,(i_{1A} + i_{1B}a + i_{1C}a^2)\,a^2/3] \\ &= 2\,[i_{1A}\,\mathrm{Re}\,(a^2) + i_{1B} + i_{1C}\,\mathrm{Re}\,(a)]/3 = i_{B1}\end{aligned}$$

where $a^* = a^2$, $aa^2 = 1$, and $\mathrm{Re}\,(a^2) = \mathrm{Re}\,(a) = -1/2$. Similarly, it can be proved that the projections of the

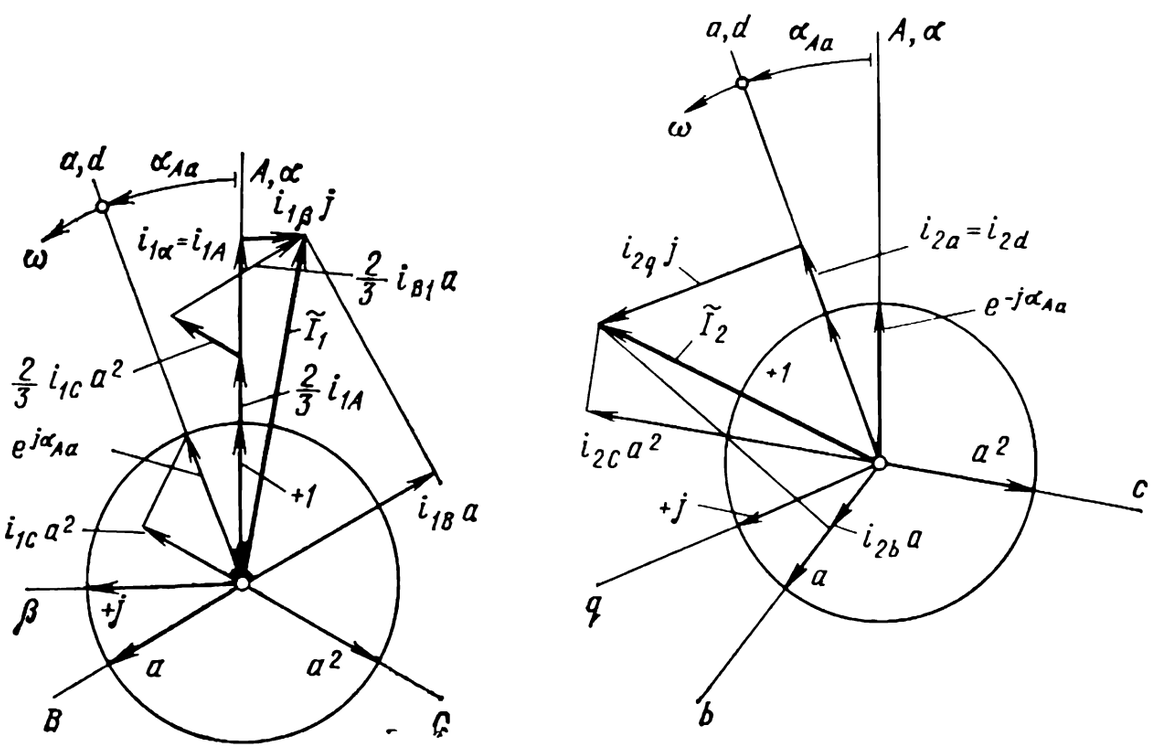

Fig. 69-2 Resultant stator and rotor current phasors, $\tilde{I}_1$ and $\tilde{I}_2$

above phasor on the other phase axes represent to scale the corresponding phase currents

$$\mathrm{Re}\,[\tilde{I}_1 \times 1] = i_{A1},$$

$$\mathrm{Re}\,[\tilde{I}_1 \times a^{*2}] = \mathrm{Re}\,[\tilde{I}_1 a] = i_{C1}$$

The phasors of stator voltage and flux linkage can be expressed in terms of phase quantities in a similar way:

$$\tilde{V}_1 = 2\,(v_{1A} + v_{1B}a + v_{1C}a^2)/3$$

$$\tilde{\Psi}_1 = 2\,(\Psi_{1A} + \Psi_{1B}a + \Psi_{1C}a^2)/3$$

Their projections on the axes of stator phases likewise represent to scale the corresponding phase quantities.

The resultant phasors of the rotor phase quantities are plotted on a rotating complex (d, q) - plane which is stationary relative to the rotor of a two-pole model (see

Fig. 69-2). If we align the real d-axis of this plane with the axis of the rotor a phase, the unit phasors a and a^2 will then line up with the b and c phase axes, respectively, and the unit phasor $\exp(-j\alpha_{Aa})$, where $\alpha_{Aa} = p_\tau\gamma$, will locate the position of the fixed axis of the stator A phase.

The resultant phasors of the rotor current, voltage and flux linkage can be expressed in terms of the respective phase quantities of the rotor as follows:

$$\begin{aligned} \tilde{I}_2 &= (2/3)\,(i_{2a} + i_{2b}a + i_{2c}a^2) \\ \tilde{V}_2 &= (2/3)\,(v_{2a} + v_{2b}a + v_{2c}a^2) \\ \Psi_2 &= (2/3)\,(\Psi_{2a} + \Psi_{2b}a + \Psi_{2c}a^2) \end{aligned} \tag{69-24}$$

Their projections on the phase axes represent to scale the corresponding phase quantities. For example

$$\text{Re}\,[\tilde{I}_2 \times a^*] = i_{2b}$$
$$\text{Re}\,[\tilde{V}_2 \times 1] = v_{2a}$$

and so on.

69-4 The α- and β-Axis Components of Stator Quantities and the d- and q-Axis Components of Rotor Quantities

The resultant phasors of stator quantities can be written as sums of α- and $j\beta$-axis components. For example, the resultant phasor of stator current, Eq. (69-22), is

$$\tilde{I}_1 = i_{1\alpha} + ji_{1\beta} \tag{69-25}$$

where

$$i_{1\alpha} = \text{Re}\,[\tilde{I}_1] = (\tilde{I}_1 + \tilde{I}_1^*)/2 = i_{1A}$$
$$i_{1\beta} = \text{Im}\,[\tilde{I}_1] = (\tilde{I}_1 - \tilde{I}_1^*)/2j = (i_{1B} - i_{1C})/\sqrt{3}$$

are the α- and β-axis components of the stator current, respectively.

The currents $i_{1\alpha}$ and $i_{1\beta}$ may be visualized as flowing in a stationary, two-phase winding, 1α and 1β, the phase axes of which are aligned with the α- and β-axes of a complex plane respectively (see Figs. 69-2 and 69-3). The two-phase (1α, 1β)-winding carrying currents $i_{1\alpha}$ and $i_{1\beta}$ (see Fig. 69-3) is equivalent to the three-phase (A, B, C) stator winding in Fig. 69-1, which carries the currents i_{1A}, i_{1B} and i_{1C}.

The resultant phasors of rotor quantities can be resolved into components directed along the rotating d- and jq-axes.

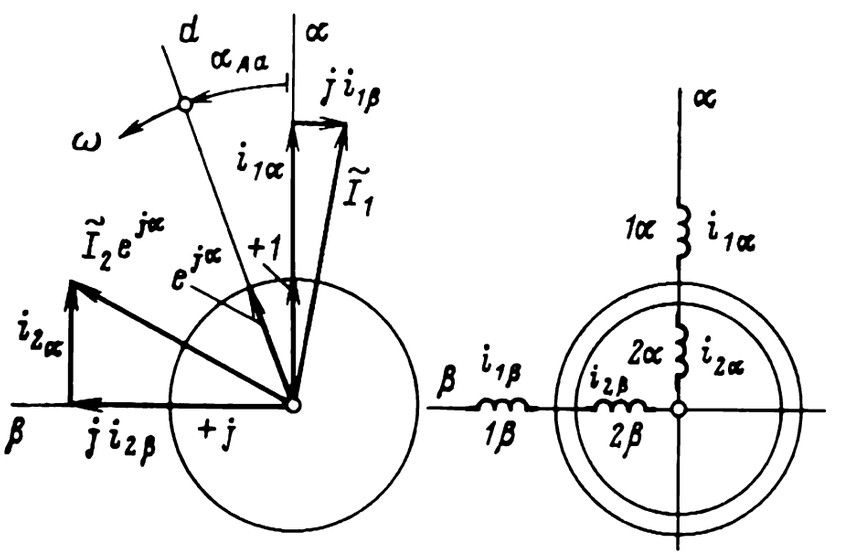

Fig. 69-3 Stator and rotor component quantities in stationary α, β coordinates

As an example, we shall demonstrate how this can be done for the resultant phasor of rotor current. On the complex

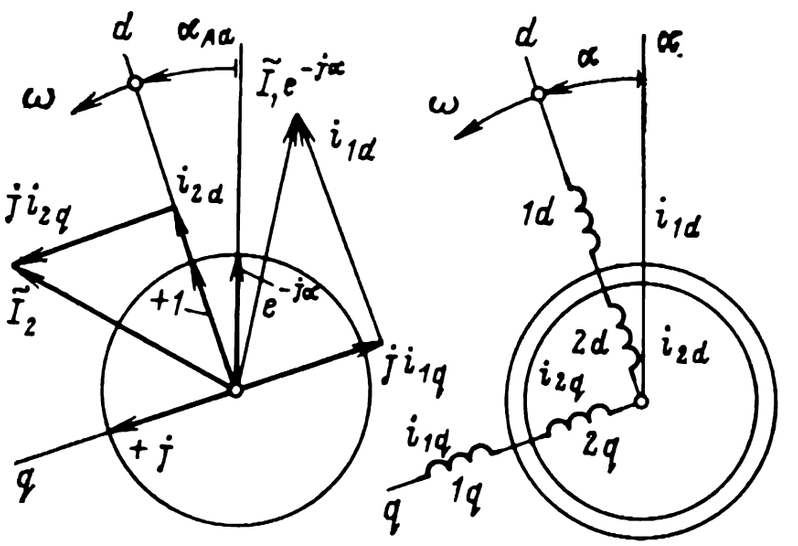

Fig. 69-4 Stator and rotor component quantities in rotating d, q coordinates

(d, jq)-plane, the rotor current defined by Eq. (69-24) is represented by a phasor

$$\tilde{I}_2 = i_{2d} + j i_{2q} \tag{69-26}$$

where

$$i_{2d} = \mathrm{Re}\,[\tilde{I}_2] = (\tilde{I}_2 + \tilde{I}_2^*)/2 = i_{2a}$$

$$i_{2q} = \mathrm{Im}\,[\tilde{I}_2] = (\tilde{I}_2 - \tilde{I}_2^*)/2j = (i_{2b} - i_{2c})/\sqrt{3}$$

are the d- and q-axis components of rotor current, respectively.

The currents i_{2d} and i_{2q} may be visualized as flowing in a rotating two-phase ($2d$, $2q$) winding the phase axes of which are aligned with the d- and q-axes of a complex plane (see Figs. 69-2 and 69-4). The rotating two-phase ($2d$, $2q$) winding in Fig. 69-4, carrying the currents i_{2d} and i_{2q}, is equivalent to the three-phase (a, b, c) winding in Fig. 69-1, which carries the currents i_{2a}, i_{2b}, and i_{2c}.

Equations for flux linkages and voltages can be derived in a similar way.

69-5 The d- and q-Axis Components of Stator Quantities and the α- and β-Axis Component of Rotor Quantities

If we wish to write equations in terms of the (α, $j\beta$) complex plane, both the stator phasors and the rotor phasors must be resolved into α-axis and $j\beta$-axis components. As an example we shall demonstrate how this can be done for the rotor current phasor, $\tilde{I}_2$, which, on the rotating (d, jq) plane, is defined by Eq. (69-26).

Because the (d, jq) complex plane is turned through an angle $\alpha = \alpha_{Aa}$ from the fixed α, $j\beta$ complex plane (see Fig. 69-2), the rotor current will be depicted on the α, $j\beta$ plane by a phasor of the form

$$\begin{aligned}\tilde{I}_{2(\alpha,\beta)} &= \tilde{I}_2 \exp(j\alpha) = (i_{2d} + ji_{2q}) \exp(j\alpha) \\ &= i_{2\alpha} + ji_{2\beta}\end{aligned} \tag{69-27}$$

The α-axis and β-axis components of the rotor current phasor

$$i_{2\alpha} = \mathrm{Re}\,[(i_{2d} + ji_{2q}) \exp(j\alpha)] = i_{2d} \cos\alpha - i_{2q} \sin\alpha$$

$$i_{2\beta} = \mathrm{Im}\,[(i_{2d} + ji_{2q}) \exp(j\alpha)] = i_{2d} \sin\alpha + i_{2q} \cos\alpha$$

are the currents in the stationary two-phase (2α, 2β) winding (see Fig. 69-3) that sets up the same magnetic field as the rotating two-phase winding which carries the currents i_{2d} and i_{2q}.

A similar transformation is applied to the resultant stator phasors in writing equations in terms of the rotating (d, jq) complex plane. For example, if on the stationary (α, $j\beta$) complex plane the stator current is depicted in accord with Eq. (69-26) by a phasor

$$\tilde{I}_1 = i_{1\alpha} + ji_{1\beta}$$

then on the (d, jq) complex plane turned through an angle $-\alpha = -\alpha_{Aa}$ from the (α, $j\beta$) plane (see Fig. 69-2), this same current will be represented by a phasor of the form

$$\begin{aligned}\tilde{I}_{1(d,q)} &= \tilde{I}_1 \exp(-j\alpha) = (i_{1\alpha} + ji_{1\beta}) \exp(-j\alpha) \\ &= i_{1d} + ji_{1q} \end{aligned} \tag{69-28}$$

The d- and q-axis components of the stator current phasor

$$i_{1d} = \text{Re}\,[(i_{1\alpha} + ji_{1\beta}) \exp(-j\alpha)] = i_{1\alpha} \cos\alpha + i_{1\beta} \sin\alpha$$

$$i_{1q} = \text{Im}\,[(i_{1\alpha} + ji_{1\beta}) \exp(-j\alpha)] = -i_{1\alpha} \sin\alpha + i_{1\beta} \cos\alpha$$

are the currents in the rotating two-phase ($1d$, $1q$) winding shown in Fig. 69-4, which sets up the same magnetic field as the stationary two-phase winding carrying the currents $i_{1\beta}$ and $i_{2\beta}$.

Equations in terms of d- and q-axis components for stator flux linkages and voltages and in terms of α- and β-axis components for rotor flux linkages and voltages can be derived in a similar way.

69-6 Flux Lnkage Phasors in Terms of Current Phasors

The stator phase flux linkages (Ψ_{A1}, Ψ_{B1}, and Ψ_{C1}) appearing in Eq. (69-20) can be expressed on the basis of Eqs. (69-20) and (69-9) in terms of phase currents, stator phase inductance L_1 and rotor-stator phase mutual inductances

$$\begin{aligned} L_{Aa} &= L_m \cos\alpha \\ L_{Ab} &= L_m \cos(\alpha + 2\pi/3) \\ L_{Ac} &= L_m \cos(\alpha + 4\pi/3) \\ L_{Ba} &= L_m \cos(\alpha + 4\pi/3), \text{ etc.} \end{aligned}$$

which are functions of the angular position of the rotor, that is, the electrical angle between the axes of the stator A phase and the rotor a phase, $\alpha = \alpha_{Aa} = p_\tau \gamma$.

Let us write the cosines of the angles between phases in exponential form

$$\cos \alpha = \mathrm{Re}\,[e] = (e + e^*)/2$$

$$\cos (\alpha + 2\pi/3) = \mathrm{Re}\,[ea] = (ea + e^* a^2)/2$$

$$\cos (\alpha + 4\pi/3) = \mathrm{Re}\,[ea^2] = (ea^2 + e^* a)/2$$

where $e = \exp(j\alpha)$, $e^* = \exp(-j\alpha)$, $a = \exp(j2\pi/3)$ and $a^* = a^2 = \exp(j4\pi/3)$ are unit phasors indicating the direction of the phase axes in Fig. 69-2. Then, turning to the equation (69-22) and (69-24) for the resultant stator and rotor current phasors, we can readily prove that the resultant stator flux linkage phasor can be written in terms of the resultant stator and rotor current phasors as follows

$$\tilde{\Psi}_1 = L_1 \tilde{I}_1 + L_{12m} \tilde{I}_2 \exp(j\alpha) = L_1 \tilde{I}_1 + L_{12m} \tilde{I}_{2(\alpha, \beta)} \qquad (69\text{-}29)$$

where

$$L_{12m} = 3L_m/2$$

is the main (useful) mutual inductance between a stator phase and the rotor phases (see Sec. 28-4),

$$\tilde{I}_{2(\alpha, \beta)} = \tilde{I}_2 \exp(j\alpha)$$

is the resultant rotor current phasor in the stationary (α, β) complex plane of the stator (see Fig. 69-2).

Similarly, using Eqs. (69-9), (69-20), (69-22) and (69-24) and applying analogous transformations, it can be shown that the rotor flux linkage phasor can be expressed in terms of the stator and rotor current phasors and the corresponding inductances

$$\tilde{\Psi}_2 = L_2 \tilde{I}_2 + L_{12m} \tilde{I}_1 \exp(-j\alpha) = L_2 \tilde{I}_2 + L_{12m} \tilde{I}_{1(d, q)} \qquad (69\text{-}30)$$

where

$$\tilde{I}_{1(d, q)} = \tilde{I}_1 \exp(-j\alpha)$$

is the resultant stator current phasor on the rotating (d, q) complex plane of the stator (see Fig. 69-2).

69-7 The Voltage Equation in Terms of the α- and β-Axis Components

If we wish to replace the three voltage equations, (69-18), each written for a particular stator phase, by an equation written in terms of resultant phasor functions, we should (1) multiply the equation for v_{1A} by 2/3, the equation for v_{1B} by $2a/3$, and the equation for v_{1C} by $2a^2/3$, and (2) add together the right- and left-hand sides of those equations termwise. Then, in view of Eqs. (69-22) and (69-23), the resultant equation will be the voltage equation of the stator in its own (α, β) complex plane

$$\tilde{V}_1 = R_1\tilde{I}_1 + \mathrm{d}\tilde{\Psi}_1/\mathrm{d}t \qquad (69\text{-}31)$$

where the stator flux-linkage phasor can be defined in terms of currents on the basis of Eq. (69-29).

Applying a similar procedure to the three voltage equations (69-18), for the individual rotor phase, we shall obtain the voltage equation of the rotor in its own (d, q) complex plane

$$\tilde{V}_2 = R_2\tilde{I}_2 + \mathrm{d}\tilde{\Psi}_2/\mathrm{d}t \qquad (69\ 32)$$

where the rotor flux linkage phasor can be defined in terms of currents on the basis of Eq. (69-30).

However, the equations for $\tilde{V}_1$ and $\tilde{V}_2$ are written in different planes and cannot be solved simultaneously. Therefore, one of them, say, the equation for V_2, must be transformed and written in terms of rotor voltage, current and flux linkage phasors defined in the (α, β) coordinates, that is, $\tilde{V}_{2(\alpha,\beta)}$, $\tilde{I}_{2(\alpha,\beta)}$, and $\tilde{\Psi}_{2(\alpha,\beta)}$. Then, in accord with Eq. (69-27),

$$\tilde{V}_2 = \tilde{V}_{2(\alpha,\beta)}\exp(-j\alpha),\ \tilde{I}_2 = \tilde{I}_{2(\alpha,\beta)}\exp(-j\alpha),$$

$$\tilde{\Psi}_2 = \tilde{I}_{2(\alpha,\beta)}\exp(-j\alpha)$$

where $\alpha = \alpha_{Aa} = \alpha(t)$ is the angle between the axes of the stator and rotor phases (see Fig. 69-2).

After the above transformations, Eq. (69-32) takes the form

$$\tilde{V}_{2(\alpha,\beta)}\exp(-j\alpha) = R_2\tilde{I}_{2(\alpha,\beta)}\exp(-j\alpha) + \frac{\mathrm{d}}{\mathrm{d}t}[\tilde{\Psi}_{2(\alpha,\beta)}\exp(-j\alpha]$$

In taking the derivative, it is important to remember that the angle between the axes of the stator and rotor phases varies with time, $\alpha = \alpha(t)$, therefore,

$$\tilde{V}_{2(\alpha,\beta)} \exp(-j\alpha) = R_2 \tilde{I}_{2(\alpha,\beta)} (\exp -j\alpha) + \exp(-j\alpha)(d\tilde{\Psi}_{2(\alpha,\beta)}/dt) + \tilde{\Psi}_{2(\alpha,\beta)}[-j \exp(-j\alpha)(d\alpha/dt)]$$

Dividing the above equation termwise by $\exp(-j\alpha)$ and recalling that $d\alpha/dt = \omega$ is the electrical angular velocity of the rotor, the rotor voltage equation may be written as

$$\tilde{V}_{2(\alpha,\beta)} = R_2 \tilde{I}_{2(\alpha,\beta)} + d\Psi_{2(\alpha,\beta)}/dt - j\omega\tilde{\Psi}_{2(\alpha,\beta)} \quad (69\text{-}33)$$

where all quantities are referenced to the stationary (α, β) complex plane. This, of course, applies to the flux linkage as well. It can be found from an equation which stems from Eqs. (69-27), (69-28) and (69-30), namely

$$\tilde{\Psi}_{2(\alpha,\beta)} = \tilde{\Psi}_2 \exp(j\alpha) = L_2 \tilde{I}_2 \exp(j\alpha) + L_{12m} \tilde{I}_{1(d,q)} \exp(j\alpha)$$
$$= L_2 \tilde{I}_{2(\alpha,\beta)} + L_{12m} \tilde{I}_1$$

where the current phasors are written in the (α, β) coordinates.

If we agree in advance that all the quantities are referenced to the (α, β) complex plane, we may drop the subscripts in the above equation and write the rotor voltage equation as

$$\tilde{V}_2 = R_2 \tilde{I}_2 + d\tilde{\Psi}_2/dt - j\omega\tilde{\Psi}_2 \quad (69\text{-}34)$$

where

$$\tilde{\Psi}_2 = L_2 \tilde{I}_2 + L_{12m} \tilde{I}_1$$

Using Eqs. (69-25) and (69-27), we can write all phasors in Eqs. (69-31) and (69-34) in terms of their α- and β-axis components. Then, instead of two voltage equations in phasor notation, there will be four equations in scalar form, namely

$$\begin{aligned} v_{1\alpha} &= R_1 i_{1\alpha} + d\Psi_{1\alpha}/dt \\ v_{1\beta} &= R_1 i_{1\beta} + d\Psi_{1\beta}/dt \\ v_{2\alpha} &= R_2 i_{2\alpha} + d\Psi_{2\alpha}/dt + \omega\Psi_{2\beta} \\ v_{2\beta} &= R_2 i_{2\beta} + d\Psi_{2\beta}/dt - \omega\Psi_{2\alpha} \end{aligned} \quad (69\text{-}35)$$

In the above equations, the flux linkage components can be expressed in terms of the corresponding current components as follows:

$$\Psi_{1\alpha} = L_1 i_{1\alpha} + L_{12m} i_{2\alpha}, \quad \Psi_{2\alpha} = L_2 i_{2\alpha} + L_{12m} i_{1\alpha}$$
$$\Psi_{1\beta} = L_1 i_{1\beta} + L_{12m} i_{2\beta}, \quad \Psi_{2\beta} = i_2 i_{2\beta} + L_{12m} i_{1\beta} \tag{69-36}$$

69-8 Voltage Equations in Terms of d- and q-Axis Components and in Terms of Components Along Axis Rotating at Arbitrary Velocity. Equivalent Circuits

Now, only Eq. (69-31) needs to be transformed. The relevant quantities can be expressed in terms of d- and q-axis components, using equations of the form of Eq. (69-28)

$$\tilde{V}_{1(d,q)} \exp(j\alpha) = R_1 \tilde{I}_{1(d,q)} \exp(j\alpha) + \frac{d}{dt}[\tilde{\Psi}_{1(d,q)} \exp(j\alpha)]$$

If, in taking the derivative, we recall that the angle between the axes of the stator and rotor phases is a time function, $\alpha = \alpha(t)$, we may write

$$\tilde{V}_{1(d,q)} \exp(j\alpha) = R_1 \tilde{I}_{1(d,q)} \exp(j\alpha) + \exp(j\alpha) \frac{d\tilde{\Psi}_{1(d,q)}}{dt} + \tilde{\Psi}_{1(d,q)}\, j \exp(j\alpha)(d\alpha/dt)$$

on cancelling out $\exp(j\alpha)$, we obtain a stator voltage equation

$$\tilde{V}_{1(d,q)} = R_1 \tilde{I}_{1(d,q)} + d\tilde{\Psi}_{1(d,q)}/dt + j\omega\tilde{\Psi}_{1(d,q)} \tag{69-37}$$

where all the quantities are referenced to the rotating (d, q) complex plane. Using Eqs. (69-27) through (69-29), the flux linkage can likewise be written in terms of currents on the (d, q) complex plane:

$$\tilde{\Psi}_{1(d,q)} = \tilde{\Psi}_1 \exp(-j\alpha)$$
$$= L_1 \tilde{I}_1 \exp(-j\alpha) + L_{12m} \tilde{I}_2(\alpha, \beta) \exp(-j\alpha)$$
$$= L_1 \tilde{I}_{1(d,q)} + L_{12m} \tilde{I}_2$$

As before, if we agree that all the quantities in Eq. (69-37) are referenced to the (d, q) complex plane, the above equa-

tion may be re-written as

$$\tilde{V}_1 = R_1\tilde{I}_1 + \mathrm{d}\tilde{\Psi}_1/\mathrm{d}t + j\omega\tilde{\Psi}_1 \qquad (69\text{-}38)$$

where

$$\tilde{\Psi}_1 = L_1\tilde{I}_1 + L_{12m}\tilde{I}_2$$

For Eqs. (69-32) and (69-38) to be re-cast in scalar form, we must express all the phasors involved in terms of projections on the d- and q-axes in accord with Eqs. (69-26) and (69-28), and separate the real and imaginary parts on the right- and left-hand sides. This will lead us to a set of four equations for the d- and q-axis stator and rotor voltages, equivalent to Eqs. (69-32) and (69-38):

$$\begin{aligned} v_{1d} &= R_1 i_{1d} + \mathrm{d}\Psi_{1d}/\mathrm{d}t - \omega\Psi_{1q} \\ v_{1q} &= R_1 i_{1q} + \mathrm{d}\Psi_{1q}/\mathrm{d}t + \omega\Psi_{1d} \\ v_{2d} &= R_2 i_{2d} + \mathrm{d}\Psi_{2d}/\mathrm{d}t \\ v_{2q} &= R_2 i_{2q} + \mathrm{d}\Psi_{2q}/\mathrm{d}t \end{aligned} \qquad (69\text{-}39)$$

The flux-linkage components in Eqs. (69-39) can be written in terms of the corresponding current components as

$$\Psi_{1d} = L_1 i_{1d} + L_{12m} i_{2d}, \quad \Psi_{2d} = L_2 i_{2d} + L_{12m} i_{1d} \qquad (69\text{-}40)$$

$$\Psi_{1q} = L_1 i_{1q} + L_{12m} i_{2q}, \quad \Psi_{2q} = L_2 i_{2q} + L_{12m} i_{1q}$$

Let us consider the d-axis rotor voltage equation (69-39) and the d-axis stator flux linkage equation (69-40) together. On differentiating Eq. (69-40) and deeming the rotor to be short-circuited, we shall obtain the following set of equations:

$$\frac{\mathrm{d}}{\mathrm{d}t}\Psi_{1d} = \frac{\mathrm{d}}{\mathrm{d}t}(L_1 i_{1d} + L_{12m} i_{2d})$$

$$0 = R_2 i_{2d} + \frac{\mathrm{d}}{\mathrm{d}t}(L_2 i_{2d} + L_{12m} i_{1d})$$

which describes the d-axis equivalent circuit in Fig. 69-5a. Applying the same reasoning to the q-axis voltage and flux-linkage equations, we shall obtain the q-axis equivalent circuit in Fig. 69-5b. The two equivalent circuits depict the transformer (inductive) coupling between the equivalent stator and rotor windings on the d- and q-axis of the machine, respectively. They are a convenient tool in the transient analysis of induction machines.

If we compare Eq. (69-31) which describes the stator voltages referenced to the stationary α- and β-axes, with Eq. (69-38) which describes the same voltages referenced to the rotating d- and q-axes, we shall notice that the latter contains one more term, $j\omega\tilde{\Psi}_1$, the rotational emf proportional to the angular velocity of the axes involved. The same finding will be made if we compare Eq. (69-32) which describes the rotor voltages referenced to the rotating d-and q-axes with Eq. (69-34) which describes the same voltages referenced to the stationary α- and β-axes. The extra term in Eq. (69-34) is $-j\omega\Psi_2$, the rotational emf proportional to the angular velocity, $-\omega$, of the α- and β-axes relative to the revolving rotor.

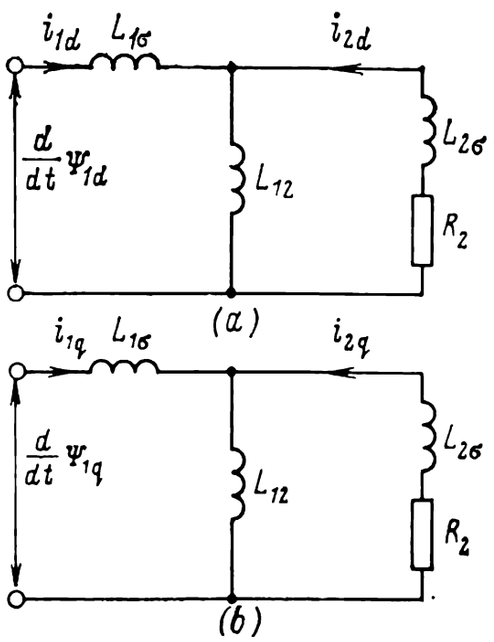

Fig. 69-5 Equivalent circuits of an induction machine: (*a*) *d*-axis and (*b*) *q*-axis

In the general case, if we write the voltage equation with reference to some axes rotating at an arbitrary velocity ω_0, it will contain an extra term representing the rotational emf which is proportional to the velocity of the axes relative to the winding involved. Thus, the equation describing the stator voltages referenced to axes rotating at ω_0 will contain an emf proportional to the velocity of those axes relative to the stationary stator winding, that is,

$$\tilde{V}_1 = R_1\tilde{I}_1 + d\tilde{\Psi}_1/dt + j\omega_0\tilde{\Psi}_1 \qquad (69\text{-}41)$$

Similarly, the equation describing the rotor voltage referenced to axes rotating at ω_0 will contain an extra emf proportional to $\omega_0 - \omega$ which is the velocity of those axes relative to the rotor revolving at velocity ω,

$$\tilde{V}_2 = R_2\tilde{I}_2 + d\tilde{\Psi}_2/dt + j(\omega_0 - \omega)\tilde{\Psi}_2 \qquad (69\text{-}42)$$

Of course, all the quantities entering Eqs. (69-41) and (69-42) must be referenced to the same complex plane rotating at ω_0. If we assume that at $t = 0$ the real axis of that complex plane is aligned with the axes of stator phase *A*

and that at time t it is displaced from stator phase A by an angle α_0, then the currents in Eqs. (69-41) and (69-42) will be

$$\tilde{I}_1 = \tilde{I}_{1(\alpha,\beta)} \exp(-j\alpha_0),$$
$$\tilde{I}_2 = \tilde{I}_{2(d,q)} \exp[-j(\alpha_0 - \alpha)] \qquad (69\text{-}43)$$

where $\tilde{I}_{1(\alpha,\beta)}$ = stator current phasor referenced to the own (α, β) complex plane

$\tilde{I}_{2(d,q)}$ = rotor current phasor referenced to the own (d, q) complex plane.

The flux linkages in Eqs. (69-41) and (69-42) can be expressed in terms of $\tilde{I}_1$ and $\tilde{I}_2$ as

$$\tilde{\Psi}_1 = L_1\tilde{I}_1 + L_{12m}\tilde{I}_2,$$
$$\tilde{\Psi}_2 = L_2\tilde{I}_2 + L_{12m}\tilde{I}_1 \qquad (69\text{-}43a)$$

69-9 Electromagnetic Torque Expressed in Terms of Resultant Current and Flux Linkage Phasors and Their Components

The equation for electromagnetic torque derived earlier, Eq. (69-21), is too unwieldy for practical purposes. Fortunately, it can be markedly simplified by using the resultant current phasors.

Let us prove that, in the general case, the electromagnetic torque can be expressed in terms of phasors in exactly the same way as the average electromagnetic torque in a balanced steady state, that is, in terms of the phasors of positive-sequence quantities (see Sec. 29-1).

Recalling that the resultant current phasors are $\sqrt{2}$ times the rms currents used to find the average electromagnetic torque in Sec. 29-1, we may write the electromagnetic torque applied to the rotor as

$$T_{em} = (3p_\tau/2)\,\mathrm{Im}\,[\tilde{\Psi}_2\tilde{I}_2^*]$$
$$= 3p_\tau(\tilde{\Psi}_2\tilde{I}_2^* - \tilde{\Psi}_2^*\tilde{I}_2)/4j \qquad (69\text{-}44)$$

and the equal electromagnetic torque applied to the stator as

$$T_{em} = (3p_\tau/2)\,\mathrm{Im}\,[\tilde{\Psi}_1^*\tilde{I}_1]$$
$$= 3p_\tau(\tilde{\Psi}_1^*\tilde{I}_1 - \tilde{\Psi}_1\tilde{I}_1^*)/4j \qquad (69\text{-}45)$$

As will be recalled, the torque acting on the rotor is assumed as positive if it is in the direction of rotation (that is, acting counter-clockwise). Conversely, the stator torque is taken as positive if it is against the direction of rotation (that is, acting clockwise).

Writing the rotor flux linkage, $\tilde{\Psi}_2$, defined by Eq. (69-3), as the sum of the self-flux linkage,

$$\tilde{\Psi}_{22}=L_2\tilde{I}_2$$

and the mutual flux linkage,

$$\tilde{\Psi}_{21}=L_{12m}\tilde{I}_1\exp(-j\alpha)$$

that is

$$\tilde{\Psi}_2=\tilde{\Psi}_{22}+\tilde{\Psi}_{21}$$

and noting that in the electromagnetic torque defined by Eq. (69-44) the component due to the interaction of current with self-flux linkage is zero,

$$3p_\tau(\tilde{\Psi}_{22}\tilde{I}_2^*-\tilde{\Psi}_{22}^*\tilde{I}_2)/4j=3p_\tau L_2(\tilde{I}_2\tilde{I}_2^*-\tilde{I}_2^*\tilde{I}_2)/4j=0$$

we can write the rotor torque in terms of mutual flux linkage as

$$\begin{aligned}T_{em}&=(3p_\tau/2)\,\mathrm{Im}\,[\tilde{\Psi}_{21}\tilde{I}_2^*]=3p_\tau(\tilde{\Psi}_{21}\tilde{I}_2^*-\tilde{\Psi}_{21}^*\tilde{I}_2)/4j\\&=-9p_\tau L_m[\tilde{I}_1\exp(-j\alpha)\tilde{I}_2^*-\tilde{I}_1^*\exp(j\alpha)\tilde{I}_2]/8j\end{aligned}\quad(69\text{-}46)$$

Similarly, on writing $\tilde{\Psi}_1$ from Eq. (69-29) as the sum of the self-flux linkage, $\tilde{\Psi}_{11}=L_1\tilde{I}_1$, and the mutual flux linkage, $\tilde{\Psi}_{12}=L_{12m}\tilde{I}_2\exp(j\alpha)$, that is,

$$\tilde{\Psi}_1=\tilde{\Psi}_{11}+\tilde{\Psi}_{12}$$

we can write the stator torque from Eq. (69-45) in terms of the mutual flux linkage

$$\begin{aligned}T_{em}&=(3p_\tau/2)\,\mathrm{Im}\,[\tilde{\Psi}_{12}^*\tilde{I}_1]=3p_\tau(\tilde{\Psi}_{12}^*\tilde{I}_1-\tilde{\Psi}_{12}\tilde{I}_1^*)\\&=9p_\tau L_m[\tilde{I}_2^*\exp(-j\alpha)\,\tilde{I}_1-\tilde{I}_2\exp(j\alpha)\tilde{I}_1^*]/8j\end{aligned}\quad(69\text{-}47)$$

As is seen, it does not differ from the electromagnetic torque acting on the rotor.

If we write the current phasors and their conjugates in the above equations in terms of the phase currents from Eqs. (69-22) and (69-24), we shall see that the electromagnetic torque found from Eqs. (69-44) and (69-46) is the same as the torque found from the general equation (69-21):

$$\begin{aligned} T_{em} &= (3p_\tau/2)\,\mathrm{Im}\,[\tilde{\Psi}_2\tilde{I}_2^*] = 9p_\tau L_m\,(\tilde{I}_1 e^{-j\alpha}\tilde{I}_2^* - \tilde{I}_1^* e^{j\alpha}\tilde{I}_2)/8j \\ &= -p_\tau L_m\,[i_{1A}\,(i_{2a}\sin\alpha_{Aa} + i_{2b}\sin\alpha_{Ab} + i_{2c}\sin\alpha_{Ac}) \\ &\quad + i_{1B}\,(i_{2a}\sin\alpha_{Ba} + i_{2b}\sin\alpha_{Bb} + i_{2c}\sin\alpha_{Bc}) \\ &\quad + i_{1C}\,(i_{2a}\sin\alpha_{Ca} + i_{2b}\sin\alpha_{Cb} + i_{2c}\sin\alpha_{Cc})] \\ &= -p_\tau L_m \sum_{k=A,B,C} i_{1k} \sum_{n=a,b,c} i_{2n}\sin\alpha_{kn} \end{aligned}$$

Finally, the electromagnetic torque can be expressed in terms of the d- and q-axis components of currents and flux linkages as

$$T_{em} = (3p_\tau/2)\,\mathrm{Im}[\tilde{\Psi}_2\tilde{I}_2^*] = (3p_\tau/2)\,(\Psi_{2q}i_{2d} - \Psi_{2d}i_{2q}) \quad (69\text{-}48)$$

or in terms of the α- and β-axis components of currents and flux linkages as

$$T_{em} = (3p_\tau/2)\,\mathrm{Im}\,[\tilde{\Psi}_1^*\tilde{I}_1] = (3p_\tau/2)\,(\Psi_{1\alpha}i_{1\beta} - \Psi_{1\beta}i_{1\alpha}) \quad (69\text{-}49)$$

69-10 Equations of a Three-Phase Induction Machine in a Balanced Steady State

In a balanced steady state, the angular velocity of the rotor, $\omega = p_\tau\Omega$, is constant, and all the electric quantities contain only positive-sequence components. For example, the positive-sequence currents in the stator phases are given by

$$\begin{aligned} i_{1A} &= \mathrm{Re}\,[\tilde{I}_{1A}] = 0.5\,(\tilde{I}_{1A} + \tilde{I}_{1A}^*) \\ i_{1B} &= \mathrm{Re}\,[\tilde{I}_{1A}a^2] = 0.5\,(\tilde{I}_{1A}a^2 + \tilde{I}_{1A}^*a) \\ i_{1C} &= \mathrm{Re}\,[\tilde{I}_{1A}a] = 0.5\,(\tilde{I}_{1A}a + \tilde{I}_{1A}^*a^2) \end{aligned}$$

where

$$\tilde{I}_{1A} = \dot{I}_{1A}\exp(j\omega_1 t)$$

is the phase A current phasor,

$$\dot{I}_{1A} = \dot{I}_{1m} = I_{1m}\exp(j\beta_1)$$

is the complex amplitude of the phase A current; $\omega_1 = 2\pi f_1$ is the angular velocity of the stator current phasors, and β_1 is the phase angle for the phase A current.

In view of the above relations Eq. (69-22) may be rewritten as

$$\begin{aligned}\tilde{I}_{1\alpha\beta} &= 2(i_{1A} + i_{1B}a + i_{1C}a^2)/3 \\ &= [\tilde{I}_{1A}(1 + a^3 + a^3) + \tilde{I}^*_{1A}(1 + a^2 + a)]/3\end{aligned}$$

whence,

$$\tilde{I}_{1\alpha\beta} = \tilde{I}_{1A} = \dot{I}_{1m}\exp(j\omega_1 t) \tag{69-50}$$

The other stator phasors referenced to the α- and β-axes can be written in a similar way:

$$\begin{aligned}\tilde{\Psi}_{1\alpha\beta} &= \tilde{\Psi}_{1A} = \Psi_{1A}\exp(j\omega_1 t, \\ \tilde{V}_{1\alpha\beta} &= \tilde{V}_{1A} = \dot{V}_{1A}\exp(j\omega_1 t)\end{aligned} \tag{69-51}$$

where

$\dot{\Psi}_{1A} = \dot{\Psi}_{1m} = \Psi_{1m}\exp(j\eta_1)$ and $\dot{V}_{1A} = \dot{V}_{1m} = V_{1m}\exp(j\varphi_1)$

and η_1 and φ_1 are the phase angles for the phase A flux linkage and voltage, respectively.

Recalling that the positive-sequence rotor quantities alternate at an angular frequency

$$\omega_2 = \omega_1 - \omega = s\omega_1$$

where ω_1 is the angular velocity of the field, the rotor phasors referenced to the d- and q-axes can be written as

$$\begin{aligned}\tilde{I}_{2dq} &= \tilde{I}_{2a} = \dot{I}_{2m}\exp(j\omega_2 t) \\ \tilde{\Psi}_{2dq} &= \tilde{\Psi}_{2a} = \dot{\Psi}_{2m}\exp(j\omega_2 t) \\ \tilde{V}_{2dq} &= \tilde{V}_{2a} = \dot{V}_{2m}\exp(j\omega_2 t)\end{aligned} \tag{69-52}$$

where

$\dot{I}_{2m} = I_{2m}\exp(j\beta_2)$, $\dot{I}_{2m} = \Psi_{2m}\exp(j\eta_2)$, $\dot{V}_{2m} = V_{2m}\exp(j\varphi_2)$

and β_2, η_2, and φ_2 are the respective phase angles.

If we wish to write steady-state equations referenced to axes which rotate at synchronous speed ω_1, we may use Eqs. (69-41) and (64-92) applicable to an arbitrary velocity ω_0. On setting $\omega_a = \omega_0$, $\alpha_0 = \alpha_1 = \omega_1 t$ and $\alpha = \omega t$, we get

$$\begin{aligned}\tilde{V}_1 &= R_1\tilde{I}_1 + p\tilde{\Psi}_1 + j\omega_1\tilde{\Psi}_1 \\ \tilde{V}_2 &= R_2\tilde{I}_2 + p\tilde{\Psi}_2 + j(\omega_1 - \omega)\tilde{\Psi}_2\end{aligned}$$

Now we can write all the phasors in Eqs. (69-50), (69-51) and (69-52) as referenced to the synchronous axes:

$$\tilde{I}_1 = \tilde{I}_{1\alpha\beta} \exp(-j\alpha_1) = \dot{I}_{1m}$$
$$\tilde{\Psi}_1 = \tilde{\Psi}_{1\alpha\beta} \exp(-j\alpha_1) = \dot{\Psi}_{1m}$$
$$\tilde{V}_1 = \tilde{V}_{1\alpha\beta} \exp(-j\alpha_1) = \dot{V}_{1m}$$
$$\tilde{I}_2 = \tilde{I}_{2dq} \exp[-j(\alpha_1 - \alpha)] = \dot{I}_{2m}$$
$$\tilde{\Psi}_2 = \tilde{\Psi}_{2dq} \exp[-j(\alpha_1 - \alpha)] = \dot{\Psi}_{2m}$$
$$\tilde{V}_2 = \tilde{V}_{2dq} \exp[-j(\alpha_1 - \alpha)] = \dot{V}_{2m}$$

Because the currents and flux linkages referenced to the synchronous axes are time-independent, the time derivatives of flux linkages are zero,

$$p\tilde{\Psi}_{1m} = 0, \quad p\tilde{\Psi}_{2m} = 0$$

Therefore, the final form of the steady-state voltage equation is as follows:

$$\dot{V}_{1m} = R_1\dot{I}_{1m} + j\omega_1\dot{\Psi}_{1m},$$
$$\dot{V}_{2m} = R_2\dot{I}_{2m} + js\omega_1\dot{\Psi}_{2m} \qquad (69\text{-}53)$$

where all the quantities are referenced to the synchronous axes and are complex amplitudes.

Now let us (1) write the flux linkages, using Eqs. (69-29) and (69-30),

$$\dot{\Psi}_{1m} = L_1\dot{I}_{1m} + L_{12m}\dot{I}_{2m} = L_{1\sigma}\dot{I}_{1m} + L_{12m}\dot{I}_{0m}$$
$$\dot{\Psi}_{2m} = L_2\dot{I}_{2m} + L_{12m}\dot{I}_{1m} = L_{2\sigma}\dot{I}_{2m} + L_{12m}\dot{I}_{0m} \qquad (69\text{-}54)$$

where $\dot{I}_{0m} = \dot{I}_{1m} + \dot{I}_{2m}$ is the complex amplitude of the magnetizing current;

(2) divide the rotor equation by $\sqrt{2}$ and the slip $s = (\omega_1 - \omega)/\omega_1 = \omega_2/\omega_1$, and

(3) divide the stator equation by $\sqrt{2}$. The result will be a set of equations

$$\dot{V}_1 = \dot{I}_1(R_1 + j\omega_1 L_{1\sigma}) + j\omega_1 L_{12m}\dot{I}_0$$
$$\dot{V}_2/s = \dot{I}_2(R_2/s + j\omega_1 L_{2\sigma}) + j\omega_1 L_{12m}\dot{I}_0 = 0 \qquad (69\text{-}55)$$

which fully checks with Eqs. (42-11) for an induction machine treated as a transformer.

This can readily be proved on recalling that $R_2/s = R_2 + R_2(1-s)/s = R_2 + R_m$, $X_1 = \omega_1 L_{1\sigma}$, $X_2 = \omega_1 L_{2\sigma}$, $X_0 = \omega_1 L_{12m}$, and $\dot{E}_2 = \dot{E}_1 = -jX_0\dot{I}_0$. It should also be remembered that in Eq. (69-55) no account is taken of magnetic losses ($R_0 = 0$) and all the rotor quantities are referred to the stator side (the referring index has been dropped).

70 Transient Phenomena in Induction Machines

70-1 Introductory Remarks

Transients in induction machines can best be analyzed in phasor notation, using Eqs. (69-32) and (69-38) where the voltages are referenced to the d- and q-axes, and Eqs. (69-31) and (69-34) where the voltages are referenced to the α- and β-axes or Eqs. (69-41) and (69-42) where the voltages are referenced to a generalized complex plane rotating at synchronous velocity, ω_0.

Combined with the equations (69-19) and (69-20) for the zero-sequence voltages v_{01} and v_{02}, the above equations give an exhaustive description (to the extent of the assumptions made) of the balanced and unbalanced steady states and transients in induction machines and may be used instead of Eqs. (69-1) through (69-4) for phase voltages.

In contrast to Eqs. (69-1) and (69-2), however, the above sets of equations are far simpler in structure, because they are sets of linear differential equations with constant coefficients. Accordingly, they can be solved analytically and lend themselves readily to solution on analog or digital computers.

It is appropriate to recall that the current coefficients (R_1, R_2, L_1, L_2, L_{12m}, L_{01}, L_{02}, and ω) in the voltage equations in the (α, β) or the (d, q) coordinate systems may be deemed constant, if we neglect:

(1) the saturation of the iron portions of the magnetic circuit;

(2) the slots on the cores;
(3) the higher and lower space harmonics of the magnetic field (which are accounted for approximately only in calculating the differential leakage);
(4) the time harmonics of currents;
(5) the magnetic losses and the eddy-current losses in the conductors, and
(6) variations in the angular velocity (that is, deeming that ω is constant).

Prior to solving a set of complex voltage equations written in a particular coordinate system, the phase quantities defining the initial conditions and the quantities whose changes lead to a transient must also be re-defined in terms of the same coordinate system. This can be done using equations like (69-25) and (69-27), or (69-26) and (69-28) or, generally, (69-43). Then, by an inverse transformation, the complex current functions thus found can be used to find the phase currents. For example, if the currents are defined in the (α, β) coordinate system to be

$$I_1(_{\alpha,\beta}) = i_{1\alpha} + ji_{1\beta} \text{ and } I_2(_{\alpha,\beta}) = i_{2\alpha} + ji_{2\beta}$$

then

$$i_{1A} = \mathrm{Re}\,[\tilde{I}_1] \qquad i_{2a} = \mathrm{Re}\,[\tilde{I}_{2(\alpha,\beta)} \exp(-j\alpha)]$$

$$i_{1B} = \mathrm{Re}\,[\tilde{I}_1 a^2] \qquad i_{2b} = \mathrm{Re}\,[\tilde{I}_{2(\alpha,\beta)} \exp(-j\alpha)\, a^2]$$

$$i_{1C} = \mathrm{Re}\,[\tilde{I}_1 a] \qquad i_{2c} = \mathrm{Re}\,[\tilde{I}_{2(\alpha,\beta)} \exp(-j\alpha)\, a]$$

During most transients, the rotor circuit of an induction machine is short-circuited, and the terminal voltage of its three-phase winding is zero, $\tilde{V}_2 = 0$. If we add a balanced set of resistances and inductances to the rotor resistances and leakage inductance, the rotor terminal voltage will remain equal to zero as before.

The mathematical description given in Chap. 69 may be extended to squirrel-cage induction machines. To this end, it will suffice to replace the polyphase squirrel-cage winding by an equivalent three-phase winding which has the same turns and dimensions as the stator winding and the same parameters as those of the squirrel-cage one referred to the stator side (see Sec. 41-4).

In an analysis of electromechanical transients (those in which the rate of change of speed is comparable with the

rate of change of electrical quantities), the complex voltage equations referenced to a particular set of axes (a particular coordinate system) must be considered together with the equation of motion for the rotor, (69-11). The electromagnetic torque in that equation can be found from Eq. (69-48) or (69-49).

70-2 Transients with the Stator Winding Open-Circuited. Disconnection of an Induction Machine from the External Circuit

Suppose that prior to disconnection the machine was operating in a steady state, the rotor velocity being ω and the external-circuit frequency being ω_1. At $t = 0$, all the stator phases are disconnected from the external circuit, and the stator current that existed prior to disconnection, $\tilde{I}_{1(t=0)}$), diminishes to zero fairly rapidly (during the time span when an arc exists between the contacts interrupting the stator circuit). If we deem the short-circuited rotor winding superconducting over that time interval and apply the principle of flux-linkage constancy, we may conclude that after the stator current vanishes the rotor flux linkage remains the same

$$\tilde{\Psi}_{2i} = L_2 \tilde{I}_{2i}$$

as it was in the previous steady state at $t = 0$,

$$\tilde{\Psi}_{2\,(t=0)} = L_2 \tilde{I}_{2\,(t=0)} + L_{12} \tilde{I}_{1\,(t=0)}$$

where $\tilde{I}_{2(t=0)}$ is the rotor current in the previous steady state.

The above flux linkages may be expressed in the same manner as in Eq. (69-43a), using any coordinate system. To simplify notation, the mutual inductance L_{12m} will be denoted simply as L_{12}.

From the equality

$$\tilde{\Psi}_{2i} = \tilde{\Psi}_{2\,(t=0)}$$

the rotor current after the stator current vanishes is found to be

$$\tilde{I}_{2i} = \tilde{\Psi}_{2\,(t=0)}/L_2 = \tilde{I}_{2\,(t=0)} + k_2 \tilde{I}_{1\,(t=0)} \qquad (70\text{-}1)$$

where $k_2 = L_{12}/L_2$ is the coupling factor of the rotor.

The subsequent transient is the decay of $\tilde{I}_2$ from its initial value $\tilde{I}_{2i}$. Because the arc exists during a very short time, it is legitimate to think that the current decay commences at $t = 0$. The rotor current phasor can be determined from the equation for the short-circuited rotor winding with the stator winding open-circuited that is, for $\tilde{I}_1 = 0$ and $\tilde{V}_2 = 0$.

Let us write the rotor equation (69-42), using a set of axes rotating at an arbitrary velocity ω_0:

$$R_2\tilde{I}_2 + [p + j(\omega_0 - \omega)]\,\tilde{\Psi}_2 = 0$$

where $\tilde{\Psi}_2 = L_2\tilde{I}_2$

The solution of the above homogeneous differential equation is

$$\tilde{I}_2 = C \exp(p_0 t)$$

The damping factor p_0 is a root of the corresponding characteristic equation

$$p + j(\omega_0 - \omega_0) + 1/T_{20} = 0$$

Hence,

$$p_0 = -1/T_{20} - j(\omega_0 - \omega)$$

where $T_{20} = L_2/R_2$ is the time constant of the rotor winding when the stator winding is open-circuited.

The constant of integration C is determined from the initial condition at $t = 0$

$$\tilde{I}_{2i} = C \exp(p_0 t) = C$$

Finally, the resultant rotor current phasor takes the form

$$\tilde{I}_2 = \tilde{I}_{2i} \exp(-t/T_{20}) \exp[-j(\omega_0 - \omega)\,t] \qquad (70\text{-}2)$$

Its physical meaning is especially easy to grasp if we use the d- and q-axes rotating at the rotor velocity, $\omega_0 = \omega$. When referenced to the rotor axes, the rotor current phasor

$$\tilde{I}_2 = \tilde{I}_{2i} \exp(-t/T_{20})$$

decays with a time constant T_{20}, remaining stationary relative to the rotor. The resultant rotor current phasor I_2 cor-

responds to a set of aperiodic currents in the rotor phases

$$i_{2a} = i_{2a,i} \exp(-t/T_{20})$$
$$i_{2b} = i_{2b,i} \exp(-t/T_{20})$$
$$i_{2c} = i_{2c,i} \exp(-t/T_{20})$$

where

$$i_{2a,1} = \mathrm{Re}[\tilde{I}_{21}], \quad i_{2b,1} = \mathrm{Re}[\tilde{I}_{21}a^2], \quad I_{2c,1} = \mathrm{Re}[\tilde{I}_{21}a]$$

are the initial values of the currents.

In the (α, β) coordinates system, $\omega_0 = 0$, and the resultant rotor current phasor

$$\tilde{I}_2 = \tilde{I}_{21} \exp(-t/T_{20}) \exp(j\omega t)$$

rotates at the rotor velocity, ω, because the mmf due to the apeoriodic currents in the rotor phases moves at exactly that velocity.

As is seen from Eq. (69-41) referenced to the α- and β-axes, that is, at $\omega_0 = 0$, the rotor currents induce in the open-circuited stator winding a voltage given by

$$\tilde{V}_1 = +\mathrm{d}\tilde{\Psi}_1/\mathrm{d}t = \tilde{V}_{11} \exp(-t/T_{20}) \exp(j\omega t) \qquad (70\text{-}3)$$

where

$$\tilde{\Psi}_1 = L_{12}\tilde{I}_2 = L_{12}\tilde{I}_{21} \exp(-t/T_{20}) \exp(j\omega t)$$
$$\tilde{\Psi}_{11} = L_{12}\tilde{I}_{21}$$
$$\tilde{V}_{11} = (j\omega - 1/T_{20})\tilde{\Psi}_{11} \approx j\omega\tilde{\Psi}_{11}$$

The above voltage varies at the rotor angular velocity ω, and its amplitude decays with a time constant T_{20}.

70-3 Transients with the Stator Winding Short-Circuited or Connected to an External Line

1. Voltage equations in terms of flux linkages. In such a case, transient analysis based on a complex plane rotating at an arbitrary velocity ω_0 involves joint consideration of the differential equations for the stator and the short-circuited rotor, that is, Eqs. (69-41) and (69-42). We assume that the stator voltage is fixed in advance, and express the flux linkage in terms of currents on the basis of Eq. (69-43*a*).

As a result, we obtain a set of equations which can be used to find the unknown currents

$$[R_1+(p+j\omega_0)L_1]\tilde{I}_1+(p+j\omega_0)L_{12}\tilde{I}_2=\tilde{V}_1$$
$$[p+j(\omega_0-\omega)]L_{12}\tilde{I}_1+[R_2+(p+j\omega_0-j\omega)L_2]\tilde{I}_2=0 \quad (70\text{-}4)$$

It is preferable, however, to use a set of equations written for the unknown flux linkages. To obtain it, we write the currents in terms of flux linkage, using Eqs. (69-43*a*)

$$\tilde{I}_1=(\tilde{\Psi}_1-k_2\tilde{\Psi}_2)/L_1' \quad (70\text{-}5)$$
$$\tilde{I}_2=(\tilde{\Psi}_2-k_1\tilde{\Psi}_1)//L_2'$$

Here,

$$L_1'=L_1-L_{12}^2L_2^{-1}=L_{1\sigma}+(L_{2\sigma}^{-1}+L_{12}^{-1})^{-1}=\sigma L_1$$

is the transient inductance of the stator when the rotor winding is short-circuited (similar to the transient inductance L_d' of a synchronous machine, Eq. (73-24)),

$$L_2'=L_2-L_{12}^2L_1^{-1}=L_{2\sigma}+(L_{1\sigma}^{-1}+L_{12}^{-1})^{-1}=\sigma L_2$$

is the transient inductance of the rotor when the stator winding is short-circuited (similar to the transient inductance L_f' of a synchronous machine, Eq. (72-23),

$k_1=L_{12}L_1^{-1}=1-\sigma_1$ is the coupling factor of the stator,

$k_2=L_{12}L_2^{-1}=1-\sigma_2$ is the coupling factor of the rotor,

$k=k_1k_2=L_{12}^2(L_1L_2)^{-1}=1-\sigma$ is the resultant coupling factor,

$\sigma_1=L_{1\sigma}L_1^{-1}=1-k_1$ is the leakage factor of the stator,

$\sigma_2=L_{2\sigma}L_2^{-1}=1-k_2$ is the leakage factor of the rotor,

$\sigma=1-L_{12}^2(L_1L_2)^{-1}=1-k$ is the resultant leakage factor.

Substituting Eq. (70-5) into Eq. (69-42) gives a set of differential equations for the stator and rotor flux linkages:

$$[R_1(L_1')^{-1}+p+j\omega_0]\tilde{\Psi}_1-k_2R_1(L_1')^{-1}\tilde{\Psi}_2=\tilde{V}_1$$
$$-k_1R_2(L_2')^{-1}\tilde{\Psi}_1+[R_2(L_2')^{-1}+p+j(\omega_0-\omega)]\tilde{\Psi}_2=0 \quad (70\text{-}6)$$

The electromagnetic torque, too, may be expressed in terms of flux linkage, without having to determine currents. On substituting $\tilde{I}_2$ expressed as a function of flux linkage from Eq. (70-5) into Eq. (69-44), and recalling that Im $[\tilde{\Psi}_2\tilde{\Psi}_2^*] = 0$ we get

$$\begin{aligned} T_{em} &= (3p_\tau/2)\,\mathrm{Im}\,[\tilde{\Psi}_2\tilde{I}_2^*] \\ &= (-3p_\tau k_1/2L_2')\,\mathrm{Im}\,[\tilde{\Psi}_2\tilde{\Psi}_1^*] \\ &= (3p_\tau k/\sigma L_{12})\,(\tilde{\Psi}_2^*\tilde{\Psi}_1 - \tilde{\Psi}_2\tilde{\Psi}_1^*)/4j \end{aligned} \qquad (70\text{-}7)$$

If the stationary α- and β-axes are chosen as reference ($\omega_0 = 0$), Eq. (70-6) will take the form

$$\begin{aligned} (p + s_{k1}\omega_1)\,\tilde{\Psi}_1 - k_2 s_{k1}\omega_1\tilde{\Psi}_2 &= \tilde{V}_1 \\ -k_1 s_{k2}\omega_1\tilde{\Psi}_1 + (p + s_{k2}\omega_1 - j\omega)\,\tilde{\Psi}_2 &= 0 \end{aligned} \qquad (70\text{-}8)$$

where

$$s_{k1}\omega_1 = R_1\,(L_1')^{-1} = 1/T_1', \quad s_{k2}\omega_1 = R_2\,(L_2')^{-1} = 1/T_2'$$

Here,

T_1' = time constant of the stator winding when the rotor winding is short-circuited and $\omega = \omega_1$;

T_2' = time constant of the rotor winding when the stator winding is short-circuited and $\omega = \omega_1$ (similar to T_f' or $T'_{sc,\,d}$ see Sec. 72-3)

$s_{k1} = R_1/(\omega_1 L_1')$ = critical slip corresponding to the maximum torque for a rotor-fed machine when the stator is short-circuited

$s_{k2} = R_2/\omega_1 L_2'$ = critical slip corresponding to the maximum torque for a stator-fed machine when the rotor is short-circuited. (In Part 4, this slip is found from Eq. (43-13).)

2. Current and flux linkage components. Assuming a constant rotor speed, ω, the response of a machine to a sudden input voltage $\tilde{V}_1$ (such that $\tilde{V}_1 = 0$ at $t < 0$ and $\tilde{V}_1 = \dot{V}_{1m} \exp(j\omega_1 t)$ at $t \geqslant 0$) is described by Eq. (70-8). For each of the two unknown flux linkages, the solution of that equation is the sum of two terms, namely a steady-state flux linkage ($\tilde{\Psi}_{1ss}$ or $\tilde{\Psi}_{2ss}$) and a force-free or transient flux linkage ($\tilde{\Psi}_{1t}$ or $\tilde{\Psi}_{2t}$)

$$\tilde{\Psi}_1 = \tilde{\Psi}_{1ss} + \tilde{\Psi}_{1t}, \quad \tilde{\Psi}_2 = \tilde{\Psi}_{2ss} + \tilde{\Psi}_{2t} \qquad (70\text{-}9)$$

Similarly the solution of Eqs. (70-4) with the aid of Eqs. (70-5) leads to two terms in the stator and rotor current:

$$\tilde{I}_1 = \tilde{I}_{1ss} + \tilde{I}_{1t} \text{ and } \tilde{I}_2 = \tilde{I}_{2ss} + \tilde{I}_{2t}$$

The steady-state flux linkages or currents are found by solving Eqs. (70-4) or (70-8) at $t = \infty$. The transient (or force-free) terms are obtained by solving Eqs. (70-4) or (70-8) on setting $\tilde{V}_1 = 0$. The solutions are presented as sums of two exponential functions. For example, the transient flux linkages can be written

$$\begin{aligned} \tilde{\Psi}_{1t} &= \tilde{I}_{1a} \exp(p_a t) + \tilde{\Psi}_{1p} \exp(p_p t) \\ \tilde{\Psi}_{2t} &= \tilde{\Psi}_{2a} \exp(p_a t) + \tilde{\Psi}_{2p} \exp(p_p t) \end{aligned} \tag{70-10}$$

where $\tilde{\Psi}_{1a}$, $\tilde{\Psi}_{2a}$ = initial values of transient flux linkages corresponding to the p_a root of the characteristic equation (here, the subscript "a" stands for "aperiodic")

$\tilde{\Psi}_{1p}$, $\tilde{\Psi}_{2p}$ = initial values of transient flux linkages corresponding to the p_p root of the characteristic equation (here, the subscript "p" stands for "periodic")

3. The characteristic equation and its roots. The characteristic equation whose roots are the damping factors p_a and p_p can be derived from Eqs. (70-8):

$$\begin{aligned} (p + s_{k1}\omega_1)\tilde{\Psi}_1 - k_2 s_{k1}\omega_1 \tilde{\Psi}_2 &= 0 \\ -k_1 s_{k2}\omega_1 \tilde{\Psi}_1 + (p + s_{k2}\omega_1 - j\omega)\tilde{\Psi}_2 &= 0 \end{aligned} \tag{70-11}$$

Eliminating $\tilde{\Psi}_1$ and $\tilde{\Psi}_2$ between them, we obtain the characteristic equation

$$p^2 + p(s_{k1} + s_{k2} - j\omega/\omega_1)\omega_1 + (\sigma s_{k1} s_{k2} - (j s_{k1}\omega/\omega_1)\omega_1^2 = 0$$

Its roots are

$$\begin{aligned} p = &-0.5(s_{k1} + s_{k2})\omega_1 + 0.5j\omega \\ &\pm 0.5\omega_1 \sqrt{(s_{k2} - s_{k1} - j\omega/\omega_1)^2 + 4(1-\sigma)s_{k1}s_{k2}} \end{aligned} \tag{70-12}$$

The "—" sign applies when $p = p_a$, and the "+" sign applies when $p = p_p$.

In the general case, the damping factor is a complex number

$$p = p_\alpha + jp_\beta$$

Because the transient term is given by

$$C \exp(pt) = C \exp(p_\alpha t) \exp(jp_\beta t)$$

the real part determines the time constant $T = -1/p_\alpha$. The coefficient p_β of the imaginary part is the angular velocity of the transient term relative to a stationary (α, β) complex plane.

In several important cases, Eq. (70-12) can be substantially simplified.

(a) *The rotor is at standstill.* Now $\omega = 0$, and both roots are real ($p_\beta = 0$):

$$p = p_\alpha = -0.5 (s_{k1} + s_{k2}) \omega_1 [1 \mp \sqrt{1 - 4\sigma s_{k1} s_{k2} (s_{k1} + s_{k2})^{-2}}]$$

Because the second term under the radical sign is negligibly small in comparison with unity, we may simplify the above expression still more without committing an appreciable error

$$p = p_\alpha = -0.5 (s_{k1} + s_{k2}) \omega_1 \{1 \mp [1 - 2\sigma s_{k1} s_{k2} (s_{k1} + s_{k2})^{-2}]\}$$

If we choose the "+" sign for the term in the brackets, we obtain the damping factor for the rapidly decaying aperiodic component

$$p_a = -(s_{k1} + s_{k2}) \omega_1 + \sigma \omega_1 s_{k1} s_{k2} (s_{k1} + s_{k2})^{-1}$$

On inserting in the above expression typical values for an induction machine ($\omega_1 = 314$ rad s^{-1}, $\omega_1 s_{k1} = 31.4$ rad s^{-1}; $\omega_1 s_{k2} = 47.1$ rad s^{-1}, $k_1 = 0.9675$, $k_2 = 0.9525$, $k = 0.92$, and $\sigma = 1 - k = 0.08$, we will see that the second term in the equation is not over 2% of the first. Discarding it, we obtain the damping factor for the rapidly decaying component

$$\begin{aligned} p_a &= -T_a^{-1} = -(s_{k1}\omega_1 + s_{k2}\omega_1) \\ &= -(T_1' + T_2')(T_1' T_2')^{-1} \end{aligned} \qquad (70\text{-}13)$$

If we choose the "—" sign for the term in the brackets, we will obtain the damping factor for the slowly decaying component

$$\begin{aligned} p_p &= -T_p^{-1} = -s_{k1} s_{k2} \omega_1^2 \sigma^2 / (s_{k1}\omega_1\sigma + s_{k2}\omega_1\sigma) \\ &= -(T_{10} + T_{20})^{-1} \end{aligned} \qquad (70\text{-}14)$$

where

$$T_{10} = 1/\sigma\omega_1 s_{k1} = L_1/R_1 = T_1'/\sigma$$

and

$$T_{20} = 1/\sigma\omega_1 s_{k2} = L_2/R_2 = T_2'/\sigma$$

are the time constants of the stator and rotor windings when the other winding is open-circuited (see Sec. 72-2).

(b) *The rotor is revolving at an arbitrary speed*, ω. Now, to simplify calculations, it is convenient in Eq. (70-12) to replace s_{k1} and s_{k2} by their average value on setting $s_{k1} = s_{k2} = s_k$, where $s_k = 0.5\,(s_{k1} + s_{k2})$. Then, approximately

$$p = p_\alpha + jp_\beta \approx -s_k\omega_1 + 0.5j\omega \pm 0.5\omega_1\sqrt{-\omega^2/\omega_1^2 + 4\,(1-\sigma)\,s_k^2}$$

When the rotor is revolving at a low speed,

$$\omega < 2\omega_1 s_k\sqrt{1-\sigma}$$

the square root in the expression for p is a real number, so the coefficients of the imaginary part are the same

$$p_{a\beta} = p_{p\beta} = 0.5\omega$$

This implies that both components of the transient response are rotating at the same angular velocity equal to half the rotor velocity. In contrast, the real parts of p in the above range of rotor velocity are different

$$p_{a\alpha} = -s_k\omega_1 - 0.5\omega_1\sqrt{4\,(1-\sigma)\,s_k^2 - \omega^2/\omega_1^2} = -T_a^{-1}$$

$$p_{p\alpha} = -s_k\omega_1 + 0.5\omega_1\sqrt{4\,(1-\sigma)\,s_k^2 - \omega^2/\omega_1^2} = -T_p^{-1}$$

The aperiodic component decays at a faster rate than the periodic component. Because

$$(p_\alpha + s_k\omega_1)^2 + p_\beta^2 = (1-\sigma)\,s_k^2\omega_1^2 = \text{constant}$$

the locus of the complex damping factor (see Fig. 70-1$_1$ is a circle with the $(-s_k\omega_1)$ point as centre and with $s_k\omega_1\sqrt{1-\sigma}$ as radius.

When the rotor is revolving at a high speed,

$$\omega > 2\omega_1 s_k\sqrt{1-\sigma}$$

the square root in the expression for p is an imaginary number and, as a consequence, the real parts of both roots are the

same

$$p_{a\alpha} = p_{p\alpha} - = - s_k\omega_1$$

This implies that both components of the transient response decay at the same average time constant

$$T_a = T_p = 1/s_k\omega_1 = 0.5\,(T_1' + T_2')$$

In contrast, the coefficients of the imaginary part in the above range of rotor velocity are distinct

$$p_{a\beta} = 0.5\omega - 0.5\omega_1\sqrt{\omega^2/\omega_1^2 - 4\,(1-\sigma)\,s_k^2}$$

$$p_{p\beta} = 0.5\omega + 0.5\omega_1\sqrt{\omega^2/\omega_1^2 - 4\,(1-\sigma)\,s_k^2}$$

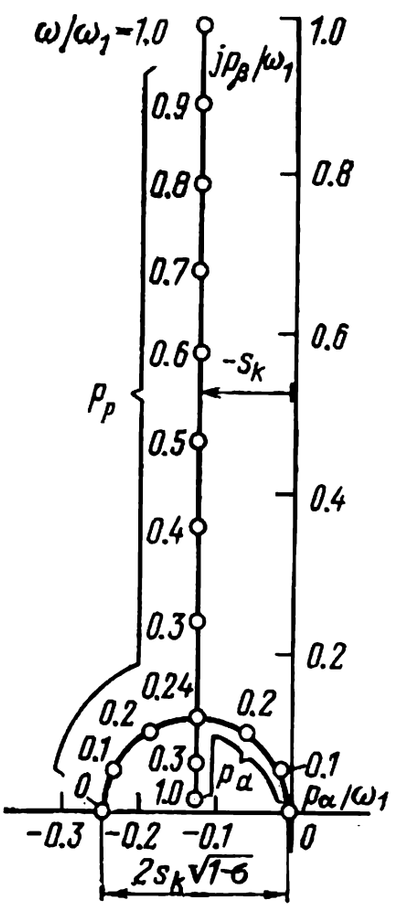

Fig. 70-1 Root locus of the characteristic equation $p = p_\alpha + jp_\beta$, in the case of a varying relative angular rotor velocity, ω/ω_1

Thus, the resultant phasors of the transient response rotate at different angular velocities, p_β and $p_{p\beta} \neq p_{a\beta}$.

The locus of p (see Fig. 70-1) is a straight line parallel to the Im-axis. Its distance from the Im-axis is $-s_k\omega_1$. The line intersects the circle at a critical angular velocity of $\omega = 2\omega_1 s_k\sqrt{1-\sigma}$.

The locus of p in Fig. 70-1 has been constructed for an induction machine having the above parameters which are given in per-unit, with ω_1 taken as the base quantity.

(c) *The rotor is revolving at a velocity nearly equal to synchronous*, $\omega \approx \omega_1$. In this case, we may allow for the difference between s_{k1} and s_{k2} more rigorously. Let us go back to the original equation for p, Eq. (70-12), and write the square root in it as $\sqrt{1-x}$, where $x \ll 1$. The procedure is as follows.

(1) Transform the radicand

$$\sqrt{(s_{k2}-s_{k1})^2 - 2j\,(s_{k2}-s_{k1})\,\omega/\omega_1 - \omega^2/\omega_1^2 + 4\,(1-\sigma)\,s_{k1}s_{k2}}$$

using the approximate expression

$$(s_{k2} - s_{k1})^2 + 4(1 - \sigma)\, s_{k1}s_{k2} = (s_{k2} + s_{k1})^2 (1 - \sigma)$$

The resultant error for a machine like the one in our case will not exceed 0.3%.

(2) Factor out $-\omega^2/\omega_1^2$ to obtain

$$j(\omega/\omega_1)\sqrt{1 - (s_{k2} + s_{k1})^2 (1 - \sigma)\, \omega_1^2/\omega^2 + 2j(s_{k2} - s_{k1})\, \omega_1/\omega_1}$$

(3) Recalling that at $\omega/\omega_1 \approx 1$ the second and third terms are small in comparison with the first, use the approximate relation $\sqrt{1 - x} \approx 1 - x/2$ to write the square root approximately as

$$j(\omega/\omega_1)\,[1 - (s_{k2} + s_{k1})^2 (1 - \sigma)\, \omega_1^2/2\omega^2 + j(s_{k2} - s_{k1})\, \omega_1/\omega]$$

(4) Using Eq. (70-12), find the roots of the characteristic equation

—for the "—" sign

$$\begin{aligned} p_a &= p_{a\alpha} + jp_{a\beta} \\ &= -s_{k1}\omega_1 + j\omega(1 - \sigma)(s_{k2} + s_{k1})^2 \omega_1^2/4\omega^2 \end{aligned} \qquad (70\text{-}15)$$

—for the "+" sign

$$\begin{aligned} p_p &= p_{p\alpha} + jp_{p\beta} \\ &= -s_{k2}\omega_1 + j\omega - j\omega(1 - \sigma)(s_{k2} + s_{k1})^2 \omega_1^2/4\omega^2 \end{aligned} \qquad (70\text{-}16)$$

It is seen from Eq. (70-15) that the phasor of the aperiodic component of the transient response decays with a time constant

$$T_1' = -p_{a\alpha}^{-1} = 1/s_{k1}\omega_1 = L_1'/R_1$$

which is the same as the time constant of the stator winding when the rotor winding is short-circuited (see above). It is also seen that it is rotating at a very low angular velocity $p_{a\beta}$ in the same direction as the rotor (at $\omega/\omega_1 \approx 1$ and the above values of parameters, $p_{a\beta} = 0.0144\omega$). Hence, the aperiodic component corresponds to the force-free (aperiodic) set of currents (flux linkages) in the stator winding.

Relative to the force-free stator current field, the rotor revolves at a velocity given by

$$\omega - p_{a\beta} = \omega\,[1 - (1 - \sigma)(s_{k1} + s_{k2})^2 \omega_1^2/4\omega^2]$$

which differs but little from ω (for the values of parameters given above, $\omega - p_{a\beta} = 0.9856\omega$). A periodic set of currents (flux linkages) is induced in the rotor winding, varying at a frequency $\omega - p_{a\beta}$.

It is seen from Eq. (70-16) that the phasor of the periodic component of the transient response decays with a time constant

$$T_2' = -p_{p\alpha}^{-1} = 1/s_{k2}\omega_1 = L_2'/R_2$$

which is the same as the time constant of the rotor winding when the stator winding is short-circuited (see above). As is seen, it rotates at an angular velocity $p_{p\beta}$ slightly lower than the rotor velocity (for the values of parameters given above, $p_{p\beta} = 0.9856\omega$). Hence, the periodic component corresponds to the set of force-free (aperiodic) currents in the rotor. This set of currents, almost stationary relative to the rotor and rotating with the rotor at $p_{p\beta}$, induces in the stator a periodic set of currents varying at a frequency

$$p_{p\beta} = \omega\,[1 - (1 - \sigma)\,(s_{k2} + s_{k1})^2\omega_1^2/4\omega^2)]$$

In view of what happens in the stator winding, the term "periodic" (the subscript "p") is assigned to both the periodically varying transient currents (flux linkages) in the stator winding and to the related set of force-free currents (flux linkages) in the rotor winding.

By the same token, the term "aperiodic" (the subscript 'a') is assigned to both the set of force-free (aperiodic) currents (flux linkages) in the stator winding, and to the periodic currents (flux linkages) induced in the rotor winding which moves at a velocity $\omega - p_{a\beta}$ relative to the set of force-free currents in the stator.

70-4 Switch-On of an Induction Machine

Switch-on is assumed to take place at an arbitrary angular velocity of the rotor, ω. At $t = 0$, the stator winding is connected to the external circuit supplying $\dot{V}_1$. In the (α, β) coordinate system, $\dot{V}_1 = 0$ at $t < 0$, and $\tilde{V}_1 = \dot{V}_{1m}\exp(j\omega_1 t)$ at $t \geqslant 0$, where $\dot{V}_{1m} = V_{1m}\exp(j\varphi_0)$.

It is assumed that during the transient the angular velocity remains equal to ω. The initial currents and flux linkages ($\tilde{I}_{11}$, $\tilde{I}_{21}$, $\tilde{\Psi}_{11}$, and $\tilde{\Psi}_{21}$), that is, those at $t = 0$, are

assumed to be fixed in advance. In the general case if a switch-on occurs at an instant when the currents following the previous switch-off have not yet decayed completely (see Sec. 70-1), the initial rotor current and flux linkage, and also the stator flux linkage may be non-zero ($\tilde{\Psi}_{1i} \neq 0$, $\tilde{\Psi}_{2i} \neq 0$, $\tilde{I}_{2i} \neq 0$). The initial stator current will be zero always.

The stator and rotor flux linkages that exist during a transient can be found from Eqs. (70-8) referenced to the stator axes, and are written as sums of a steady-state and a transient component:

$$\tilde{\Psi}_1 = \tilde{\Psi}_{1ss} + \tilde{\Psi}_{1t}, \quad \tilde{\Psi}_2 = \tilde{\Psi}_{2ss} + \tilde{\Psi}_{2t} \tag{70-17}$$

where

$$\tilde{\Psi}_{1t} = \tilde{\Psi}_{1a} \exp(p_a t) + \tilde{\Psi}_{1p} \exp(p_p t)$$

$$\tilde{\Psi}_{2t} = \tilde{\Psi}_{2a} \exp(p_a t) + \tilde{\Psi}_{2p} \exp(p_p t)$$

Similar expressions may be written for currents

$$\tilde{I}_1 = \tilde{I}_{1ss} + \tilde{I}_{1t}, \quad \tilde{I}_2 = \tilde{I}_{2ss} + \tilde{I}_{2t} \tag{70-18}$$

where

$$\tilde{I}_{1t} = \tilde{I}_{1a} \exp(p_a t) + \tilde{I}_{1p} \exp(p_p t)$$

$$\tilde{I}_{2t} = \tilde{I}_{2a} \exp(p_a t) + \tilde{I}_{2p} \exp(p_p t)$$

In the general case, the damping factors p_a and p_p are found from Eq. (70-12). The real and imaginary parts of p_a and p_p substantially depend on the angular velocity of the rotor.

When the rotor is at standstill, $\omega = 0$, they may be found from Eqs. (70-13) and (70-14). When the rotor velocity is nearly equal to synchronous, this can be done with Eqs. (70-15) and (70-16). The steady-state values of flux linkages are found from Eq. (70-8) for $t = \infty$.

Recalling that steady-state flux linkages vary harmonically, their resultant phasors referenced to the stator axes may be written as

$$\tilde{\Psi}_1 = \dot{\Psi}_{1m} \exp(j\omega_1 t), \quad \tilde{\Psi}_2 = \dot{\Psi}_{2m} \exp(j\omega_1 t)$$

Then, noting that

$$p\tilde{\Psi}_1 = j\omega_1 \tilde{\Psi}_1 \text{ and } p\tilde{\Psi}_2 = j\omega_1 \tilde{\Psi}_2$$

the following equations can be derived from Eq. (70-8) for steady-state voltages referenced to the stator axes:

$$\begin{aligned}\omega_1 (j + s_{k1})\,\tilde{\Psi}_1 - k_2 s_{k1}\omega_1 \tilde{\Psi}_2 &= \tilde{V}_1 \\ -k_1 s_{k2}\omega_1 \tilde{\Psi}_1 + \omega_1 (sj + s_{k2})\,\tilde{\Psi}_2 &= 0\end{aligned} \tag{70-19}$$

where $s = (\omega_1 - \omega)/\omega_1$ is the relative slip.

Solving Eqs. (70-19) simultaneously gives

$$\begin{aligned}\tilde{\Psi}_{1ss} = \tilde{\Psi}_1 &= \frac{\tilde{V}_1 (s_{k2} + js)}{j\omega_1 [(s_{k2} + ss_{k1}) + j (s - \sigma s_{k1} s_{k2})]} \\ \tilde{\Psi}_{2ss} = \tilde{\Psi}_2 &= \frac{\tilde{V}_1 k_1 s_{k2}}{j\omega_1 [(s_{k2} + ss_{k1}) + j (s - \sigma s_{k1} s_{k2})]}\end{aligned} \tag{70-20}$$

Approximately, when $R_1 = 0$ and $s_{k1} = 0$,

$$\tilde{\Psi}_1 = \tilde{V}_1 / j\omega_1, \quad \tilde{\Psi}_2 = \tilde{V}_1 k_1 s_{k2} / j\omega_1 (s_{k2} + js)$$

Using Eq. (70-5), we can readily find the steady-state currents

$$\begin{aligned}\tilde{I}_{1ss} = \tilde{I}_1 &= \frac{\tilde{V}_1 (\sigma s_{k2} + js)}{j\omega_1 L_1' [(s_{k2} + ss_{k1}) + j (s - \sigma s_{k1} s_{k2})]} \\ \tilde{I}_{2ss} = \tilde{I}_2 &= \frac{\tilde{V}_1 (-k_1 js)}{j\omega_1 L_2' [(s_{k2} + ss_{k1}) + j (s - \sigma s_{k1} s_{k2})]}\end{aligned} \tag{70-21}$$

The four unknown phasor coefficients in the expressions for the transient (force-free) flux linkages or currents, (70-17) or (70-18), are found, using the initial conditions at $t = 0$. On substituting the initial conditions at $t = 0$ into, say, Eq. (70-17),

$$\begin{aligned}\tilde{\Psi}_1 = \tilde{\Psi}_{1i} &= \tilde{\Psi}_{1ss} + \tilde{\Psi}_{1a} + \tilde{\Psi}_{1p} \\ \tilde{\Psi}_2 = \tilde{\Psi}_{2i} &= \tilde{\Psi}_{2ss} + \tilde{\Psi}_{2a} + \tilde{\Psi}_{2p}\end{aligned} \tag{70-22}$$

we obtain two of the four necessary equations. Two more equations can be obtained on recalling that the homogeneous differential equation (70-11) must be satisfied for both aperiodic and periodic components of flux linkages. On substituting the aperiodic components $\tilde{\Psi}_{1a} \exp(p_a t)$ and $\tilde{\Psi}_{2a} \exp(p_a t)$ into the first of Eqs. (70-11) and the periodic components $\tilde{\Psi}_{1p} \exp(p_p t)$ and $\tilde{\Psi}_{2p} \exp(p_p t)$ into the second of Eqs. (70-11) and cancelling out $\exp(p_a t)$ or $\exp(p_p t)$,

we obtain

$$\begin{aligned}\tilde{\Psi}_{2a} &= \tilde{\Psi}_{1a}(p_a + s_{k1}\omega_1)/(k_2 s_{k1}\omega_1) = k_{21a}\tilde{\Psi}_{1a}\\ \tilde{\Psi}_{1p} &= \tilde{\Psi}_{2p}(p_p + s_{k2}\omega_1 - j\omega)/(k_1 s_{k2}\omega_1) = k_{12p}\tilde{\Psi}_{2p}\end{aligned} \tag{70-23}$$

where

$$k_{21a} = (p_a + s_{k1}\omega_1)/k_2 s_{k1}\omega_1$$

$$k_{12p} = (p_p + s_{k2}\omega_1 - j\omega)/k_1 s_{k2}\omega_1$$

When the rotor is spinning at a speed close to synchronous ($\omega \approx \omega_1$), the relations between flux linkages are noticeably simplified. Now, using Eqs. (70-15) and (70-16), we obtain

$$\begin{aligned}k_{21a} &= jk_1\omega_1 (s_{k1} + s_{k2})^2/(4s_{k1}\omega) \approx jk_1 s_{k2}\omega_1/\omega\\ k_{12p} &= -jk_2\omega_1 (s_{k1} + s_{k2})^2/4s_{k2}\omega \approx -jk_2 s_{k1}\omega_1/\omega\end{aligned} \tag{70-24}$$

Equations (70-24) have been derived on replacing

$$(s_{k1} + s_{k2})/2 \approx \sqrt{s_{k1}s_{k2}}$$

which gains in accuracy as the difference between s_{k1} and s_{k2} decreases. Considering Eqs. (70-22) and (70-23) together, we get

$$\begin{aligned}\tilde{\Psi}_{2p} &= [k_{21a}(\tilde{\Psi}_{1i} - \tilde{\Psi}_{1ss}) - \tilde{\Psi}_{2i} - \tilde{\Psi}_{2ss}]/(k_{12p}k_{21a} - 1)\\ \tilde{\Psi}_{1a} &= [k_{12p}(\tilde{\Psi}_{2i} - \tilde{\Psi}_{2ss}) - (\tilde{\Psi}_{1i} - \tilde{\Psi}_{1ss})]/(k_{12p}k_{21a} - 1)\end{aligned} \tag{70-25}$$

Then, using Eq. (70-23), we can determine $\tilde{\Psi}_{1p}$ and $\tilde{\Psi}_{2a}$. If, prior to switch-on, there were no currents flowing in the windings ($\tilde{I}_{1i} = \tilde{I}_{2i} = \tilde{\Psi}_{1i} = \tilde{\Psi}_{2i} = 0$), then from Eq. (70-25) we get

$$\begin{aligned}\tilde{\Psi}_{2p} &= (\tilde{\Psi}_{2ss} - k_{21a}\tilde{\Psi}_{1ss})/(k_{12p}k_{21a} - 1)\\ \tilde{\Psi}_{1a} &= (\tilde{\Psi}_{1ss} - k_{12p}\tilde{\Psi}_{2ss})/(k_{12p}k_{21a} - 1)\end{aligned} \tag{70-26}$$

The currents $\tilde{I}_1$ and $\tilde{I}_2$ or their components can be found from Eq. (70-5). Using Eqs. (70-26) and (70-5), we can express the coefficients of the transient currents $\tilde{I}_{1a}$, $\tilde{I}_{1p}$, $\tilde{I}_{a2}$ and $\tilde{I}_{2p}$ in Eq. (70-18) in terms of the specified initial

and steady-state currents $\tilde{I}_{1i}$, $\tilde{I}_{2i}$, $\tilde{I}_{1ss}$, and $\tilde{I}_{2ss}$:

$$\tilde{I}_{1a} = \frac{(1-k_2k_{21a})}{\sigma(k_{12p}k_{21a}-1)}[(1-k_1k_{12p})(\tilde{I}_{1ss}-\tilde{I}_{1i}) + (k_1/k_2)(k_2-k_{12p})(\tilde{I}_{2ss}-\tilde{I}_{2i})]$$

$$\tilde{I}_{1p} = \frac{k_{12p}-k_2}{\sigma(k_{12p}k_{21a}-1)}[(k_1-k_{21a})(\tilde{I}_{1ss}-\tilde{I}_{1i}) + (k_1/k_2)(1-k_2k_{21a})(\tilde{I}_{2ss}-\tilde{I}_{2i})] \qquad (70\text{-}27)$$

$$\tilde{I}_{2a} = \tilde{I}_{1a}\frac{k_2(k_{21a}-k_1)}{k_1(1-k_2k_{21a})}; \tilde{I}_{2p} = \tilde{I}_{1p}\frac{k_2(1-k_1k_{12p})}{k_1(k_{12p}-k_2)}$$

As an example, consider the switch-on of an induction motor for which (in per-unit where applicable) $f_1 = 50$ Hz, $\omega_1 = 2\pi f_1 = 314$ rad s^{-1}, $\omega_1 L_{12} = 3.0$, $\omega_1 L_{1\sigma} = 0.11$, $\omega_1 L_{2\sigma} = 0.14$, $\omega_1 L_1' = 0.2441$, $\omega_1 L_2' = 0.2465$, $R_1 = 0.02441$, $R_2 = 0.03696$, $s_{k1} = 0.1$, $s_{k2} = 0.15$, $k_1 = 0.9646$, $k_2 = 0.9554$, $\sigma = 0.0785$.

The motor is running at $\omega = \omega_1(1-s)$ which remains constant for the duration of the transient. The relative slip is $s = 0.03794$. The supply voltage is taken to be equal to rated, that is, $V_{1m} = 1$. The voltage phasor in the (α, β) plane is

$$\tilde{V}_1 = V_{1m}\exp[j(\omega_1 t - \pi/2)]$$

where $V_{1m} = 1$. In the synchronous $(+, +j)$ complex plane which rotates at ω_1 and whose real "+"- axis at $t = 0$ is turned through $-\pi/2$ from the α-axis (or the phase A axis), the voltage is represented by a phasor $\tilde{V}_1 = 1$. In Fig. 70-2, it is shown coincident with the "+"-axis of the synchronous plane.

In the synchronous complex plane, the direction of the phase A axis (or of the α-axis) is defined by a unit phasor

$$\exp j(\pi/2 - \omega_1 t) = \exp[2\pi j(0.25 - \omega_1 t/2\pi)]$$

At $t = 0$, the phasor is in line with the imaginary axis (it is $\exp(j\pi/2)$. At an arbitrary time t, its direction is defined by the relative time $t/T_1 = \omega_1 t/2\pi$, expressed as a fraction of the period $T_1 = 2\pi/\omega_1 = 1/f_1$. The relative time scale is plotted on the locus of the unit phasor of phase A, shown in Fig. 70-2 as a circle. It is assumed that prior to the switch-on there were no currents flowing in the winding, that is, $I_{1i} = I_{2i} = 0$.

The steady-state currents can be found from Eqs. (70-21):

$$\tilde{I}_{1ss} = 1.029 \exp(-j\,0.5354)$$

$$\tilde{I}_{2ss} = 0.9391 \exp(j\,2.907)$$

At the given slip, the above currents are equal to rated very

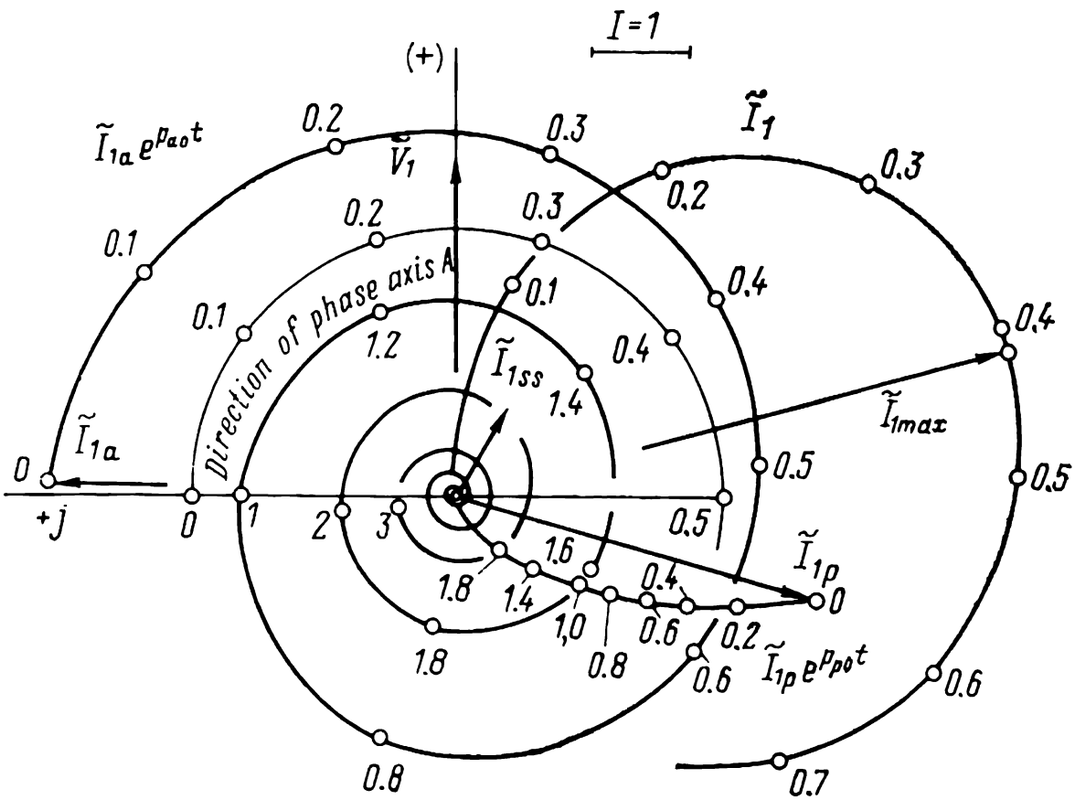

Fig. 70-2 Changes in currents following the switch-on of a running synchronous motor [$\omega = \omega_1 (1 - s)$, $s = 0.0394$]

nearly. Using Eqs. (70-24), we can find the necessary auxiliary coefficients

$$k_{21a} = j\,0.1505, \quad k_{12p} = -j\,0.09930$$

Then, using Eqs. (70-27), we can find the coefficients of the transient currents:

$$\tilde{I}_{1a} = 4.218 \exp(j\,1.533) \qquad \tilde{I}_{2a} = 4.038 \exp(-j\,1.62)$$

$$\tilde{I}_{1p} = 3.843 \exp j(\pi + 1.291) \qquad \tilde{I}_{2p} = 3.98 \exp(j\,1.283)$$

For a solution in the (α, β) complex plane, the roots of the characteristic equation are found from Eqs. (70-15) and (70-16):

$$p_a = p_{a\alpha} + jp_{a\beta}$$

$$p_p = p_{p\alpha} + jp_{p\beta}$$

where $p_{a\alpha} = -31.4$ rad s^{-1}, $p_{p\alpha} = -47.1$ rad s^{-1}, $p_{a\beta} = 4.701$ rad s^{-1}, and $p_{p\beta} = 297.5$ rad s^{-1}.

For a solution in the synchronous $(+, +j)$ complex plane, the roots of the characteristic equation are found with allowance for the velocity at which the synchronous plane travels relative to the stationary complex plane:

$$p_{a,0} = p_{a\alpha,0} + jp_{a\beta,0}$$

$$p_{p,0} = p_{p\alpha,0} + jp_{p\beta,0}$$

where $p_{a\alpha,0} = p_{a\alpha} = -31.4$ rad s^{-1}, $p_{p\alpha,0} = p_{p\alpha} = -47.1$ rad s^{-1}, $p_{a\beta,0} = p_{a\beta} - \omega_1 = 4.701 - 100\pi = -309.5$ rad s^{-1}, and $p_{p\beta,0} = p_{p\beta} - \omega_1 = 297.5 - 100\pi = -16.55$ rad s^{-1}.

In the synchronous complex plane, the total currents during a transient, as defined by Eq. (70-18), can be written

$$\tilde{I}_1 = \tilde{I}_{1ss} + \tilde{I}_{1a} \exp(p_{a,0}t) + \tilde{I}_{1p} \exp(p_{p,0}t)$$

$$\tilde{I}_2 = \tilde{I}_{2ss} + \tilde{I}_{2a} \exp(p_{a,0}t) + \tilde{I}_{2p} \exp(p_{p,0}t)$$

The loci of the stator current, $\tilde{I}_1$, and of its components are shown in Fig. 70-2. The manner in which the current phasors traverse their loci can be judged for the relative time scale, $t/T_1 = 0$, 0.2, 0.4, ... As is seen, at $t = 0$, $\tilde{I}_1 = 0$; at $t = 0.42T_1$, $\tilde{I}_1$ is a maximum $\tilde{I}_{1,\max} = 5.8$. Subsequently, as the aperiodic component $\tilde{I}_{1a} \exp(p_{a,0}t)$ and the periodic component $\tilde{I}_{1p} \exp(p_{p,0}t)$ decay, $\tilde{I}_1$ asymptotically approaches its steady-state value, $\tilde{I}_{1ss}$.

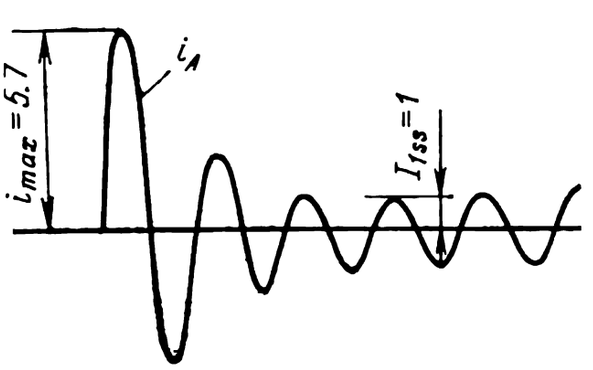

Fig. 70-3 Oscillogram of stator current at switch-on of a running induction motor [$\omega = \omega_1(1 - s)$, $s = 0.0394$]

To find the phase A current (or the current component on the α-axis), $\tilde{I}_1$ or its components must be projected onto the phase A direction:

$$i_{1,A} = \mathrm{Re}\,[\tilde{I}_1 \exp j(\omega_1 t - \pi/2)]$$

The waveform of the phase A current generated by an analog computer for the specified conditions of switch-on appears in Fig. 70-3. As is seen, the maximum current ex-

ceeds the steady-state value by a factor of

$$I_{1,\,max}/I_{1ss} = 5.8/1.029 = 5.63$$

So that the electromagnetic torque can be written in per-unit, let us write Eq. (69-46), using the synchronous complex plane as reference

$$T_{em} = \frac{3p_\tau L_{12}(\tilde{I}_1\tilde{I}_2^* - \tilde{I}_1^*\tilde{I}_2)}{4j} = \frac{3p_\tau L_{12}}{2}\,\mathrm{Im}\,[\tilde{I}_1\tilde{I}_2^*]$$

and define the base torque as

$$T_{em,b} = S_R/\Omega_1 = 3V_{1,R}I_{1,R}p_\tau/2\omega_1$$

Then,

$$T_{em*12} = T_{em}/T_{em,b} = X_{*12}\,\mathrm{Im}\,[\tilde{I}_{*1}I_{*2}^*]$$

$$= \frac{X_{*12}(\tilde{I}_{*1}I_{*2}^* - \tilde{I}_{*1}^*\tilde{I}_{*2}}{2j} \qquad (70\text{-}28)$$

where $X_{*12} = \omega_1 L_{12}I_{1,R}/V_{1,\,R} = (\omega_1 L_{12})_*$

On introducing into Eqs. (70-28) the per-unit values of $\tilde{I}_1$, $\tilde{I}_2$ and $X_{*12} = (\omega_1 L_{12})_* = 3.0$, we can plot variation

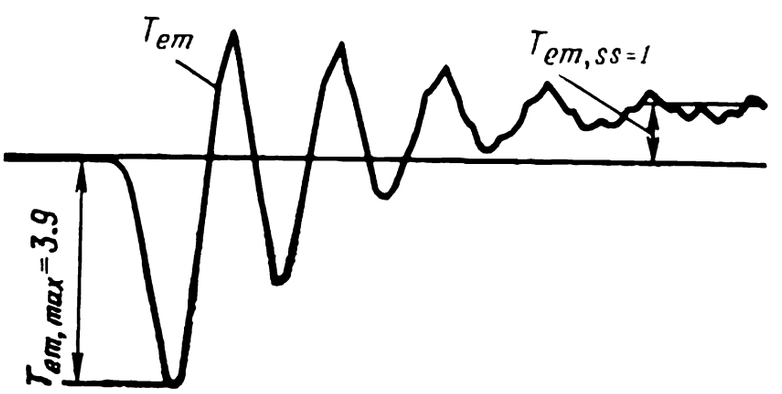

Fig. 70-4 Oscillogram of electromagnetic torque at switch-on of a running induction motor [$\omega = \omega_1(1 - s)$, $s = 0.0394$]

in the electromagnetic torque during the transient. Such a plot generated by an analog computer is shown in Fig. 70-4. As is seen, the maximum electromagnetic torque is 3.9 times its steady-state value.

70-5 Transients during a Balanced Short-Circuit in the Stator Winding of an Induction Machine

We shall be concerned with a short-circuit which occurs from an initial steady state without a prior interruption of the stator circuit. In the circumstances, the transient may

be treated as if resulting from the application of $\tilde{V}_1 = 0$ to an induction machine whose windings carry initial currents $\tilde{I}_{1i}$ and $\tilde{I}_{2i}$.

With such an approach, we may analyze the short-circuit, using the same mathematical description as was used for a switch-on (see Sec. 70-4). If we know in advance the machine performance data, the initial steady-state voltage $\tilde{V}_{1,0}$ and the initial steady-state slip s, then the initial steady-state currents $\tilde{I}_{1ss,0}$ and $\tilde{I}_{2ss,0}$, which are, at the same time, the initial currents for the short-circuit, can be found from Eq. (70-21).

Taking, as an example, the steady-state considered in the example of Sec. 70-4 ($V_{1,0} = 1$ and $s = 0.03794$), the initial currents will be

$$\tilde{I}_{1i} = \tilde{I}_{1ss,0} = 1.029 \exp(-j\,0.5354)$$

$$\tilde{I}_{2i} = \tilde{I}_{2ss,0} = 0.9391 \exp(j\,2.907)$$

Obviously, at the end of the transient following a short-circuit (or application of $\tilde{V}_1 = 0$), the currents are zero:

$$\tilde{I}_{1ss} = \tilde{I}_{2ss} = 0$$

Using the above basic data and the results of Sec. 70-4, we can readily find the coefficients of the transient currents by invoking Eq. (70-27). For the motor specified in Sec. 70-4, the coefficients of the transient currents that exist on a short-circuit will differ from the corresponding coefficients at switch-on only in sign (see above):

$$\tilde{I}_{1a} = -4.218 \exp(j\,1.533) \qquad \tilde{I}_{2a} = -4.038 \exp(j1.62)$$

$$\tilde{I}_{1p} = -3.843 \exp j(\pi + 1.291) \qquad \tilde{I}_{2p} = -3.98 \exp(j\,1.283)$$

In the synchronous complex plane, the total currents existing during the transient which follows a short-circuit and defined by Eq. (70-18), can be written

$$\tilde{I}_1 = \tilde{I}_{1a} \exp(p_{a,0}t) + \tilde{I}_{1p} \exp(p_{p,0}t)$$

$$\tilde{I}_2 = \tilde{I}_{2a} \exp(p_{a,0}t) + \tilde{I}_{2p} \exp(p_{p,0}t)$$

where $p_{a,0}$ and $p_{p,0}$ are the roots of the characteristic equation, as found in Sec. 70-4.

The above total currents contain transient components which differ from those existing at switch-on only in sign. Subject to that qualification, variations in the stator current following a short-circuit can be assessed by reference to Fig. 70-2 if we neglect $\tilde{I}_{1ss}$. Because $\tilde{I}_{1ss}$ plays a relatively minor role, the maximum stator current on a short-circuit is nearly the same as it is at a switch-on; it exceeds the initial steady-state current by a factor of $I_{1max}/I_{1i} = 5.2$

71 Mathematical Description of Transient and Asynchronous Conditions in Synchronous Mahines

71-1 Statement of the Problem. Simplifying Assumptions

We shall consider a three-phase synchronous machine with a complete damper winding and a *d*-axis field winding. The machine may have a salient- or nonsalient-pole rotor.

During transients or under asynchronous conditions ($\omega \neq \omega_1$), changes of flux linkages give rise to emfs not only in the stator phases, but also in the rotor circuits, that is the damper winding and the field winding.* These emfs give in turn rise to currents, and the current induced in the field winding is superimposed on the direct excitation current.

To determine the currents in the rotor circuits, we should be able to calculate their resistances, self-inductances, and mutual inductances with the other stator and rotor circuits. The currents induced in the rotor circuits contribute to the mutual field and the flux linkages with the stator phases. In order to determine those flux linkages, we need to know the mutual inductances between the rotor circuits and the stator phases.

---

* In nonsalient-pole machines, the part of a damper winding is played by slot wedges and the substantial rotor core.

In order to simplify calculations and to obtain an analytical description for the transients, it appears necessary to make the following simplifying assumptions.

1. The relative permeability of the iron parts of the magnetic circuit is assumed to be infinite, $\mu_{rc} = \infty$.
2. In calculating the mutual field, account will be taken only of the fundamental (p-cycle) terms of the radial gap flux density.

On the first assumption, the magnetic field in a machine may be treated as a sum of the fields set up in each circuit by each current taken separately. This assumption enables the analyst (or designer) to determine the inductive variables of each rotor circuit independently.

71-2 Equivalent Circuits for the Damper Winding

As a rule, the damper winding of a synchronous machine is formed by a fairly large number of bars connected to two short-circuiting end rings. The slots of each pole holds n_b bars; ordinarily, $n_b \geqslant 4$ (in Figs. 71-1 and 71-2, six bars are shown, numbered 1, 2, 3, 3′, 2′, and 1′).

A change (say, a decrease) in the d-axis flux (Fig. 71-1) causes a set of d-axis circuit currents ($i_{sc\,d1}$, $i_{sc\,d2}$, and $i_{sc\,d3}$) to flow in the damper winding, which oppose the change that caused them. (Here, the subscript "sc" denotes the short-circuited damper winding.) Similarly, a change (say, a decrease) in the q-axis flux (see Fig. 71-2) causes a set of q-axis circuit currents ($i_{sc\,q1}$, $i_{sc\,q2}$, and $i_{sc\,q3}$) to flow in the damper winding, which oppose the change in the q-axis flux.

The currents induced in the d-and q-axis circuits of the damper winding could be found by solving the set of simultaneous differential equations written for the d- and q-axis circuits of the stator winding, the field winding, and all the circuits of the damper winding. Unfortunately, this would call for an extremely unwieldy mathematical description of all transients and a detailed consideration of all the circuits in the damper winding. A way out is to simplify the mathematics involved by replacing the multicircuit damper winding by two equivalent damper circuits per pole pitch,

namely an equivalent d-axis circuit carrying a current $i_{sc\,d}$ (see Fig. 71-1) and an equivalent q-axis circuit carrying a current $i_{sc\,q}$ (see Fig. 71-2). These circuits are arranged at the poles in such a way that the d-axis circuit interacts solely with the d-axis field, and the q-axis circuit solely with the q-axis field.

Either equivalent circuit is permitted to have an arbitrary number of turns, w_{eq}. Their currents are expressed in

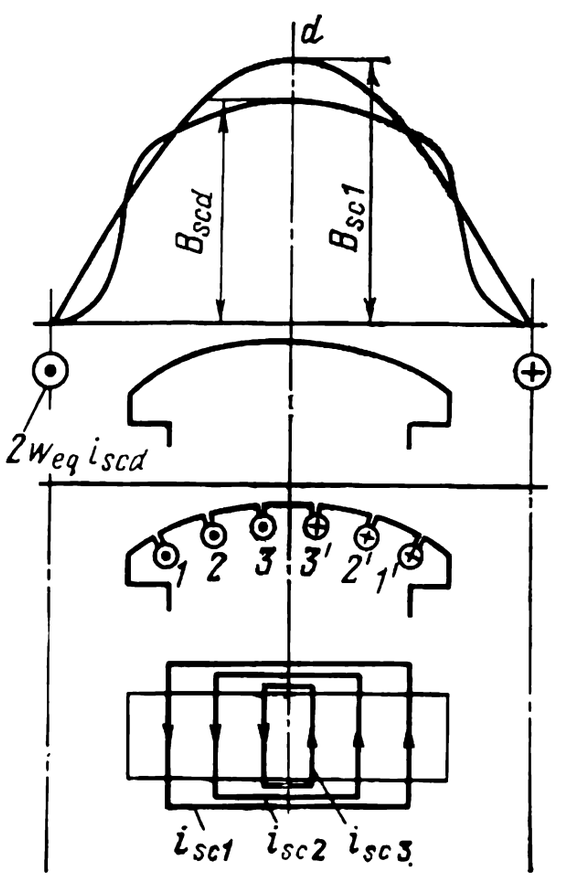

Fig. 71-1 Equivalent representation of the d-axis currents in a damper winding

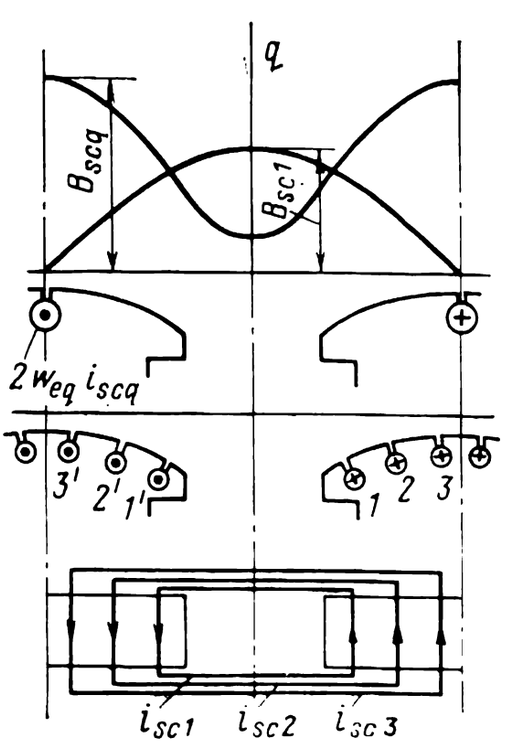

Fig. 71-2 Equivalent representation of the q-axis currents in a damper winding

terms of the currents induced in the actual circuits of the actual damper winding. The current in the equivalent d-axis circuit must produce the same fundamental term of the gap flux density, $B_{sc\,d1}$, as the set of d-axis circuit currents ($i_{sc\,d1}$, $i_{sc\,d2}$, and $i_{sc\,d3}$) in the actual damper winding (see Fig. 71-1). Similarly, the current in the equivalent q-axis circuit must produce the same fundamental term of the gap flux density, $B_{sc\,q1}$, as the set of q-axis circuit currents ($i_{sc\,q1}$, $i_{sc\,q2}$, and $i_{sc\,q3}$) in the actual damper winding (see Fig. 71-2).

As will be shown in more detail later, the parameters of the equivalent circuits can be expressed in terms of the pa-

rameters of the damper-winding circuits formed each by two adjacent bars and the parts of the short-circuiting end rings between the bars. The resistances of the equivalent d- or q-axis circuit, $R_{sc\,d}$ or $R_{sc\,q}$, are chosen to be such that the I^2R losses in them due to $i_{sc\,d}$ and $i_{sc\,q}$ will be the same as in the actual damper winding due to the d- or q-axis set of circuit currents. The leakage inductance of the d-axis equivalent circuit, $L_{sc\,d\sigma}$ and $L_{sc\,q\sigma}$, is chosen so as to have the same energy as is associated with the leakage field of the d- or q-axis circuit currents in the actual damper winding.

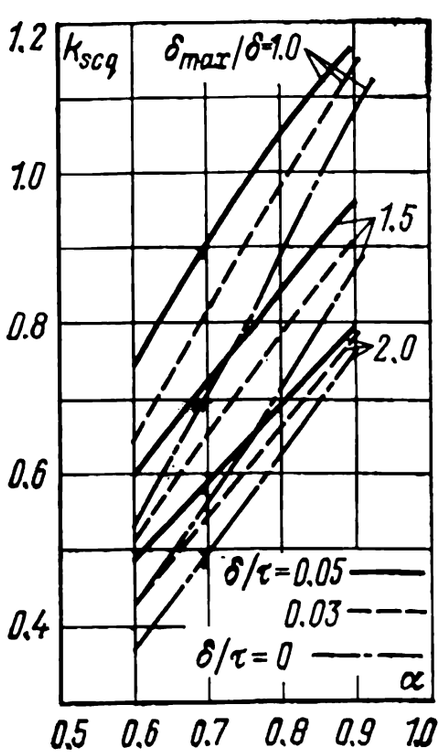

Fig. 71-3 Field factor of the q-axis damper winding

The circuit flux linkages under transient conditions are found with allowance for the field produced by the mmf of the equivalent d-axis circuit of the damper winding,

$$F_{sc\,d} = w_{eq} i_{sc\,d}$$

and the mmf of the equivalent q-axis circuit

$$F_{sc\,q} = w_{eq} i_{sc\,q}$$

The flux density due to $F_{sc\,d}$ (see Fig. 71-1) can be described in terms of the d-axis field form factor for the damper winding

$$k_{sc\,d} = B_{sc\,d1}/B_{sc\,d} = k_f \quad (71.1)$$

which is seen to be equal to the field form factor of the field winding, k_f (see Fig. 53-3).

The flux density due to $F_{sc\,q}$ (see Fig. 71-2) can be described in terms of the q-axis field form factor for the damper winding

$$k_{sc\,q} = B_{sc\,q1}/B_{sc\,q} \quad (71\text{-}2)$$

which is equal to the ratio of the fundamental term of the flux density due to $F_{sc\,q}$ and the peak value of the same flux density as found for a uniform radial air gap, $\delta' = \delta k_\delta$ between the stator and rotor cores. The value of $k_{sc\,q}$ can be found from Fig. 71-3.

71-3 Referring the Rotor Circuits to the Stator Side

Replacing the multicircuit damper winding by equivalent d- and q-axis circuits leaves the rotor (Fig. 71-4) with three single-phase windings, namely the d-axis field winding having w_f turns and carrying a current i_f, the equivalent d-axis damper-winding circuit having w_{eq} turns and carrying a current $i_{sc\,d}$, and the equivalent q-axis damper-winding circuit having w_{eq} turns and carrying a current $i_{sc\,q}$. Both w_f and w_{eq} are turns per pole. In Fig. 71-3, $w_f = 1.5$ and $w_{eq} = 0.5$.

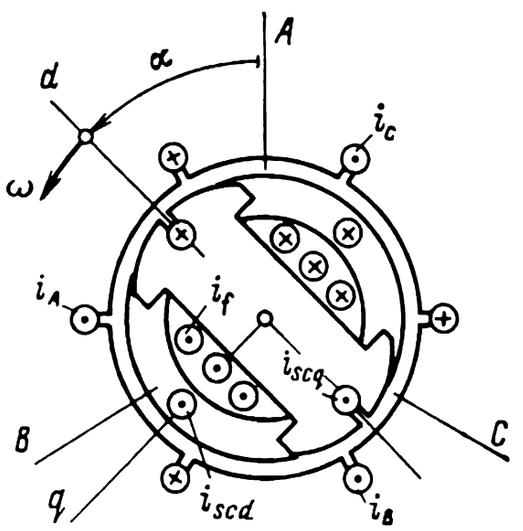

Fig. 71-4 Three-phase salient-pole synchronous machine ($2p = 2$) with equivalent d- and q-axis damper circuits

So that we could use the concepts of resultant phasors introduced in Chap. 69, the single-phase rotor windings of a synchronous machine should be replaced with appropriately oriented three-phase windings which do not differ in arran-

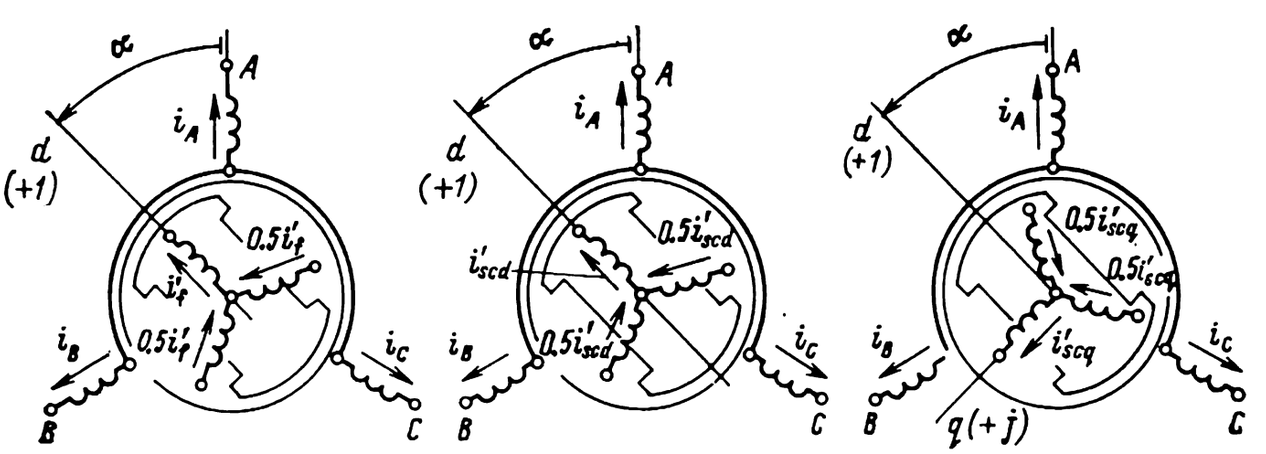

Fig. 71-5 Referring the d- and q-axis rotor circuits to the stator side

gement from the stator winding (Fig. 71-5). This replacement is called *referring* (or *transferring*), and the equivalent three-phase windings that replace the rotor circuits (see Fig. 71-4) are called the *rotor circuits referred to the stator side*, or simply the *referred rotor circuits*.

As is seen from Fig. 71-4, the main (datum) phase of a three-phase winding used to replace a particular rotor circuit

must be arranged to lie on the same axis as the original circuit, and the currents in the phases of the referred rotor circuit should produce the same fundamental component of the gap flux (in magnitude and direction) as the current in the actual rotor circuit. For the field to be aligned in its original direction, the main phase of the referred circuit should carry the total referred circuit current in the positive direction, whereas the other two phases of that circuit should carry each half that current in the negative direction. In Fig. 71-5, the referred field current is denoted as i'_f, the referred d-axis damper-winding current as $i'_{\mathrm{sc}\,d}$, and the referred q-axis damper-winding current as $i'_{\mathrm{sc}\,q}$.

To obtain the desired fundamental term of the field, the referred circuit current should be equal to the product of the circuit current by the referring factor:

$$i'_f = m_{1f} i_f, \quad i'_{\mathrm{sc}d} = m_{1,\mathrm{sc}d} i_{\mathrm{sc}d}, \quad i'_{\mathrm{sc}q} = m_{1,\mathrm{sc}q} i_{\mathrm{sc}q} \tag{71-3}$$

The referring factors for the field current, the d-axis damper-winding current, and the q-axis damper-winding current are:

$$m_{1f} = \frac{\pi p_\tau w_f k_f}{m_1 w_1 k_{\mathrm{w}1} k_d}, \quad m_{1,\mathrm{sc}d} = \frac{\pi p_\tau w_{\mathrm{eq}} k_{\mathrm{sc}d}}{m_1 w_1 k_{\mathrm{w}1} k_d}$$
$$m_{1,\mathrm{sc}q} = \frac{\pi p_\tau w_{\mathrm{eq}} k_{\mathrm{sc}q}}{m_1 w_1 k_q} \tag{71-4}$$

Here,

m_1 = number of phases in the stator winding (usually, $m_1 = 3$)
$k_{\mathrm{w}1}$ = winding factor of the stator for the fundamental (see Sec. 24-6)
k_d = field form factor for the armature winding on the d-axis
k_q = field form factor for the armature winding on the q-axis
k_f = field form factor for the field winding
$k_{\mathrm{c}\,d}$ = field form factor for the damper winding on the d-axis
$k_{\mathrm{s}\,q}$ = field form factor for the damper winding on the q-axis (see Figs. 54-4, 53-3 and 71-3)

The resistive and inductive parameters of the rotor circuits should likewise be referred to the stator side. The referred resistance of a rotor circuit is the phase resistance of the equivalent three-phase winding such that the electric (copper) loss associated with the set of referred currents in

the phases of that winding is the same as the copper loss in the rotor circuit itself. By the same token, the referred leakage inductance of a rotor circuit is the phase inductance of the equivalent three-phase winding such that the energy of the magnetic field established by the set of referred currents in the phases of that winding is the same as the energy of the leakage field of the rotor circuit itself.

The referred resistances and inductances are found as the product of the original quantity by the referring factor:

$$\begin{aligned} R'_f &= m_{Rf} R_f \\ L'_{f\sigma} &= m_{Lf} L_{f\sigma} \\ &\cdots\cdots\cdots \end{aligned} \tag{71-5}$$

The referring factors for the resistance and leakage inductance turn out to be the same

$$\begin{aligned} m_{Rf} &= m_{Lf} = 2m_1 \left(\frac{w_1 k_{w1} k_d}{\pi p_\tau w_f k_f} \right)^2 \\ m_{R,scd} &= m_{L,scd} = 2m_1 \left(\frac{w_1 k_{w1} k_d}{\pi p_\tau w_{eq} k_{scd}} \right)^2 \\ m_{R,scq} &= m_{L,scq} = 2m_1 \left(\frac{w_1 k_{w1} k_q}{\pi p_\tau w_{eq} k_{scq}} \right)^2 \end{aligned} \tag{71-6}$$

The referred rotor-circuit voltages are found in a similar way

$$v'_f = m_{vf} v_f, \quad v'_{scd} = m_{v,scd} v_{scd}, \quad v'_{scq} = m_{v,scq} v_{scq} \tag{71-7}$$

where $m_{vf} = m_{Rf} m_{if}$, $m_{v,scd} = m_{R,scd} m_{i,scd}$, and $m_{v,scq} = m_{R,scq} m_{i,scq}$ are the referring factors of the rotor-circuit voltages.

71-4 Resistive and Inductive Parameters of a Salient-oPle Synchronous Machine with Referred Rotor Circuits

The calculation of a three-phase armature winding has been covered in Chap. 58. Here, we need only to include the main inductances of the armature phases and the main mutual inductances between them, the mutual inductances between the armature phases and the referred rotor circuits, and also the parameters of the referred rotor circuits.

(i) Main Inductances of the Armature Phases and the Mutual Inductances Between Them

The main (useful) inductance of an armature phase, associated with the mutual field, depends on the position of the rotor with respect to the phase axis. As is seen from Fig. 71-6, when the d-axis of the rotor is aligned with the phase A axis (that is, when $\alpha = \alpha_A = 0$ or $\alpha_A = \pi$), the main (useful) inductance of phase A is a maximum

$$L_{AA} = L_{AA\max} = L_{md}$$

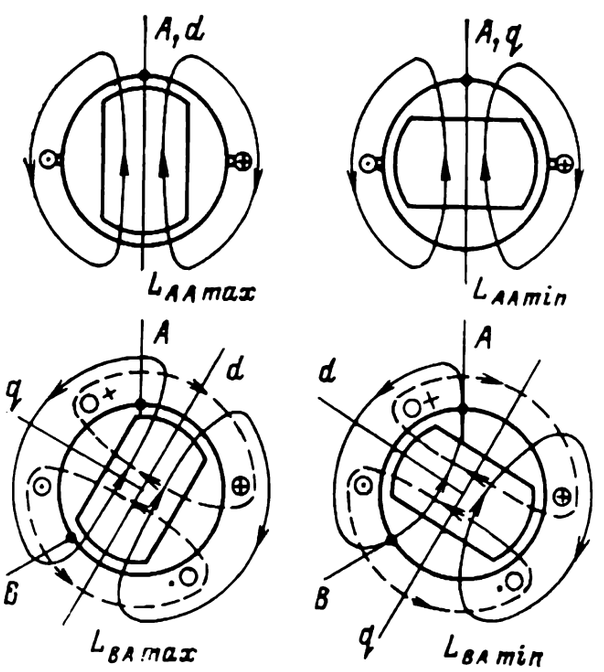

Fig. 71-6 Rotor positions in which the inductive parameters of phase A taken on extremal values

Similarly, when the q-axis of the rotor is aligned with the phase axis (that is, when $\alpha = \alpha_A = \pm\pi/2$), the useful inductance of phase A is a minimum

$$L_{AA} = L_{AA\min} = L_{mq}$$

The above reasoning applies to the other phases as well:

$$L_{BB\max} = L_{CC\max} = L_{md},$$

$$L_{BB\min} = L_{CC\min} = L_{mq}$$

Equations giving the main phase inductances on the d- and q-axes can readily be derived from Eqs. (54-25) and (54-26) on setting $m_1 = 3$:

$$\begin{aligned} L_{md} &= \frac{2}{3} L_{ad} = (4\mu_0/p_\tau \pi^2)\,(w_1 k_{w1})^2\,\lambda_{ad} \\ L_{mq} &= \frac{2}{3} L_{aq} = (4\mu_0/p_\tau \pi^2)\,(w_1 k_{w1})^2\,\lambda_{aq} \end{aligned} \qquad (71\text{-}8)$$

where $\lambda_{ad} = k_d \tau l_\delta / k_\delta \delta$ and $\lambda_{aq} = k_q \tau l_\delta / k_\delta \delta$ are the d- and q-axis permeances of the gap, respectively.

To find the main inductance of, say, phase A at an arbitrary angle between the d-axis of the rotor and the phase axis (Fig. 71-7), the phase A current must be resolved into a d-axis component $i_{Ad} = i_A \cos\alpha$ and a q-axis component $i_{Aq} = -i_A \sin\alpha$, each of which establishes only a d-axis field or only a q-axis field. The d- and q-axis flux linkages

due to the phase current can be written in terms of the respective main phase inductances

$$\Psi_d = i_{Ad} L_{md}, \quad \Psi_q = i_{Aq} L_{mq}$$

The flux linkage of the d- and q-axis field with a phase is found as the sum of the projections of the Ψ_d and Ψ_q phasors on the phase axis

$$\Psi_{AA} = L_{AA} i_A$$
$$= \Psi_d \cos\alpha - \Psi_q \sin\alpha$$

Hence, the main (useful) inductance of phase A is

$$L_{AA} = \Psi_{AA}/i_A$$
$$= L_{md}\cos^2\alpha + L_{mq}\sin^2\alpha$$
$$= L_{m,0} - L_{m,\sim}\cos 2\alpha$$

where $L_{m,0} = (L_{md} + L_{mq})/2$ is the mean main inductance of the phase, and $L_{m,\sim} = (L_{md} - L_{mq})/2$ is the amplitude of the alternating component of the main inductance of the phase.

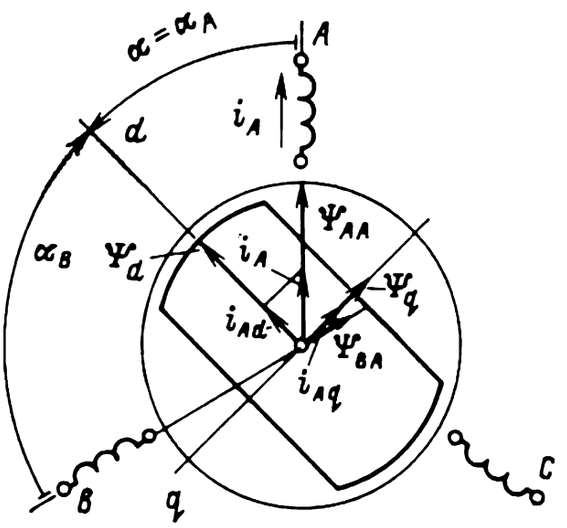

Fig. 71-7 Calculation of the flux linkages produced by the phase A current

Equations for the main inductances of the other phases are derived by analogy, on setting $\alpha_B = \alpha - 2\pi/3$ and $\alpha_C = \alpha - 4\pi/3$:

$$\begin{aligned} L_{BB} &= L_{m,0} + L_{m,\sim}\cos(2\alpha + 2\pi/3) \\ L_{CC} &= L_{m,0} - L_{m,\sim}\cos(2\alpha - 4\pi/3) \end{aligned} \qquad (71\text{-}9)$$

To be able to find the main mutual inductance between armature phases A and B, we should first determine the flux linkage of the phase A field with phase B (see Fig. 71-7)

$$\Psi_{BA} = L_{BA} i_A = \Psi_d \cos\alpha_B - \Psi_q \sin\alpha_B$$

Turning to the equations for Ψ_d and Ψ_q (given earlier) and applying simple trigonometric rules we get

$$L_{BA} = L_{AB} = \Psi_{BA}/i_A = -L_{m,0}/2 + L_{m,\sim}\cos(2\alpha + 4\pi/3)$$

Equations for the other main mutual inductances can be derived by analogy:

$$\begin{aligned} L_{CA} &= L_{AC} = -L_{m,0}/2 + L_{m,\sim}\cos(2\alpha + 2\pi/3) \\ L_{BC} &= L_{CB} = -L_{m,0}/2 + L_{m,\sim}\cos 2\alpha \end{aligned} \qquad (71\text{-}10)$$

The rotor positions where the main mutual inductance L_{AB} takes on extremal values are shown in Fig. 71-6. A maximum value (in absolute terms)

$$L_{AB\max} = -(3L_{md} - L_{mq})/4$$

occurs at $\alpha = -\pi/6$ or $5\pi/6$, and a minimum value (a negative maximum)

$$L_{AB\min} = -(3L_{mq} - L_{md})/4$$

at $\alpha = \pi/3$ or $-2\pi/3$.

If $L_{mq} > L_{md}/3$, the mutual inductance L_{AB} will remain negative at any position of the rotor.

(ii) Mutual Inductances Between the Armature Phases and the Referred Rotor Circuits

The referred rotor circuits are three-phase windings oriented along the *d*- and *q*-axes and having the same values as the stator winding (see Fig. 71-5). To find the mutual inductance between stator phase *A* and the referred field winding, suppose that the latter carries a set of currents, i'_f, $-0.5i'_f$, and $-0.5i'_f$, shown in Fig. 71-5. The *d*-axis field set up by those currents is displaced from the phase *A* axis through an angle $\alpha_{Ad} = \alpha$ and its flux linkage with that phase is

$$\Psi_{Af} = (3/2)\, L_{md} i'_f \cos\alpha$$

Hence, the mutual inductance of the referred field winding with stator phase *A* and, by analogy, the mutual inductances with the other phases are:

$$\begin{aligned} L_{Af} &= \Psi_{Af}/i'_f = (3/2)\, L_{md} \cos\alpha \\ L_{Bf} &= (3/2)\, L_{md} \cos(\alpha + 4\pi/3) \\ L_{Cf} &= (3/2)\, L_{md} \cos(\alpha + 2\pi/3) \end{aligned} \qquad (71\text{-}11)$$

where L_{md} is defined by Eq. (71-8).

The *d*-axis mutual inductances between the referred damper winding and the phases of the stator winding are the same as the corresponding mutual inductances of the field winding:

$$L_{Af} = L_{Ascd},\ L_{Bf} = L_{Bscd},\ L_{Cf} = L_{Cscd} \qquad (71\text{-}12)$$

The *q*-axis mutual inductances between the referred damper winding and the stator phases can be expressed in terms

of L_{mq} and the cosine of the angles between the q-axis and the phase axes (see Fig. 71-5):

$$L_{Ascq} = (3/2)\, L_{mq} \cos \alpha_{Aq} = -(3/2)\, L_{mq} \sin \alpha$$
$$L_{Bscq} = -(3/2)\, L_{mq} \sin (\alpha + 4\pi/3) \qquad (71\text{-}13)$$
$$L_{Cscq} = -(3/2)\, L_{mq} \sin (\alpha + 2\pi/3)$$

In deriving equations for the mutual inductance between a stator phase and the main phase of a referred rotor circuit it is important to remember that now the field is solely set up by one stator phase, whereas in writing equations for the inverse quantities, Eqs. (71-11), (71-12) and (71-13), the field was assumed to be established by the set of currents in all the phases of the referred rotor circuit. Therefore, the mutual inductance between a stator phase and the main phase of a referred rotor circuit is not equal to the inverse mutual inductance, that is, the mutual inductance between a referred rotor circuit and a stator phase, being two-thirds of the former:

$$L_{fA} = (2/3)\, L_{Af}, \qquad L_{fB} = (2/3)\, L_{Bf}, \ \ldots$$
$$L_{scdA} = (2/3)\, L_{Ascd}, \quad L_{scdB} = (2/3)\, L_{Bscd}, \ \ldots \qquad (71\text{-}14)$$
$$L_{scqA} = (2/3)\, L_{Ascq}, \quad L_{scqB} = (2/3)\, L_{Bscq}, \ \ldots$$

(iii) Parameters of the Rotor Circuits

The main inductances of the referred rotor circuits can be found from the gap field produced by the set of referred currents in all the phases of the referred winding. By the main mutual inductance we mean the ratio of the flux linkage of that field to the referred current in the main phase. For example, the main inductance of the referred field winding is (here and elsewhere the referring superscript will be dropped):

$$L_{ff} = \Psi'_{ff}/i'_f = 3L_{md}/2$$

The same goes for the d-axis main inductance of the damper winding

$$L_{scdd} = 3L_{md}/2 \qquad (71\text{-}15)$$

Similarly, the q-axis main inductance of the damper winding is

$$L_{scqq} = 3L_{mq}/2 \qquad (71\text{-}16)$$

The d-axis mutual inductance between the referred rotor circuits (the field winding and the damper winding) can be written similarly

$$L_{dscf} = L_{dfsc} = \Psi'_{fscd}/i'_f = 3L_{md}/2 \qquad (71\text{-}17)$$

The referred resistances and leakage inductances of the rotor circuits are found as the products of the respective original quantities by the referring factor defined in Eqs. (71-6).

The resistance of the referred field winding is

$$R_f = (24/p_\tau\pi^2)\,(w_1 k_{w1} k_d/k_f)^2\ (\rho_f l_f/S_f w_f) \qquad (71\text{-}18)$$

where

ρ_f = resistivity of the field winding
l_f = mean half-turn length
S_f = cross-sectional of the conductor

The d-axis resistance of the referred damper winding is

$$R_{scb} = (6/p_\tau)\,(w_1 k_{w1} k_d/k_f)^2\,\rho_b l_b k_{scd}/(1 - k_{dsc})\,n_{sc} S_b \qquad (71\text{-}19)$$

where

ρ_b = resistivity of a damper-winding bar
l_b = length of a bar
S_b = cross-sectional area of a bar
n_{sc} = number of bars per pole in the damper winding
$k_{dsc} = \dfrac{\sin(n_{sc}\alpha_{sc})}{n_{sc}\sin\alpha_{sc}}$ = distribution factor of the damper winding, where $\alpha_{sc} = \pi t_{Z2}/\tau$ and t_{Z2} is the spacing between bars
c_{scd} = 1.05 to 1.1 = coefficient taking care of the effect of the short-circuiting elements

The q-axis resistance of the referred damper winding is

$$R_{scq} = k_{qR} R_{scd} \qquad (71\text{-}20)$$

where k_{qR} = 0.75 = for a damper winding with complete short-circuiting rings
$k_{qR} \approx$ 10 for a damper winding with insulated short-circuiting segments between adjacent poles.

The leakage inductance of the referred field winding is

$$L_{f\sigma} = (12/p_\tau\pi^2)\,(w_1 k_{w1} k_d/k_f)^2 \mu_0 l_\delta \lambda_{f\sigma} \qquad (71\text{-}21)$$

where $\lambda_{f\sigma}$ is the specific permeance for the leakage flux linkage of the field winding (permeance per unit effective core length per pole).

The d-axis leakage inductance of the referred damper winding is

$$L_{\mathrm{sc}d\sigma} = (12/p_\tau \pi^2)\,(w_1 k_{w1} k_d/k_f)^2\,\mu_0 l_\delta \lambda_{\mathrm{sc}d\sigma} \qquad (71\text{-}22)$$

where $\lambda_{\mathrm{sc}\,d\sigma}$ is the d-axis specific permeance for the leakage flux linkage of the damper winding (permeance per unit effective core length per pole).

The q-axis leakage inductance of the referred damper winding is

$$L_{\mathrm{sc}\,q\sigma} = k_{qL} L_{\mathrm{sc}\,d\sigma} \qquad (71\text{-}23)$$

where $k_{qL} = 0.75$ for a complete damper winding with short-circuiting end rings, and $k_{qL} = 4$ for a damper winding with insulated short-circuiting segments between adjacent poles.

The values of $\lambda_{f\sigma}$ and $\lambda_{\mathrm{sc}\,d\sigma}$ depend on the shape of the gap between the cores and the manner in which the conductors are arranged in the gap. Equations for $\lambda_{f\sigma}$ and $\lambda_{\mathrm{sc}\,d\sigma}$ can be found in [13].

71-5 Circuit Voltage Equations in Terms of Phase Quantities

Taking the same approach as for induction machines (see Chap. 69), let us separate from all the stator phase quantities the components that do not contain zero-sequence terms, that is, the quantities given by

$$\begin{aligned} i_A &= i_{A\Sigma} - i_0 \\ i_B &= i_{B\Sigma} - i_0 \\ &\cdots\cdots\cdots \\ \Psi_A &= \Psi_{A\Sigma} - \Psi_0 \\ \Psi_B &= \Psi_{B\Sigma} - \Psi_0 \\ &\cdots\cdots\cdots \end{aligned} \qquad (71\text{-}24)$$

where

$$\begin{aligned} i_0 &= (i_{A\Sigma} + i_{B\Sigma} + i_{C\Sigma})/3 \\ \Psi_0 &= (\Psi_{A\Sigma} + \Psi_{B\Sigma} + \Psi_{C\Sigma})/3 \\ &\cdots\cdots\cdots\cdots\cdots \end{aligned}$$

The above procedure need not be applied to the referred rotor quantities, because the set of currents in the referred three-phase rotor circuits is free from zero-sequence terms. As is seen from Fig. 71-5, the sum of zero-sequence currents

taken over all the three phases is zero always. For example,

$$i'_f + (-0.5i'_f) + (-0.5i'_f) = 0$$

Separation of the zero-sequence terms from the phase quantities leads to two sets of voltage equations for synchronous machines. In one, the phase quantities involved do not contain zero-sequence terms. In the other, the voltage equations are written in terms of zero-sequence phase quantities.

The former set for all the phases can be written as

$$\begin{aligned} v_A &= Ri_A + \mathrm{d}\Psi_A/\mathrm{d}t \\ v_B &= Ri_B + \mathrm{d}\Psi_B/\mathrm{d}t \\ v_C &= Ri_C + \mathrm{d}\Psi_C/\mathrm{d}t \end{aligned} \qquad (71\text{-}25)$$

For the main phases of the referred three-phase rotor circuits shown in Fig. 71-5, they take the form

$$\begin{aligned} v_f &= R_f i_f + \mathrm{d}\Psi_f/\mathrm{d}t \\ v_{\mathrm{sc}\,d} &= R_{\mathrm{sc}\,d} i_{\mathrm{sc}\,d} + \mathrm{d}\Psi_{\mathrm{sc}\,d}/\mathrm{d}t \\ v_{\mathrm{sc}\,q} &= R_{\mathrm{sc}\,q} i_{\mathrm{sc}\,q} + \mathrm{d}\Psi_{\mathrm{sc}\,q}/\mathrm{d}t \end{aligned} \qquad (71\text{-}26)$$

A zero-sequence voltage equation for one of the stator phases takes the form

$$v_0 = Ri_0 + \mathrm{d}\Psi_0/\mathrm{d}t \qquad (71\text{-}27)$$

As will have been noted, in Eqs. (71-25), (71-26) and others written in terms of referred rotor quantities, the referring superscript has been dropped so as to facilitate their use in transient analysis.

The flux linkages in Eqs. (71-25) and (71-26) are expressed in terms of stator phase currents, main rotor phase currents, and the corresponding inductances, (see above). For example, the flux linkage of stator phase A is

$$\begin{aligned} \Psi_A = {} & L_{AA\Sigma} i_A + L_{AB\Sigma} i_B + L_{AC\Sigma} i_C + L_{Af} i_f \\ & + L_{A\mathrm{sc}\,d} i_{\mathrm{sc}\,d} + L_{A\mathrm{sc}\,q} i_{\mathrm{sc}\,q} \end{aligned} \qquad (71\text{-}28)$$

The flux linkage of the main phase in the referred field winding is

$$\Psi_f = L_{fA} i_A + L_{fB} i_B + L_{fC} i_C + L_f i_f + L_{f\mathrm{sc}\,d} i_{\mathrm{sc}\,d} \qquad (71\text{-}29)$$

The d-axis flux linkage of the main phase in the referred damper winding is

$$\Psi_{sc\,d} = L_{sc\,dA}\,i_A + L_{sc\,dB}i_B + L_{sc\,dC}i_C + L_{sc\,df}i_f + L_{sc\,d}i_{sc\,d} \tag{71-30}$$

The q-axis flux linkage of the main phase in the referred damper winding is

$$\Psi_{sc\,q} = L_{sc\,qA}i_A + L_{sc\,qB}i_B + L_{sc\,qC}i_C + L_{sc\,q}i_{sc\,q} \tag{71-31}$$

The zero-sequence flux linkage is

$$\Psi_0 = L_0 i_0 \tag{71-32}$$

where

$L_0 = L_{AA\sigma} + L_{AB\sigma} + L_{AC\sigma}$ is the stator phase inductance for the zero-sequence currents (see Chap. 69). The flux linkages of phases B and C can be written in a similar way.

The total inductances $L_{AA\Sigma}$, $L_{AB\Sigma}$, and $L_{AC\Sigma}$ in Eq. (71-28) for phase A and the inductances $L_{BB\Sigma}$, $L_{CC\Sigma}$ and others in similar equations for phases B and C are each the sum of the main inductances defined in Eqs. (71-9) and (71-10), and the leakage inductances explained in Chap. 69:

$$\begin{aligned} &L_{AA\Sigma} = L_{AA} + L_{AA\sigma},\quad L_{BB\Sigma} = L_{BB} + L_{BB\sigma},\\ &L_{CC\Sigma} = L_{CC} + L_{CC\sigma}\\ &L_{AB\Sigma} = L_{AB} + L_{AB\sigma},\quad L_{AC\Sigma} = L_{AC} + L_{AC\sigma},\\ &L_{BC\Sigma} = L_{BC} + L_{BC\sigma} \end{aligned} \tag{71-33}$$

The main-phase total inductances of the referred rotor circuits are likewise each the sum of the corresponding main (useful) inductance defined in Eqs. (71-15) and the leakage inductance defined by Eqs. (71-21) and (71-23):

$$\begin{aligned} L_f = L_{ff} + L_{f\sigma},\quad L_{sc\,d} = L_{sc\,dd} + L_{sc\,d\sigma},\\ L_{sc\,q} = L_{sc\,qq} + L_{sc\,q\sigma} \end{aligned} \tag{71-34}$$

71-6 Circuit Votlage Equations in the d, q-Plane

The set of differential equations, (71-25) through (71-27), completely describes transients in a synchronous machine. Unfortunately, for the reasons explained in Chap. 69 they are difficult to solve.

The task can be simplified, if Eqs. (71-25) through (71-26) set up in terms of phase quantities are transformed in a manner similar to that used for the induction machine in Chap. 69. Then the phase quantities (currents, voltages and flux linkages) will be replaced by new variables in the form of resultant complex functions (phasors) expressed in terms of the corresponding phase quantities. It is most convenient to present such phasors in the (d, q) complex plane oriented along the axes of magnetic symmetry of the rotor. Then the real axis of the complex plane will be aligned with the d-axis of the rotor, and the imaginary axis of the complex plane with the q-axis of the rotor.

It is simplest of all to write phasors for the d-axis quantities of the rotor circuits the main phase of which is oriented along the d-axis (see Fig. 71-5 and Eqs. (69-22) and (69-23)). It can be shown that the resultant d-axis current phasors are equal to the referred circuit currents flowing in the main phases, and are in line with the d-axis

$$\begin{aligned}\tilde{I}_f &= (2/3)\,[i_f + (-0.5i_f)\,a + (-0.5i_f)\,a^2] = i_f \\ \tilde{I}_{scd} &= (2/3)\,[i_{scd} + (-0.5i_{scd})a + (-0.5i_{scd})\,a^2] = i_{scd}\end{aligned} \tag{71-35}$$

Recalling that the main phase of the damper-winding q-axis circuit is aligned with the imaginary axis of the complex plane (see Fig. 71-5), the respective q-axis damper-winding current phasor is

$$\tilde{I}_{scq} = j2\,[i_{scq} + (-0.5i_{scq})\,a + (-0.5i_{scq})\,a^2]/3 = ji_{scq} \tag{71-36}$$

As is seen, the magnitude of the above phasor is equal to the referred q-axis damper-winding current and is directed along the q-axis.

The resultant rotor-circuit voltage and flux linkage phasors can be expressed in terms of the respective referred quantities in a similar way:

$$\begin{aligned}\tilde{V}_f &= v_f \quad \tilde{V}_{scd} = v_{scd} \quad \tilde{v}_{scq} = jv_{scq} \\ \tilde{\Psi}_f &= \Psi_f \quad \tilde{\Psi}_{scd} = \Psi_{scd} \quad \tilde{\Psi}_{scq} = j\Psi_{scq}\end{aligned} \tag{71-37}$$

In the (α, β) complex plane whose real axis is aligned with the axis of phase A, the resultant phasor for, say, the stator current can be found from Eq. (69-22)

$$\tilde{I}_{(\alpha,\beta)} = 2\,(i_A + i_B a + i_C a^2)/3$$

In the (d, q) complex plane which rotates together with the rotor and makes an angle α with the (α, β) complex plane, the stator currents defined by Eq. (69-28) can be represented by a resultant phasor of the form

$$\begin{aligned}\tilde{I} &= \tilde{I}_{(\alpha,\beta)} \exp(-j\alpha) \\ &= (2/3)(i_A + i_B a + i_C a^2) \exp(-j\alpha)\end{aligned} \quad (71\text{-}38)$$

The resultant stator voltage and flux linkage phasors are found in a similar manner

$$\begin{aligned}\tilde{V} &= \tilde{V}_{(\alpha,\beta)} \exp(-j\alpha) \\ &= (2/3)(v_A + v_B a + v_C a^2) \exp(-j\alpha)\end{aligned} \quad (71\text{-}39)$$

$$\begin{aligned}\tilde{\Psi} &= \tilde{\Psi}_{(\alpha,\beta)} \exp(-j\alpha) \\ &= (2/3)(\Psi_A + \Psi_B a + \Psi_C a^2) \exp(-j\alpha)\end{aligned}$$

To re-cast Eqs. (71-25) in terms of the resultant phasors in the (α, β) complex plane, it will suffice to multiply the equation for v_A by 2/3, the equation for v_B by $2a/3$, and the equation for v_C by $2a^2/3$, and to add together the right- and left-hand sides of those equations termwise. The result will be only one equation in the (α, β) complex plane

$$\tilde{V}_{(\alpha,\beta)} = R\tilde{I}_{(\alpha,\beta)} + \frac{\mathrm{d}}{\mathrm{d}t}\tilde{\Psi}_{(\alpha,\beta)}$$

All of the quantities in the above equation can be presented in the (d, q) complex plane on the basis of Eqs. (71-38) and (71-39) as

$$\tilde{V}\exp(j\alpha) = R\tilde{I}\exp(j\alpha) + \frac{\mathrm{d}}{\mathrm{d}t}[\tilde{\Psi}\exp(j\alpha)]$$

If, in taking the derivative, we recall that the angle α is a function of time, and cancel out $\exp(j\alpha)$ in all the terms we shall obtain the stator voltage equation in the (d, q) complex plane

$$\tilde{V} = R\tilde{I} = \mathrm{d}\tilde{\Psi}/\mathrm{d}t + j\omega\tilde{\Psi} \quad (71\text{-}40)$$

where

$$\omega = \mathrm{d}\alpha/\mathrm{d}t = p_\tau\Omega$$

is the electrical angular velocity of the rotor.

The rotor-circuit voltage equations need no transformation and may be left as Eqs. (71-26) where the referred rotor quantities are at the same time the projections of the corresponding resultant phasors on the d- or q-axis [see Eqs.

(71-35), (71-36) and (71-37)]. Transformation needs only to be applied to the sum of the terms involving stator phase currents in the equations for the flux linkages of the rotor circuits. As an example, let us show how this transformation is applied to the field-winding flux linkage produced by the stator currents. The flux linkage corresponds to the first three terms in Eq. (71-29). The stator phase currents in those terms are expressed as the projections of the resultant current phasor $\tilde{I}$, Eq. (71-38), on the phase axes or their extensions (for phase A, on the direction defined by $e^* = \exp(-j\alpha)$ relative to the (d, q) complex plane, for phase B on the direction defined by e^*a, and for phase C on the direction defined by e^*a^2)

$$i_A = \text{Re}\,[\tilde{I}e] = 0.5\,(\tilde{I}e + \tilde{I}^*e^*)$$

$$i_B = \text{Re}\,[\tilde{I}ea^2] = 0.5\,(\tilde{I}ea^2 + \tilde{I}e^*a)$$

. . . . . .

Using Eqs. (71-11) and (71-14), the mutual inductances L_{fA}, L_{fB} and L_{fC} can be expressed in terms of the cosines of the angles α, $\alpha + 4\pi/3$ and $\alpha + 2\pi/3$, which can in turn be written in phasor notation as

$$L_{fA} = L_{md}\cos\alpha = 0.5L_{md}\,(e + e^*)$$

$$L_{fB} = L_{md}\cos(\alpha + 4\pi/3) = 0.5L_{md}\,(ea^2 + e^*a)$$

. . . . . .

On substituting and manipulating, we obtain

$$i_AL_{fA} + i_BL_{fB} + i_CL_{fC} = 0.5\,(\tilde{I} + \tilde{I}^*)\,L_{ad}$$

where $L_{ad} = 3L_{md}/2$ is the main (useful) inductance of the armature on the d-axis.

Noting that $0.5\,(\tilde{I} + I^*)$ is the projection of the resultant current phasor on the d-axis, that is, the current i_d, we can obtain from Eq. (71-29) the following expression for the flux linkage of the referred field winding:

$$\Psi_f = i_d\,L_{ad} + i_f\,(L_{ad} + L_{f\sigma}) + i_{\text{sc}\,d}L_{ad} \qquad (71\text{-}41)$$

The flux linkages of the referred damper windings can be written in similar fashion

$$\begin{aligned}\Psi_{\text{sc}\,d} &= i_dL_{ad} + i_fL_{ad} + i_{\text{sc}\,d}\,(L_{ad} + L_{\text{sc}\,d\sigma})\\ \Psi_{\text{sc}\,q} &= i_qL_{aq} + i_{\text{sc}\,q}\,(L_{aq} + L_{\text{sc}\,q\sigma})\end{aligned} \qquad (71\text{-}42)$$

where $L_{ad} + L_{f\sigma} = L_f$, $L_{ad} + L_{sc\,d\sigma} = L_{sc\,d}$, and $L_{aq} + L_{sc\,q\sigma} = L_{sc\,q}$ are the total d- and q-axis inductances of the referred field and damper windings.

The resultant stator flux linkage phasor in Eq. (71.40) can be expressed in terms of the components of the current phasors. To this end, it will suffice in Eq. (71-39) to write the phase flux linkages as functions of currents and inductances (i.e. Eq. (71-28) and similar equations for Ψ_B and Ψ_C), and to take into account the manner in which the inductances vary with angle α in Eqs. (71-9) and (71-17). Also, if we write all trigonometric functions as algebraic expressions which solely contain complex numbers, all the necessary transformations can be carried out in complex form and the stator flux linkage phasor can be written as

$$\tilde{\Psi} = \Psi_d + j\Psi_q \tag{71-43}$$

where

$\Psi_d = L_d i_d + L_{ad} i_f + L_{ad} i_{sc\,d}$ and $\Psi_q = L_q i_q + L_{aq} i_{sc\,q}$

are the projections of the resultant phasor on the d- and q-axis;

$$i_d = (\tilde{I} + \tilde{I}^*)/2 \quad \text{and} \quad i_q = (1/2j)(\tilde{I} - \tilde{I}^*)$$

are the projections of the resultant current phasor on the d- and q-axis;

$$L_{ad} = 3L_{md}/2 \text{ and } L_{aq} = 3L_{mq}/2$$

are the main armature inductances on the d- and q-axes;

$$L_d = L_{ad} + L_\sigma \text{ and } L_q = L_{aq} + L_\sigma$$

are the total d- and q-axis inductances of the armature; and

$$L_\sigma = L_{AA\sigma} - L_{AB\sigma}$$

is the leakage inductance of an armature phase (with allowance for the effect of the other phases).

On expressing the voltage, current and flux linkage phasors in Eq. (71-4) in terms of the d- and q-axis components, the equation breaks up into two equations, one for the d-axis stator voltage, and the other for the q-axis stator voltage

$$\begin{aligned} v_d &= Ri_d + d\Psi_d/dt - \omega\Psi_q \\ v_q &= Ri_q + d\Psi_q/dt + \omega\Psi_d \end{aligned} \tag{71-44}$$

The quantities entering Eq. (71-44) characterize the events taking place in the d- and q-axis stator circuits which are rotating three-phase windings. The main phases of those windings carrying currents i_d and i_q and oriented respectively along the d- and q-axes, and also the main phases of the referred rotor circuits carrying currents i_f, i_{scd} and i_{scq}, are shown in Fig. 71-8 (the referring superscript is omitted).

In transient analysis, Eqs. (71-44) must be considered together with the rotor-circuit voltage equations (71-26)

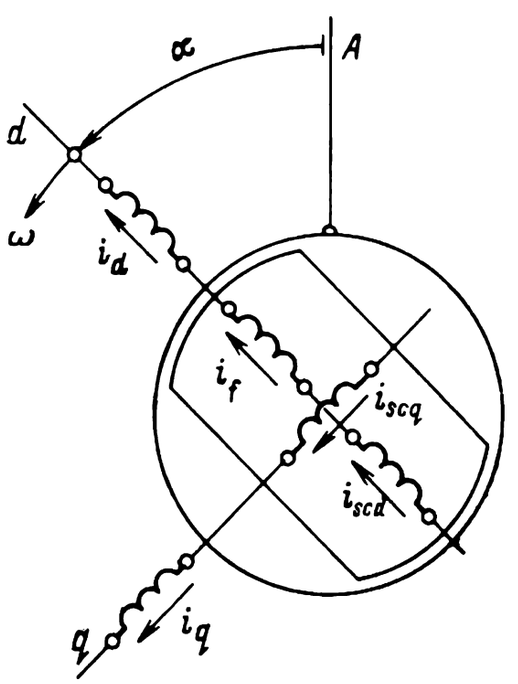

Fig. 71-8 Main (datum) phases of the referred stator and rotor circuits aligned with the d- and q-axes

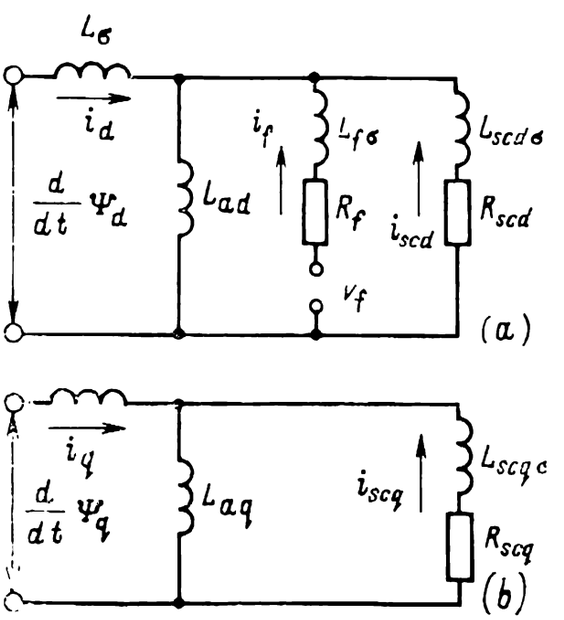

Fig. 71-9 Equivalent circuit of a synchronous machine: (a) the d-axis and (b) the q-axis

written in terms of referred quantities (here, as elsewhere, the prime on the referred quantities is omitted). The flux linkages in Eqs. (71-44) and (71-26) are expressed in terms of the d- and q-axis currents on the basis of Eqs. (71-41) through (71-43).

Consider together the d-axis rotor-circuit voltage equations, (71-26), subject to Eqs. (71-41) and (71-42), and also the d-axis stator flux linkage equation (71-43). On differentiating the last mentioned equation, we get

$$\mathrm{d}\Psi_d/\mathrm{d}t = \frac{\mathrm{d}}{\mathrm{d}t}[L_d i_d + L_{ad}(i_f + i_{scd})]$$

$$v_f = R_f i_f + \frac{\mathrm{d}}{\mathrm{d}t}[L_f i_f + L_{ad}(i_d + i_{scd})]$$

$$0 = R_{scd} i_{scd} + \frac{\mathrm{d}}{\mathrm{d}t}[L_{scd} i_{scd} + L_{ad}(i_d + i_f)]$$

The applicable *d*-axis equivalent circuit appears in Fig. 71-9*a*. Using the same procedure for the *q*-axis rotor-circuit voltage equation and the *q*-axis stator flux linkage equation, we shall obtain the *q*-axis equivalent circuit shown in Fig. 71-9*b*. The two equivalent circuits depict the inductive coupling (transformer action) between the equivalent stator and rotor circuits whose axes are directed along the *d*- and *q*-axes, respectively. The use of *d*- and *q*-axis equivalent circuits facilitates transient analysis of synchronous machines.

The fact that the coefficients of the currents in Eqs. (71-41) through (71-43) are independent of the angular position of the rotor enables transients to be analyzed on the basis of the transformed set of equations. Also, it simplifies programming and the development of analog set-ups in solving those equations on digital or analog computers.

When handled analytically, the set of equations referenced to the *d*- and *q*-axes is often written and solved in operator notation. Then the derivative d/dt is replaced by the operator p.

71-7 Electromagnetic Torque and the Equation of Motion for the Rotor

In a synchronous machine, the electromagnetic torque may be looked upon as one acting either on the rotor or on the stator. In the latter case, recourse may be had to the equations derived for induction machines [see Eq. (69-45)].

Using the notation adopted for synchronous machines, the equation of electromagnetic torque may be written

$$T_{em} = (3p_\tau/2)\,\mathrm{Im}\,[\tilde{\Psi}^*\tilde{I}] = 3p_\tau\,(\tilde{\Psi}^*\tilde{I} - \tilde{\Psi}\tilde{I}^*)/4j$$

$$= (3p_\tau/2)\,(\Psi_d i_q - \Psi_q i_d) \qquad (71\text{-}45)$$

where $\tilde{\Psi} = \Psi_d + i\Psi_q$ is the resultant stator flux linkage phasor, and $\tilde{I} = i_d + ji_q$ is the resultant stator current phasor.

The electromagnetic torque on the rotor is taken to be positive if it is acting in the direction of rotation.

The equation of motion for the rotor of a synchronous machine does not differ from that for an induction machine, Eq. 69-11.

71-8 Equations of a Three-Phase Synchronous Machine in a Balanced Synchronous Steady State

In a balanced synchronous steady state, the angular velocity of the rotor, $\omega = p_\tau \Omega$, is constant and does not differ from the angular frequency of the stator currents, voltages and flux linkages, that is, $\omega = \omega_1$. Also, all stator quantities contain only positive-sequence terms.

Referenced to the stationary α, β-axes, the resultant phasors of stator quantities (as with induction machines, see Sec. 69-10) are the same as the phasors of the corresponding quantities of stator phase A, namely

$$\tilde{I}_{\alpha\beta} = \tilde{I}_A = \dot{I}_A \exp(j\omega_1 t)$$

where $\dot{I}_A = \dot{I}_m = I_m \exp(j\beta_1)$,

$$\tilde{\Psi}_{\alpha\beta} = \tilde{\Psi}_A = \dot{\Psi}_A \exp(j\omega_1 t)$$

where $\dot{\Psi}_A = \dot{\Psi}_m = \Psi_m \exp(j\eta_1)$,
and

$$\tilde{V}_{\alpha\beta} = \tilde{V}_A = \dot{V}_A \exp(j\omega_1 t)$$

where $\dot{V}_A = \dot{V}_m = V_m \exp(j\varphi_1)$.

In the (d, q) coordinates, the phasors of stator quantities are time-invariant:

$$\tilde{I}_{dq} = \tilde{I}_{\alpha\beta} \exp(-j\alpha) = \dot{I}_m$$

$$\tilde{\Psi}_{dq} = \tilde{\Psi}_{\alpha\beta} \exp(-j\alpha) = \dot{\Psi}_m$$

$$\tilde{V}_{dq} = \tilde{V}_{\alpha\beta} \exp(-j\alpha) = \dot{V}_m$$

which can readily be proved if we recall that $\alpha = \omega t = \omega_1 t$.

Referring to the stator voltage equation, (71-40), written in terms of the resultant phasors in the (d, q) reference, we can readily see that the transformer emf, $d\tilde{\Psi}/dt$, vanishes (because $\tilde{\Psi}$ is time-invariant). Therefore, in a synchronous steady state, the right-hand side retains only the rotational

(or motional) emf. $-j\omega_1\tilde{\Psi}$, so it may be re-cast as

$$\dot{V}_s = R\dot{I}_m + j\omega_1\dot{\Psi}_m \qquad (71\text{-}46)$$

where the subscript "s" stands for "supply", that is, the voltage applied to the stator (armature) winding from an external source.

Because the rotor is revolving at synchronous speed, the stator currents are formally constant and give rise to constant flux linkages with the rotor circuits. As a consequence, they do not induce any emf in those circuits. Therefore, as an analysis of Eq. (71-26), would show, when the d- and q-axis circuits of the damper winding are short-circuited ($v_{sc\,d} = v_{sc\,q} = 0$), there are no currents flowing in the damper-winding circuits ($i_{sc\,d} = i_{sc\,q} = 0$), whereas the constant current in the field winding, i_f, is determined by the source of constant voltage, v_f, feeding the field winding:

$$i'_f = v'_f/R'_f = m_{i,f}\,(v_f/R_f) = m_{i,f}i_f \qquad (71\text{-}47)$$

On expressing Ψ_m in Eq. (71-46) in terms of stator and field currents on the basis of Eq. (71-43)

$$\dot{\Psi}_m = \Psi_{d,m} + j\Psi_{q,m} = L_d i_d - L_{ad}i_f + jL_q i_q$$

$$= L_d\dot{I}_{d,m} + L_q\dot{I}_{q,m} + L_{ad}\dot{I}_{f,m}$$

and dividing Eq. (71-46) by $\sqrt{2}$, we get

$$\dot{E}_f = \dot{V} + R\dot{I} + jX_q\dot{I}_q + jX_d\dot{I}_d \qquad (71\text{-}48)$$

. . . . . .

which is the same as Eq. (55-14) derived for the steady state. In comparing them, it should be recalled that

$$\dot{E}_f = -jX_{ad}\dot{I}_f, \quad \dot{V} = -\dot{V}_s, \quad X_{ad} = \omega L_{ad}$$

$$\dot{I} = i_d - ji_q = \dot{I}_d + \dot{I}_q, \qquad X_d = \omega L_d$$

$$\dot{I}_f = i_f \qquad X_q = \omega L_q$$

72 Transients in Synchronous Machines Caused by Changes in and Synppression of Field Excitation

72-1 General Remarks

Normal and abnormal transients in synchronous machines are many and diverse. Some of them, related to substantial changes in speed (such as pulling into step during synchronization and re-synchronization, asynchronous starting, response to load shedding and switch-on, etc.), have been examined under a number of simplifying assumptions in Part 5.

This chapter will be limited to an analysis of the electromagnetic transients observed in synchronous machines at constant speed. In doing so, we shall base ourselves on the mathematical formalism set forth in Chap. 71. We shall proceed from the simple transients to the more complex ones, starting with those caused by changes in and removal (suppression) of the field excitation.

Such transients are at their simplest in synchronous machines without a damper winding on the rotor, and grow in complexity when a damper winding is added. The course of a transient substantially depends on whether the stator winding is short- or open-circuited.

72-2 Transients in a Synchronous Machine with No Damper Winding (with the Stator Winding Open-Circuited)

In this case, the transients are solely associated with changes in the circuit feeding the field winding, and can be described by the equation for that winding

$$R_f i_f + \mathrm{d}\Psi_f/\mathrm{d}t = v_f$$

where

$$\Psi_f = L_f i_f$$

Assuming that the iron parts of the magnetic circuit have an infinite permeability and that the field and all the other windings have a constant inductance, we may write a first-

order linear differential equation with constant coefficients

$$R_f i_f + L_f \mathrm{d}i_f/\mathrm{d}t = v_f$$

On recalling that $p = \mathrm{d}/\mathrm{d}t$, the equation may be recast in operator notation as

$$R_f i_f + L_f p i_f = v_f \qquad (72\text{-}1)$$

As will be recalled, the solution of Eq. (72-1) has two terms, namely:

(*a*) a steady-state term given by the right-hand of the equation and defining the current at $t = \infty$, when the transients have all died out and $pi_f = 0$. If the transients have been caused by a sudden change in input voltage at $t = 0$, then v_f will be zero at $t < 0$ and constant at $t \geqslant 0$, so the steady-state term is

$$i_{f,\mathrm{ss}} = v_f/R_f$$

(*b*) a transient (or force-free) term given by the solution of the homogeneous differential equation

$$R_f i_{f,t\mathrm{t}} + L_f p i_{f,\mathrm{t}} = 0$$

The solution has the form

$$i_{f,\mathrm{t}} = C \exp(\beta t)$$

where $\beta = -R_f/L_f = -1/T_f$ is a root of the characteristic equation

$$R_f + L_f \beta = 0,$$

C is the constant of integration, and

$$T_f = L_f/R_f$$

is the time constant of the field winding.

The current in the field winding is the sum of the above two terms

$$i_f = i_{f,\mathrm{ss}} + i_{f,\mathrm{t}} = i_{f,\mathrm{ss}} + C \exp(-t/T_f)$$

Consider the transient response to a sudden change in the field voltage, v_f. Suppose that prior to that change the initial current in the field winding is $i_{f,\mathrm{i}}$. Then at $t = 0$, the constant of integration can be found from the last equation as

$$C = i_{f,\mathrm{i}} - i_{f,\mathrm{ss}}$$

On substituting it in the above equation, we get

$$i_f = i_{f,\mathrm{ss}} + (i_{f,\mathrm{i}} - i_{f,\mathrm{ss}}) \exp(-t/T_f) \qquad (72\text{-}2)$$

The solution obtained is equally applicable to an increase in excitation, when $i_{f,\mathrm{ss}} > i_{f,\mathrm{i}}$ (Fig. 72-1*a*), and to a decrease in excitation, when $i_{f,\mathrm{ss}} < i_{f,\mathrm{i}}$ (Fig. 72-1*b*). The time constant of the field winding is relatively long, being from one to 12 seconds (notably in large machines). Therefore, for a rapid build-up of the field, it is customary to boost the exciter voltage. More specifically, the exciter voltage is raised to its limiting value

$$v_{f,m} = k_{\mathrm{lim}} v_{f,\mathrm{R}}$$

which is k_{lim} times the rated voltage, $v_{f,\mathrm{R}}$. In such a case, the field current rises as shown in Fig. 72-1*a* by a dashed curve.

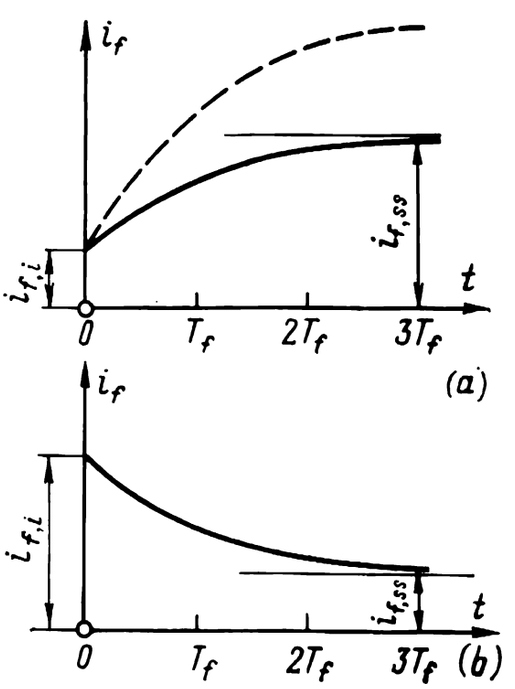

Fig. 72-1 Transients following a change in field voltage

The excitation systems are capable of boosting the field voltage 1.4 times in general-purpose machines, and by a factor of 2.0 in hydrogenerators, turboalternators, and synchronous condensers.

Equation (72-2) is equally applicable to transient analysis in the case of excitation suppression (removal). For excitation removal, the field winding is first shorted via a series resistor, R_{s}, then disconnected from the exciter. Then, $i_{f,\mathrm{ss}} = 0$ and

$$i_f = i_{f,i} \exp(-t/T_{f,\mathrm{s}}) \qquad (72\text{-}3)$$

where $T_{f,\mathrm{s}}$ is the time constant with which the field is being suppressed.

In calculating $T_{f,\mathrm{s}}$ and the field voltage, account must be taken not only of the resistance of the field winding, R_f, but also of the series (field-suppressing) resistor, R_{s}. The time constant of field suppression

$$T_{f,\mathrm{s}} = L_f / R_{f,\mathrm{s}}$$

is by a factor of $R_{f,s}/R_{f,0}$ shorter than that of the field winding, T_f. Here,

$$R_{f,s} = R_{f,0} + R_s^*$$

The voltage across the field-suppression resistor,

$$v_{f,s} = i_f R_s$$

is the same as the transient voltage across the field winding

$$R_{f,0} i_f + L_f p i_f$$

This follows from Eq. (72-1), if we recall that at field suppression, $v_f = 0$ and $R_f = R_{f,0} + R_f$. Then,

$$R_{f,0} i_f + p L_f i_f = -R_s i_f = v_{f,s}$$

Because the initial current in the field winding, $i_{f,i}$, is decided by the initial voltage, $v_{f,i}$

$$i_{f,i} = v_{f,i}/R_{f,0}$$

the transient voltage across the field winding is

$$v_{f,s} = v_f R_s = R_s/R_{f,0}\, v_{f,i} \exp(-t/T_{f,s})$$

Immediately after the field winding is shorted by the field-suppression resistor, that is, at $t = 0$, the voltage across the field winding is $R_s/R_{f,0}$ times the initial voltage. In choosing the value of the field-suppression resistor, it is important to strike the balance between two conflicting requirements. On the one hand, the field must be killed as rapidly as practicable so as to avoid a breakdown. On the other, the resultant voltage should not rise to a point where it might damage the insulation. The two requirements are met to a sufficient degree at $R_s \approx 5R_{f,0}$. Then the time constant is reduced by a factor of $5 + 1 = 6$, and the voltage rises not more than five-fold.

---

* It is always essential to take account of the resistances in the field winding circuit presented by the leads, sliding contacts, exciter armature, and excitation system elements.

72-3 Transients in a Synchronous Machine with a Damper Winding and with the Stator Open-Circuited

For a machine with a damper winding, the need arises to consider together two differential equations, one for the field winding and the other for the equivalent circuit of the damper winding, Eq. (71-26). Let us write the two equations in operator notation

$$\begin{aligned} R_f i_f + p\,(L_f i_f + L_{ad} i_{scd}) &= v_f \\ R_{scd} i_{scd} + p\,(L_{scd} i_{scd} + L_{ad} i_f) &= 0 \end{aligned} \qquad (72\text{-}4)$$

Suppose that, as in the previous case, the field voltage undergoes a sudden change at $t = 0$ and remains constant from that instant on (a step input). Then the field current will change from its initial value

$$i_{f,i} = v_{f,i}/R_f$$

at $t = 0$ to a steady-state value

$$i_{f,ss} = v_f/R_f$$

at $t = \infty$, and will be the sum of a steady-state and a transient component

$$i_f = i_{f,ss} + i_{f,t}$$

The damper winding will carry only a transient (force-free) current, because at the end of the transients there will be no other current flowing in it ($i_{scd,ss} = 0$):

$$i_{scd} = i_{scd,t}$$

The transient (force-free) currents in the two windings are found by solving the set of homogeneous equations derived from (72-4) at $v_f = 0$:

$$\begin{aligned} R_f i_{f,t} + pL_f i_{f,t} + pL_{ad} i_{scd,t} &= 0 \\ R_{scd} i_{scd,t} + pL_{scd}\, i_{scd,t} + pL_{ad} i_{f,t} &= 0 \end{aligned} \qquad (72\text{-}5)$$

As will be recalled from the theory of differential equations, the solution of the above set has the form

$$\begin{aligned} i_{f,t} &= i_{f1} \exp(-t/T_1) + i_{f2} \exp(-t/T_2) \\ i_{scd,t} &= i_{scd1} \exp(-t/T_1) + i_{scd2} \exp(-t/T_2) \end{aligned} \qquad (72\text{-}6)$$

where i_{f1}, i_{f2}, i_{scd1} and i_{scd2} are the arbitrary initial currents determined from the initial conditions and Eqs. (72-4)

T_1 and T_2 are the time constants that must be found from the characteristic equation.

To set up the characteristic equation, we differentiate Eqs. (72-5) and eliminate between the four equations the damper-winding current and its first and second derivatives, that is, $i_{\mathrm{sc}\,d,\mathrm{t}}$, $pi_{\mathrm{sc}\,d,\mathrm{t}}$ and $p^2 i_{\mathrm{sc}\,d,\mathrm{t}}$. This will result in the following equation for the field current:

$$\sigma T_f T_{\mathrm{sc}\,d} p^2 i_{f,\mathrm{t}} + (T_f + T_{\mathrm{sc}\,d})\, p i_{f,\mathrm{t}} + i_{f,\mathrm{t}} = 0 \qquad (72\text{-}7$$

where $T_f = L_f/R_f$ is the time constant of the field winding when all the other windings are open-circuited; $T_{\mathrm{sc}\,d} = L_{\mathrm{sc}\,d}/R_{\mathrm{sc}\,d}$ is the d-axis time constant of the damper winding when all the other windings are open-circuited; and $\sigma = 1 - L_{\mathrm{a}\,d}^2/L_f L_{\mathrm{sc}\,d}$ is the leakage factor of the field and damper windings.

The characteristic equation corresponding to Eq. (72-7) has the form

$$\sigma T_f T_{\mathrm{sc}\,d} \beta^2 + (T_f + T_{\mathrm{sc}\,d})\, \beta + 1 = 0$$

Its roots are the damping factors β_1 and β_2 which can be expressed in terms of the time constants in Eq. (72-6):

$$T_1 = -1/\beta_1$$

$$T_2 = -1/\beta_2$$

On substituting $\beta = -1/T$, we obtain a quadratic equation

$$T^2 - (T_f + T_{\mathrm{sc}\,d})\, T + \sigma T_{\mathrm{sc}\,d} T_f = 0 \qquad (72\text{-}8)$$

whose roots are the desired time constants

$$T_1 = -1/\beta_1 = \frac{T_f + T_{\mathrm{sc}\,d}}{2} + \sqrt{\left(\frac{T_f + T_{\mathrm{sc}\,d}}{2}\right)^2 - \sigma T_f T_{\mathrm{sc}\,d}} \qquad (72\text{-}9)$$

$$T_2 = -1\ \beta_2 = \frac{T_f + T_{\mathrm{sc}\,d}}{2} - \sqrt{\left(\frac{T_f + T_{\mathrm{sc}\,d}}{2}\right)^2 - \sigma T_f T_{\mathrm{sc}\,d}}$$

As a rule, T_f is many times $T_{\mathrm{sc}\,d}$, because $R_{\mathrm{sc}\,d} \gg R_f$. Because of this, the roots of Eq. (72-8) change little, if at all, if the coefficient of T is increased by $\sigma T_{\mathrm{sc}\,d}$, and the free term by $\sigma T_{\mathrm{sc}\,d}^2$. But then

$$T^2 - [(T_f + T_{\mathrm{sc}\,d}) + \sigma T_{\mathrm{sc}\,d}]\, T + (T_f + T_{\mathrm{sc}\,d})\, \sigma T_{\mathrm{sc}\,d} = 0$$

or

$$[T - (T_f + T_{\mathrm{sc}\,d})]\, (T - \sigma T_{\mathrm{sc}\,d}) = 0$$

On solving the above equation, we obtain the following approximate expressions for the time constants:

$$T_1 \approx T_f + T_{scd},\quad T_2 \approx \sigma T_{scd} \tag{72-10}$$

Because

$$\sigma = 1 - L_{ad}^2/L_f L_{scd} < 1$$

it follows that

$$T_1 = T_f + T_{scd} \gg T_2$$

and each of the force-free (transient) currents in Eq. (72-6) is the sum of a "slow" component (with the subscript "1")

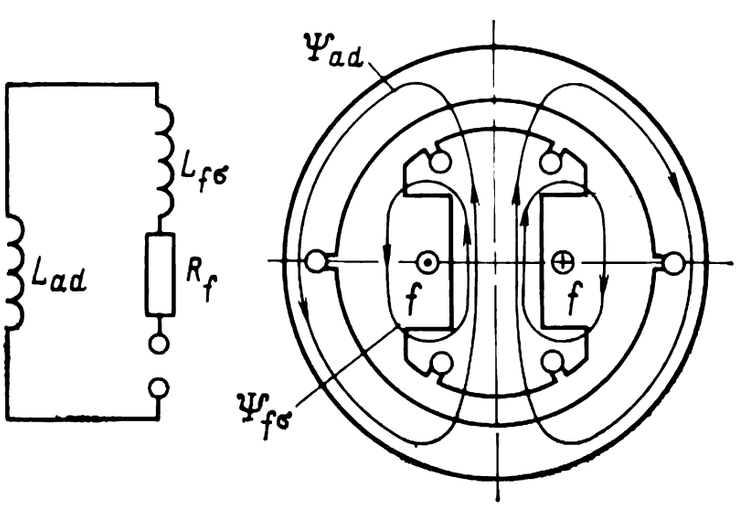

Fig. 72-2 Equivalent circuit and the flux pattern for finding the inductance of the field winding, L_f

which decays with the time constant T_1, and a "fast" component (with the subscript "2") which decays with the time constant T_2.

The "slow" component is mainly associated with the field current and the flux of the field winding. Therefore, the time constant of the slow component differs but little from that of the field winding

$$T_1 \approx T_f + T_{scd} \approx T_f = L_f/R_f$$

An equivalent circuit for which the time constant is T_f is shown in Fig. 72-2. It is easily seen that this equivalent circuit can be derived from the general equivalent circuit in Fig. 71-9 if we open-circuit the stator and damper windings. Figure 72-2 also shows the flux pattern produced by the current in the field winding when all the other windings are open-circuited.

The time constant of the fast component

$$T_2 \approx \sigma T'_{sc\,d} = \sigma L_{sc\,d}/R_{sc\,d}$$

can be expressed in terms of the inductance

$$\sigma L_{sc\,d} = L_{sc\,d} + (1/L_{a\,d} + 1/L_{f\delta})^{-1}$$

possessed by the d-axis damper winding when the field winding is short-circuited and its resistance is deemed equal to

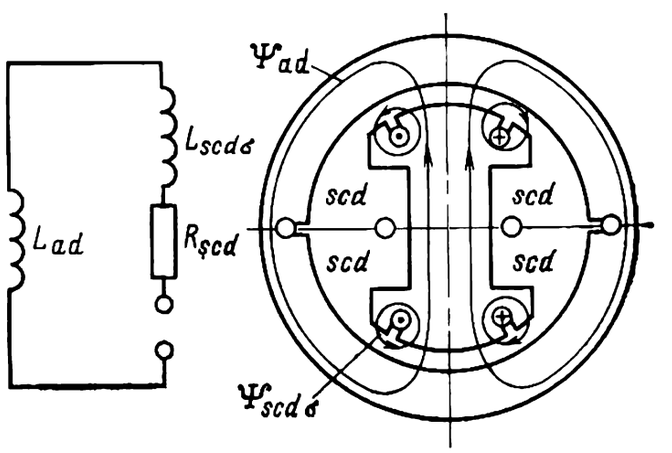

Fig. 72-3 Equivalent circuit and the flux pattern for finding the inductance of the d-axis damper winding, $L_{sc\,d}$

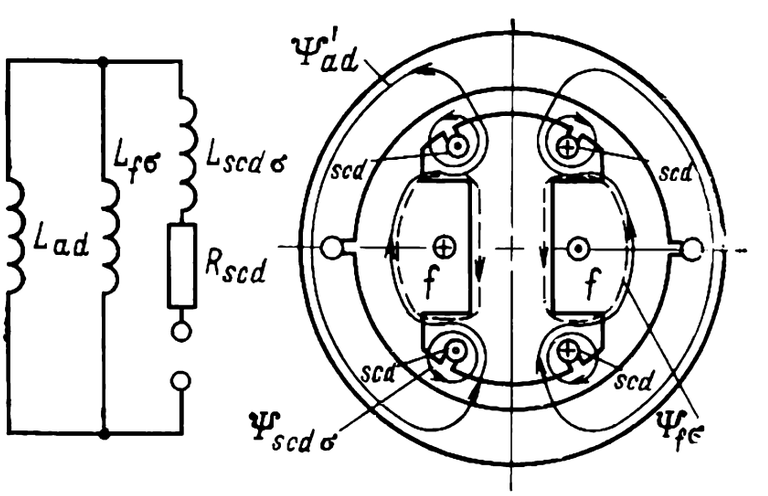

Fig. 72-4 Equivalent circuit and the flux pattern for finding the inductance of the d-axis damper winding when the field winding is short-circuited, $\sigma L_{sc\,d}$

zero (a "superconducting" winding). The time constant of the fast component, T_2, differs markedly from $T_{sc\,d}$. An equivalent circuit with a time constant equal to $T_{sc\,d}$ appears in Fig. 72-3 which also shows the flux pattern produced by the damper winding when all the other windings are open-circuited. An equivalent circuit whose time constant is T_2 and whose inductance is $\sigma L_{sc\,d}$ is shown in Fig. 72-4

which also presents the flux pattern set up by the fast components, with the "superconducting" field winding short-circuited. It is easy to check that the equivalent circuits in Figs. 72-3 and 72-4 can be derived from the general equivalent circuit in Fig. 71-9 on meeting appropriate requirements.

We can readily prove that the field winding may be deemed "superconducting" in the analysis of fast transients. On substituting the fast components from Eq. (72-6) into Eq. (72-5) for the field winding

$$R_f i_{f2} e^{-t/T_2} - (L_f/T_2)\, i_{f2} e^{-t/T_2} - (L_{ad}/T_2)\, i_{scd2} e^{-t/T_2} = 0$$

we can see that at $R_f \ll R_{scd}$ it is always legitimate to neglect the first term which has the meaning of the ohmic voltage drop, in comparison with the second term having the meaning of an emf of self-induction:

$$R_f \ll L_f/T_2 = R_{scd} L_f/\sigma L_{scd}$$

where $L_f \approx L_{scd}$ and $\sigma < 1$.

This implies that, in analysing the fast transients, we may, without committing a grave error, deem the field winding "superconducting", $R_f = 0$.

The damper-winding inductance for the fast component of current, i_{scd2}, with allowance for the effect of i_{f2} induced in the "superconducting" field winding, can be expressed in terms of the resultant damper-winding flux linkage as

$$L = \Psi_{scd}/i_{scd2} = (L_{scd} i_{scd2} + L_{ad} i_{f2})/i_{scd2} \qquad (72\text{-}11)$$

The current i_{f2} in Eq. (72-11) can be found from Eq. (72-5) on setting $R_f = 0$ and $d\Psi_f/dt = 0$, where

$$\Psi_f = L_f i_{f2} + L_{ad} i_{scd2}$$

is the flux linkage of the field winding due to the fast component of current. On integrating the above equation, we will see that during a transient the flux linkage of the "superconducting" short-circuited field winding, and of any "superconducting" short-circuited circuit in general remains unchanged and does not differ from the initial flux linkage, or mathematically

$$\Psi_f = \Psi_{f0} = \text{constant} \quad \text{and} \quad \Psi = \Psi_0 = \text{constant} \qquad (72\text{-}12)$$

The above finding is widely utilized in and markedly simplifies transient analysis.

In our case, the flux linkage of the "superconducting" field winding due to the fast current components must be zero, because those currents do not exist prior to the onset of the transient:

$$\Psi_f = L_f i_{f2} + L_{ad} i_{\mathrm{sc}\,d2} = \Psi_{f0} = 0$$

Therefore, the following relation must apply to the fast components

$$i_{f2} = (-L_{ad}/L_f)\, i_{\mathrm{sc}\,d2} \tag{72-13}$$

Substituting Eq. (72-13) into Eq. (72-12) gives an expression for the damper-winding inductance when the field winding is short-circuited. It is analogous to that obtained earlier:

$$L = \Psi_{\mathrm{sc}d}/i_{\mathrm{sc}d2} = L_{\mathrm{sc}d\sigma} + (1/L_{ad} + 1/L_{f\sigma})^{-1}$$
$$= \sigma L_{\mathrm{sc}d} \tag{72-14}$$

The inductance defined by Eq. (72-14) corresponds to the flux pattern in Fig. 72-4. This can readily be checked, if we recall that the inductances are proportional to the permeabilities of the nonmagnetic parts through which the associated fluxes are closed. As follows from Eqs. (71-21), (71-22) and (71-43),

$$L_{\mathrm{ad}} = w_1^2 \Lambda_{ad},\ L_{f\sigma} = w_1^2 \Lambda_{f\sigma},\ L_{\mathrm{sc}\,d\sigma} = w_1^2 \Lambda_{\mathrm{sc}\,d\sigma}$$

where Λ_{ad} = gap permeance for the d-axis flux linkage in Fig. 72-2 or 72-3

$\Lambda_{f\sigma}$ = permeance between poles for the leakage flux linkage of the field winding, $\Psi_{f\sigma}$, in Fig. 72-2

$\Lambda_{\mathrm{sc}\,d\sigma}$ = permeance of the nonmagnetic parts to the leakage flux linkage of the d-axis damper winding, $\Psi_{\mathrm{sc}\,d\sigma}$ in Fig. 72-3.

Similarly, L may be written in terms of the corresponding permeance:

$$L = w_1^2 \Lambda$$

On writing the inductances in Eq. (72-14) in terms of permeances, we obtain

$$\Lambda = \Lambda_{\mathrm{sc}\,d\sigma} + \Lambda'_{ad}$$

where $1/\Lambda'_{ad} = 1/\Lambda_{f\sigma} + 1/\Lambda_{\mathrm{sc}\,d\sigma}$.

As is seen, the permeance for the total flux linkage is the sum of the shunt permeances $\Lambda_{\mathrm{sc}\,d\sigma}$ and Λ'_{ad} through which $\Psi_{\mathrm{sc}d\sigma}$ and Ψ'_{ad} close (see Fig. 72-4), whereas Λ'_{ad} is the per-

meance of two series-connected nonmagnetic parts namely, the gap whose permeance is Λ_{ad}, and the spacings between the poles whose permeance is $\Lambda_{f\sigma}$. It is those series-connected permeance that form a closed path for the flux giving rise to Ψ'_{ad} (see Fig. 72-4). Penetration of Ψ'_{ad} inside the field circuit is blocked by i_{f2} (see Fig. 72-13) induced in the field winding. (The flux linkage of the field circuit is equal to zero, so there are no lines of flux linking the circuit!) Therefore, the flux giving rise to Ψ'_{ad} has to close via the permeance $\Lambda_{f\sigma}$, that is, along the same path as the leakage flux of the field winding, (in Fig. 72-4), the associated lines of flux are shown as dashed lines).

Now let us find the maximum (initial) values of the fast transient currents, i_{f2} and $i_{\mathrm{sc}\,d2}$, and of the slow transient currents, i_{f1} and $i_{\mathrm{sc}\,d1}$, in Eq. (72-6). One of the equations needed to determine those currents has already been obtained; this is Eq. (72-13). Assuming that the initial current $i_{f\mathrm{i}}$ and the steady-state current $i_{f,\mathrm{ss}}$ in the field winding are fixed in advance, the initial current may be written with the aid of Eq. (72-6) as follows:

$$\begin{aligned} i_{f,\,\mathrm{i}} &= i_{f(t=0)} = i_{f,\,\mathrm{ss}} + i_{f,\,\mathrm{t}(t=0)} \\ &= i_{f,\,\mathrm{ss}} + i_{f1} + i_{f2} \end{aligned} \tag{72-15}$$

Recalling that at $t = 0$ there is no initial current flowing in the damper winding, we may write, subject to Eq. (72-6):

$$i_{\mathrm{sc}d(t=0)} = i_{\mathrm{sc}d1} + i_{\mathrm{sc}d2} = 0 \tag{72-16}$$

A fourth equation needed to find arbitrary currents is derived, using the equation of the damper-winding circuit, (72-5), over a time interval sufficient for the fast component to completely decay, that is,

$$\exp\,(-t/T_2) = 0$$

On substituting Eq. (72-6) into (72-5) and cancelling out the common factor $\exp\,(-t/T_1)$, we obtain

$$R_{\mathrm{sc}\,d} i_{\mathrm{sc}\,d1} - (1/T_1)\,(L_{\mathrm{sc}\,d} i_{\mathrm{sc}\,d1} + L_{\mathrm{a}\,d} i_{f1}) = 0 \tag{72-17}$$

Solving Eqs. (72-13) and (72-17) simultaneously gives

$$\begin{aligned} i_{f1} &= (i_{f\mathrm{i}} - i_{f\mathrm{ss}})\,\frac{T_1 - T_{\mathrm{sc}d}}{T_1 - T_2} \\ i_{f2} &= (i_{f\mathrm{i}} - i_{f\mathrm{ss}})\,\frac{T_{\mathrm{sc}d} - T_2}{T_1 - T_2} \\ i_{\mathrm{sc}d1} &= -i_{\mathrm{sc}d2} = (i_{f\mathrm{i}} - i_{f\mathrm{ss}})\,\frac{L_{ad} T_{\mathrm{sc}d}}{L_{\mathrm{sc}d}\,(T_1 - T_2)} \end{aligned} \tag{72-18}$$

Plots of i_f and $i_{sc\,d}$ based on Eqs. (72-6) and (72-18) in the case of field suppression are shown in Fig. 72-5 by full lines. They have been plotted for $T_f = 0.8T_1$, $T_{sc\,d} = 0.2T_1$, $L_{sc\,d}/L_{a\,d} = 1.1$, $L_f/L_{a\,d} = 1.14$, $\sigma = 0.2$, and $T_2 = 0.04T_1$. The same figure shows (by a dashed line) a plot of i_f in the case of field suppression when the damper winding is open-circuited, $i_{sc\,d} = 0$, and the transient decays with a time constant

$$T_f = T_1 - T_{sc\,d}$$

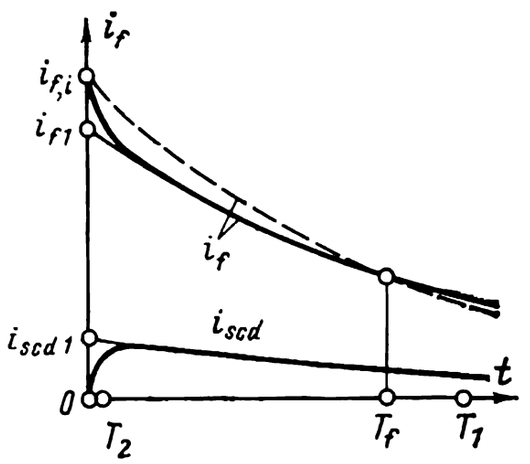

Fig. 72-5 Changes in i_f and i_{scd} following field removal: with the damper winding closed (*solid*); with the damper winding open-circuited (*dashed*)

As is seen, at $t < T_f$, the field current decays faster when the damper winding is short-circuited. At $t = T_f$, however, the full and the dashed lines intersect, and at $t > T_f$ the field current decays faster when the damper winding is open-circuited (because $T_f < T_1 = T_f + T_{sc\,d}$). Thus, in the long run, the damper winding prolongs the transients.

It is of interest to see how the damper winding affects the decay of the stator voltage in the case of field suppression. The stator voltage is given by

$$V = \sqrt{v_d^2 + v_q^2}$$

where v_d and v_q are found from Eq. (71-44). When the stator winding is open-circuited, $i_d = i_q = i_{sc\,q} = 0$. Accordingly,

$$\Psi_q = i_q L_q + i_{sc\,q} L_{a\,q} = 0$$

and the only non-zero quantity is the d-axis flux linkage

$$\begin{aligned}\Psi_d &= L_{a\,d}\,(i_f + i_{sc\,d}) \\ &= \Psi_{d1} \exp(-t/T_1) + \Psi_{d2} \exp(-t/T_2) \qquad (72\text{-}19)\end{aligned}$$

where

$$\Psi_{d1} = i_{f,\,i} L_{ad} \frac{T_1 - \sigma_1 T_{scd}}{T_1 - T_2}, \quad \Psi_{d2} = i_{f,\,i} L_{ad} \frac{\sigma_1 T_{scd} - T_2}{T_1 - T_2}$$

$$\sigma_1 = 1 - L_{ad}/L_{scd}$$

Since

$$v_q = \omega\Psi_d = \omega\Psi_{d1} \exp(-t/T_1) + \omega\Psi_{d2} \exp(-t/T_2)$$

and

$$v_d = d\Psi_d/dt = -(\Psi_{d1}/T_1) \exp(-t/T_1) - (\Psi_{d2}/T_2) \exp(-t/T_2)$$

it is easy to demonstrate that at power frequency ($f = 50$ Hz) and at the time constants ordinarily encountered in synchronous machines, namely $T_1 \approx 1$ to 12 s and T_2 from $0.02T_1$ to $0.06T_1$, the voltage v_q, identical with the rotational emf, is many times the voltage v_d, identical with the transformer emf. Therefore, in the case of field removal the stator voltage is proportional to and varies in step with the d-axis flux linkage $V = v_d = \omega\Psi_d$.

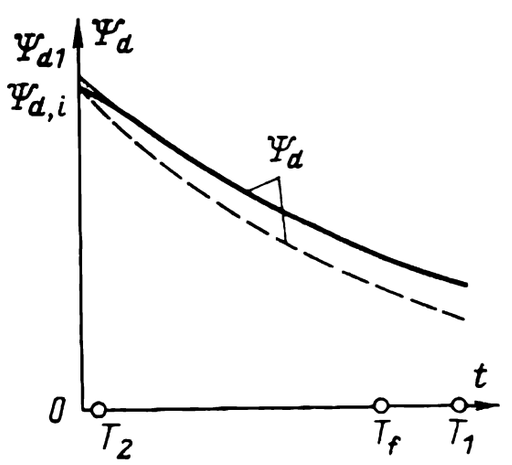

Fig. 72-6 Changes in Ψ_d following field removal: with the damper winding closed (*solid*); with the damper winding open-circuited (*dashed*)

A plot of Ψ_d based on Eq. (72-19) and drawn for the same conditions as the one in Fig. 72-5 appears in Fig. 72-6 (the full line). As is seen, Ψ_d contains a very small fast component, $\Psi_{d2} \exp(-t/T_2)$, and a very large slow component, $\Psi_d \exp(-t/T_1)$. The dashed line in the same figure represents the d-axis flux linkage

$$\Psi_d = \Psi_{d,i} \exp(-t/T_f)$$

existing when the damper winding is open-circuited. This component decays faster at any stage of the transient than when the damper winding is short-circuited.

To sum up, the damper winding serves to slow down the transients caused by field removal. The same goes for the transients caused by changes in field excitation.

72-4 Transients in a Synchronous Machine without a Damper Winding, with the Stator Short-Circuited

Now the current induced in the short-circuited stator winding has a strong effect on the flux and flux linkage produced by the field winding. Therefore, transient analysis must be

based on the equation (71-26) for the field winding

$$R_f i_f + p\Psi_f = v_f \tag{72-20}$$

where $\Psi_f = L_f i_f + L_{ad} i_d$, and the equation (70-44) for the d- and q-axis stator circuits shorted ($v_d = v_q = 0$):

$$Ri_d + p\Psi_d - \omega\Psi_q = 0 \tag{72-21}$$

$$Ri_q + p\Psi_q + \omega\Psi_d = 0 \tag{72-22}$$

Because $| Ri_d | \ll | \omega\Psi_q |$ and $| p\Psi_d | \ll | \omega\Psi_q |$, we may conclude, on the basis of Eq. (72-21), that

$$\Psi_q = L_q i_q = 0$$

and, as a consequence, only the d-axis current, i_d, exists in the stator winding, as it does under a steady-state short circuit (see Chap. 61), whereas the q-axis current, i_q, is non-existent. Then from Eq. (72-22) it follows that

$$\Psi_d = L_d i_d + L_{ad} i_f = 0$$

Hence,

$$i_d = -L_{ad} i_f / L_d$$

On introducing i_d into the expression for Ψ_f, we can see how the short-circuited stator winding affects the self-inductance of the field winding

$$\Psi_f = L_f i_f + L_{ad} i_d = (L_f - L_{ad}^2 / L_d)\, i_f = L_f' i_f$$

where

$$L_f' = \Psi_f / i_f = L_f - L_{ad}^2 / L_d = L_{f\sigma} + (1/L_{ad} + 1/L_\sigma)^{-1} \tag{72-23}$$

Owing to a demagnetizing effect, the current i_d tends to buck the flux of the field winding. The associated flux linkage is expressed in terms of L_f', the self-inductance of the field winding when the stator winding is short-circuited, which is always smaller than L_f, the self-inductance of the field winding when the other windings are open-circuited.

The excitation flux pattern existing when the stator winding is short-circuited and the applicable equivalent circuit having L_f' and $T_f' = L_f'/R_f$ are shown in Fig. 72-7. It can be readily seen that the equivalent circuit in Fig. 72-7 is a special case of the general equivalent circuit drawn in Fig. 71-9 for the damper winding open-circuited and the stator winding short-circuited. It is also seen that the flux

linkage of the field winding is the sum of $\Psi_{f\sigma}$, the leakage flux linkage proportional to $\Lambda_{f\sigma}$, and Ψ'_{ad}, proportional to Λ'_{ad}, where Λ'_{ad} is the permeance of two series-connected nonmagnetic parts, namely the air gap with Λ_{ad}, and the parts through which the stator leakage flux closes, with

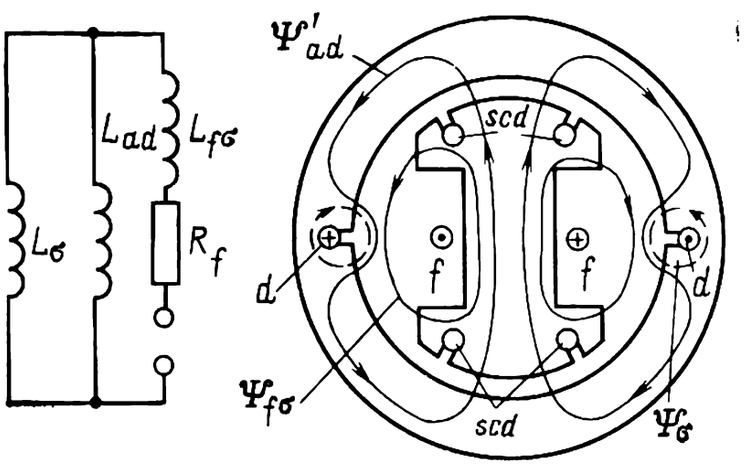

Fig. 72-7 Equivalent circuit and the flux pattern for finding the inductance of the field winding, when the stator winding is short-circuited, L'_f

permeance Λ_σ. Therefore, when the stator winding is short-circuited, the self-inductance of the field winding is

$$L'_f = \Psi_f/i_f = w_1^2\Lambda'_f = w_f^2\,[\Lambda_{f\sigma} + (1/\Lambda_{ad} + 1/\Lambda_\sigma)^{-1}]$$
$$= L_{f\sigma} + (1/L_{ad} + 1/L_\sigma)^{-1}$$

which checks with Eq. (72-23) derived earlier. Expressing Ψ_f in Eq. (72-20) in terms of L'_f and i_f

$$R_f i_f + pL'_f i_f = v_f \qquad (72\text{-}24)$$

leads us to a differential equation which differs from Eq. (72-1) only in that it contains L'_f instead of L_f. Therefore, instead of solving it again, we may use what has been found in the analysis of the transients caused by changes in the field voltage when all the other windings are open-circuited (see Sec. 72-2), and replace L'_f for L_f. The field current equation can be derived from Eq. (72-2).

$$i_f = i_{f,\,\mathrm{ss}} + (i_{f,\mathrm{i}} - i_{f,\mathrm{ss}}) \exp(-t/T'_f) \qquad (72\text{-}25)$$

where $T'_f = L'_f/R_f$ is the time constant of the field winding when the stator winding is short-circuited.

Because $T'_f > T_f$, the transients caused by field suppression and by changes in field excitation take a shorter time to complete when the stator winding is short-circuited.

72-5 Transients in a Synchronous Machine with a Damper Winding and the Stator Winding Short-Circuited

Now, we need to consider jointly three equations, namely the equation (71-26) for the field winding

$$R_f i_f = p\Psi_f = v_f \tag{72-26}$$

an equation for the damper winding

$$R_{sc\,d} i_{sc\,d} + p\Psi_{sc\,d} = 0 \tag{72-27}$$

and the equations (71-44) for the stator winding shorted, that is, for $v_d = v_q = 0$,

$$Ri_d + p\Psi_d - \omega\Psi_q = 0 \tag{72-28}$$

$$Ri_q + p\Psi_q + \omega\Psi_d = 0 \tag{72-29}$$

Because $|Ri_d| \ll |\omega\Psi_q|$ and $|p\Psi_d| \ll |\omega\Psi_q|$, we may conclude, on the basis of Eq. (72-28) that

$$\Psi_q = L_q i_q + L_{ad} i_{sc\,q} = 0$$

and, as a consequence, $i_q = i_{sc\,q} = 0$. Then from Eq. (72-29) we get

$$\Psi_d = L_d i_d + L_{ad}\,(i_f + i_{sc\,d}) = 0$$

Hence,

$$i_d = -\frac{L_{ad}\,(i_f + i_{sc\,d})}{L_d}$$

On expressing i_d in Ψ_f, Eq. (72-26), in terms of i_f and $i_{sc\,d}$, we get

$$\Psi_f = L_f i_f + L_{ad} i_d + L_{ad} i_{sc\,d} = L'_f i_f + L'_{ad} i_{sc\,d} \tag{72-30}$$

where L'_f = field-winding inductance when the stator winding is short-circuited, as defined in Eq. (72-23)

$L'_{ad} = (1/L_{a\,d} + 1/L_\sigma)^{-1}$ = mutual inductance between the field and damper windings, when the stator winding is short-circuited.

It is seen from Fig. 72-7 that the mutual inductance L_{ad} is determined by the flux linkage with the damper winding, Ψ'_{ad}, the stator winding being short-circuited. Therefore,

$$L'_{ad} = \Psi'_{ad}/i_f = w_1^2 \Lambda'_{ad} = w_1^2\,(1/\Lambda_{ad} + 1/\Lambda_\sigma)^{-1}$$
$$= (1/L_{a\,d} + 1/L_\sigma)^{-1} \tag{72-31}$$

Similarly, on expressing i_d in $\Psi_{sc\,d}$, Eq. (72-27), in terms of i_f and $i_{sc\,d}$, we get

$$\begin{aligned}\Psi_{sc\,d} &= L_{sc\,d} i_{sc\,d} + L_{ad} i_d + L_{ad} i_f \\ &= L'_{sc\,d} i_{sc\,d} + L'_{a\,d} i_f \end{aligned} \tag{72-32}$$

where

$$L'_{sc\,d} = L_{sc\,d\sigma} + (1/L_{ad} + 1/L_\sigma)^{-1} \tag{72-33}$$

is the d-axis self-inductance of the damper winding, when the stator winding is short-circuited and the field winding is open-circuited (Fig. 72-8).

Introducing Ψ_f and $\Psi_{sc\,d}$ expressed in terms of i_f and $i_{sc\,d}$ into Eqs. (72-26), (72-27) and (72-4) leads us to a set of diffe-

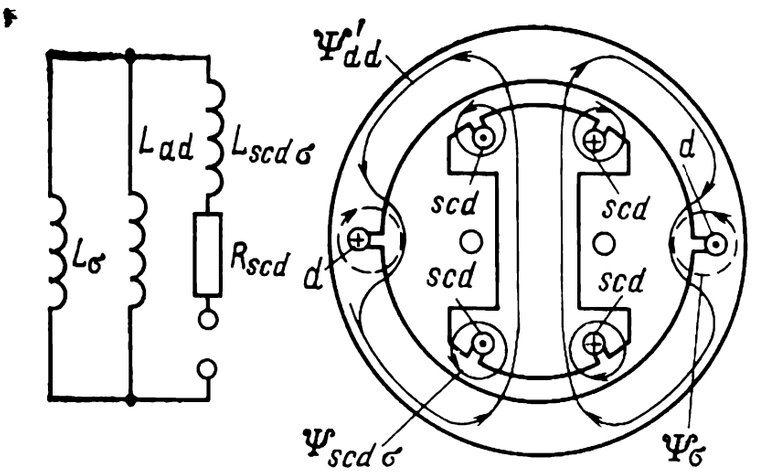

Fig. 72-8 Equivalent circuit and the flux pattern for finding the inductance of the d-axis damper winding when the stator winding is short-circuited, L'_{scd}

rential equations which differ from Eqs. (72-4) written for the stator winding open-circuited only in that they contain the inductances L'_f, $L'_{sc\,d}$ and L'_{ad} instead of L_f, $L_{sc\,d}$, and L_{ad}, respectively. Because the inductances in the case of a short-circuited stator winding have the same order of magnitude as when the stator winding is open-circuited, all the assumptions made in solving Eqs. (72-4) may be extended to Eqs. (72-26) and (72-27). Also, instead of solving Eqs. (72-26) and (72-27) once again, we may use the solution of Eqs. (72-4), on introducing the modified inductances into all the equations. Then the equations will contain the following new variables:

—the time constant of the field winding, with the stator winding short-circuited

$$T'_f = L'_f / R_f \tag{72-34}$$

—the time constant of the d-axis damper winding, with the stator winding short-circuited

$$T'_{\mathrm{sc}\,d} = L'_{\mathrm{sc}\,d}/R_{\mathrm{sc}\,d} \tag{72-35}$$

—the leakage factor of the field and damper windings, with the stator winding short-circuited

$$\sigma' = 1 - (L'_{ad})^2/L'_f L'_{\mathrm{sc}\,d} \tag{72-36}$$

—the time constants of the slow and fast components of field current

$$T'_1 = T'_f + T'_{\mathrm{sc}\,d}$$

$$T'_2 = \sigma' T'_{\mathrm{sc}\,d} \tag{73-37}$$

—the maximum values of the slow and fast field-current components

$$i'_{f1} = (i_{f,\,\mathrm{i}} - i_{f,\,\mathrm{ss}}) \frac{T'_1 - T'_{\mathrm{sc}d}}{T'_1 - T'_2}$$

$$i'_{f2} = (i_{f,\,\mathrm{i}} - i_{f,\,\mathrm{ss}}) \frac{T'_{\mathrm{sc}d} - T'_2}{T'_1 - T'_2} \tag{72-38}$$

—the maximum values of the slow and fast damper winding component currents

$$i'_{\mathrm{sc}d1} = -i'_{\mathrm{sc}d2} = (i_{f,\,\mathrm{i}} - i_{f,\,\mathrm{ss}}) \frac{L'_{ad} T'_{\mathrm{sc}d}}{L'_{\mathrm{sc}d}(T'_1 - T'_2)} \tag{72-39}$$

—equations for the currents in the field and damper windings, when the stator winding is short-circuited [by analogy with Eq. (72-6)]

$$i_f = i_{f,\mathrm{ss}} + i'_{f1} \exp(-t/T'_1) + i'_{f2} \exp(-t/T'_2)$$
$$i_{\mathrm{sc}\,d} = i'_{\mathrm{sc}\,d1} \exp(-t/T'_1) + i_{\mathrm{sc}\,d2} \exp(-t/T'_2) \tag{72-40}$$

Because $T'_1 < T_1$ and $T'_2 < T_2$, the transients caused by changes in excitation, when the stator winding is short-circuited, die out faster than they do when the stator winding is open-circuited.

73 Transients Caused by a Balanced Short-Circuit on the Stator WInding of a Synchronous Machine

73-1 General Remarks. Initial and Terminal Conditions

The transient response to a balanced short-circuit on the stator winding of a synchronous machine may be treated as a special case of the transient caused by a sudden decrease or increase in the external voltage V_e in the line with which the machine is operating in parallel.

Suppose that at $t < 0$ (that is, prior to the onset of the transient) the machine is running in a steady state in parallel with the external circuit. The initial condition (see Sec. 71-8) is characterized by the field current i_f and the stator flux linkage components

$$\Psi_{d,\mathrm{i}} = i_{d,\mathrm{i}} L_d + i_{f,\mathrm{i}} L_{ad} \text{ and } \Psi_{q,\mathrm{i}} = i_{q,\mathrm{i}} L_q$$

to which there correspond the currents

$$i_{q,\mathrm{i}} = \Psi_{q,\mathrm{i}}/L_q \text{ and } i_{d,\mathrm{i}} = (\Psi_{d,\mathrm{i}} - E_{f,\mathrm{i}}/\omega)/L_d \qquad (73\text{-}1)$$

where $E_{f,\mathrm{i}} = \omega L_{ad} i_{f,\mathrm{i}}$ is the initial field emf.

From Eq. (71-44) it follows that

$$\begin{aligned} R i_{d,\mathrm{i}} + p\Psi_{d,\mathrm{i}} - e_{d,\mathrm{i}} &= v_{d,\mathrm{i}} \\ R i_{q,\mathrm{i}} + p\Psi_{q,\mathrm{i}} - e_{q,\mathrm{i}} &= v_{q,\mathrm{i}} \end{aligned} \qquad (73\text{-}2)$$

where $e_{d,\mathrm{i}} = \omega\Psi_{q,\mathrm{i}}$ and $e_{q,\mathrm{i}} = -\Psi\omega_{d,\mathrm{i}}$ are the components of the generated emf, E_{i}, in the initial state.

Neglecting the small terms $Ri_{d,\mathrm{i}}$ and $Ri_{q,\mathrm{i}}$ and noting that $p\Psi_{d,\mathrm{i}} = p\Psi_{q,\mathrm{i}} = 0$ the total emf along the d- and q-axis will be

$$v_{d,\mathrm{i}} + e_{d,\mathrm{i}} = 0, \quad v_{q,\mathrm{i}} + e_{q,\mathrm{i}} = 0 \qquad (73\text{-}3)$$

Thus, in the initial steady state the initial external voltage $V_{e\mathrm{i}}$ (composed of $v_{d,\mathrm{i}}$ and $v_{q,\mathrm{i}}$) is balanced by the generated or internal emf, E_i (composed of $e_{d\mathrm{i}}$ and $e_{q\mathrm{i}}$), so the total emf in the d-axis and the q-axis circuits is zero.

At $t = 0$, the external voltage undergoes a sudden change to V_e (composed of v_d and v_q). It is no longer balanced out by E_{i}, and the resultant total emfs in the d- and q-axis stator

circuits

$$v_d + e_{d,1} = v_d - v_{d,1},$$
$$v_q + e_{q,1} = v_q - v_{q,1} \tag{73-4}$$

give rise to a transient at the end of which the emfs attain a new state of equilibrium. In this new state, the values of $i_{d,ss}$, $i_{q,ss}$, $\Psi_{d,ss} = L_d i_{d,ss} + L_{ad} i_{f,1}$, and $\Psi_{q,ss} = i_{q,ss} L_q$ are such that a balance of emfs is struck again:

$$v_q + e_{q,ss} = 0 \text{ and } v_d + e_{d,ss} = 0 \tag{73-5}$$

where $e_{d,ss} = \omega \Psi_{q,ss}$ and $e_{q,ss} = -\omega \Psi_{d,ss}$.

When a balanced short-circuit is applied at time $t = 0$, the external (applied) voltage disappears altogether, ($V_e = v_d = v_q = 0$), and the transients that are brought about in the stator circuits are solely due to the uncompensated emfs, Eq. (73-4):

$$e_{d,1} = -v_{d,1}, \; e_{q,1} = -v_{q,1} \tag{73-6}$$

At the end of the transient, the emfs in the short-circuited stator circuits, Eq. (73-5), strike a balance, the internal emfs take on steady-state values $e_{q,ss} = -v_q = 0$ and $e_{d,ss} = -v_d = 0$, which correspond to steady-state d- and q-axis flux linkages

$$\Psi_{q,ss} = L_q i_{q,ss} = 0 \text{ and } \Psi_{d,ss} = L_d i_{d,ss} \; L_{ad} i_{f,1} = 0$$

and there appears a steady-state short-circuit current which consists of a d-axis component alone

$$i_{d,ss} = -L_{ad} i_{f,1} / L_d = -E_{f,1} / \omega L_d = -E_{f,1} / X_d \tag{73-7}$$

Here and elsewhere, the equations are written in terms of referred quantities, and the capitals denote their peak values.

Transient currents on a balanced short-circuit could be found by solving the complete set of differential equations for a synchronous machine, Eqs. (71-26) and (71-44), namely two equations for the armature winding, two equations for the damper winding, and one for the field winding. Unfortunately, in order to determine the time constants of the transient response we would have to solve a fifth-degree characteristic equation, which could only be done numerically and no general solution could be effected. Therefore, we set out to find an approximate (but sufficiently accurate)

analytical solution for the above set of equations from the physics of the processes involved, on making some simplifying assumptions.

In contrast to the transients caused by changes in the field circuit, those brought about by a short-circuit on the stator winding involve aperiodically damped force-free (transient) currents not only in the rotor circuits, but also in the stator circuits. In the rotor circuits, they set up fields which are stationary relative to the rotor and which induce periodic currents in the stator phases. The loss in the stator resistances due to those currents are made up for by mechanical power input, so the decay time constants of the transient currents in the rotor are independent of the stator resistances. Therefore, we may safely set the latter equal to zero.

In the stator phases, the *aperiodically damped* transient currents set up fields which are stationary relative to the stator and which induce alternating currents in the rotor circuits. The loss in the rotor resistances due to those currents are made up for by mechanical power input, so the decay time constant of the transient currents in the stator circuits is independent of the resistances of the short-circuited rotor circuits. Therefore, we may set the latter equal to zero.

To sum up, two sets of transient currents are produced in the machine circuits, and they are termed according to the manner in which the various component currents vary in the stator phases.

Thus, the transient currents in the rotor circuits and the corresponding periodic (alternating) transient currents in the stator phases are referred to as *periodic*. The aperiodic transient currents in the stator phases and the corresponding alternating transient currents in the rotor circuits are referred to as *aperiodic*.

The transient current in each of the circuits can be visualized as a sum of a periodic and an aperiodic current in that circuit. Therefore, to simplify the procedure, the analysis is carried out in two steps. In the first step, one finds the periodic currents on the valid assumption that the stator winding is "superconducting". In the second, one finds the aperiodic currents meeting the specified initial conditions, on the assumption that the rotor circuits are "superconducting".

73-2 Equations for Transient Currents

As follows from Eq. (73-6), the transient occurring at $t = 0$, that is, the instant of a balanced short-circuit when the terminal voltages $v_{d,\mathrm{i}}$ and $v_{q,\mathrm{i}}$ vanish, may be visualized as a process accompanying the generation of unbalanced emfs in the short-circuited stator winding

$$-v_{d,\mathrm{i}} = e_{d,\mathrm{i}} = \omega\Psi_{q,\mathrm{i}}, \quad -v_{q,\mathrm{i}} = e_{q,\mathrm{i}} = -\omega\Psi_{d,\mathrm{i}}$$

In the stator and rotor circuits, the unbalanced emfs induce periodic transient currents $i_{d\mathrm{p}}$, $i_{q\mathrm{p}}$, $i_{f\mathrm{p}}$, $i_{\mathrm{sc}\,d\mathrm{p}}$, and $i_{\mathrm{sc}\,q\mathrm{p}}$, and aperiodic transient currents $i_{d\mathrm{a}}$, $i_{q\mathrm{a}}$, $i_{f\mathrm{a}}$, $i_{\mathrm{sc}\,d\mathrm{a}}$, and $i_{\mathrm{sc}\,q\mathrm{a}}$. Therefore, the total currents in the various circuits of the machine are each a sum of a transient and a steady-state term

$$\begin{aligned} i_d &= i_{d\mathrm{p}} + i_{d\mathrm{a}} + i_{d,\mathrm{ss}} \\ i_q &= i_{q\mathrm{p}} + i_{q\mathrm{a}} + i_{q,\mathrm{ss}} \\ i_f &= i_{f\mathrm{p}} + i_{f\mathrm{a}} + i_{f,\mathrm{ss}} \\ i_{\mathrm{sc}\,d} &= i_{\mathrm{sc}\,d\mathrm{p}} + i_{\mathrm{sc}\,d\mathrm{a}} + i_{\mathrm{sc}\,d,\mathrm{ss}} \\ i_{\mathrm{sc}\,q} &= i_{\mathrm{sc}\,q\mathrm{p}} + i_{\mathrm{sc}\,q\mathrm{a}} + i_{\mathrm{sc}\,q,\mathrm{ss}} \end{aligned} \tag{73-8}$$

Here, the steady-state currents are those existing at $t = \infty$ and are given by

$$\begin{aligned} i_{d,\mathrm{ss}} &= -E_{f,\mathrm{i}}/X_d \text{ (from Eq. (73-7))} \\ i_{q,\mathrm{ss}} &= 0 \\ i_{f,\mathrm{ss}} &= i_{f,\mathrm{i}} \\ i_{\mathrm{sc}\,d,\mathrm{ss}} &= i_{\mathrm{sc}\,q,\mathrm{ss}} = i_{\mathrm{sc}\,d,\mathrm{i}} = i_{\mathrm{sc}\,q,\mathrm{i}} = 0 \end{aligned}$$

The transient currents appearing on a short circuit can be found from the set of equations for the short-circuited stator winding, extended to include $e_{d,\mathrm{i}}$ and $e_{q,\mathrm{i}}$ [see Eqs. (71-26) and (71-44)]

$$\begin{aligned} R\,(i_{d\mathrm{p}} + i_{d\mathrm{a}}) + p\,(\Psi_{d\mathrm{p}} + \Psi_{d\mathrm{a}}) - \omega\,(\Psi_{q\mathrm{p}} + \Psi_{q\mathrm{a}}) &= e_{d,\mathrm{i}} \\ R\,(i_{q\mathrm{p}} + i_{q\mathrm{a}}) + p\,(\Psi_{q\mathrm{p}} + \Psi_{q\mathrm{a}}) + \omega\,(\Psi_{d\mathrm{p}} + \Psi_{d\mathrm{a}}) &= e_{q,\mathrm{i}} \end{aligned} \tag{73-9}$$

and from the equations for the shorted rotor circuits

$$R_f\,(i_{f\mathrm{p}} + i_{f\mathrm{a}}) + p\,(\Psi_{f\mathrm{p}} + \Psi_{f\mathrm{a}}) = 0 \tag{73-10}$$

$$\left.\begin{aligned} R_{\mathrm{sc}\,d}\,(i_{\mathrm{sc}\,d\mathrm{p}} + i_{\mathrm{sc}\,d\mathrm{a}}) + p\,(\Psi_{\mathrm{sc}\,d\mathrm{p}} + \Psi_{\mathrm{sc}\,d\mathrm{a}}) = 0 \\ R_{\mathrm{sc}\,q}\,(i_{\mathrm{sc}\,q\mathrm{p}} + i_{\mathrm{sc}\,q\mathrm{a}}) + p\,(\Psi_{\mathrm{sc}\,q\mathrm{p}} + \Psi_{\mathrm{sc}\,q\mathrm{a}}) = 0 \end{aligned}\right\} \tag{73-11}$$

On the assumptions made earlier as regards the resistances of the stator and rotor circuits, the above system breaks up into two independent sets of equations, one for periodic components and the other for aperiodic components.

The periodic currents are induced in the circuits by $e_{d,1}$ and $e_{q,1}$ injected into the stator circuits. In the stator circuits, the two emfs should be treated as forced, whereas in the rotor circuits, they may be looked upon as force-free. Therefore, the periodic components may be found from the following set of equations

$$\left.\begin{aligned} Ri_{dp} + p\Psi_{dp} - \omega\Psi_{qp} &= e_{d,1} = \omega\Psi_{q,1} \\ Ri_{qp} + p\Psi_{qp} + \omega\Psi_{dp} &= e_{q,1} = -\omega\Psi_{d,1} \end{aligned}\right\} \quad (73\text{-}12)$$

$$R_f i_{fp} + p\Psi_{fp} = 0 \quad (73\text{-}13)$$

$$\left.\begin{aligned} R_{scd} i_{scdp} + p\Psi_{scdp} &= 0 \\ R_{scq} i_{scqp} + p\Psi_{scqp} &= 0 \end{aligned}\right\} \quad (73\text{-}14)$$

which should be solved on assuming that $R = 0$ and that Ψ_{dp} and Ψ_{qp} contain no force-free components.

The aperiodic currents in the stator phases are damped transient currents; the aperiodic currents in the rotor circuits may be looked upon as forced currents. Therefore, the aperiodic currents must be found from a set of homogeneous differential equations with their right-hand sides set equal to zero. Formally, such a set can be derived by subtracting the equations for the periodic components, Eqs. (73-12) through (73-14), from the equations for transient components, Eqs. (73-9) through (73-11):

$$\left.\begin{aligned} Ri_{da} + p\Psi_{da} - \omega\Psi_{da} &= 0 \\ Ri_{qa} + p\Psi_{qa} + \omega\Psi_{da} &= 0 \end{aligned}\right\} \quad (73\text{-}15)$$

$$R_f i_{fa} + p\Psi_{fa} = 0 \quad (73\text{-}16)$$

$$\left.\begin{aligned} R_{scd} i_{scda} + p\Psi_{scda} &= 0 \\ R_{scq} i_{scqa} + p\Psi_{scqa} &= 0 \end{aligned}\right\} \quad (73\text{-}17)$$

73-3 Periodic Currents

The periodic components are found from Eqs. (73-12) through (73-14) as those arising upon a sudden injection of $e_{d,1}$ and $e_{q,1}$ into the stator circuits. The injected emfs are found from the initial conditions defined by Eqs. (73-1) and (73-2) at $t \geqslant 0$, and are equal to zero at $t < 0$.

As already noted, Ψ_{dp} and Ψ_{qp} contain no force-free components (which do exist in Ψ_{da} and Ψ_{qa}). Also, the armature resistance has no effect on the periodic components and may therefore be taken as zero. Hence, Eqs. (73-12) are satisfied only when $p\Psi_{dp} = p\Psi_{qp} = 0$, and take the form

$$\begin{aligned} \Psi_{dp} &= (i_{d\infty} + i_{dp}) L_d + (i_{fp} + i_{sc\,d}) L_{ad} = -\Psi_{d,1} \\ \Psi_{qp} &= (i_{q\infty} + i_{qp}) L_q + i_{sc\,q} L_{aq} = -\Psi_{q,1} \end{aligned} \qquad (73\text{-}18)$$

In the above equations, i_{dp} and i_{qp} are the periodic transient components in the stator circuits, which owe their existence to the force-free rotor currents (i_{fp}, $i_{sc\,d}$, and $i_{sc\,q}$) and decay together with them. The currents $i_{d\infty}$ and $i_{q\infty}$ appear in the stator circuits at $t = \infty$, after the force-free currents in the rotor circuits and the transient currents in the stator circuits have all died out. On putting $i_{dp} = i_{qp} = i_{fp} = i_{sc\,dp} = i_{scqp} = 0$, we obtain from Eq. (73-18)

$$i_{d\infty} = -\Psi_{d,1}/L_d, \quad i_{q\infty} = -\Psi_{q,1}/L_q \qquad (73\text{-}19)$$

The transient periodic currents are found by solving the homogeneous differential equations including (73-13) and (73-14), and the equations derived from (73-18) upon eliminating $i_{d\infty}$ and $i_{q\infty}$ with the aid of (73-19):

$$\begin{aligned} i_{dp} L_d + (i_{fp} + i_{sc\,d}) L_{ad} &= 0 \\ i_{qp} L_q + i_{sc\,q} L_{aq} &= 0 \end{aligned} \qquad (73\text{-}20)$$

(1) A machine without a damper winding. To begin with, let us find the periodic currents. In the case on hand, $i_{sc\,dp} = i_{sc\,qp} = 0$, and, as is seen from Eq. (73-20), $i_{qp} = 0$. Therefore, it will suffice to consider Eq. (73-20) for the d-axis alone and Eq. (73-13)

$$\begin{aligned} i_{dp} L_d + i_{fp} L_{ad} &= 0 \\ R_f i_{fp} + p\,(i_{fp} L_f + i_{dp} L_{ad}) &= 0 \end{aligned} \qquad (73\text{-}21)$$

Such a system of homogeneous equations has already been solved in Sec. 72-2 in the analysis of transients caused by changes in the excitation of a machine without a damper winding and with the stator winding short-circuited:

$$i_{fp} = i_{f1} \exp(-t/T'_f) \qquad (73\text{-}22)$$

where $T'_f = L'_f/R_f$ is the time constant of the field winding when the stator winding is short-circuited.

Also, it follows from Eq. (73-21) that

$$i_{dp} = -(L_{ad}/L_d)\, i_{fp} = i_{d1} \exp(-t/T'_f) \qquad (73\text{-}23)$$

The unknown initial values of the periodic components of field and stator currents can be found from Eq. (73-13) for $t = 0$, when the field established by the stator current has not yet found its way into the field circuit, and its flux linkage is zero:

$$\Psi_{fp(t=0)} = L_f i_{f1} + L_{ad}\,(i_{d\infty} + i_{d1}) = 0$$

Subject to the above condition, the initial field current can be written in terms of the initial stator current as

$$i_{f1} = -(L_{ad}/L_f)\,(i_{d\infty} + i_{d1})$$

Now, we substitute the above current in Eq. (73-18) for the direct axis at $t = 0$,

$$(i_{d\infty} + i_{d1})\, L_d - (L_{ad}^2/L_f)\,(i_{d\infty} + i_{d1}) = -\Psi_{d,1}$$

Hence,

$$i_{d\infty} + i_{d1} = -\Psi_{d,1}/L'_d \qquad (73\text{-}24)$$

where $L'_d = L_\sigma + L'_{ad,f}$ is the d-axis transient inductance the stator winding of with $L'_{ad,f} = (1/L_{f\sigma} + 1/L_{ad})^{-1}$.

The stator winding has such an inductance when the magnetic field set up by the current, $i_{d\infty} + i_{d1}$, suddenly appearing in it does not link the superconducting field winding and closes via the permeances for its leakage fluxes. The applicable flux pattern and the equivalent circuit having L'_d are shown in Fig. 73-1. Because $L'_{ad,f} < L_{ad}$, the d-axis transient inductance of the stator winding, L'_d, is always smaller than L_d.

From Eqs. (73-19) and (73-24) we conclude that

$$i_{d1} = -\Psi_{d,1}/L'_d + i_{d\infty} = -\Psi_{d,1}\,(1/L'_d - 1/L_d)$$

and can write the following expression for the periodic component of the stator current in a synchronous machine without a damper winding

$$i_{dp} = -\Psi_{d,1}\,(1/L'_d - 1/L_d) \exp(-t/T'_f) \qquad (73\text{-}25)$$

This component is the difference between the initial and final values of the d-axis current, decaying with a time constant T'_f.

(2) A machine with a damper winding The d-axis. In this case, in order to find the transient periodic components of currents, we need to consider the complete set of homogeneous differential equations, including the two equations in (73-20) and the equations (73-13) and (73-14) for the short-

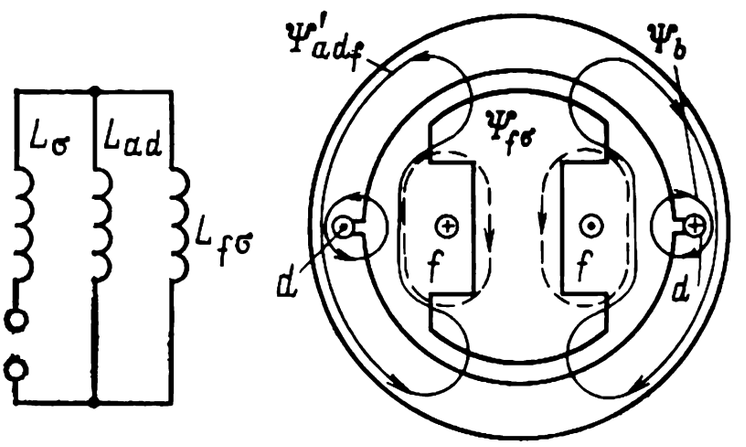

Fig. 73-1 Equivalent circuit and the flux pattern for finding the transient inductance of the stator winding (in a machine without a damper winding)

circuited rotor circuits. This set can be broken down into two independent sets of equations for the d- and q-axis currents.

The d-axis transient periodic components of currents must satisfy the following system of equations

$$\begin{aligned} i_{dp}L_d + (i_{fp} + i_{scdp})\,L_{ad} &= 0 \\ R_f i_{fp} + p\,[i_{fp}L_f + (i_{dp} + i_{scdp})\,L_{ad}] &= 0 \\ R_{scd} i_{scdp} + p\,[i_{scdp}L_{scd} + (i_{dp} + i_{fp})\,L_{ad}] &= 0 \end{aligned} \qquad (73\text{-}26)$$

Resolving the first line for the stator current

$$i_{dp} = -(i_{fp} + i_{scdp})\,(L_{ad}/L_d) \qquad (73\text{-}27)$$

and substituting it in the second and third lines, we obtain a new set of equations

$$\begin{aligned} R_f i_{fp} + p\,(L'_f i_{fp} + L'_{ad} i_{scdp}) &= 0 \\ R_{scd} i_{scdp} + p\,(L'_{scd} i_{scdp}) + L'_{ad} i_{fp}) &= 0 \end{aligned} \qquad (73\text{-}28)$$

which has already been solved in Sec. 72-2 in the analysis of the transients caused by changes in the excitation of a machine with a damper winding, when the stator winding is short-circuited [see Eqs. (72-37) and (72-40)].

The force-free (transient) currents in the rotor circuits are each a sum of a slow and a fast component

$$\begin{aligned} i_{fp} &= i_{f1} \exp(-t/T_1') + i_{f2} \exp(-t/T_2') \\ i_{\mathrm{sc}\,dp} &= i_{\mathrm{sc}\,d1} \exp(-t/T_1') + i_{\mathrm{sc}\,d2} \exp(t/T_2') \end{aligned} \tag{73-29}$$

decaying, respectively, with the time constants T_1' and T_2' which can be found from Eq. (72-37).

In the theory of synchronous machines, the slow components decaying with the time constant T_1' are referred to as *transient currents.* The fast components decaying with the time constant T_2' are referred to as *subtransient currents.* Accordingly, T_1' is the *d-axis transient time constant* and is given the symbol T_d'. The shorter time constant T_2' is called the *d-axis subtransient time constant* and is given the symbol T_d''

$$\begin{aligned} T_1' &= T_d' = T_f' + T_{\mathrm{sc}\,d}' \\ T_2' &= T_d'' = \sigma' T_{\mathrm{sc}\,d}' \end{aligned} \tag{73-30}$$

where σ', $T_{\mathrm{sc}\,d}'$ and T_f' are defined in Eqs. (72-34) through (72-36).

Considering Eqs. (73-27) and (73-29) jointly, we can note that the *d*-axis stator current likewise is a sum of a slow and a fast component decaying each at a time constant of its own and similar to those considered above:

$$i_{dp} = i_{d1} \exp(-t/T_1') + i_{d2} \exp(-t/T_2') \tag{73-31}$$

where

$$\begin{aligned} i_{d1} &= -(i_{f1} + i_{\mathrm{sc}\,d1})\,(L_{ad}/L_d), \\ i_{d2} &= -(i_{f2} + i_{\mathrm{sc}\,d2}) \times (L_{ad}/L_d) \end{aligned}$$

The unknown initial currents in the *d*-axis stator and rotor circuits at $t = 0$ are given by

$$\begin{aligned} i_{d0} &= i_{d\infty} + i_{dp(t=0)} = i_{d\infty} + i_{d1} + i_{d2} \\ i_{f0} &= i_{fp(t=0)} = i_{f1} + i_{f2} \\ i_{\mathrm{sc}\,d0} &= i_{\mathrm{sc}\,d(t=0)} = i_{\mathrm{sc}\,d1} + i_{\mathrm{sc}\,d2} \end{aligned} \tag{73-32}$$

They can be found using Eq. (73-18) at $t = 0$, when the field set up by the stator current has not yet entered the rotor circuits, and its flux linkage with the rotor circuits is zero:

$$\begin{aligned} \Psi_{fp(t=0)} &= L_f i_{f0} + L_{ad}\,(i_{d0} + i_{\mathrm{sc}\,d0}) \quad = 0 \\ \Psi_{\mathrm{sc}\,d(t=0)} &= L_{\mathrm{sc}\,d} i_{\mathrm{sc}\,d0} + L_{ad}\,(i_{d0} + i_{f0}) = 0 \end{aligned}$$

From the above equations, the currents i_{f0} and i_{scd0} are found to be

$$i_{f0} = -\frac{L_{ad}^2 - L_{ad}L_{scd}}{L_{ad}^2 - L_f L_{scd}} i_{d0} \text{ and } i_{scd0} = -\frac{L_{ad}^2 - L_{ad}L_f}{L_{ad}^2 - L_f L_{scd}} i_{d0} \tag{73-33}$$

On substituting the above currents in Eq. (73-18) at $t = 0$

$$i_{d0}L_d + (i_{f0} + i_{scd0})\, L_{ad} = -\Psi_{d,1}$$

we can write the initial current in the d-axis stator circuit:

$$i_{d0} = -\Psi_{d,1}/L_d''$$

where

$$L_d'' = L_\sigma + (1/L_{f\sigma} + 1/L_{scd\sigma} + 1/L_{ad})^{-1} = L_\sigma + L_{ad}'' \tag{73-34}$$

is the d-axis subtransient inductance of the stator winding. The armature winding has such an inductance when the

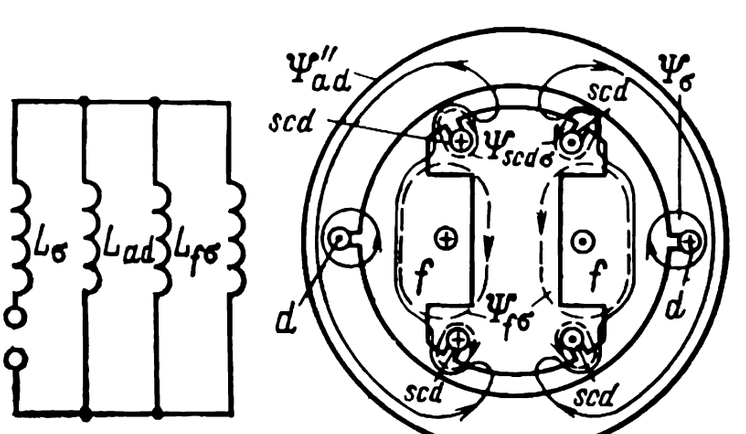

Fig. 73-2 Equivalent circuit and the flux pattern for finding the d-axis subtransient inductance of the stator winding

magnetic field set up by the suddenly appearing current i_{d0} does not link the superconducting rotor circuits and closes via the permeances for the leakage fluxes of those circuits. The applicable flux pattern and equivalent circuit having L_d'' are shown in Fig. 73-2.

From Eqs. (73-32) and (73-34) it follows that the initial d-axis current can be written in terms of L_d'' as

$$i_{d0} = i_{d\infty} + i_{d1} + i_{d2} = -\Psi_{d,1}/L_d'' \tag{73-35}$$

By analogy, the initial d-axis current which is the sum of the steady-state current $i_{d\infty}$ and the initial value of the slow (transient) component can be written in terms of the

transient inductance of the stator winding $L'_{d(sc)}$ as

$$i_{d\infty} + i_{d1} = -\Psi_{d,1}/L'_{d(sc)} \tag{73-36}$$

The stator-winding transient inductance, $L'_{d(sc)}$, is found from the stator flux linkage due to the initial slow-decaying currents in the d-axis circuits of the stator winding, $i_{d\infty} + i_{d1}$, the field winding, i_{f1}, and the damper winding, i'_{scd1}. In a synchronous machine without a damper winding, $L'_{d(sc)} = L'_d$ from Eq. (73-24).

Considering Eqs. (73-35) and (73-36) jointly with Eq. (73-19), we get

$$\begin{aligned} i_{d1} &= -\Psi_{d,1}\,(1/L'_{d(sc)} - 1/L_d) \\ i_{d2} &= -\Psi_{d,1}\,(1/L''_d - 1/L'_{d(sc)}) \end{aligned} \tag{73-37}$$

To find the transient inductance, we need to know the initial values of the slow component currents in the rotor circuits, i_{f1} and i_{scd1}. Firstly, we express the rotor circuit currents in Eq. (73-29) in terms of the slow components i_{f1} and i_{scd1}, using Eq. (73-32)

$$\begin{aligned} i_{fp} &= i_{f1} \exp(-t/T'_1) + (i_{f0} - i_{f1}) \exp(-t/T'_2) \\ i_{scdp} &= i_{scd1} \exp(-t/T'_1) + (i_{scd0} - i_{scd1}) \exp(-t/T'_2) \end{aligned} \tag{73-38}$$

and substitute them in the rotor-circuit equations (73-28). Noting that the equations will be satisfied at any stage of the transients only if the coefficients of $\exp(-t/T'_1)$ and $\exp(-t/T'_2)$ are equal to zero, we may write the following equations leading to i_{f1} and i_{scd1}:

$$\begin{aligned} (R_f T'_1 - L'_f)\, i_{f1} - L'_{ad} i_{scd1} &= 0 \\ (R_{scd} T'_2 - L'_{scd})\,(i_{scd0} - i_{scd1}) - L'_{ad}\,(i_{f0} - i_{f1}) &= 0 \end{aligned} \tag{73-39}$$

On solving Eqs. (73-39) for i_{f1} and i_{scd1} subject to Eq. (73-33), and using Eq. (73-31), we find the current i_{d1}

$$i_{d1} = -(i_{f1} + i_{scd1})\,(L_{ad}/L_d)$$

Then, on substituting the above current in Eq. (73-36), we obtain an expression for the transient inductance of the stator winding (with allowance for the effect of both the field and damper windings)

$$L'_{d(sc)} = L'_d \left[1 - \frac{T_2 - T'_2}{T'_1 - T'_2}\,(1 - T'_1/T_1)\right]^{-1} \tag{73-40}$$

where T_1' and T_2' are defined in Eq. (73-30), and T_1 and T_2, in Eq. (72-10).

From the equation thus derived it follows that in a machine with a damper winding which has a higher resistance than the field winding, so that $T_2 \ll T_1$ and $T_2' \ll T_1'$, the inductance $L'_{d(\mathrm{sc})}$ does not differ from the transient inductance L'_d found from Eq. (73-24) for a machine without a damper winding.

Once $L'_{d(\mathrm{sc})}$ is found, the periodic component of the d-axis stator current defined in Eqs. (73-31) and (73-37) can be written as the sum of a subtransient current decaying with time constant $T_2' = T_d''$, and of a transient current decaying with time constant $T_1' = T_d'$:

$$\begin{aligned} i_{d\mathrm{p}} = &-\Psi_{d,1}[(1/L_d'' - 1/L'_{d(\mathrm{sc})}) \exp(-t/T_2') \\ &+ (1/L'_{d(\mathrm{sc})} - 1/L_d) \exp(-t/T_1')] \end{aligned} \qquad (73\text{-}41)$$

(3) A machine with a damper winding. The q-axis. The q-axis periodic components of current are found from the second line in Eqs. (73-18) and the second lines in Eqs. (73-20) and (73-14) which are quite similar to the d-axis equations for a machine without a damper winding (the first lines in Eqs. (73-18) and (73-21)). Because on the q-axis only the damper-winding circuit interacts with the stator circuit, all the equations may be written by analogy with the equations for the d-axis of a machine without a damper winding—in such a machine, too, there is only one circuit on the rotor, the field winding. By analogy with Eq. (73-25), we can write (without derivation) an expression for the q-axis periodic component of stator current

$$i_{q\mathrm{p}} = -\Psi_{q,1}(1/L_q'' - 1/L_q) \exp(-t/T'_{\mathrm{sc}\,q}) \qquad (73\text{-}42)$$

where the time constant of the q-axis damper winding, with the stator winding short-circuited, is obtained from Eq. (73-22)

$$T'_{\mathrm{sc}q} = L'_{\mathrm{sc}q}/R_{\mathrm{sc}q} \qquad (73\text{-}43)$$

where $L'_{\mathrm{sc}q} = L_{\mathrm{sc}q\sigma} + L'_{\mathrm{a}q}$ and $L'_{\mathrm{a}q} = (1/L_\sigma + 1/L_{\mathrm{a}q})^{-1}$. On the basis of Eq. (72-33), and the subtransient inductance of the q-axis stator winding is

$$L_q'' = L_\sigma + L'_{\mathrm{a}q\mathrm{sc}} \qquad (73\text{-}44)$$

where $L'_{\mathrm{a}q\mathrm{sc}} = (1/L_{\mathrm{sc}q\sigma} + 1/L'_{\mathrm{a}q})^{-1}$.

The stator winding has such an inductance when the magnetic field set up by the suddenly appearing current does

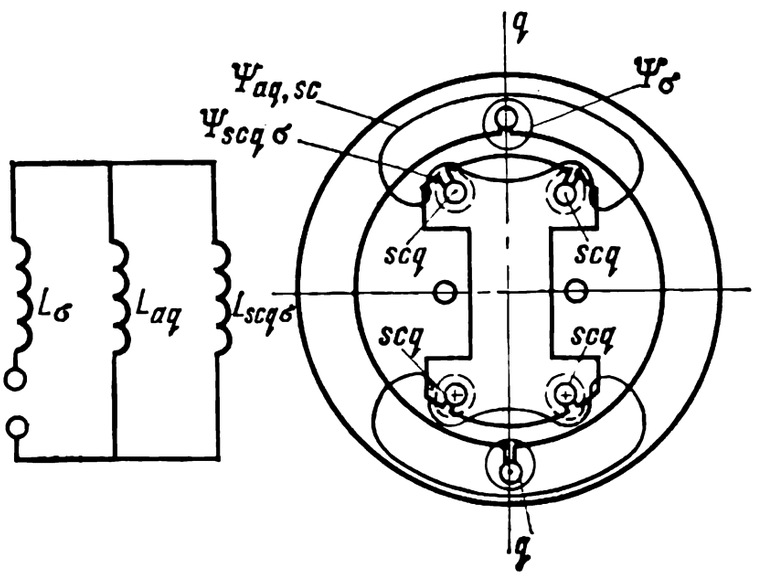

Fig. 73-3 Equivalent circuit and the flux pattern for finding the q-axis subtransient inductance of the stator winding

not link the superconducting q-axis damper winding, but closes via the permeance for its leakage flux. The applicable flux pattern and the equivalent circuit having L_q'' are shown in Fig. 73-3.

73-4 Aperiodic Current Components

The aperiodic current components are found by solving Eqs. (73-15) through (73-17) on the assumption made, namely $R_f = R_{sc\,d} = R_{sc\,q} = 0$.

On that assumption, instead of the differential equations (73-16) and (73-17), we may consider jointly with Eq. (73-15), the equations for the flux linkages of the rotor circuits, assuming that those flux linkages are equal to zero:

$$\begin{aligned} \Psi_{f\,a} &= L_f i_{f\,a} + L_{a\,d}\,(i_{d\,a} + i_{sc\,d\,a}) = 0 \\ \Psi_{sc\,d\,a} &= L_{sc\,d} i_{sc\,d\,a} + L_{a\,d}\,(i_{d\,a} + i_{f\,a}) = 0 \\ \Psi_{sc\,q\,a} &= L_{sc\,q} i_{sc\,q\,a} + L_{aq} i_{q\,a} = 0 \end{aligned} \qquad (73\text{-}45)$$

The above equations can then be used to express $i_{f\,a}$ and $i_{sc\,d\,a}$ in terms of $i_{d\,a}$, and $i_{sc\,q\,a}$ in terms of $i_{q\,a}$. On substituting the resultant expressions in the equations for the stator flux linkages on the direct and quadrature axes, we may write the flux linkages in terms of $i_{d\,a}$ and $i_{q\,a}$ as:

$$\Psi_{d\,a} = L_d'' i_{d\,a}, \quad \Psi_{q\,a} = L_q'' i_{q\,a} \qquad (73\text{-}46)$$

where L''_d is from Eq. (73-34) and L''_q is from Eq. (73-44). On substituting Ψ_{da} and Ψ_{qa} thus derived into Eq. (73-15), we get two differential equations for i_{da} and i_{qa}:

$$\begin{aligned} Ri_{da} + L''_d p i_{da} - \omega L''_q i_{qa} &= 0 \\ Ri_{qa} + L''_q p i_{qa} + \omega L''_d i_{da} &= 0 \end{aligned} \tag{73-47}$$

Eliminating i_{qa} between them, we obtain an expression for i_{da} of the form

$$L''_d L''_q p^2 i_{da} + R\,(L''_d + L''_q)\,p i_{da} + (\omega^2 L''_d L''_q + R^2)\,i_{da} = 0$$

The corresponding characteristic equation defining the exponents is

$$L''_d L''_q \beta^2 + R\,(L''_d + L''_q)\,\beta + (\omega^2 L''_d L''_q + R^2) = 0$$

Its two roots

$$\beta = -\frac{R\,(L''_d + L''_q)}{2L''_d L''_q} \pm j\omega \sqrt{1 - \left[\frac{R\,(L''_d - L''_q)}{2\omega L''_d L''_q}\right]^2} \tag{73-48}$$

are complex conjugates, $-\beta_1 \pm j\beta_2$. Therefore, the solution to the differential equations (73-47) is written as

$$\begin{aligned} i_{da} &= [C_{1d} \exp(+j\beta_2 t) + C_{2d} \exp(-j\beta_2 t)] \exp(-\beta_1 t) \\ &= (i_{da1} \cos\beta_2 t + i_{da2} \sin\beta_2 t) \exp(-\beta_1 t) \\ i_{qa} &= [C_{1q} \exp(j\beta_2 t) + C_{2q} \exp(-j\beta_2 t)] \exp(-\beta_1 t) \\ &= (i_{qa1} \cos\beta_2 t + i_{qa2} \sin\beta_2 t) \exp(-\beta_1 t) \end{aligned} \tag{73-49}$$

As is seen from Eq. (73-49), the aperiodic currents vary at frequency β_2, and their amplitude decays with a time constant

$$T''_a = 1/\beta_1 = \frac{2L''_d L''_q}{R\,(L''_d + L''_q)} \tag{73-50}$$

In a machine without a damper winding, this time constant would be given by

$$T'_a = 1/\beta_1 = \frac{2L'_d L_q}{R\,(L'_d + L_q)} \tag{73-51}$$

The frequency of variations in aperiodic currents is

$$\beta_2 = \omega \sqrt{1 - \left[\frac{R\,(L''_d - L''_q)}{2\omega L''_d L''_q}\right]^2} \tag{73-52}$$

In a machine without a damper winding, it would be

$$\beta_2 = \omega \sqrt{1 - \left[\frac{R(L'_d - L_q)}{2\omega L'_d L_q}\right]^2} \qquad (73\text{-}53)$$

Because the resistance is small ($R \ll L''_d \approx L''_q$), it may be deemed with a high degree of accuracy that

$$\beta_2 = \omega \qquad (73\text{-}54)$$

In determining the arbitrary constants i_{da1}, i_{da2}, i_{qa1} and i_{qa2} in Eq. (73-49), we will adopt the above assumption for a machine with a damper winding. From that general case it will be an easy matter to go over to a machine without a damper winding on setting $X''_d = X'_d$ and $X''_q = X'_q$. At $t = 0$, we have from Eq. (73-49):

$$i_{da,i} = i_{da1}, \quad i_{qa,i} = i_{qa1}$$

On substituting the above currents into Eq. (72-8) at $t = 0$, we obtain the following equations:

$$i_{d,i} = i_{dp,i} + i_{da,i} + i_{d,ss}$$
$$i_{q,i} = i_{qp,i} + i_{qa,i} + i_{q,ss}$$

where $i_{d,i}$ and $i_{q,i}$ are the currents prior to a short-circuit, as defined in Eq. (73-1), $i_{d,ss}$ and $i_{q,ss}$ are the steady-state short-circuit currents as defined in Eq. (73-7) and equal to zero, and

$$i_{dp,i} = -\Psi_{d,i}(1/L''_d - 1/L_d), \quad i_{qp,i} = -\Psi_{q,i}(1/L''_q - 1/L_q)$$

are the initial values of periodic components from Eq. (73-41).

On solving the above equations for $i_{da,i}$ and $i_{qa,i}$, we get

$$i_{da,i} = i_{da1} = \Psi_{d,i}/L''_d, \quad i_{qa,i} = i_{qa1} = \Psi_{q,i}/L''_q \qquad (73\text{-}55)$$

To find i_{da2} and i_{qa2}, let us substitute i_{da} and i_{qa} from Eqs. (73-49), (73-50) and (73-54) into the first line of Eq. Eq. (73-47) and cancel the common factor $\exp(-t/T'_a)$:

$$R(i_{da1}\cos\omega t - i_{da2}\sin\omega t) - (L''_d/T''_a)(i_{da1}\cos\omega t + i_{da2}\sin\omega t) + L_d\omega(-i_{da1}\sin\omega t + i_{da2}\cos\omega t) - L''_q\omega(i_{qa1}\cos\omega t + i_{qa2}\sin\omega t) = 0$$

The above equation must be satisfied at any instant during the transient (at any value of t). This can only happen,

if the coefficients of sin ωt and cos ωt are equal to zero, that is,

$$(R - L''_d/T''_a)\, i_{da2} - \omega L''_d i_{da1} - \omega L''_q i_{qa2} = 0$$
$$(R - L''_d/T''_a)\, i_{da1} + \omega L''_d i_{da2} - \omega L''_q i_{qa1} = 0$$

Because the coefficient of the first term in the above equations is negligibly small in comparison with that of the last term,

$$|(R - L''_d/T''_a)| = |(RL''_q - L''_d)/2L''_q| \ll \omega L''_q$$

we obtain, subject to Eq. (73-55)

$$i_{da2} = i_{qa1}(L''_q/L''_d) = \Psi_{q,i}/L''_d,$$
$$i_{qa2} = -i_{da1}(L''_d/L''_q) = -\Psi_{d,i}/L''_q \qquad (73\text{-}56)$$

On substituting Eqs. (73-55), (73-56), (73-50) and (73-54) into Eq. (73-49), we obtain expressions for the aperiodic components of stator currents

$$i_{da} = (I/L''_d)(\Psi_{d,i}\cos\omega t + \Psi_{q,i}\sin\omega t)\exp(-t/T''_a)$$
$$i_{qa} = (I/L''_q)(\Psi_{q,i}\cos\omega t - \Psi_{d,i}\sin\omega t)\exp(-t/T''_a) \qquad (73\text{-}57)$$

73-5 Total Short-Circuit Currents in the d- and q-Axis Stator Circuits

Equations for the total short-circuit currents on the d- and q-axis can be obtained by substituting Eqs. (73-7), (73-41), (73-42) and (73-57) into Eq. (73-8):

$$i_d = -\Psi_{d,i}[(1/L''_d - 1/L'_{d(sc)})\exp(-t/T'_2)$$
$$+(1/L'_{d(sc)} - 1/L_d)\exp(-t/T'_1)]$$
$$+(1/L''_d)[\Psi_{d,i}\cos\omega t + \Psi_{q,i}\sin\omega t]\exp(-t/T''_a) - E_{f,i}/\omega L_d \qquad (73\text{-}58)$$

$$i_q = -\Psi_{q,i}(1/L''_q - 1/L_q)\exp(-t/T'_{scq})$$
$$+(1/L''_q)[\Psi_{q,i}\cos\omega t$$
$$-\Psi_{d,i}\sin\omega t]\exp(-t/T''_a) \qquad (73\text{-}59)$$

where $E_{f,i} = \omega L_{ad} i_{f,i}$ is the emf corresponding to the initial field current.

For a machine without a damper winding, the equations of short-circuit currents take the form

$$i_d = -\Psi_{d,1}(1/L'_d - 1/L_d)\exp(-t/T'_f) + 1/L'_d\,[\Psi_{d,1}\cos\omega t + \Psi_{q,1}\sin\omega t]\exp(-t/T'_a) - E_{f,1}/\omega L_d \tag{73-60}$$

$$i_q = (1/L_q)\,[\Psi_{q,1}\cos\omega t - \Psi_{d,1}\sin\omega t]\exp(-t/T'_a) \tag{73-61}$$

It is to be noted that prior to a short-circuit the initial flux linkage depends on the loading condition

$$\Psi_{d,1} = i_{d,1}L_d + i_{f,1}L_{ad} = -e_{q,1}/\omega = v_{q,1}/\omega = (V_e/\omega)\cos\theta$$

$$\Psi_{q,1} = i_{q,1}L_q = e_{d,1}/\omega = -v_{d,1}/\omega = +(V_e/\omega)\sin\theta$$

In the special case of a short-circuit at no-load, that is, at $\theta = 0$, $i_{d,1} = 0$, $i_{q,1} = 0$, and $\Psi_{q,1} = 0$, we have

$$\Psi_{d,1} = V_e/\omega = E_{f,1}/\omega = L_{ad}i_{f,1}$$

and the expressions for currents are markedly simplified

$$i_d = -(E_{f,1}/\omega)\,[(1/L''_d - 1/L'_{d(sc)})\exp(-t/T'_2) + (1/L'_{d(sc)} - 1/L_d)\exp(-t/T'_1) - (1/L''_d)\exp(-t/T''_a)\cos\omega t + 1/L_d] \tag{73-62}$$

$$i_q = -(E_{f,1}/\omega L''_q)\exp(-t/T'_a)\sin\omega t$$

73-6 Currents in the Stator Phases

To find the short-circuit currents in the stator phases, we need first to express the resultant stator current phasor in terms of the (d, q) components:

$$\tilde{I} = i_d + ji_q$$

Then, using Eq. (71-38), we should reference the above phasor to the α- and β-axes stationary relative to the stator, namely

$$\tilde{I}_{\alpha,\beta} = \tilde{I}\exp(j\alpha)$$

where $\alpha = \omega t - \alpha_0$ is the angle between the d-axis of the rotor and the axis of phase A (see Fig. 71-4), and α_0 is the angle of lag between the d-axis and the phase A axis at $t = 0$.

Then the projections of the phasor $\tilde{I}_{\alpha,\beta}$, on the directions of the phase axes, found on the basis of Eq. (69-23), will give the phase currents:

$$i_A = \mathrm{Re}\,[\tilde{I}_{\alpha,\beta}] = \frac{\tilde{I}e^{j\alpha} + \tilde{I}^* e^{-j\alpha}}{2} = i_d \cos\alpha - i_q \sin\alpha$$

$$i_B = \mathrm{Re}\,[\tilde{I}_{\alpha,\beta} a^*] = i_d \cos(\alpha - 2\pi/3) - i_q \sin(\alpha - 2\pi/3) \quad (73\text{-}63)$$

$$i_C = \mathrm{Re}\,[\tilde{I}_{\alpha,\beta} a] = i_d \cos(\alpha - 4\pi/3) - i_q \sin(\alpha - 4\pi/3)$$

To obtain the most general expressions for the short-circuit currents in the stator phases, we ought to substitute i_d and i_q from Eqs. (73-58) and (73-59) into Eq. (73-63). For simplicity, however, we will limit ourselves to a short-circuit from no-load, when i_d and i_q are found from Eq. (73-62). Then for a machine with a damper winding

$$\begin{aligned} i_A = -(E_{f,1}/\omega) \Big\{ & [1/L_d + (1/L'_{d(sc)} - 1/L_d)\exp(-t/T'_1) \\ & + (1/L''_d - 1/L'_{d(sc)}\exp)(-t/T'_2)]\cos(\omega t - \alpha_0) \\ & - \Big[(1/L''_d + 1/L''_q)\cos(\alpha_0/2) \\ & + (1/L''_d - 1/L''_q)\frac{\cos(2\omega t - \alpha_0)}{2}\Big]\exp(-t/T''_a)\Big\} \end{aligned} \quad (73\text{-}64)$$

and for a machine without a damper winding

$$\begin{aligned} i_A = -(E_{f,1}/\omega) \Big\{ & [1/L_d + (1/L'_d - 1/L_d)\,e^{-t/T'_t}]\cos(\omega t - \alpha_0) \\ & - \Big[(1/L'_d + 1/L_q)\frac{\cos\alpha_0}{2} + (1/L'_d - 1/L_q) \\ & \times \frac{\cos(2\omega t - \alpha_0)}{2}\Big] e^{-t/T'_a}\Big\} \end{aligned} \quad (73\text{-}65)$$

The expressions for the currents in phases B and C differ from those for the current in phase A only in that the angle α_0 is replaced by $(\alpha_0 + 2\pi/3)$ for phase B and the angle $(\alpha_0 + 4\pi/3)$ for phase C. It is seen from Eq. (74-64) that the current in phase A is the sum of three terms, namely:

(1) a periodic current varying at frequency ω, which decays to a steady-state amplitude $E_{f,1}/\omega L_d$ (this term is in turn a sum of a periodic component and a steady-state short-circuit current);

(2) a part of an aperiodic component, with an initial value proportional to cos α_0, which decays with a time constant T''_a;

(3) the remainder of the aperiodic component, varying at a frequency 2ω, which decays with a time constant T'_a.

Let us find the maximum value of the instantaneous short-circuit current in phase A. From an analysis of Eq. (73-64), it will be seen that the current is a maximum a half-cycle after the instant of a short-circuit, when $\omega t = \pi$, cos $(\omega t - \alpha_0) = -\cos \alpha_0$, and the instantaneous aperiodic current is combined with the instantaneous periodic current which is acting in the same direction. Obviously, a half-cycle after the application of a short-circuit, the short-circuit current will be a maximum if $\cos \alpha_0 = \pm 1$, that is, if the short-circuit occurs when the pole axis aligns itself with the phase A axis, and $\alpha = -\alpha_0 = 0$ or π.

The periodic and aperiodic components of stator phase A under the above initial conditions and also the steady-state short-circuit current in the same phase are shown in Fig. 73-4. As is seen from Eq. (73-64) for $\alpha_0 = 0$ or $\omega t = \pi$, or from the figure, the maximum instantaneous current on a short-circuit from no-load is given by

$$i_{max} = 2E_{f,1}/\omega L''_d = 2E_{f,1}/X''_d \qquad (73\text{-}66)$$

Here, $E_{f,1}$ is the peak value of excitation emf, which is $\sqrt{2}$ times its rms value, $E_{f,1(ms)}$. It should be remembered that Eq. (73-66) has been derived for the time constants T'_1, T'_2, and T''_a which are many times the time, $t = \pi/\omega$, elapsing from the onset of the transient to the appearance of the maximum short-circuit current. On such an assumption, the peak values of the short-circuit current components do not practically differ from their initial values, and the equation for i_{max} takes the form of Eq. (73-66).

The maximum instantaneous short-circuit current and the corresponding extremal currents that concurrently appear in the rotor circuits are responsible for the electromagnetic forces that act on the coil ends (overhangs) and the core parts. Under a relevant USSR state standard, synchronous machines should stand up without damage to a balanced no-load short-circuit at a voltage which is 1.05 times the rated value, when $E_{f,1} = 1.05V_R$ (here, V_R is the peak value of the rated phase voltage). Then, the per-unit maximum instantaneous short-circuit current (with the peak value

of rated current taken as the base) will be

$$i_{*\max} = i_{\max}/I_R = (2 \times 1.05V_R)/I_R X''_d = 2.1/X''_{*d} \tag{73-67}$$

For machines with a damper winding, whose subtransient inductive reactance, X''_d, is from 0.12 to 0.3 per-unit, the

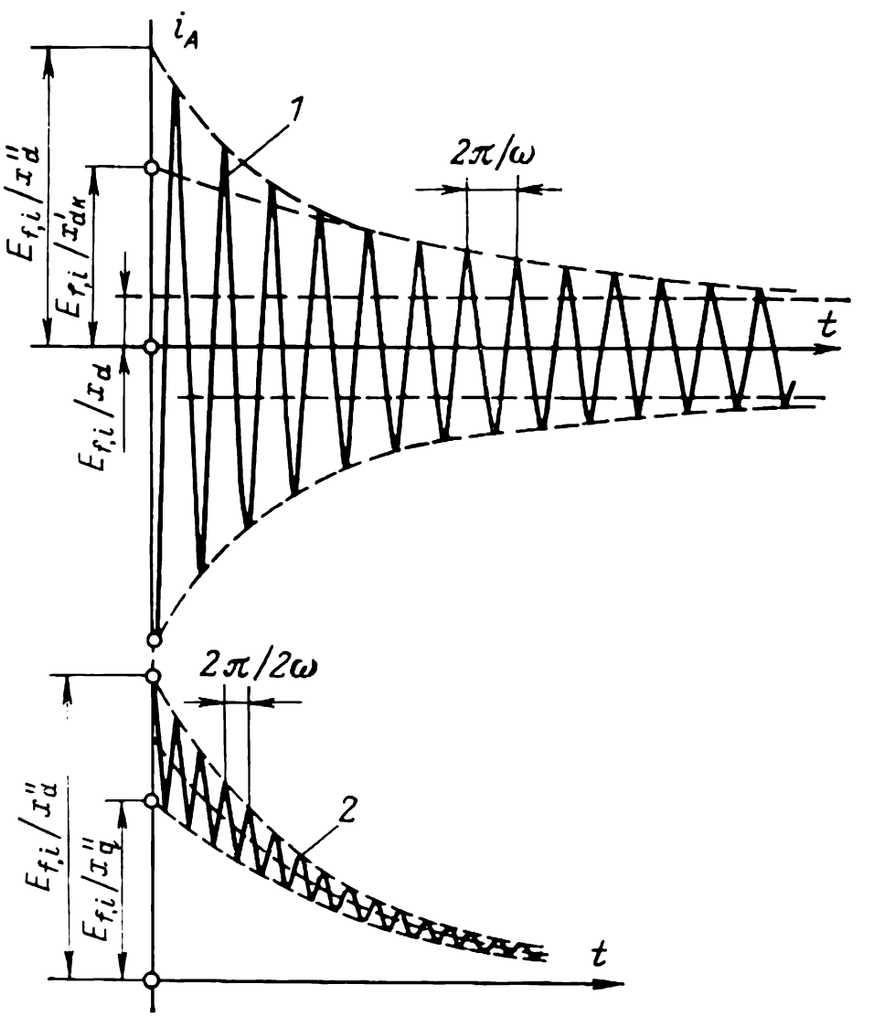

Fig. 73-4 Current in stator phase *A* following a short-circuit from no-load: *1*—periodic and steady-state short-circuit currents; *2*—aperiodic component

maximum instantaneous short-circuit current may be 7 to 17.5 times the peak value of rated current. In machines without a damper winding for which the subtransient and the transient reactive inductances are the same, the figure is 4.5 to 8.5 times.

73-7 Currents in the Rotor Windings

(1) A machine without a damper winding. The field current is the sum of the initial field current which is the same as the steady-state current, $i_{f,\mathrm{i}} = i_{f,\mathrm{ss}}$, a periodic term, $i_{f,\mathrm{p}}$, and an aperiodic term, $i_{f,\mathrm{a}}$.

The periodic and aperiodic components can be found from the same equations as were used to find the corresponding components in the stator winding. The relation between the aperiodic components in the field winding and in the stator winding can be deduced from the flux-linkage equation for the field winding, (73-45). Hence,

$$i_{f,\,a} = -i_{da}\,(L_{ad}/L_f) = -i_{da}\,\frac{L'_d - L_\sigma}{L_{f\sigma}} \qquad (73\text{-}68)$$

Substituting i_{da} from Eq. (73-57) into Eq. (73-68) and noting that in a machine without a damper winding $L''_d = L'_d$ and $L''_q = L_q$, we obtain

$$i_{f,\,a} = -(1/L_{f\sigma})\,(1 - L_\sigma/L'_d)\,(\Psi_{d,\,i}\cos\omega t + \Psi_{q,\,i}\sin\omega t)\,e^{(-t/T'_a)} \qquad (73\text{-}69)$$

The relation between the periodic currents in the field and stator windings has been derived earlier, Eq. (73-23). On substituting the periodic stator current from Eq. (73-25), we get

$$i_{f,\,p} = (-L_d/L_{ad})\,i_{dp} = \Psi_{d,\,i}\,\frac{L_d - L'_d}{L'_d L_{ad}}\exp(-t/T'_f) \qquad (73\text{-}70)$$

Noting that

$$\frac{L_d - L'_d}{L'_d L_{ad}} = (1/L_{f\sigma})\,(1 - L_\sigma/L'_d)$$

we may write a general equation for the current in the field winding as follows:

$$i_f = i_{f,\,i} + \frac{L_d - L'_d}{L'_d L_{ad}}\,[\Psi_{d,\,i}\exp(-t/T'_f) - (\Psi_{d,\,i}\cos\omega t + \Psi_{q,\,i}\sin\omega t)\exp(-t/T'_a)] \qquad (73\text{-}71)$$

In the special case of a short-circuit from no-load, when

$$\Psi_{d,i} = E_{f,1}/\omega = i_{f,1}L_{ad} \text{ and } \Psi_{q,1} = 0$$

the expression for current is markedly simplified

$$i_f = i_{f,\,i}\left[1 + \frac{L_d - L'_d}{L'_d}\,(e^{-t/T'_f} - \cos\omega t e^{-t/T'_a})\right] \qquad (73\text{-}72)$$

(2) A machine with a damper winding. In this case, too, the aperiodic and periodic current components can be found

from the same equations as were derived in the analysis of stator currents.

From Eq. (73-45) for the flux linkages of the rotor circuits, we can readily express the aperiodic currents in the rotor circuits, i_{fa}, i_{scda} and i_{scqa}, in terms of the known currents i_{da} and i_{qa}:

$$\begin{aligned} i_{fa} &= -\frac{L_{scd\sigma}L_{ad}}{L_f L_{scd} - L_{ad}^2} i_{da} = -\frac{L_d'' - L_\sigma}{L_{f\sigma}} i_{da} \\ i_{scda} &= -\frac{L_{f\sigma}L_{ad}}{L_f L_{scd} - L_{ad}^2} i_{da} = -\frac{L_d'' - L_\sigma}{L_{scd\sigma}} i_{da} \\ i_{scqa} &= -(L_{ad}/L_{scq})\, i_{qa} = -\frac{L_q'' - L_\sigma}{L_{scq\sigma}} i_{qa} \end{aligned} \tag{73-73}$$

Substituting i_{da} and i_{qa} from Eq. (73-57) into Eq. (73-73) gives

$$\begin{aligned} i_{fa} &= -\frac{1}{L_{f\sigma}}\left(1 - \frac{L_\sigma}{L_d''}\right)(\Psi_{d,\,i}\cos\omega t + \Psi_{q,\,i}\sin\omega t)\, e^{-t/T_a''} \\ i_{scda} &= -\frac{1}{L_{scd\sigma}}\left(1 - \frac{L_\sigma}{L_d''}\right)(\Psi_{d,\,i}\cos\omega t + \Psi_{q,\,i}\sin\omega t)\, e^{-t/T_a''} \\ i_{scqa} &= -\frac{1}{L_{scq\sigma}}\left(1 - \frac{L_\sigma}{L_q''}\right)(\Psi_{q,\,i}\cos\omega t - \Psi_{d,\,i}\sin\omega t)\, e^{-t/T_a''} \end{aligned} \tag{73-74}$$

The periodic components, i_{fp} and i_{scdp}, of the d-axis rotor circuit currents contain slow terms decaying with a time constant T_1' and fast terms decaying with a time constant T_2' [see Eq. (73-29)]. Their initial values (at $t = 0$) can be found, if we recall that the sum of periodic and aperiodic terms at that instant must be zero:

$$i_{f,\,i} = i_{fp(t=0)} + i_{fa(t=0)} = 0, \quad i_{scd,\,i} = i_{scdp(t=0)} + i_{scda(t=0)} = 0$$

Hence,

$$\begin{aligned} i_{fp(t=0)} &= i_{f0} = i_{f1} + i_{f2} = -i_{fa(t=0)} \\ &= (1/L_{f\sigma})(1 - L_\sigma/L_d'')\,\Psi_{d,\,i} \\ i_{scd(t=0)} &= i_{scd0} = i_{scd1} + i_{scd2} = -i_{scda(t=0)} \\ &= (1/L_{scd\sigma})(1 - L_\sigma/L_d'')\,\Psi_{d,\,i} \end{aligned} \tag{73-75}$$

It can be readily proved that Eqs. (73-75) are identical with Eqs. (73-33).

Now it only remains to deduce the initial values of the slow and fast components, i_{f1}, i_{scd1} and i_{f2}, i_{scd2}, of the decaying currents in Eqs. (73-75). If the damper winding has a sufficiently high resistance, $R_{scd} \gg R_f$, it may be deemed that the slow (transient) component of field current does not differ from the periodic component of field current if the same machine had no damper winding [see Eq. (73-70)]. Then the initial value of the slowly decaying field current is

$$i_{f1} = \Psi_{d,1} \frac{L_d - L'_d}{L'_d L_{ad}} = (\Psi_{d,1}/L_{f\sigma})(1 - L_\sigma/L'_d) \quad (73\text{-}76)$$

Now, we can use Eqs. (73-75) to find the initial value of the fast decaying component of field current

$$i_{f2} = i_{f0} - i_{f1} = -(L_\sigma/L_{f\sigma})(1/L''_d - 1/L'_d)\Psi_{d,1} \quad (73\text{-}77)$$

Neglecting the very small slow term of the damper-winding current, the initial value of the fast component of that current can be found from Eqs. (73-75)

$$i_{scd2} \approx i_{scd0} = (1/L_{scd\sigma})(1 - L_\sigma/L''_d)\Psi_{d,1} \quad (73\text{-}78)$$

More accurate values of the slow components of currents, i_{f1} and i_{scd1}, can be obtained by solving Eqs. (73-39). They are:

$$i_{f1} = \frac{i_{f0} + i_{scd0}(L'_{ad}/L'_f)}{(1 + T'_{scd}/T'_f)} \quad (73\text{-}79)$$

$$i_{scd1} = \frac{i_{scd0} + i_{f0}(L'_f/L'_{ad})}{(1 + T'_f/T'_{scd})} \quad (73\text{-}80)$$

After obtaining the more accurate values of i_{f1} and i_{scd1} we can find i_{f2} and i_{scd2} from Eqs. (73-75). It can readily be proved that at $T'_f \gg T'_{scd}$, Eq. (73-79) is the same as Eq. (73-76), Eq. (73-80) yields $i_{scd1} = 0$, and i_{scd2} is found from Eq. (73-78).

For the q-axis damper winding, the initial value of the periodic current is found in a similar way from Eq. (73-74)

$$i_{scqp(t=0)} = i_{scq0} = -i_{scqa(t=0)} = -(1/L_{scq\sigma})(1 - L_\sigma/L''_q)\Psi_{q,1} \quad (73\text{-}81)$$

The final expressions for the currents that exist in the field winding and the d- and q-axis damper windings in the case of a balanced short-circuit are obtained by combining the component currents found earlier from Eqs. (73-74)

and (73-78) or, more accurately, from Eq. (73-79) and (73-80):

$$\begin{aligned} i_f &= i_{f,\mathrm{i}} + i_{f\mathrm{a}} + i_{f\mathrm{p}} = i_{f,i} + i_{f\mathrm{a}} + i_{f1} \exp(-t/T'_1) \\ &\quad + i_{f2} \exp(-t/T'_2) \\ i_{\mathrm{sc}\,d} &= i_{\mathrm{sc}\,d\mathrm{a}} + i_{\mathrm{sc}\,d\mathrm{p}} = i_{\mathrm{sc}\,d\mathrm{a}} + i_{\mathrm{sc}\,d1} \exp(-t/T'_1) \\ &\quad + i_{\mathrm{sc}\,d2} \exp(-t/T'_2) \\ i_{\mathrm{sc}\,q} &= i_{\mathrm{sc}\,q\mathrm{a}} + i_{\mathrm{sc}\,q\mathrm{p}} = i_{\mathrm{sc}\,q\mathrm{a}} + i_{\mathrm{sc}\,q0} \exp(-t/T'_{\mathrm{sc}\,q}) \end{aligned} \tag{73-82}$$

If a short-circuit occurs from no-load and $T'_f \gg T'_{\mathrm{sc}\,d}$,

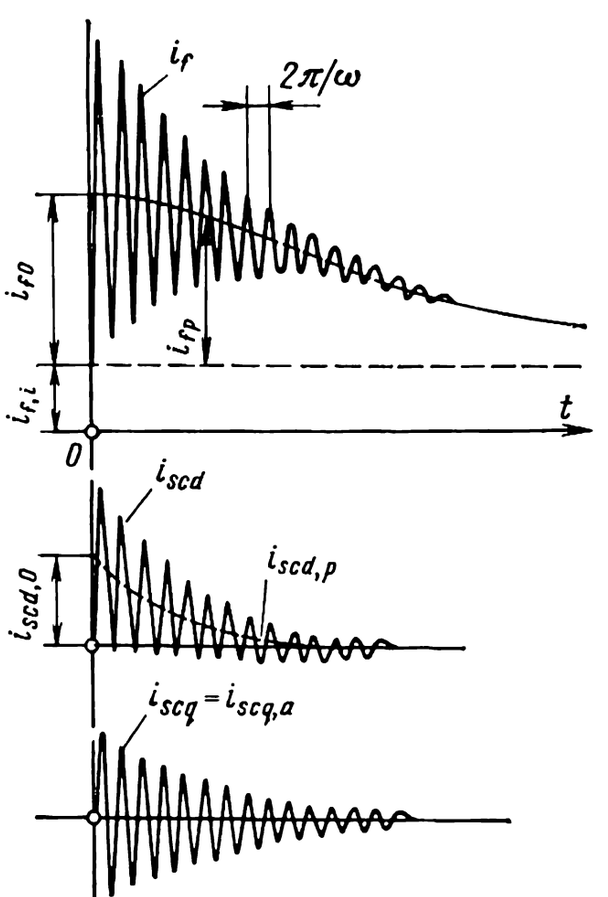

Fig. 73-5 Currents in the rotor circuits on a short-circuit from no-load

the equations for the rotor-circuit currents take the form:

$$\begin{aligned} i_f &= i_{f,\,i}\{1 + (L_{ad}/L_{f\sigma})[(1 - L_\sigma/L'_d)\, e^{-t/T'_1} \\ &\quad - L_\sigma (1/L''_d - 1/L'_d) \exp(-t/T'_2) \\ &\quad - (1 - L_\sigma/L''_d)\, e^{-t/T''_{\mathrm{a}}} \cos \omega t]\} \\ i_{\mathrm{scd}} &= i_{f,\,\mathrm{i}} (L_{ad}/L_{\mathrm{scd}\sigma})(1 - L_\sigma/L''_d)(e^{-t/T'_2} - e^{-t/T''_{\mathrm{a}}} \cos \omega t) \\ i_{\mathrm{scq}} &= i_{f,\,\mathrm{i}} (L_{ad}/L_{\mathrm{scq}\sigma})(1 - L_\sigma/L''_q)\, e^{-t/T''_{\mathrm{a}}} \sin \omega t \end{aligned} \tag{73-83}$$

For the above special case, the waveforms of the currents in the rotor circuits are shown in Fig. 73-5.

Appendix

Conductor Materials for Electrical Machines and Transformers

1. **Copper.** The windings of electrical machines and transformers are wound with conductors fabricated from special grades of copper (see the Table below). These grades of copper are obtained by electrolytic refining and show an extremely high purity (the best Soviet-made grade of copper, labelled MO, is 99.95% pure).

Round copper conductors can be fabricated from hard (non-annealed) copper (labelled MT in the USSR) and soft (annealed) copper (labelled MM in the USSR). Such conductors come in diameters from 0.03 to 10 mm.

Copper strip (or rectangular) conductors are likewise made of either hard or soft copper (respectively labelled МГТ and МГМ). Strip conductors come in sizes 0.83-12.5 for the smaller side and 2.1-35 mm for the larger side.

2. **Aluminium.** As a conductor material, aluminium is widely used for transformers and, although on a smaller scale, in electrical machines. Busbars and wires are fabricated from commercial-purity aluminium (labelled A6, A5 and AE under a relevant USSR state standard). These grades of aluminium are 99.5% to 99.6% pure.

Aluminium wire is fabricated from AE aluminium. Round aluminium wire comes in three grades, namely AT (hard), АПТ (semihard), and AM (soft), in the diameter range from 0.08 to 10 mm. Aluminium strip (rectangular) conductors come in two grades, AT and AM, with 1.56 to 12.5 on the small side and from 2.1 to 45 mm on the larger side.

Bibliography

To Part Six

63. Бертинов А. И., Варлей В. В. *Электрические машины с катящимся ротором.* Энергия, Москва, 1969.
64. Гурин Я. С., Курочкин М. Н. *Проектирование машин постоянного тока.* Госэнергоиздат, Москва — Ленинград, 1961.
65. Рабинович И. Н., Шубов И. Г. *Проектирование электрических машин постоянного тока.* Энергия, Ленинград, 1967.
66. Толвинский В. А. *Электрические машины постоянного тока.* Госэнергоиздат, Москва — Ленинград, 1956.
67. Овчинников И. Е., Лебедев Н. И. *Бесконтактные двигатели постоянного тока автоматических устройств.* Наука, Ленинград, 1966.
68. *Двигатели постоянного тока с полупроводниковыми коммутаторами.* Наука, Ленинград, 1972.
69. Бертинов А. И., Алиевский Б. Л., Троицкий С. Р. *Униполярные электрические машины.* Энергия, Москва, 1966.
70. Сандлер А. С. *Регулирование скорости вращения асинхронных двигателей.* Энергия, Москва, 1966.
71. Костенко М. П., Гнедин Л. Н. *Теория и расчет трехфазных коллекторных машин и каскадных систем.* Наука, Москва — Ленинград, 1964.

To Part Seven

72. Горев А. А. *Переходные процессы синхронной машины.* Госэнергоиздат, Москва — Ленинград, 1950.
73. Грузов Л. Н. *Методы математического исследования электрических машин.* Госэнергоиздат, Москва – Ленинград, 1953.
74. Казовский Е. Я. *Переходные процессы в электрических машинах переменного тока.* Изд-во АН СССР, Москва – Ленинград, 1962.
75. Кимбарк Э. *Синхронные машины и устойчивость электрических систем.* Госэнергоиздат, Москва — Ленинград, 1960.
76. Ковач К. П., Рац И. *Переходные процессы в машинах переменного тока.* Перев. с венгерского. Госэнергоиздат, Москва — Ленинград, 1963.
77. Сорокер Т. Г. *Переходные процессы синхронных машин.* Высшая школа, Москва, 1960.
78. Веников В. А. *Переходные электромеханические процессы в электрических* системах. Высшая школа, Москва, 1970.
79. Конкордия Ч. *Синхронные машины — переходные и установившиеся процессы.* Госэнергоиздат, Москва — Ленинград, 1959.
80. Лайбл Т. *Теория синхронной машины при переходных процессах.* Госэнергоиздат, Москва — Ленинград, 1957.
81. Трещев И. И. *Методы исследования электромагнитных процессов в машинах переменного тока.* Энергия, Ленинград, 1969.
82. Урусов И. Д. *Линейная теория колебаний синхронной машины.* Изд-во АН СССР, Москва — Ленинград, 1960.
83. Постников И. М. *Обобщенная теория и переходные процессы электрических машин.* Техніка, Киев, 1966.

Index

A.C. commutator motors
  repulsion, 161
  single-phase, 155
    compensated series, 168
  three-phase, 139
A. C. motors
  commutation in, 147
Amplidyne, 108
Armature emf, 30
  on load, 32
Armature reaction, 49
Armature windings, 17
  drum, 17
  frog-leg, 26
  lap, 19
  wave, 22

Brush angle, 161
Brush sparking, 65

Chording, 36
Coil group, 18
Coil width, 18
Commutation, 59
  a.c. motors, 59
  early, 63
  late, 63
  straight-line, 62
Commutator, 9
  as frequency changer, 135
  mechanical, 9
  solid-state, 121
Commutator action
  in a.c. machines, 134
Commutator winding, 33
Compensating winding, 58
Conduction pump, 113
Control generator, 107

Damper winding, 213
D. C. electromagnetic pump, 113
D. C. generator, 10, 71
  armature characteristics of, 74
  armature current on short-circuit, 77
  compound, 77
  Krämer, 102
  output characteristics of, 76
  parallel operation of, 83
  Rosenberg, 104
  series-wound, 72
  shunt, 77
  split-pole, 102
D. C. machines
  acyclic, 111
  construction, 13
  electromagnetic torque, 38
  energy conversion by, 56
  homopolar, 111
  magnetic circuit calculation, 43 48
  mmfs, 40
  permanent-magnet, 100
  principle of operation, 17
  resistances, 40
  solid-state commutator, 121
  special-purpose, 100
  voltage calculations, 48
D. C. motors, 9, 84
  compound-wound, 87
  fractional-hp transistor, 124
  printed-armature, 110
  round-armature, 110
  series-wound, 93
  starting of, 84
  steady-state characteristics, 86
  thyristor-commutated, 130
Deri motor, 164
Dynamotors,
  a.c.-to-d.c., 118
  d.c.-to-d.c., 116

Equalizers, 28
  first-order, 28
  second-order, 29
Electric loading, 41

Field removal, 235
Flashover, 68

Frequency conversion
by mechanical commutator, 136

Generator buildup, 77

Induction machines
switch-on, 203
Induction motors,
power factor control, 148
speed control, 148

MHD machines, 113
Motor-generator sets, 115

Pitch
back, 18
brush, 20
front, 18
resultant, 20

Rapidyne, 108
Referring rotor to stator, 216
Repulsion motor, 161
RICHTER, 139
Rotary converters, 115
Rotary power amplifiers, 107
cross-field, 108

Scheribus scheme, 151
Schrage motor, 139
Short-pitching, 36
Speed control schemes, 148-155

Thompson motor, 161
Transients, 165
in induction machines, 166, 191
at switch-on, 203
mathematical description, 166-191, 212-234
synchronous machines, 212-276

Printed in the Union of Soviet Socialist Republics